THE DESIGN AND SYNTHESIS OF PHOSPHORUS CONTAINING HEMILABLE LIGANDS.

By

Joanne Wheatley

A Thesis submitted in partial fulfillment for the award of

Doctor of Philosophy

School of Chemistry

University of St. Andrews

North Haugh

St. Andrews

Fife

KY16 9ST.

31 March 2004

DECLARATION.

I, Joanne Wheatley, hereby certify that this thesis, which is approximately 35,000 words in length, has been written by me, that it is the record of work carried out by me and that it has not been submitted in any previous application for a higher degree.

Date 3/12/04 signature of candidate.

I was admitted as a research student in September 2000 and as a candidate for the degree of Doctor of Philosophy in September 2001; the higher study for which this is a record was carried out in the University of St. Andrews between 2000 and 2003.

Date 3/12/04 signature of candidate.

I hereby certify that the candidate has fulfilled the conditions of the Resolution and Regulations appropriate for the degree of Doctor of Philosophy in the University of St. Andrews and that the candidate is qualified to submit this thesis in application for that degree.

Date 3.12.04 signature of supervisor.

In submitting this thesis to the University of St. Andrews I understand that I am giving permission for it to be made available for use in accordance with the regulations of the University Library for the time being in force, subject to any copyright vested in the work not being affected thereby. I also understand that the title and abstract will be published, and that a copy of the work may be made and supplied to any *bona fide* library or research worker.

Date..3/12/04... signature of candidate.

ABSTRACT.

This thesis describes the preparation and complexation of a range of hemilable ligands.

2-Diphenyl(phosphinohydrazino)pyridine, ($Ph_2PNHNHpy$), was prepared and oxidised to form $Ph_2P(E)NHNHpy$ (E = O, S, Se) or reacted with appropriate metal complexes such as $[PtCl_2(cod)]$, $[PtMe_2(cod)]$, $[\{Pd(\mu\text{-}Cl)(\eta^3\text{-}C_3H_5)\}_2]$, $[\{Rh(\mu\text{-}Cl)(C_8H_{12})\}]$, $[\{RuCl_2(\eta^3\text{:}\eta^3\text{-}C_{10}H_{16})\}_2]$, $[\{RuCl(\mu\text{-}Cl)(\eta^6\text{-}p\text{-}MeC_6H_4{}^iPr)_2\}]$, $[\{IrCl(\mu\text{-}Cl)(\eta^5\text{-}C_5Me_5)\}_2]$ and $[Cu(MeCN)_4][PF_6]$ to give a range of new monodentate complexes.

p-$Ph_2PNHCH_2(C_6H_4)CH_2NHPPh_2$, was oxidised to form (*p*-$Ph_2P(E)NHCH_2(C_6H_4)CH_2NHP(E)Ph_2$) (E = O, S, Se) or reacted with appropriate metal complexes such as $[\{PtCl(\mu\text{-}Cl)(PEt_3)\}_2]$, $[\{PtCl(\mu\text{-}Cl)(PPhMe_2)\}_2]$, $[\{MCl(\mu\text{-}Cl)(\eta^5\text{-}C_5Me_5)\}_2]$ (M = Rh, Ir), $[\{RuCl(\mu\text{-}Cl)(\eta^6\text{-}p\text{-}MeC_6H_4{}^iPr)_2\}]$, $[\{Pd(\mu\text{-}Cl)(\eta^3\text{-}C_3H_5)\}_2]$, $[\{Rh(\mu\text{-}Cl)(C_8H_{12})\}]$ and [AuCl(tht)] to give a range of new bidentate bridging complexes.

N-allylaminodiphenylphosphine, ($Ph_2PNH(C_3H_5)$, was used as a precursor to form $Ph_2P(E)NH(C_3H_5)$ (E = O, S, Se) or reacted with appropriate metals such as $[PtCl_2(cod)]$, $[PdCl_2(cod)]$, $[\{MCl(\mu\text{-}Cl)(\eta^5\text{-}C_5Me_5)\}_2]$ (M = Rh, Ir), $[\{RuCl(\mu\text{-}Cl)(\eta^6\text{-}p\text{-}MeC_6H_4{}^iPr)_2\}]$, [AuCl(tht)], $[\{PtCl(\mu\text{-}Cl)(PEt_3)\}_2]$ and $[\{PtCl(\mu\text{-}Cl)(PPhMe_2)\}_2]$, to give a range of new monodentate complexes.

N-allylaminobisdiphenylphosphine, ($(Ph_2P)_2N(C_3H_5)$), was oxidised to form $(Ph_2P(E))_2N(C_3H_5)$ (E = O, S, Se) or reacted with appropriate metals such as $[PtCl_2(cod)]$, $[PdCl_2(cod)]$, $[\{MCl(\mu\text{-}Cl)(\eta^5\text{-}C_5Me_5)\}_2]$ (M = Rh, Ir), $[\{RuCl(\mu\text{-}Cl)(\eta^6\text{-}p\text{-}MeC_6H_4{}^iPr)_2\}]$, [AuCl(tht)], $[Mo(CO)_4(nbd)]$, and $[Cu(MeCN)_4][PF_6]$ to give a range of new bidentate complexes.

N-allylaminodiphenylphosphine, ($Ph_2PNH(C_3H_5)$), was oxidised to form $Ph_2P(E)NH(C_3H_5)$ (E = O, S, Se) or reacted with appropriate metals such as $[PtCl_2(C_8H_{12})]$, $[PdCl_2(C_8H_{12})]$, $[PtMe_2(C_8H_{12})]$, $[\{Rh(\mu\text{-}Cl)(C_8H_{12})\}]$, $[\{RuCl(\mu\text{-}Cl)(\eta^6\text{-}p\text{-}MeC_6H_4{}^iPr)_2\}]$, and $[Mo(CO)_4(nbd)]$ to give a range of new monodentate and bidentate complexes.

Z-1-diphenylphosphino-3,3-dimethyl-2-phenylthiobut-1-ene and *Z*-1-diphenylphosphino-2-phenylthiopropene react with appropriate metal complexes such as $[PtCl_2(C_8H_{12})]$, $[PdCl_2(C_8H_{12})]$, $[\{RuCl(\mu\text{-}Cl)(\eta^6\text{-}p\text{-}MeC_6H_4{}^iPr)_2\}]$, $[\{IrCl(\mu\text{-}Cl)(\eta^5\text{-}C_5Me_5)\}_2]$, $[\{Pd(\mu\text{-}Cl)(\eta^3\text{-}C_3H_5)\}_2]$, and [AuCl(tht)] to give a range of new complexes that are either only phosphorus bound or phosphorus-sulfur bound.

Molecular modelling of imidazolidine and benzimidazole derivatives provides the opportunity to investigate the likelihood of reactions proceeding as proposed. Suitable candidates are suggested for future work with the possibility of developing new hemilabile ligands.

ACKNOWLEDGEMENTS

Firstly I would like to give special thanks to Matt for all his support (despite my tantrums) during this work and for making me believe that I can do it. I would also like to give special thanks to both Derek and Alex for funding and encouragement when times were difficult. Thanks also for the opportunity to learn new techniques which were both interesting and challenging.

Thanks go to Alan Aitkin for preparing *Z*-1-diphenylphosphino-3,3-dimethyl-2-phenylthiobut-1-ene and *Z*-1-diphenylphosphino-2-phenylthiopropene and allowing me to use them to make new metal complexes. They gave me a very valuable and much needed chapter though I do not miss the smell that these two ligands produced.

The guys in the lab, Steve thanks for all your help especially the metals complexes that were invaluable (you are still missed but I hope you are having loads of fun in Loughborough), Prav thanks for all the advice and help (good luck for the future) and Petr thanks for your help with NMR and any other silly little questions you have had to put up with since Steve and Prav left (good luck to both you and Petra). To Colin, Stu, David, and Ian thanks for making the lab a fun place and to Heather for putting up with me in the office and for the crystallography. Best wishes to you all in whatever you decide to do.

CONTENTS

LIST OF FIGURES

LIST OF TABLES

LIST OF SCHEMES.

3.1.2 Reaction of 2 $Ph_2PNH(C_3H_5)$ with $[MCl_2(cod)]$ (M = Pt, Pd; cod = C_8H_{12})).

3.1.3 Reaction of $Ph_2PNH(C_3H_5)$ with $[MCl_2(cod)]$ (M = Pt, Pd; cod = C_8H_{12})).

3.1.4 Reaction of $Ph_2PNH(C_3H_5)$ with $[\{MLCl_2\}_2]$ (M = Rh, Ir; L = η^5-C_5Me_5).

3.2.1 Formation of $(C_3H_5)N(Ph_2P)_2$.

3.2.2 Reaction of $(Ph_2P)_2N(C_3H_5)$ with $[\{RuCl(\mu\text{-}Cl)(\eta^6\text{-}p\text{-}MeC_6H_4{}^iPr)\}_2]$.

3.2.3 Reaction of $(Ph_2P)_2N(C_3H_5)$ with $[\{MCl(\mu\text{-}Cl)(\eta^5\text{-}C_5Me_5)\}_2]$ (M = Rh, Ir).

3.3.1 Reaction of $(C_3H_5)_2NH$ with PR_3.

3.3.2 Formation of $Ph_2PN(C_3H_5)_2$ and $Ph_2P(E)N(C_3H_5)_2$ ligands (E = O, S, Se).

3.3.3 Reaction of $Ph_2PN(C_3H_5)_2$ with $[PtCl_2(cod)]$.

4.1 Reaction of a β-phosphinothioketonate coordinated ligand with PMe_3.

4.2 Suggested formation of ligands **67** and **74**.

4.3 Formation of *P,S*-chelated complexes.

ABBREVIATIONS

This list contains abbreviations, which may have been used in this thesis without definition.

Å	Angstrom unit 10^{-10} m
^{t}Bu	*t*-Butyl, -C(CH_3)$_3$
cm^{-1}	wavenumber
cod	1,5-cyclooctadiene, C_8H_{12}
dcm	dichloromethane, CH_2Cl_2
dppa	bis(diphenylphosphino)amine, $Ph_2PNHPPh_2$
dppe	bis(diphenylphosphino)ethane, $Ph_2PCH_2CH_2PPh_2$
dppm	bis(diphenylphosphino)methane, $Ph_2PCH_2PPh_2$
dpptb	*Z*-1-diphenylphosphino-3,3-dimethyl-2-phenylthiobut-1-ene
dpptp	*Z*-1-diphenylphosphino-2-phenylthiopropene
Et	ethyl, -C_2H_5
ES	Electrospray mass spectrometry
FAB	Fast Atomic Bombardment
FT	Fourier transform (for NMR or IR)
Hz	Hertz, sec^{-1}
IR	Infra-red
J	coupling constant, Hz
Me	methyl, -CH_3
m/z	mass-to-charge ratio
nbd	2,5-norbornadiene, C_7H_8
NMR	Nuclear Magnetic Resonance
Ph	phenyl, -C_6H_5

ppm	parts per million
^{i}Pr	*i*-propyl, -$CH(CH_3)_2$
PR_3	phosphine
py	pyridyl, -C_5H_4N
$^{31}P\{^{1}H\}$	phosphorus, proton decoupled
thf	tetrahydrofuran, C_4H_8O
tht	tetrahydrothiophene, C_4H_8S

GENERAL EXPERIMENTAL CONDITIONS

Unless otherwise stated all reactions were performed under an atmosphere of oxygen free nitrogen using standard Schlenk procedures. All glassware was oven dried at 100 °C or flame dried under vacuum prior to use.

All solvents and reagents were purchased from Aldrich, Strem, Fisher or Lancaster and used as received. In addition toluene, thf, Et_2O and hexane were distilled from sodium-benzophenone; dichloromethane from CaH_2 under nitrogen. Deuterated solvents were dried over molecular sieves and used as supplied. Et_3N was dried over CaH_2 under nitrogen prior to distillation and Ph_2PCl was purified by distillation. Water was deionised and degassed prior to use.

Infra-red spectra were recorded as KBr discs in the range 4000-200 cm^{-1} or thin films between KBr plates on a Perkin-Elmer 2000 FTIR/RAMAN spectrometer. NMR spectra were recorded on a Gemini 2000 (operating at 121.4 MHz for ^{31}P and 300 MHz for ^{1}H) or on a Jeol Delta FT (270 MHz) spectrometers. ^{1}H NMR spectra were referenced internally to deuterated solvents; CD_2Cl_2 δ 5.35 ppm, $CDCl_3$ δ 7.27 ppm. ^{31}P NMR were referenced externally to 85 % H_3PO_4. Mass spectra were performed by the St. Andrews University service and EPSRC mass spectrometry service centre (University of Wales, Swansea). Microanalyses were carried out by the service at the University of St. Andrews

CHAPTER 1: INTRODUCTION

1.1 *An introduction to hemilabile ligands.*

The area of hemilabile chemistry has received a vast amount of interest in recent years. This is the study of coordinated complexes containing mixed functionality ligands that enables a variety of complexes to be formed and investigated. The area that has received the most interest in recent years is when the ligands formed contain one strongly bound atom such as phosphorus and one weakly bound labile atom such as nitrogen, oxygen or sulfur. These hemilabile ligands[1] as they are most commonly known show distinctive characteristics by allowing the relatively weakly bound atom the ability to fill a reaction site temporarily until a more reactive species appears in the reaction. The labile fragment of the ligand is reattached after the more reactive species has undergone a transformation that makes it unattractive to the transition metal centre and is hence removed. The use of these bifunctional hemilabile ligands has been developed in homogeneous catalysis, chemical sensing, small molecule metal complex activation and stabilisation of reactive, unsaturated transition metal species.

The term hemilabile ligand was first introduced in 1979 by Jeffrey and Rauchfuss[2] and has since been used to describe a wide range of coordinated groups with a variety of reactivity's on a variety of metal centres. The basic characteristics of hemilabile ligands are shown in scheme 1.1.

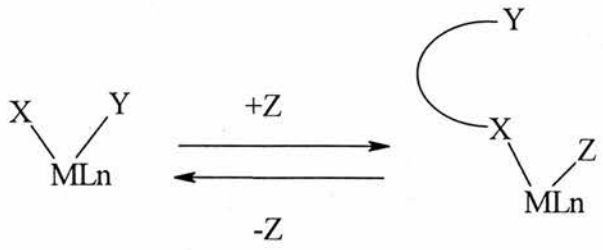

X= substitutionally inert group
Y= substitutionally labile group
Z= ligand or solvent

Scheme 1.1. Basic characteristics of hemilabile ligands.

1.2 *Phosphorus Based Hemilabile Ligands.*

The best studied area of hemilabile chemistry involves phosphorus-based ligands. In this instance the phosphorus atom is a substitutionally inert group and the ligand can contain a variety of labile moieties including nitrogen, carbon and sulfur, which will be discussed here. Phosphorus-nitrogen based ligands in particular phosphine-amine ligands have been extensively studied in recent years and were one of the first reported types of hemilabile ligand known containing phosphorus coordinated to transition metal centres. This hemilability was demonstrated by Mann and Watson[3] who showed that they could displace the amino group from *o*-dimethylaminophenyldiethylphosphine Pd(II) with SCN^-. Since this work it has been shown that phosphorus- amino ligands can behave both irreversibily and reversible depending on the coordinating moiety used for the displacement.

1.3 *Aminophosphine Ligands.*

Werner *et al*[4] studied a phosphine-amine ligand complexed to an iridium centre and showed that the complex was inert in the presence of ethylene though

in the presence of CO the amine moiety dissociated from the metal centre allowing the CO to coordinate to the iridium. This dissociation was subsequently shown by Roundhill *et al*[5] in another study, which showed the displacement of the chelated amino group with acetonitrile and pyridine ligands, thus illustrating that the amino group is susceptible to dissociation in the presence of strong π-acceptor ligands such as CO and by σ-donors including acetonitrile. However, this is not always true as other factors may influence the dissociation of the amino group including metal oxidation state, the substituents present on both the phosphine and amino groups and what other ligands are present with the metal complex.

1.4 *Pyridylphosphine Ligands.*

Phosphorus based hemilabile ligands containing pyridine have also been described. This group of ligands has shown both substitutionally inert and hemilabile characteristics. Rigo and coworkers[6, 7] investigated the reactivity of complexes containing pyridyl-phosphine ligands in a variety of coordinating molecules. In the presence of small molecules like acetonitrile or pyridine it was shown that reactions of osmium (II) complexes of 1-(diphenylphosphino)-2-(2-pyridyl)ethane did not proceed with the displacement of the chelated pyridyl moiety but in the presence of CO it was shown that the pyridyl could be displaced in a hemilabile fashion. In another example it was shown that the analogous ruthenium (II) complex readily reacted with CO in CH_2Cl_2 to dissociate a bound pyridyl fragment[7] unlike the related phosphine-amine ligands, which did not react in the presence of CO[8]. This finding shows the inherent

difference in the lability of the aliphatic and aromatic moieties involved on the metal centre.

As described previously for phosphine-amine systems fluxional ligand exchanges can also occur with pyridyl-phosphorus ligands[9, 10, 11]. The ligand 2-(diphenylphosphino)pyridine was shown to participate in a chelate isomerisation reaction[9] by ^{1}H NMR spectroscopy and the process occurs equally at ambient temperatures. However, as the temperature at which the isomerisation was observed increased the amount of the non-chelated complex present in the reaction decreased. The utilisation of both 2-(diphenylphosphino)pyridine (Ph_2Ppy) and 2,6-bis(diphenylphosphino)pyridine [$(Ph_2P)_2py$] to prepare bimetallic and polymetallic complexes[12, 13, 14] has been achieved due to the strained chelate that is formed in the ligands.

1.4.1 *Synthesis of pyridylphosphine ligands.*

The first reported synthesis of pyridylphosphine[15] ligands was by Mann and Davies[16] in 1944 when they studied the optical resolution of tertiary phosphines. They studied the reaction of phenyl(4-bromophenyl)chlorophosphine with 2-pyridylmagnesium bromide or 3-pyridylmagnesium phosphine to afford the 2-{phenyl(4-bromophenyl)phosphine} pyridine (5 %) **A** and 3-{phenyl(4-bromophenyl)phosphine} pyridine (7 %) **B** respectively.

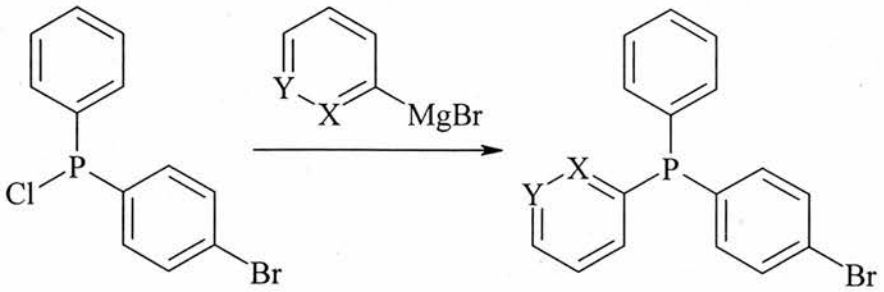

A X = N, Y = CH
B X = CH, Y = N

Scheme 1.2. Reaction of phenyl-(4-bromophenyl)chlorophosphine.

Further pyridylphosphines were prepared using 2-pyridylmagnesium bromide and PCl_3 in particular tris-2-(diphenylphosphino)pyridine **E** (13 %) and in 1948[17] the synthetic procedure was extended to prepare di-2-(diphenylphosphino)pyridine **D** and 2-(diphenylphosphino)pyridine **C**.

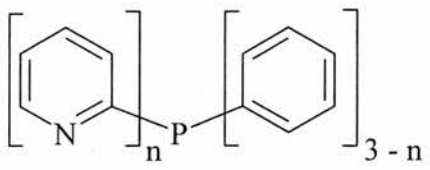

C (n=1)
D (n=2)
E (n=3)

Figure 1.1. Mono-, di- and tris- (diphenylphosphino)pyridines.

Improvements were made to the preparation of pyridylphosphine ligands that included the utilisation of 2-lithiopyridines at significantly lower temperatures (-65 °C to – 100 °C), in place of the 2-pyridylmagnesium bromides. These modifications were used in the resynthesis of tris-2-(diphenylphosphino)pyridine which resulted in an increased yield of 66 %[18]. Other phosphines were prepared

in a similar way using the appropriate pyridyllithium species and PCl_3 or $MePCl_2$.

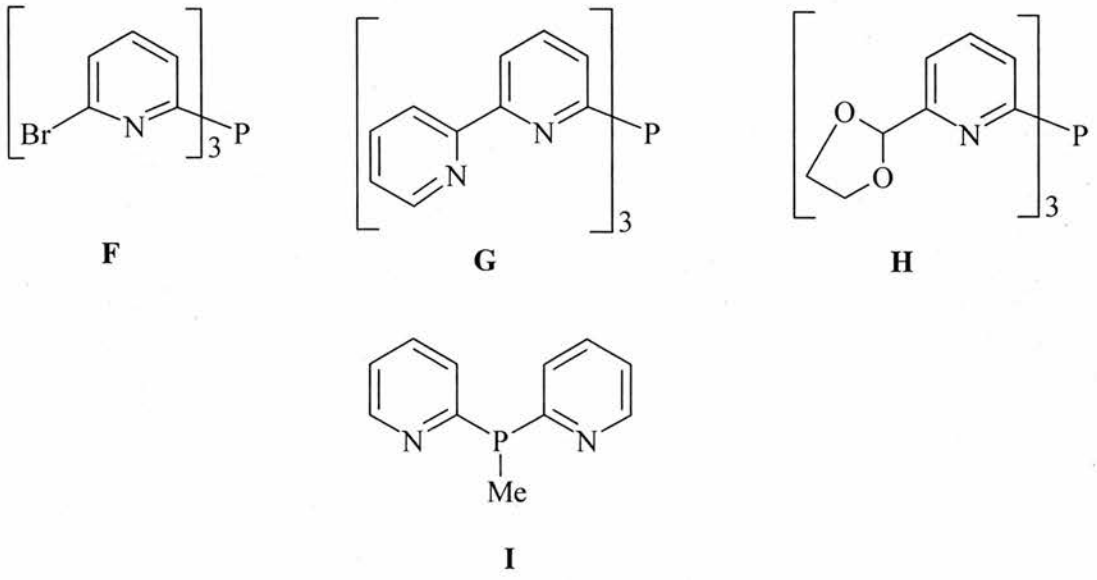

Figure 1.2. Phosphines prepared by reaction of pyridyllithium species with PCl_3 or $MePCl_2$.

Direct nucleophilic substitution on halopyridines by metal phosphides was reported in 1965[18] when 9-chloroacridine was treated with $KP(C_6H_5)_2$ in dioxane to yield 9-diphenylphosphinoacridine. However, unsubstituted acridine, when treated with $LiP(C_6H_5)_2$ yielded the dihydro derivative. This procedure has since been extended to prepare numerous phosphines substituted pyridines along with their α-phosphinomethyl derivatives and this work has resulted in a wide range of phosphorus nitrogen donor ligands that have the potential to be poly-dentate.

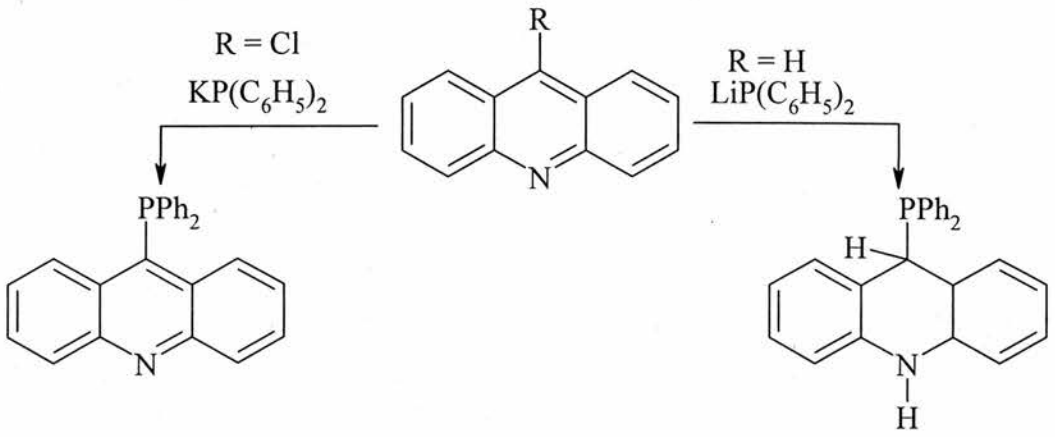

Scheme 1.3. Reactions of acridine.

1.5 *Phosphinoalkene Ligands.*

Another class of ligand that has been studied for use as a hemilabile ligand is one that contains an olefinic moiety. Many researchers have investigated this area of coordination chemistry in recent years and in early work the olefinic fragment was used as a stabilising group with strongly bonding phosphine ligands and this enabled the study of transition metal complexes containing olefins[19, 20]. More recently the study of phosphine-alkene ligands has focused on the weakly ligating nature of the alkene. The hemilabile nature of these ligands has been investigated in a similar way to the phosphine-amine and pyridyl-phosphine ligands described previously by reaction of their complexes with small molecules. One example of this was shown by Brookes[21] who displaced the olefinic groups of a rhodium complex with a tetraphenylborate anion to yield a piano stool effect metal complex.

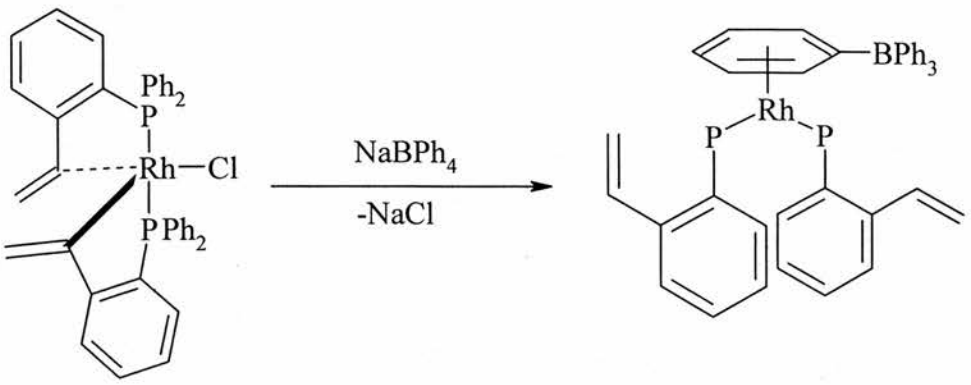

Scheme 1.4. Reaction showing the displacement of η^2-alkenes.

A further example of phosphine-alkene ligand complexes was demonstrated by Lindner *et al*[22] who studied phopshinoalkylfuran ligands. They showed that the furan ring could ligate to metal centres in a η^1- fashion through the oxygen atom or by a η^2-fashion through the C-C double bonds. The most favoured coordination mode of these type of phosphine-alkene ligands was shown to be the η^2-fashion as the partial donation of the lone pair from the oxygen makes the η^1-fashion coordination less favourable due to the oxygen being a poorer σ-donor than the olefinic groups. Diphenylvinylphosphine (DPVP) was shown by the Barthel-Rosa research group to be a hemilabile ligand when coordiniated to ruthenium (II) centres[23, 24]. They determined that the η^3-DPVP-ruthenium (II) complex could react both reversibly and irreversible depending on the small molecule that was used in the reaction. A reversible reaction was observed when acetonitrile was used however, in the presence of CO the reaction was found to be irreversible but in both instances the DPVP ligand underwent a η^3- to η^1- shift that opened up a coordination site on the metal centre.

Dynamic ligand exchange processes have also been studied due to the labile nature of the alkene group in phosphorus-alkene complexes.

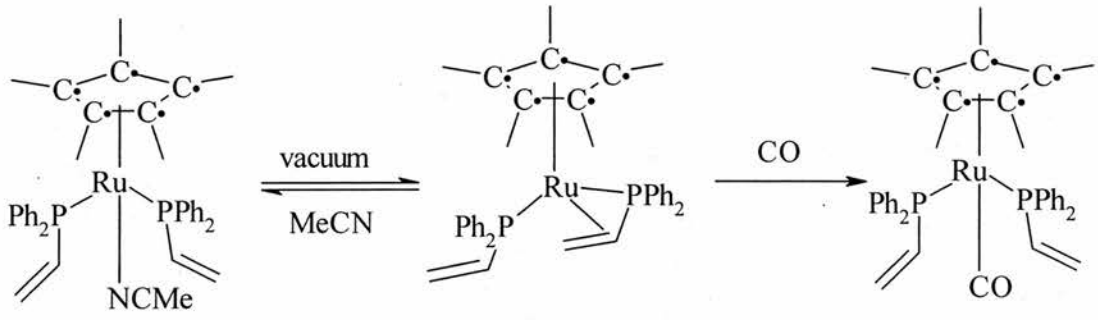

Scheme 1.5. Reaction showing the labile properties of alkene groups.

Garrou and Hartwell[25] observed one example of this type of exchange process that saw the rapid exchange of the olefinic groups of a platinum complex by ^{31}P NMR spectroscopy.

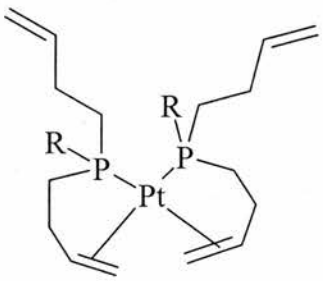

Figure 1.3. Platinum complex used to observe rapid ligand exchange of alkenes.

Despite many phosphino-alkene ligands displaying hemilabile properties there are also many phosphine-alkene ligands that have not shown any[26-45].

π-bonded and σ-bonded alkene groups in organometallic complexes have been shown to react with small molecules such as phosphines[46] and carbon monoxide[47, 48] to displace the hemilabile alkene moiety. Greco *et al*[46] reacted

fluoro-alkenes with (π-allyl)tricarbonyl cobalt complexes and isolated complexes containing hemilabile carbon-alkene ligands. These complexes were then reacted with PPh_3 to show that the alkene moiety was in fact hemilabile and this displacement was further confirmed by NMR and IR spectroscopy. Greco *et al*[46] also showed that heating the unchelated complex vigorously in xylene causes one of the carbon monoxide groups to dissociate and allow the alkene moiety to associate again.

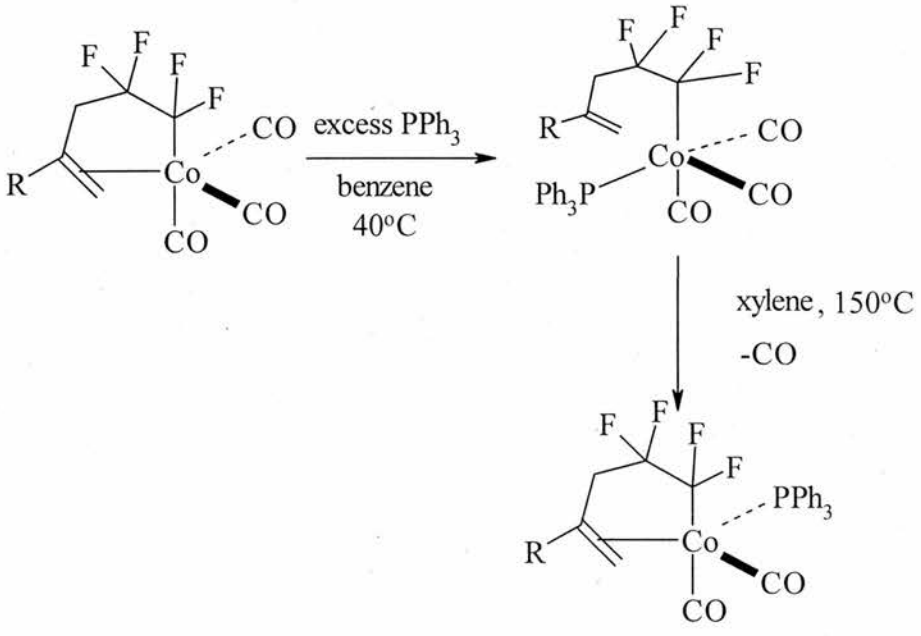

Scheme 1.6. Reaction showing hemilabile properties of alkenes.

The above examples provide a flavour of the opportunities and complexity of hemilabile ligands. In this project we undertook to develop the synthesis of a range of this class of ligands and conduct some preliminary studies on their coordination chemistry.

1.6 *An Introduction into NMR.*

Throughout this work the use of NMR proved very useful in the determination of the structure and composition of the compounds made. The main NMR handles used throughout this work were ^{31}P and ^{1}H NMR.

NMR nuclei occur in varying abundances naturally. ^{31}P has a natural abundance of 100 %, which gives a singlet on the NMR spectrum when no other NMR active species are present (excepting hydrogen which can be decoupled). Due to the high abundance of ^{31}P these spectra are quickly accumulated and can therefore, give a quick spectrum to interpret. ^{1}H occurs in 99.99 % abundance and is used to give the differing environments of the protons within the compound. Other NMR active nuclei that have been observed within this work are ^{195}Pt, which has an abundance of 33.8 % and in the presence of other NMR active nuclei satellites are observed with the pattern 1:4:1. Table 1.1 shows some typical coupling constants for ^{195}Pt-^{31}P reported by Pregosin *et* al[49]

Table 1.1. Typical $^{1}J\{^{195}Pt$-$^{31}P\}$ couplings for simple platinum complexes are shown below.

R	X	*Trans*$PtX_2(PR_3)_2$
Bu	Cl	2400
Bu	Br	2327
Et	Cl	2400
O-o-tol	Cl	4405
Bu	I	2265

Another nucleus used was ^{103}Rh, which has a natural abundance of 100 % with a spin of ½. When present in a compound containing other NMR active

nuclei the pattern observed is a doublet of equal heights. The final NMR active nucleus studied in this work was ^{77}Se and has a natural abundance of only 7.63 %.

Table 1.2. Typical $^{1}J\{X\text{-}^{31}P\}$ couplings for simple complexes of rhodium and selenium are shown below (X = Rh, Se).

Compound	Coupling	Magnitude/Hz
trans-$RhCl(CO)(PBu_3)_2$	$^{1}J\{^{103}Rh\text{-}^{31}P\}$	116
fac-$RhCl_3(PEt_3)_3$	$^{1}J\{^{103}Rh\text{-}^{31}P\}$	114
$R_3P{=}Se$	$^{1}J\{^{77}Se\text{-}^{31}P\}$	ca 750

1.7 *An Introduction into IR.*

Infrared (IR) is a technique that uses molecular vibrations. The usual range used for IR spectra is between 4000cm^{-1} and 625 cm^{-1}. There are two types of vibration observed within IR and these are known as stretching and bending vibrations. Stretching vibrations fall into two categories, symmetric and asymmetric stretches whilst bending vibrations can be categorised as bending or scissoring, rocking, twisting and wagging. Figure 1.4 shows how these vibrations can be shown.

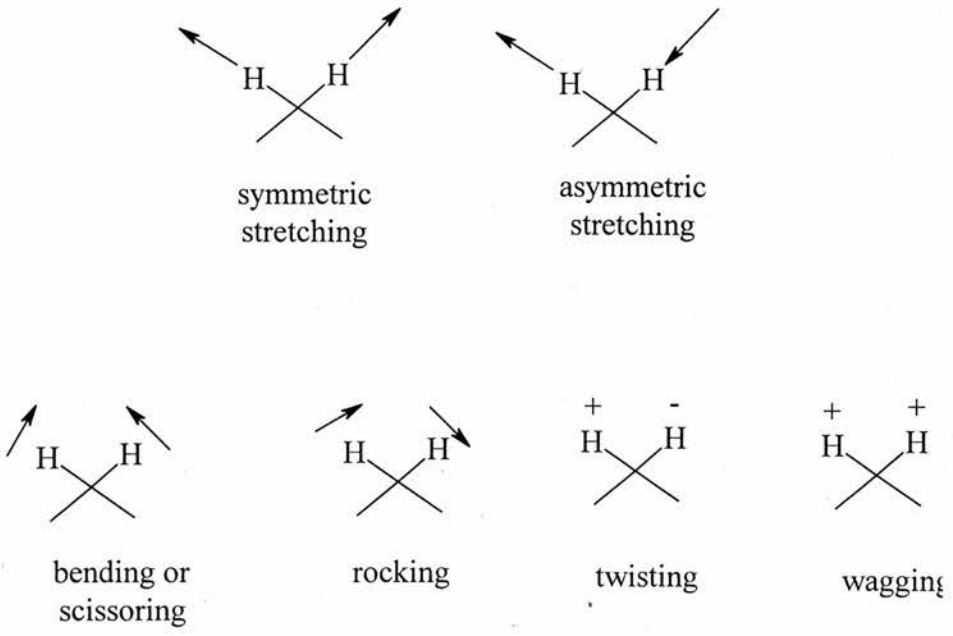

Figure 1.4. Stretching and bending vibrations observed in IR.

Different functional groups vibrate in different regions of the IR spectrum and these regions are used when new complexes are prepared as a basis for determining the structure. This can be seen when assigning ν_{CN}, for example, which moves when bound to a metal centre from its original position. However, the use of IR as a tool for the assignation of structure should only be a guide as in some regions, in particular the fingerprint region, a lot of vibrations occur and interpretation can sometimes prove difficult. Tables of characteristic group frequencies are available and Fleming and Williams[50] show these characteristic frequencies of functional groups typically observed in organic chemistry.

1.8 *An Introduction into the metal complexes used.*

The metal complexes used in this work were chosen because they are easily prepared, from well-documented procedures, purified and characterised. Their chemistry has been studied thoroughly and many useful comparisons can be made in this work from these studies. Many of these characteristics have been discussed previously in this chapter. They were also chosen for their

characteristic NMR profiles when complexes are prepared with phosphorus containing ligands. The various Pt, Rh and P containing complexes all offer easy NMR handles to observe any changes brought about by addition of ligands. As an integral aspect of this is the values given by the various coupling constants that can be elucidated from the NMR spectra. Important observations about the geometry and coordination around the metals can be derived from these *J* values. Of particular interest is the interaction of the various allyl protons found in this work with these NMR active metal centres, the coupling shown in the ^{1}H NMR is perhaps the easiest way to definitively determine whether the ligand is chelating via the allyl group.

References.

1. C. S. Sloane; D. A. Weinberger; C. A. Mirkin, *Progress in Inorganic Chemistry*, 1999, **48**, 233.
2. J. C. Jeffrey; T. B. Rauchfuss, *Inorg. Chem.*, 1979, **18**, 2658.
3. F. G. Mann; H. R. Watson, *J. Chem. Soc.*, 1957, 3950.
4. H. Werner; M. Schultz; B. Windmůller, *Organometallics*, 1995, **14**, 3659.
5. S. Park; D. Hedden; D. M. Roundhill, *Organometallics*, 1986, **5**, 2151.
6. A. Del Zotto; A. Mezzetti; P. Rigo, *J. Chem. Soc. Dalton Trans.*, 1994, 2257.
7. L. Costella; A. Del Zotto; A. Mezzetti; E. Zangrando; P. Rigo, *J. Chem. Soc. Dalton Trans.*, 1993, 3001.
8. T. B. Rauchfuss; F. T. Patino; D. M. Roundhill, *Inorg. Chem.*, 1975, **14**, 652.
9. J. P. Farr; F. E. Wood; A. L. Balch, *Inorg. Chem.*, 1983, **22**, 3387.

10. K. Tani; M. Yabuta; S. Nakamura; T. Yamagata, *J. Chem. Soc. Dalton Trans.*, 1993, 2781.

11. A. Del Zotto; G. Nardin; P. Rigo, *J. Chem. Soc. Dalton Trans.*, 1995, 3343.

12. C. Woods; L. J. Tortorelli, *Polyhedron*, 1988, **7**, 1751.

13. F. E. Wood; J. Hvoslef; A. L. Balch, *J. Am. Chem. Soc.*, 1983, **105**, 6986.

14. A. L. Balch; L. A. Fossett; M. M. Olmstead, *Inorg. Chem.*, 1986, **25**, 4526.

15. G. R. Newkome, *Chem. Rev.*, 1993, **93**, 2067.

16. W. C. Davies; F. G. Mann, *J. Chem. Soc.*, 1944, 276.

17. F. G. Mann; J. Watson, *J. Org. Chem.*, 1948, **13**, 502.

18. K. Issleib; L. Brusehaber, *Z. Naturfosch.*, 1965, **20b**, 181.

19. L. V. Interrante; M. A. Bennet; R. S. Nyholm, *Inorg. Chem.*, 1966, **5**, 2212.

20. M. A. Bennet; L. V. Interrante; R. S. Nyholm, *Z. Naturforsch., B: Anorg. Chem. Org. Chem.*, 1965, **20**, 633.

21. P. R, Brookes, *J. Organomet. Chem.*, 1972, **42**, 415.

22. E. Lindner; C. Scheytt; P. Wegner, *J. Organomet. Chem.*, 1986, **308**, 311.

23. L. P. Barthel-Rosa; K. Maitra; J. Fischer; J. H. Nelson, *Organometallics*, 1997, **16**, 1714.

24. H. –L. Ji; J. H. Nelson; A. DeCian; J. Fischer; L. Solujic; E. B. Milosavljevic, *Organometallics*, 1992, **11**, 401.

25. M. A. Bennet; K. J. Cavell; K. Y. Chan, *Inorg. Chim. Acta*, 1989, **163**, 153.

26. G. R. Clark; C. M. Cochrane; P. W. Clark, *J. Organomet. Chem.*, 1982, **236**, 197.

27. P. W. Clark, *J. Organomet. Chem.*, 1976, **110**, C13.

28. P. E. Garrou; J. L. S. Curtis; G. E. Hartwell, *Inorg. Chem.*, 1976, **15**, 3094.

29. R. R. Ryan; R. Schaeffer; P. Clark; G. Hartwell, *Inorg. Chem.*, 1975, **14**, 3039.

30. P. W. Clark; G. E. Hartwell, *J. Organomet. Chem.*, 1975, **102**, 387.

31. P. W. Clark; G. E. Hartwell, *J. Organomet. Chem.*, 1975, **96**, 451.

32. P. E. Garrou; G. E. Hartwell, *J. Organomet. Chem.*, 1973, **55**, 331.

33. P. W. Clark; G. E. Hartwell, *Inorg. Chem.*, 1970, **9**, 1948.

34. K. D. Tau; D. W. Meek; T. Sorrell; J. A. Ibers, *Inorg. Chem.*, 1978, **17**, 3454.

35. P. R. Brookes, *J. Organomet. Chem.*, 1972, **42**, 459.

36. M. A. Bennett; L. L. Welling, *Polyhedron*, 1989, **8**, 2193.

37. M. A. Bennett; R. N. Johnson; I. B. Tomkins, *J. Organomet. Chem.*, 1976, **118**, 205.

38. M. A. Bennett; S. J. Gruber; E. J. Hann; R. S. Nyholm, *J. Organomet. Chem.*, 1971, **29**, c12.

39. M. A. Bennett; E. J. Hann, *J. Organomet. Chem.*, 1971, **29**, c15.

40. M. A. Bennett; G. B. Robertson; I. B. Tomkins; P. O. Whimp, *Chem. Commun.*, 1971, 341.

41. M. A. Bennett; R. S. Nyholm; J. D. Saxby, *J. Organomet. Chem.*, 1967, **10**, 301.

42. W. Hewertson; I. C. Taylor, *Chem. Commun.*, 1970, 428.

43. D. I. Hall; R. S. Nyholm, *Chem. Commun.*, 1970, 488.

44. L. V. Interrante; G. V. Nelson, *Inorg. Chem.*, 1968, **7**, 2059.

45. M. C. Browning; J. R. Mellor; D. J. Morgan; S. A. J. Pratt; L. E. Sutton; L. M. Venanzi, *J. Chem. Soc.*, 1962, 693.

46. A. Greco; M. Green; F. G. A. Stone, *J. Chem. Soc. (A)*, 1971, 3476.

47. G. Carturan; M. Graziani; U. Belluco, *J. Chem. Soc. (A)*, 1971, 2509.

48. G. Carturan; M. Graziani; R. Ros; U. Belluco, *J. Chem. Soc. Dalton Trans.*, 1972, 262.

49. P. S. Pregosin, *Coordination Chem. Rev.* 1982, **44**, 247.

50. D. H. Williams; I. Fleming, *Spectroscopic Methods in Organic Chemistry*, 1995.

CHAPTER 2.1: PREPARATION AND COORDINATION CHEMISTRY OF 2-(DIPHENYLPHOSPHINOHYDRAZINO)PYRIDINE ($Ph_2PNHNHpy$).

2.1.1 *Introduction.*

Hemilabile phosphines are of interest in both homogenous catalysis and coordination chemistry[1]. Phosphorus- nitrogen containing ligands have particular use in catalysis where it is necessary for part of the ligand to dissociate to allow an organic fragment to coordinate and undergo transformation. The presence of P-N bidentate ligands enables many different and important catalytic processes to occur including asymmetric hydroboration[2], carbonylation of alkynes[3], Stille coupling[4] and asymmetric hydrogenation of highly substituted alkenes[5] to name a few. Some of these processes have had pyridyl phosphines such as 2-(diphenylphosphino)pyridine applied to them successfully[6]. The properties of this ligand have been extensively studied [1,6,7]. Together with related ligands containing organic spacer units which have been developed to increase the distance between the phosphorus and pyridyl nitrogen donor sites and these include $Ph_2PCH(R)py$ (where R=H[8-10], CH_2OEt[11,12], or PPh_2[13-17]) and $Ph_2PCH_2CH_2py$[18-26].

Relatively few examples of amino containing pyridylphosphine ligands are known despite the relative ease of formation of phosphorus-nitrogen bonds compared to phosphorus-carbon bonds. Examples include 2-(diphenylphosphinoamino)pyridine[27], 2-(phenylphosphino)bisaminopyridine[27] and 2-(trisaminopyridyl)phosphine[27]. Aucott *et al* have recently reported studies on 2-(diphenylphosphinoamino)pyridine[27] and demonstrated that it displays

three, possibly four different coordination modes. Katti *et al*[28,29] reported the inclusion of phosphorus donors within the hydrazine ligand to develop new ligand systems. These ligands possess either N-N-P-N-N or P-N-N-P backbones.

In this work we report the preparation of a new phosphine that has a hydrazine backbone and the potential to act as a hemilable ligand. Illustrative coordination complexes have been prepared.

Results and Discussion.

2.1.2 *Synthesis and chalcogen derivatives of $Ph_2PNHNHpy$*

Reaction of 2-hydrazinopyridine with one equivalent of Ph_2PCl in the presence of NEt_3, proceeds in thf to give **1** which was isolated (50 % yield) by filtration from the $Et_3NH^+Cl^-$ as a white crystalline solid upon recrystallisation from chloroform (Scheme 2.1.1).

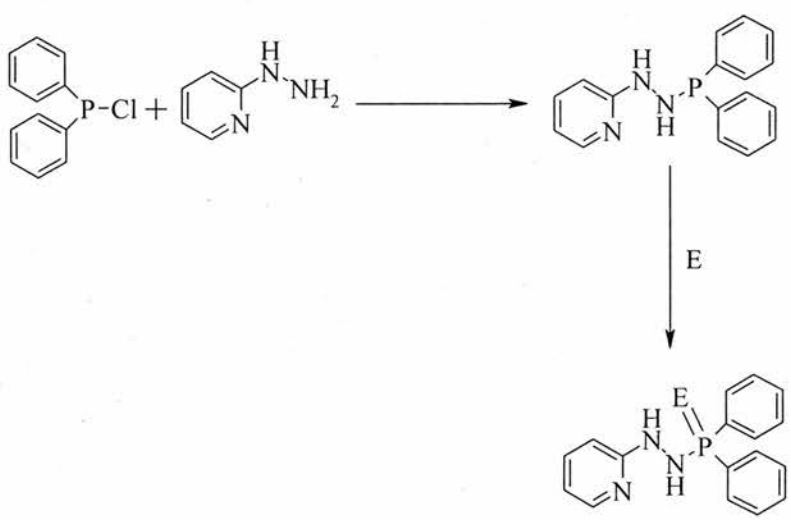

Scheme 2.1.1. Formation of $Ph_2NHNHpy$ and $Ph_2P(E)NHNHpy$ ligands {E=O (**2**), S (**3**), Se (**4**)}.

The $^{31}P\{^1H\}$ NMR spectrum of **1** consists of a singlet at δ_p 49.6 ppm. In the IR spectrum two bands are observed at 3313 and 3200 cm^{-1} which are assigned to the two ν_{NH} vibrations whilst the $\nu_{CN[py]}$ and ν_{PN} vibrations are observed at 1602 and 989 cm^{-1} respectively. The FAB mass spectrum gave the expected parent ion and fragmentation pattern and microanalysis gave satisfactory results. In the solid state structure (Figure 2.1.1) The N(14)-C(13)-N(2)-N(1) backbone of this ligand is almost planar, with the phosphorus being above this plane by 1.65 Å. **1** forms an infinite chain of hydrogen bonded dimer pairs in the solid state, *via* the interaction of the hydrazine N-H groups with the pyridyl N on adjacent molecules [N(14)---N(2A) separation 2.99 Å, the N(14)---H(2n) 1.89 Å, N(2)-H(2n)---N(14) 159.5°]. A second weaker hydrogen bond from the other N-H group links these dimers together to form infinite chains [N(14B)---N(1) 3.33 Å, N(14B)---H(1n) distance of 2.29 Å, N(1)-H(1n)---N(14B) of 153°] .

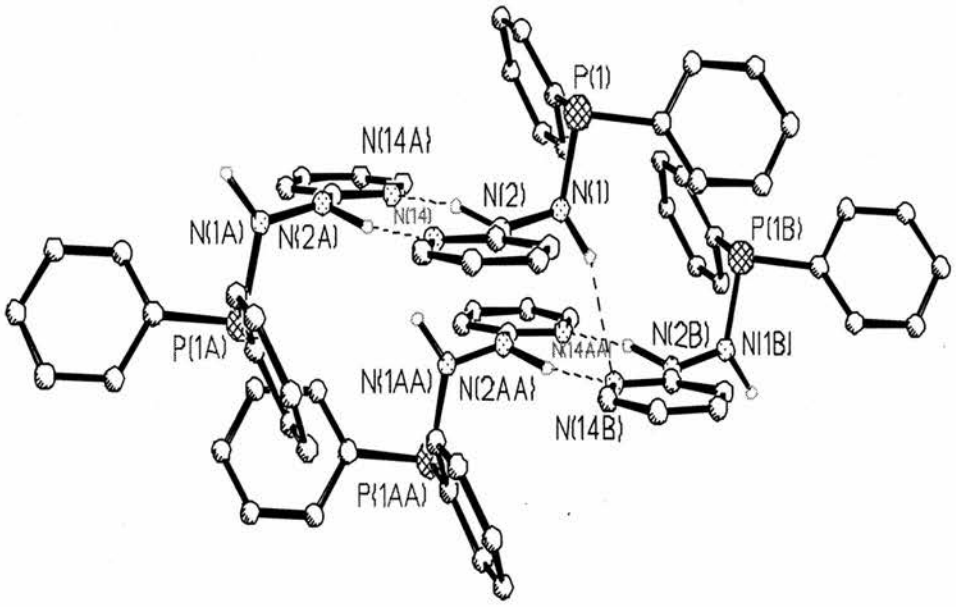

Figure.2.1.1. The X-ray structure of $Ph_2PNHNHpy$ (**1**).

The oxide (**2**) $Ph_2P(O)NHNHpy$ was easily prepared by the addition of excess aqueous hydrogen peroxide to **1** in thf whilst the sulfur (**3**) and seleno (**4**) analogues were prepared by the addition of elemental S or Se to the ligand in toluene. Satisfactory microanalyses were obtained for **3** and **4** though **2** proved difficult to purify completely [this may be due to overoxidation] and the EI^+ mass spectral data gave the expected parent ion and fragmentation patterns. $^{31}P\{^1H\}$ NMR show single resonances ($CDCl_3$) at δ_P 26.9 and 63.8 ppm for the oxide and the sulfide respectively. The selenide analogue exhibits a single $^{31}P\{^1H\}$ NMR resonance ($CDCl_3$) at δ_P 61.0 ppm with selenium satellites $^1J(^{31}P\text{-}^{77}Se)$ 768 Hz which is typical for a P=Se group. In the solid state the sulfur and selenide analogues are isomorphous; the Se compound **4** is reported since this behaved better crystallographically. The P-N bond in **4** is significantly shorter than that in **1** The N(14)-C(13)-N(2)-N(1) backbone is planar, and the phosphorus is not as far out of plane in **4** [1.18 Å] as is the case in **1**. The hydrogen-bonding motif observed here is considerably different to that of **1**. There are two types of H bond N-N…N and N-H…Se to give an infinite chain. [N(1)…N(14A) 2.94, H(1n)---N(14) 1.99 Å , N(1)-H(1n)---N(14) 163 °; N(2)…Se(1B) 3.75, H(2N)…Se(1B) 2.78 Å N(2)-H(2N) …Se(1B) 169 °]. (Figure 2.1.2).

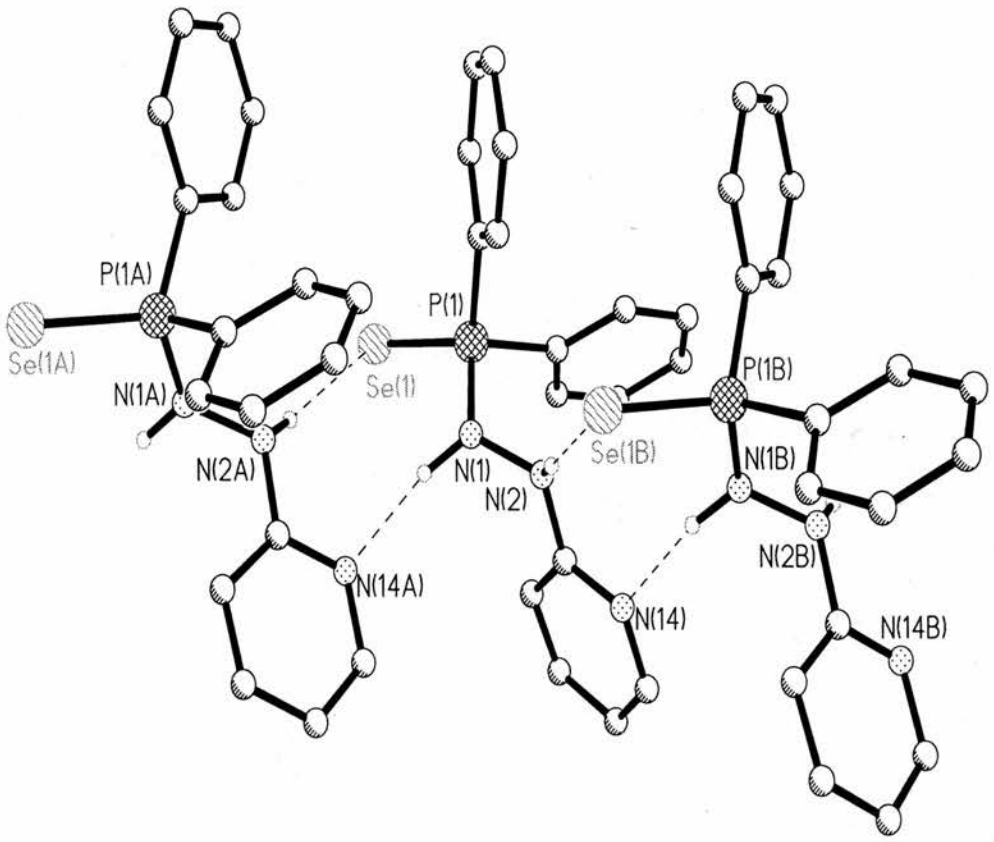

Figure. 2.1.2. The X-ray structure of $Ph_2P(Se)NHNHpy$ (**4**)

Table 2.1.1. Selected bond lengths (Å) and angles (°) for $Ph_2PNHNHpy$ and $Ph_2P(Se)NHNHpy$.

Selected bond lengths (Å) and angles (°)	*(1)*	*(4)*
P(1)-N(1)	1.709(7)	1.656(5)
Se(1)-P(1)	-	2.1145(15)
N(14)-C(13)	1.356(9)	1.332(7)
P(1)-C(7)	1.842(8)	1.797(5)
P(1)-C(1)	1.821(8)	1.814(6)
N(2)-C(13)	1.346(9)	1.390(7)
N(1)-N(2)	1.411(8)	1.410(6)
N(1)-P(1)-C(1)	98.5(4)	106.5(3)
C(1)-P(1)-C(7)	100.1(4)	105.4(3)
N(1)-N(2)-C(13)	118.9(7)	118.0(5)
N(2)-C(13)-C(18)	125.1(8)	122.7(5)
N(1)-P(1)-C(7)	104.5(4)	108.7(3)
P(1)-N(1)-N(2)	117.8(5)	120.7(4)
N(2)-C(13)-N(14)	113.7(7)	114.2(5)
N(14)-C(13)-C(18)	121.2(8)	123.2(6)
C(7)-P(1)-Se(1)	-	112.45(18)
N(1)-P(1)-Se(1)	-	109.18(18)
C(1)-P(1)-Se(1)	-	114.2(2)

2.1.3 *Coordination chemistry of $Ph_2PNHNHpy$.*

Reaction of $[PtCl_2(cod)]$ with $Ph_2PNHNHpy$ gives $[PtCl_2(Ph_2PNHNHpy)_2$-*P*$]$ **5** in good yield (72%), however, there was no evidence of *P,N* chelate formation..

The FAB mass spectrum of **5** contains the expected parent ion and fragmentation pattern and the complex displays a single resonance with platinum satellites in the $^{31}P\{^{1}H\}$ NMR spectrum (δ_p 44.0 ppm, $^{1}J\{^{31}P\text{-}^{195}Pt\}$ 3855 Hz), which indicates the presence of Cl^- *trans* to P. The IR spectrum has ν_{NH} at 3143 cm^{-1}, $\nu_{CN[py]}$ and ν_{PN} at 1600 and 997 cm^{-1} respectively and two ν_{PtCl} bands at 307 and 288 cm^{-1} which support the *cis* geometry.

Reaction of $[PtMe_2(cod)]$ with two equivalents of $Ph_2PNHNHpy$ gives $[PtMe_2(Ph_2PNHNHpy)_2\text{-}P]$ **6** (δ_p 71 ppm , $^{1}J\{^{31}P\text{-}^{195}Pt\}$ 1985 Hz). IR spectral analysis showed that the pyridyl N is not bound in this complex as $\nu_{CN[py]}$ is observed at 1598 cm^{-1}. $[PtMeCl(Ph_2PNHNHpy)_2\text{-}P]$ **7** was prepared in a similar manner (eqn 1). The complex was isolated by filtration in a yield of 40 % and its microanalyses gave satisfactory results for the bis(phosphine) species formed. The FAB mass spectrum contains M-Cl^- at 796 whilst $^{31}P\{^{1}H\}$ NMR spectroscopy revealed a single sharp resonance with platinum satellites, (δ_p 60.4 ppm, $^{1}J\{^{31}P\text{-}^{195}Pt\}$ 3183 Hz), indicating the two phosphorus atoms are *trans* to each other. The IR bands observed at 3251, 3224, 1600, 997 and 266 cm^{-1} represent ν_{NH}, ν_{NH}, $\nu_{CN[py]}$, ν_{PN} and ν_{PtCl} respectively.

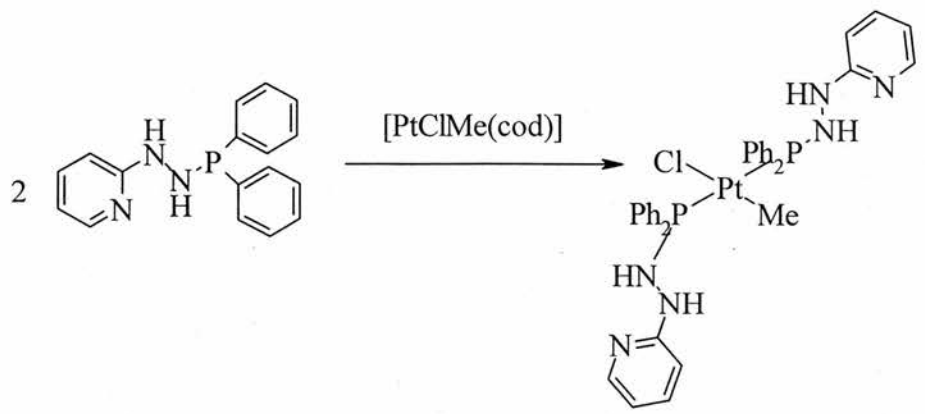

Scheme 2.1.2. Reaction of $Ph_2PNHNHpy$ with [PtClMe(cod)] (**7**).

The reaction of $Ph_2PNHNHpy$ with $[Pd(\mu\text{-}Cl)(\eta^3\text{-}C_3H_5)]_2$ gave the expected product $[PdCl(\eta^3\text{-}C_3H_5)(Ph_2PNHNHpy)\text{-}P]$ (**8**). The ^{31}P NMR ($CDCl_3$) showed a single broad peak at 66.4 ppm, indicating that the complex is fluxional. The IR spectrum was again useful in determining the coordination of the ligand around the Pd centre. The peak observed at 1601 cm^{-1} indicating the pyridyl N is not bound to the metal centre and the Pd-Cl stretch is observed at 280 cm^{-1}.

Upon slow addition of $[RhCl(cod)]_2$ to $Ph_2PNHNHpy$, $[Rh(cod)Cl(Ph_2PNHNHpy\text{-}P)]$ **9** was obtained in a yield of 68 %. Microanalysis gave only fairly satisfactory results though the ^{31}P $\{^1H\}$ NMR ($CDCl_3$) displayed the expected peak at δ_p 71.0 ppm with a coupling constant of $^1J\{^{31}P\text{-}^{103}Rh\}$ of 156 Hz. FAB mass spectral analysis gave the expected parent ion and fragmentation pattern and the IR spectrum showed bands at 3206, 996 and 250 cm^{-1} that are assigned as ν_{NH}, ν_{PN} and ν_{RhCl} vibrations respectively. The presence of the $\nu_{CN[py]}$ at 1597 cm^{-1} is indicative of a non-chelated complex. However, upon further analysis of the NMR and IR spectra we believe that the complex formed was fluxionally chelated due to the existence of broad peaks in

the $^{31}P\{^1H\}$ spectrum. Also in the IR spectrum there appeared to be a shoulder at 1610 cm^{-1} that also indicated that this complex was fluxionally chelated.

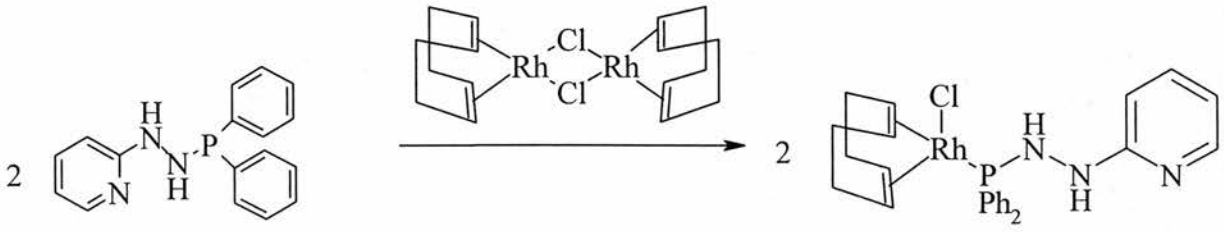

Scheme 2.1.3. Reaction of $Ph_2PNHNHpy$ with $[\{Rh(cod)Cl\}_2]$.(**9**)

Reaction of $[RuCl_2(\eta^3:\eta^3\text{-}C_{10}H_{16})]_2$ with $Ph_2PNHNHpy$ gives $[RuCl_2(\eta^3:\eta^3\text{-}C_{10}H_{16})(Ph_2PNHNHpy\text{-}P)]$ **10** in 42% yield. The IR spectrum showed characteristic bands of ν_{NH}, $\nu_{CN[py]}$ and ν_{PN} at 3279, 1596 and 984 cm^{-1} respectively with bands at 305 and 245 cm^{-1} corresponding to the presence of ν_{RuCl} vibrations. A single resonance was observed in the $^{31}P\{^1H\}$ NMR spectrum at δ_p 69.5 ppm. Microanalysis and FAB mass spectral data gave satisfactory results for the suggested structure. In the solid state the compound exhibits monodentate coordination, there is an intramolecular N-H…Cl H-bond [N(1)…Cl(1) 3.75 , H(1N)…Cl(1) 2.99 Å N-H…Cl 135°] (Figure 2.1.3).

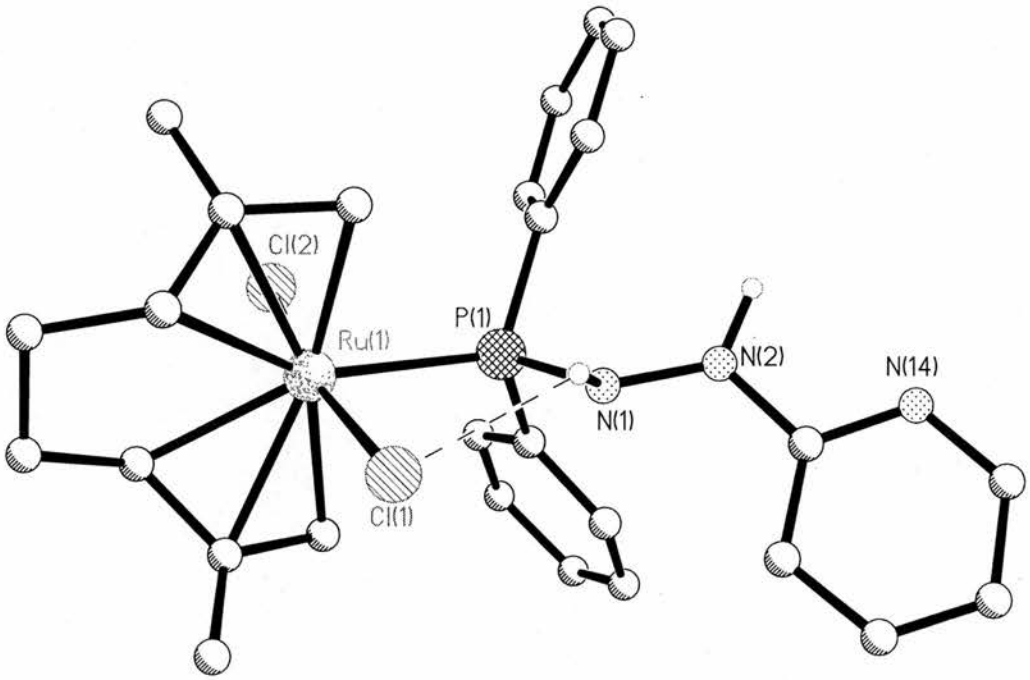

Figure. 2.1.3. The X-ray structure of [$RuCl_2(\eta^3:\eta^3$-$C_{10}H_{16})Ph_2PNHNHpy$-*P*] (**10**).

We also prepared [$IrCp^*Cl_2(Ph_2PNHNHpy$-*P*] **12**. In the solid state the X-ray structure contains two independent molecules [the second molecule is numbered by addition of 30 to all atom labels]. The bond lengths and the hydrogen bonding is the same for each independent molecule. Both display a intramolecular H ..Cl [N(1)…Cl(1) 3.15 , H(1N)…Cl(1) 2.64 Å N-H…Cl 112°] and intermolecular NH..N to form dimer pairs [N(2)…N(14A) 3.09, H(2N)…N(14A) 2.11 Å N(2)-H(2N) …N(14A) 179°] (Figure. 2.1.4).

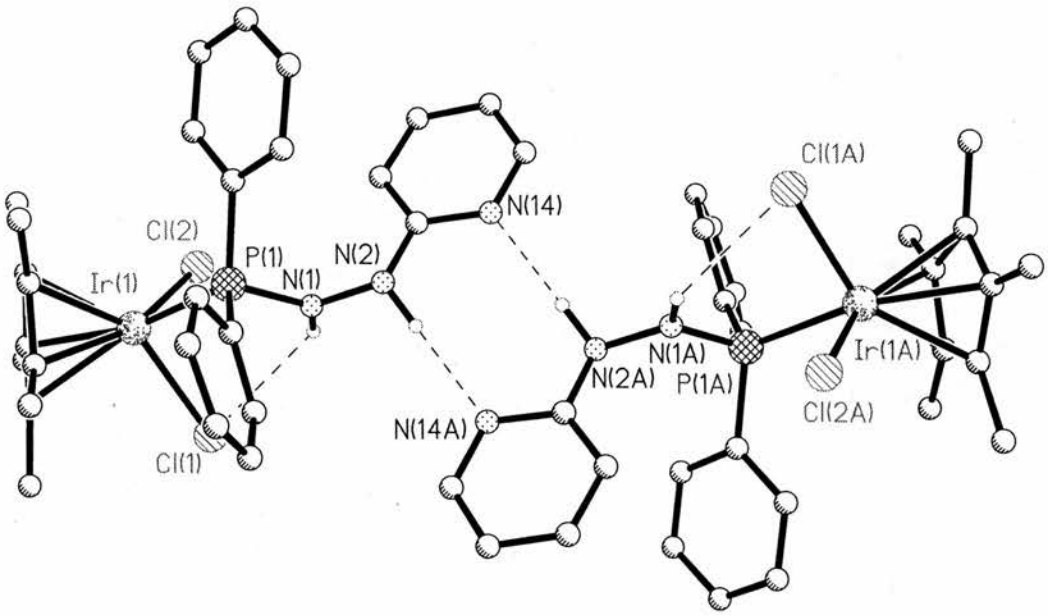

Figure. 2.1.4. The X-ray structure of [IrCp*Cl_2(Ph_2PNHNHpy *P*)] (**12**).

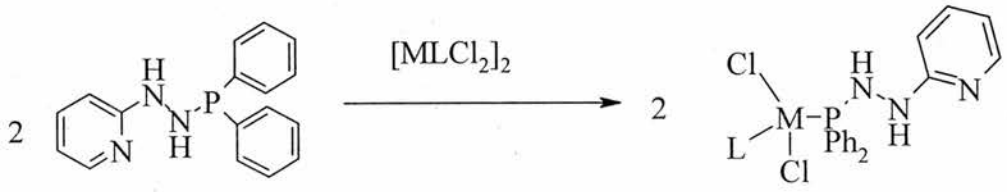

M = Ru (**11**), L = η^3:η^3-$C_{10}H_{16}$; Ir (**12**), L = η^5-C_5Me_5

Scheme 2.1.4. Reaction of Ph_2PNHNHpy with [{$MLCl_2$}$_2$].

Table 2.1.2. Selected bond length (Å) and angles (°) for [$RuCl_2(\eta^3:\eta^3$-$C_{10}H_{16}$)($Ph_2PNHNHpy$-*P*)] and [$IrCp^*Cl_2(Ph_2PNHNHpy$-*P*)].

Selected bond lengths (Å) and angles (°)	*(10)*	*(12)*
M(1)-Cl(1)	2.458(3)	2.4009(15)
M(1)-Cl(2)	2.422(3)	2.4284(14)
M(1)-P(1)	2.432(3)	2.2928(13)
Average M(1)-C(L)	2.25	2.19
P(1)-N(1)	1.698(8)	1.660(4)
N(14)-C(13)	1.352(13)	1.355(6)
N(2)-C(13)	1.379(14)	1.362(7)
N(1)-N(2)	1.406(11)	1.404(5)
P(1)-M(1)-Cl(2)	80.71(10)	88.48(5)
Cl(1)-M(1)-Cl(2)	170.07(11)	88.43(5)
N(1)-P(1)-M(1)	108.3(4)	108.27(16)
N(2)-N(1)-P(1)	119.2(8)	122.4(3)
N(14)-C(13)-N(2)	113.3(11)	113.6(5)
C(13)-N(2)-N(1)	118.2(10)	118.9(5)
Cl(1)-M(1)-P(1)	82.40(8)	88.71(5)

$[Cu(MeCN)_4][PF_6]$ formed the bis-chelate complex $[Cu(Ph_2PNHNHpy)_2][PF_6]$ **13** in good yield (71 %), isolated as a cream coloured solid. No NMR data observed for this complex since it is diamagnetic. Microanalysis and FAB mass spectral determination gave the expected results for the presence of the bis-chelate complex and this was subsequently confirmed by the existence of the $\nu_{CN[py]}$ vibration at 1614 cm^{-1} in the IR spectrum.

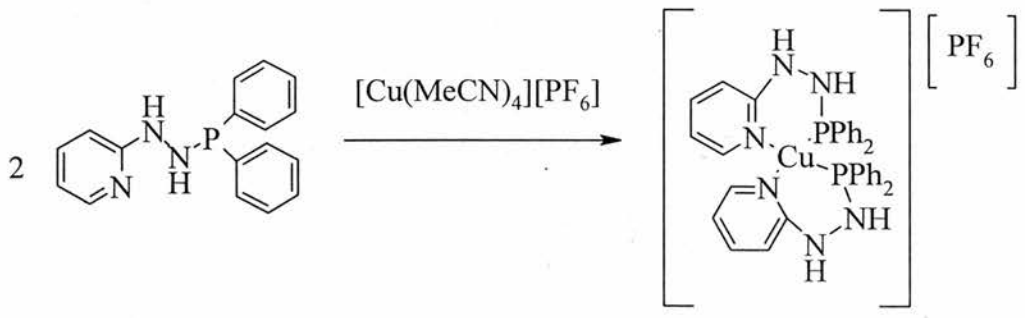

Scheme 2.1.5. Reaction of $Ph_2PNHNHpy$ with $[Cu(MeCN)_4][PF_6]$ (**13**).

2.1.4 *Crystallography*

X-ray diffraction studies were performed at 293 K using a Rigaku AFC7S with Cu-K_α radiation [compound **1**] or a Bruker SMART diffractometer with graphite-monochromated Mo-K_α radiation. The structures were solved by direct methods, non-hydrogen atoms were refined with anisotropic displacement parameters; hydrogen atoms bound to carbon were idealised, the NH protons were located by a *F* map. Structural refinements were by the full-matrix least-squares method on *F* [compound **1,** TeXsan[31]] or F^2 using SHELXTL.[32] Details of the data collections are summarised in Appendix 2.

2.1.5 *Coordination chemistry of $Ph_2P(S)NHNHpy$ (3).*

Similar reactions to those described above can be performed using $Ph_2P(S)NHNHpy$. Reaction with $[Rh(cod)Cl]_2$ in toluene formed $[Rh(cod)(Ph_2P(S)NHNHpy\text{-}S,N)][Cl]$ **14** in good yield (79 %). Analysis by FAB mass spectrometry gave the parent ion at $M\text{-}Cl^-$ =536 and microanalysis gave satisfactory results. The presence of υ_{NH}, $\upsilon_{CN[py]}$, υ_{PN} and υ_{PS} vibrations in the IR spectrum were observed at 3163, 1611, 998 and 640 cm^{-1} respectively. A single NMR resonance in $CDCl_3$ was observed in the $^{31}P\{^1H\}$ spectrum at δ_p 64.3 ppm. The existence of the $\upsilon_{CN[py]}$ vibration at 1611 cm^{-1} indicated that the complex formed is a chelate with the Cl acting as a counter ion.

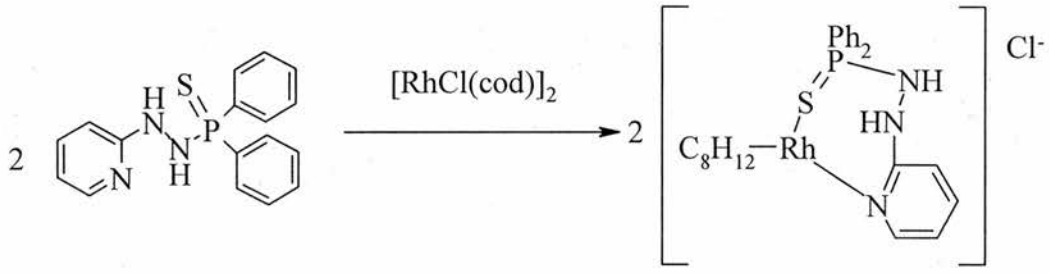

Scheme 2.1.6. Reaction of $Ph_2P(S)NHNHpy$ with $[\{Rh(\mu\text{-}Cl)(cod)\}_2]$.(**14**)

The reaction of $Ph_2P(S)NHNHpy$ with $[RuCl_2(p\text{-}Cy)]_2$ [Cy = cymene] proceeded in good yield (80 %) to give the chelate complex $[Ru(p\text{-}Cy)(Ph_2P(S)NHNHpy\text{-}S,N)][Cl_2]$ **15**. FAB mass spectral analysis gave the expected fragmentation pattern and parent ion at $M\text{-}Cl_2$ =559. Elemental analysis of this complex gave satisfactory results and the $^{31}P\{^1H\}$ NMR spectrum showed a single resonance at δ_p 81.1 ppm. Analysis by IR indicated the presence of vibrations at 3448, 3178, 1611, 995 and 635 cm^{-1} which

correspond to υ_{NH}, υ_{NH}, $\upsilon_{CN[py]}$, υ_{PN} and υ_{PS} respectively. The absence of any υ_{RuCl} vibrations in the IR spectrum indicated that the complex formed was a chelate and this was further confirmed by the presence of $\upsilon_{CN[py]}$ at 1611 cm^{-1}.

$[Cu(MeCN)_4][PF_6]$ reacts with $Ph_2P(S)NHNHpy$ similarly to $Ph_2PNHNHpy$ to form the bis-chelate complex $[Cu(Ph_2P(S)NHNHpy\text{-}S,N)][PF_6]$ **16**, in good yield (77 %). Analysis by $^{31}P\{^1H\}$ NMR gave a single broad resonance at δ_p 65.9 ppm. Elemental analysis confirmed the suggested bis-chelate structure, as did FAB mass spectral analysis with the parent ion occurring at M-PF_6 =713. The IR spectrum also confirmed the presence of the bischelate structure with existence of $\nu_{CN[py]}$ vibrations at 1611 cm^{-1}. Other vibrations present in the IR spectrum include ν_{NH}, ν_{PN} and ν_{PS} at 3262, 997 and 622 cm^{-1} respectively.

2.1.6 *Use of $\nu_{CN[py]}$ to determine binding mode.*

This chapter used the $\nu_{CN[py]}$ as a tool to determine the binding of the ligand to the metal centre. In the complexes where the pyridyl nitrogen has chelated to the metal centre the value of $\nu_{CN[py]}$ has shifted to lower frequency from 1602 cm^{-1} in free pyridine. Aucott *et al* [27] and Clarke *et al*[30] gave examples of this type of coordination.

Table 2.1.3. Characterisation data for $Ph_2PNHNHpy$ and its derivatives. ([a] $^1J\{^{31}P\text{-}^{77}Se\}$ 768 Hz.). ([b] $^1J\{^{31}P\text{-}^{195}Pt\}$ 3855 Hz), ([c] $^1J\{^{31}P\text{-}^{195}Pt\}$ 1984 Hz), ([d] $^1J\{^{31}P\text{-}^{195}Pt\}$ 3183 Hz), ([e] $^1J\{^{31}P\text{-}^{103}Rh\}$ 156 Hz)

Compound	*$^{31}P\text{-}\{^1H\}$ NMR*	*IR/cm^{-1}*					*Microanalysis/ % Found (calc.)*		
	δ_p/ppm	ν_{PN}	ν_{NH}	ν_{NH}	$\nu_{CN[py}$	ν_{MCl}	C	H	N
$Ph_2PNHNHpy$ (1)	49.6	989	3313	3200	1602	-	69.09	5.29	14.01
							(69.60)	(5.50)	(14.33)
$Ph_2P(O)NHNHpy$ (2)	26.9	997	3344	3076	1595	1312	64.64	4.42	11.83
							(66.01)	(5.21)	(13.59)
$Ph_2P(S)NHNHpy$ (3)	63.8	991	3276	3090	1602	648	62.91	4.67	13.12
							(62.75)	(4.96)	(12.92)
$Ph_2P(Se)NHNHpy$ (4)[a]	61.0[a]	992	3255	3076	1601	587	55.16	4.18	10.98
							(54.85)	(4.33)	(11.29)

Table continued

$[PtCl_2(Ph_2PNHNHpy\text{-}P)_2]$ (5)	44.0[b]	997	-	3143	1600	307, 288	48.30 (47.90)	3.15 (3.78)	9.88 (9.86)
$[PtMe_2(Ph_2PNHNHpy\text{-}P)_2]$ (6)	71.2[c]	985	3341	3051	1598	-	53.66 (53.27)	5.29 (4.72)	9.90 (10.35)
$[PtClMe(Ph_2PNHNHpy\text{-}P)_2]$ (7)	60.4[d]	997	3251	3224	1600	266	51.61 (50.52)	3.87 (4.24)	10.17 (10.10)
$[PdCl(\eta^3\text{-}(C_3H_5)(Ph_2PNHNHpy\text{-}P)]$ (8)	66.4	997	3202	3051	1601	285	50.28 (50.44)	4.37 (4.44)	8.28 (8.82)
$[Rh(C_8H_{12})Cl(Ph_2PNHNHpy\text{-}P)]$ (9)	71.0[e]	996	3206	-	1597	250	52.51 (55.65)	4.57 (5.23)	7.90 (7.79)
$[RuCl_2(\eta^3:\eta^3\text{-}C_{10}H_{16})(Ph_2PNHNHpy\text{-}P)]$ (10)	69.5	984	3279	-	1596	305, 245	54.51 (53.90)	5.42 (5.37)	6.98 (6.99)
$[RuCl_2(\eta^6\text{-}p\text{-}MeC_6H_4{}^iPr)(Ph_2PNHNHpy\text{-}P)]$ (11)	72.7	987	3332	3296	1597	294	54.17 (54.08)	4.21 (5.05)	6.96 (7.01)

Table continued									
[Ir(η^5-C_5Me_5)Cl_2(Ph_2PNHNHpy-P)] (12)	45.0	987	3318	3057	1598	285	46.60	4.45	5.74
							(46.75)	(4.80)	(6.06)
[Cu(Ph_2PNHNHpy-P,N)$_2$][PF_6] (13)	-	999	3291	-	1614	-	51.04	4.05	10.86
							(51.36)	(4.06)	(10.57)
[Rh(C_8H_{12})(Ph_2P(S)NHNHpy-S,N)][Cl] (14)	64.3	998	-	3168	1611	640	53.08	4.73	7.28
							(52.50)	(4.93)	(7.35)
[Ru(η^6-*p*-$MeC_6H_4{}^iPr$)(Ph_2P(S)NHNHpy-S,N][Cl_2] (15)	81.1	995	3448	3178	1611	635	50.88	4.41	6.46
							(51.34)	(4.79)	(6.66)
[Cu(Ph_2P(S)NHNHpy-S,N][PF_6] (16)	65.9	997	-	3262	1611	622	47.30	3.66	9.70
							(47.55)	(3.76)	(9.79)

Experimental

General

General experimental conditions and instruments were as set out on page xvii. Unless otherwise stated, all reactions were carried out under an oxygen-free nitrogen atmosphere using standard Schlenk techniques. Diethyl ether and thf were purified by reflux over sodium-benzophenone and distillation under nitrogen. Dichloromethane was heated to reflux over calcium hydride and distilled under nitrogen. Toluene and hexane were heated to reflux over sodium and distilled under nitrogen. The complexes $[MCl_2(cod)]$ (M = Pt or Pd; cod = cycloocta-1,5-diene)[33, 34], $[PtMeX(cod)]$ (X = Cl or Me)[35], $[Pd(\mu\text{-}Cl)(\eta^3\text{-}C_3H_5)]_2$[36], $[\{Rh(\mu\text{-}Cl)(cod)\}_2]$[37], $[\{RuCl_2(\eta^3{:}\eta^3\text{-}C_{10}H_{16})\}_2]$[38], $[\{RuCl(\mu\text{-}Cl)(\eta^6\text{-}p\text{-}MeC_6H_4{}^iPr)_2\}]$[39], $[\{IrCl(\mu\text{-}Cl)(\eta^5\text{-}C_5Me_5)\}_2]$[40], $[Cu(MeCN)_4][PF_6]$[41] and $Ph_2PNHNHpy$ **1** was prepared as described previously[30]. Infra-red spectra were recorded as KBr discs in the range 4000-200 cm^{-1} on a Perkin-Elmer 2000 FTIR/RAMAN spectrometer. NMR spectra were recorded on a Gemini 2000 spectrometer (operating at 121.4 MHz for ^{31}P and 300 MHz for ^1H). Microanalyses were performed by the St. Andrews University service and mass spectra by the Swansea Mass Spectrometer Service.

$Ph_2P(O)NHNHpy$ (2): $Ph_2PNHNHpy$ (300 mg, 1 mmol) was dissolved in THF (20 cm^3). H_2O_2 (35 mg, 1 mmol) was added dropwise over 5 minutes to give a colourless solution. The reaction mixture was stirred at room temperature for one hour before removing all the solvent on the vacuum line. The solid formed was dissolved in CH_2Cl_2 before reducing the volume to 0.5 cm^3 on the vacuum line. Diethyl ether (2 cm^3) was added to precipitate the product, which was

isolated by filtration. Yield 203 mg, 64 %. Microanalysis: Found (calculated for $C_{17}H_{16}N_3OP$) C 64.64 (66.01), H 4.42 (5.21), N 11.83 (13.59). δ_p ($CDCl_3$) 26.9 ppm. δ_H ($CDCl_3$) 8.1 (m, 5 H, aromatic), 7.2-7.7 (m, 9 H, aromatic), 6.7 (m, 1 H, NH), 6.1 (d, 1 H, $^1J\{^1H\text{-}^1H\}$ 21 Hz, NH). IR (KBr) cm^{-1} υ_{NH} 3344, υ_{NH} 3076, $\upsilon_{CN[py]}$ 1595, υ_{PO} 1312, υ_{PN} 997. Mass spec (EI^+): 309(M^+).

$Ph_2P(S)NHNHpy$ (3): Elemental sulfur (219 mg, 0.7 mmol) and $Ph_2PNHNHpy$ (2 g, 0.7 mmol) were dissolved together under nitrogen in dry toluene (18 cm^3). The reaction mixture was sonicated to ensure that the entire solid was dissolved before heating with a heat gun. The reaction mixture was left to cool overnight with stirring, which precipitated out a solid that was isolated by filtration. Yield 1.9 g, 85 %. Microanalysis: Found (calculated for $C_{17}H_{16}N_3PS$) C 62.91 (62.75), H 4.67 (4.96), N 13.12 (12.92). δ_p ($CDCl_3$) 63.8 ppm. δ_H ($CDCl_3$) 7.9-8.1 (m, 4 H, aromatic), 7.4-7.55 (m, 8 H, aromatic), 6.8 (d, 1 H, aromatic), 6.65 (t, 1 H, aromatic), 6.4 (br. s, 1 H, NH[py]), 5.0 (d, 1 H, $^2J\{^{31}P\text{-}^1H\}$ 19 Hz, NH[P]). IR (KBr) cm^{-1} υ_{NH} 3276, υ_{NH} 3090, $\upsilon_{CN[py]}$ 1602, υ_{PN} 991, υ_{PS} 648. Mass spec (NOBA Marix): 348(M+Na), 325(M^+).

$Ph_2P(Se)NHNHpy$ (4): Elemental selenium (40 mg, 0.5 mmol) and $Ph_2PNHNHpy$ (150 mg, 0.5 mmol) were dissolved together under nitrogen in dry toluene (10 cm^3). The reaction mixture was heated for four hours, and then most of the solvent was removed under reduced pressure. The remaining mixture was placed in the fridge overnight and a white powder precipitated from the solution, which was isolated by filtration. Yield 119 mg, 63 %. Microanalysis: Found (calculated for $C_{17}H_{16}N_3PSe$) C 55.16 (54.85), H 4.18 (4.33), N 10.98 (11.29). δ_p ($CDCl_3$) 61 ppm $^1J\{^{31}P\text{-}^{77}Se\}$ 768 Hz. δ_H 7.9-8.1 (m, 4 H, aromatic), 7.4-7.5

(m, 8 H, aromatic), 6.8 (d, 1 H, aromatic), 6.65 (t, 1 H, aromatic), 6.5 (br. s, 1 H, NH[py]), 5.0 (d, 1 H, $^2J\{^{31}P\text{-}^1H\}$ 19 Hz, NH[P]). IR (KBr) cm^{-1} υ_{NH} 3255, υ_{NH} 3076, $\upsilon_{CN[py]}$ 1601, υ_{PN} 992, υ_{PSe} 587. Mass spec (EI^+): 373(M^+).

[$PtCl_2(Ph_2PNHNHpy)_2$-*P*] (5): A CH_2Cl_2 (5 cm^3) solution of [Pt(cod)Cl_2] (64 mg, 0.1 mmol) was added dropwise to a CH_2Cl_2 (5 cm^3) solution of $Ph_2PNHNHpy$ (100 mg, 0.3 mmol). The resulting solution was stirred for a few hours before, the white solid that formed on stirring, being isolated by filtration. Yield 104 mg, 72 %. Microanalysis: Found (calculated for $C_{34}H_{32}N_6P_2Cl_2Pt$) C 48.30 (47.90), H 3.15 (3.78), N 9.88 (9.86). δ_p ($CDCl_3$) 44.0 ppm $^1J\{^{31}P\text{-}^{195}Pt\}$ 3855Hz. δ_H ($CDCl_3$) 7.9-8.1 (m, 8 H, aromatic), 7.4-7.55 (m, 16 H, aromatic), 6.8 (d, 2 H, aromatic), 6.65 (t, 2 H, aromatic), 6.4 (br. s, 2 H, NH[py]), 5.0 (d, 2 H, $^2J\{^{31}P\text{-}^1H\}$ 19 Hz, NH[P]). IR (KBr) cm^{-1} υ_{NH} 3143, $\upsilon_{CN[py]}$ 1600, υ_{PN} 997, υ_{PtCl} 307, υ_{PtCl} 288. Mass spec (NOBA Matrix): 817(M-Cl^-), 780(M-2Cl^-).

[$PtMe_2(Ph_2PNHNHpy$-*P*)$_2$-*P*] (6): $Ph_2PNHNHpy$ (150 mg, 0.5 mmol) and [$PtMe_2$(cod)] (85 mg, 0.5 mmol) were dissolved together in CH_2Cl_2 (7 cm^3) under nitrogen and stirred for 5 minutes. Excess hexane was added, then most of the solvent removed under reduced pressure. The solid formed was subsequently isolated by filtration. Yield 54 mg, 13 %. Microanalysis: Found (calculated for $C_{36}H_{38}N_6P_2Pt$) C 53.66 (53.27), H 5.29 (4.72), N 9.90 (10.35). δ_p ($CDCl_3$) 71.2 ppm $^1J\{^{31}P\text{-}^{195}Pt\}$ 1984 Hz. IR (KBr) cm^{-1} υ_{NH} 3341, υ_{NH} 3051, $\upsilon_{CN[py]}$ 1598, υ_{PN} 985.

[PtMeCl($Ph_2PNHNHpy$)$_2$-*P*] (7): $Ph_2PNHNHpy$ (87 mg, 0.3 mmol) and [PtMeCl(cod)] (50 mg, 0.1 mmol) were dissolved under nitrogen in dry toluene

(10 cm^3). The resulting solution was stirred vigorously for a few hours yielding a white precipitate that was isolated by filtration. Yield 98 mg, 40 %. Microanalysis: Found (calculated for $C_{35}H_{35}N_6P_2ClPt$) C 51.61 (50.52), H 3.87 (4.24), N 10.17 (10.10). δ_p ($CDCl_3$) 60.4 ppm $^1J\{^{31}P\text{-}^{195}Pt\}$ 3183 Hz. δ_H ($CDCl_3$) 7.8-8.1 (m, 9 H, aromatic), 7.2-7.6 (m, 16 H, aromatic), 6.7 (m, 5 H, NH and aromatic), 6.3 (s, 2 H, NH), 0.0 (s, 3 H, $^2J\{^{195}Pt\text{-}^1H\}$ 829 Hz, CH_3). IR (KBr) cm^{-1} υ_{NH} 3251, υ_{NH} 3224, $\upsilon_{CN[py]}$ 1600, υ_{PN} 997, υ_{PtCl} 266. Mass spec (NOBA Matrix): 796(M-Cl^-).

[PdCl(η^3-C_3H_5)($Ph_2PNHNHpy$-*P*)] (8): A CH_2Cl_2 (10 cm^3) solution of $Ph_2PNHNHpy$ (113 mg, 0.39 mmol, 2 eq.) was added dropwise by use of a syringe pump to a CH_2Cl_2 (3 cm^3) solution of [Pd(μ-Cl)(η^3-C_3H_5)]$_2$ (71 mg, 0.195 mmol) under nitrogen over 2.5 hours with stirring. The solvent volume was removed under pressure before excess hexane was added to precipitate a beige solid after cooling overnight then isolated by filtration. Yield 92 mg, 50 %. Microanalysis: Found (calculated for $C_{21}H_{21}ClN_3PPd$) C 50.28 (50.44), H 4.37 (4.44), N 8.28 (8.82). δ_p ($CDCl_3$) 66.4 ppm. δ_H ($CDCl_3$) 7.9 (m, 4 H, aromatic), 7.7 (d, 1 H, aromatic), 7.4 (m, 6 H, aromatic), 7.1 (t, 1 H, aromatic), 6.7 (d, 1 H, aromatic), 6.5 (t, 1 H, aromatic), 6.1 (s, 1 H, NH[py]), 5.5 (d, 1 H, $^2J\{^{31}P\text{-}^1H\}$ 8 Hz, NH[P]), 5.4 (t, 2 H, $J\{^1H\text{-}^1H\}$ 22 Hz, CH_2), 4.7 (t, 1 H, $J\{^1H\text{-}^1H\}$ 14 Hz, CH), 3.7 (t, 2 H, $J\{^1H\text{-}^1H\}$ 24 Hz, CH_2). IR (KBr) cm^{-1} υ_{NH} 3202, υ_{NH} 3051, $\upsilon_{CN[py]}$ 1601, υ_{PN} 997, υ_{PdCl} 285. Mass spec (NOBA Matrix): 440(M-Cl^-).

[Rh(C_8H_{12})Cl$Ph_2PNHNHpy$-*P*] (9): A toluene (5 cm^3) solution of [{Rh(μ-Cl)(cod)}$_2$] (84 mg, 0.2 mmol) was added dropwise to a toluene solution of

$Ph_2PNHNHpy$ (100 mg, 0.3 mmol) under nitrogen. The resulting solution was stirred for 10 minutes before the solvent volume was reduced and hexane added to precipitate a brown solid that was isolated by filtration. Yield 126 mg, 68 %. Microanalysis: Found (calculated for $C_{25}H_{28}PClN_3Rh$) C 52.51 (55.65), H 4.57 (5.23), N 7.90 (7.79). δ_p ($CDCl_3$) 71.0 ppm, d, $^1J\{^{31}P\text{-}^{103}Rh\}$ 156 Hz. δ_H ($CDCl_3$) 7.9 (d, 1 H, pyC[6]H), 7.1-7.6 (m, 12 H, aromatic), 6.7 (d, 1 H, aromatic), 6.5 (t, 1 H, aromatic), 6.1 (s, 1 H, NH[py]), 4.5 (d, 1 H, $^2J\{^{31}P\text{-}^1H\}$ 12 Hz, NH[P]), 4.0 (br. s, 4 H, C_8H_{12}), 2.3 (m, 4 H, C_8H_{12}), 1.7 (m, 4 H, C_8H_{12}). IR (KBr) cm^{-1} υ_{NH} 3206, $\upsilon_{CN[py]}$ 1597, υ_{PN} 996, υ_{RhCl} 250. Mass spec (NOBA Matrix): 540(M+H), 504 ($M\text{-}Cl^-$).

[$RuCl_2(\eta^3:\eta^3\text{-}C_{10}H_{16})Ph_2PNHNHpy\text{-}P$] (10): $Ph_2PNHNHpy$ (50 mg, 0.1 mmol) and [{$RuCl_2(\eta^3:\eta^3\text{-}C_{10}H_{16})$}$_2$] (52 mg, 0.08 mmol) were dissolved under nitrogen in dry toluene (10 cm^3). The resulting solution was stirred for an hour before reducing the solvent volume to 2 cm^3. Diethyl ether was added to form a precipitate, which redissolved on the addition of excess ether. The solvent was reduced before hexane was added drop wise to form an orange/yellow precipitate that was then isolated by filtration. Yield 43 mg, 42 %. Microanalysis: Found (calculated for $C_{27}H_{32}N_3PCl_2Ru$) C 54.51 (53.90), H 5.42 (5.37), N 6.98 (6.99). δ_p ($CDCl_3$) 69.5 ppm. δ_H ($CDCl_3$) 7.9-8.1 (m, 4 H, aromatic), 7.4-7.55 (m, 8 H, aromatic), 6.8 (d, 1 H, aromatic), 6.65 (t, 1 H, aromatic), 6.4 (br. s, 1 H, NH[py]), 5.0 (d, 1 H, $^2J\{^{31}P\text{-}^1H\}$ 19 Hz, NH[P]), 5.2 (br m, 2 H, CH_c), 4.3 (d, 2 H, $J\{^1H\text{-}^{31}P\}$ 8.8 Hz, CH_a), 3.4 (m, 2 H, CH_b), 3.2 (d, 2 H, $J\{^1H\text{-}^{31}P\}$ 3.3 Hz, CH), 2.7 (m, 2 H, CH_2), 2.2 (s, 6 H, CH_3). IR (KBr) cm^{-1} υ_{NH} 3279, $\upsilon_{CN[py]}$

1596 , υ_{PN} 984, υ_{RuCl} 305, υ_{RuCl} 245. Mass spec (NOBA Matrix): 624(M+Na), 602(M+H).

[$RuCl_2(\eta^6$-*p*-$MeC_6H_4{}^iPr)Ph_2PNHNHpy$-*P*] (11): $Ph_2PNHNHpy$ (200 mg, 0.7 mmol) and [{$RuCl(\mu$-Cl)(η^6-*p*-$MeC_6H_4{}^iPr)_2$}] were dissolved under nitrogen in dry CH_2Cl_2 (10 cm^3). The resulting red/orange solution was stirred for 15 minutes before the solvent was reduced to 2 cm^3. Hexane was added to precipitate an orange solid that was isolated by filtration. Yield 330 mg, 81 %. Microanalysis: Found (calculated for $C_{27}H_{30}N_3PCl_2Ru$) C 54.17 (54.08), H 4.21 (5.05), N 6.96 (7.01). δ_p ($CDCl_3$) 72.7 ppm. δ_H ($CDCl_3$) 7.9 (m, 4 H, aromatic), 7.7 (d, 1 H, aromatic), 7.4 (m, 6 H, aromatic), 7.1 (t, 1 H, aromatic), 6.7 (d, 1 H, aromatic), 6.5 (t, 1 H, aromatic), 6.1 (s, 1 H, NH[py]), 5.4 (d, 1 H, $^2J\{^{31}P\text{-}^1H\}$ 12 Hz, NH[P]),5.3 (d, 2 H, $^1J\{^1H\text{-}^1H\}$ 2 Hz, cymene), 5.2 (d, 2 H, $^1J\{^1H\text{-}^1H\}$ 6 Hz, cymene), 2.5 (m, 1 H, ArCH), 1.9 (s, 3 H, $ArCH_3$), 0.9 (d, 6 H, $ArCH_3$). IR (KBr) cm^{-1} υ_{NH} 3332, υ_{NH} 3296, $\upsilon_{CN[py]}$ 1597, υ_{PN} 987, υ_{RuCl} 294. Mass spec (NOBA Matrix): 622(M+Na), 600(M+H), 564(M-Cl^-), 528(M-$2Cl^-$).

[$IrCl_2(\eta^5$-$C_5Me_5)(Ph_2PNHNHpy$-*P*)] (12): A CH_2Cl_2 (10 cm^3) solution of $Ph_2PNHNHpy$ (78 mg, 0.26 mmol) was added dropwise by a syringe pump to a CH_2Cl_2 (3 cm^3) solution of [{$IrCl(\mu$-Cl)(η^5-C_5Me_5)}$_2$] (105 mg, 0.13 mmol) under nitrogen over 2 hours with stirring. The solvent was reduced under pressure before excess hexane was added to precipitate an orange solid after cooling overnight that was isolated by filtration. Yield 157 mg, 86 %. Microanalysis: Found (calculated for $C_{27}H_{33}Cl_2N_3PIr$) C 46.60 (46.75), H 4.45 (4.80), N 5.74 (6.06). δ_p ($CDCl_3$) 45.0 ppm. δ_H ($CDCl_3$) 7.9 (m, 4 H, aromatic), 7.8 (d, 1 H, aromatic), 7.4 (m, 6 H, aromatic), 7.15 (t, 1 H, aromatic), 6.6 (d, 1 H,

aromatic), 6.4 (t, 1 H, aromatic), 6.05 (s, br, 1 H, NH), 5.8 (d, 1 H, $J\{^{31}P\text{-}^{1}H\}$ 33.1 Hz, NH[P]), 1.4 (d, 15 H, Cp*). IR (KBr) cm^{-1} υ_{NH} 3318, υ_{NH} 3057, $\upsilon_{CN[py]}$ 1598, υ_{PN} 987, υ_{IrCl} 285. Mass spec (NOBA Matrix): 692(M^+), 656(M-Cl^-), 619(M-2Cl^-).

[Cu(Ph$_2$PNHNHpy-*P*,*N*)$_2$][PF$_6$] (13): $Ph_2PNHNHpy$ (200 mg, 0.6 mmol) and $[Cu(MeCN)_4][PF_6]$ (127 mg, 0.3 mmol) were dissolved under nitrogen in dry CH_2Cl_2 (5 cm^3). The resulting solution was stirred for about 10 minutes before the solvent volume was reduced on the vacuum line to 2 cm^3. Dry diethyl ether (8 cm^3) was added to yield a creamy white precipitate, which was isolated by filtration and washed with excess ether then dried on the vacuum line. Yield 193 mg, 71 %. Microanalysis: Found (calculated for $C_{34}H_{32}N_6P_3F_6Cu$) C 51.04 (51.36), H 4.05 (4.06), N 10.86 (10.57). IR (KBr) cm^{-1} υ_{NH} 3291, $\upsilon_{CN[py]}$ 1614, υ_{PN} 999. Mass spec (NOBA Matrix): 649(M-PF_6^-).

[Rh(C$_8$H$_{12}$)Ph$_2$P(S)NHNHpy-*S*,*N*][Cl] (14): $Ph_2P(S)NHNHpy$ (200 mg, 0.6 mmol) was dissolved under nitrogen in dry toluene (8 cm^3). $[\{Rh(\mu\text{-}Cl)(cod)\}_2]$ (152 mg, 0.3 mmol) was dissolved in dry toluene (5 cm^3) under nitrogen. The rhodium complex solution was added dropwise over about 10 minutes with stirring. The reaction mixture was then stirred for 20 minutes at room temperature, to yield a yellow precipitate that was isolated by filtration, washed with ether and dried on the vacuum line. Yield 274 mg, 79 %. Microanalysis: Found (calculated for $C_{25}H_{30}N_3PSRhCl$) C 53.08 (52.50), H 4.73 (4.93), N 7.28 (7.35). δ_p ($CDCl_3$) 64.3 ppm. δ_H ($CDCl_3$) 7.9-8.1 (m, 4 H, aromatic), 7.4-7.55 (m, 8 H, aromatic), 6.8 (d, 1 H, aromatic), 6.65 (t, 1 H, aromatic), 6.4 (br. s, 1 H, NH[py]), 5.0 (d, 1 H, $^2J\{^{31}P\text{-}^{1}H\}$ 19 Hz, NH[P]), 4.0 (br. s, 4 H, C_8H_{12}), 2.3 (m,

4 H, C_8H_{12}), 1.7 (m, 4 H, C_8H_{12}). IR (KBr) cm^{-1} υ_{NH} 3163, $\upsilon_{CN[py]}$ 1611, υ_{PN} 998, υ_{PS} 640. Mass spec (NOBA Matrix): 536($M-Cl^-$).

[Ru(η^6-*p*-$MeC_6H_4{}^iPr$)$Ph_2P(S)NHNHpy$-*S*,*N*][Cl_2] (15): $Ph_2P(S)NHNHpy$ (200 mg, 0.6 mmol) and [{RuCl(μ-Cl)(η^6-*p*-$MeC_6H_4{}^iPr)_2$}] (188 mg, 0.3 mmol) were dissolved together under nitrogen in dry CH_2Cl_2 (10 cm^3). The resulting dark orange solution was stirred for 20 minutes before removing the solvent on the vacuum line. Dry hexane (2 cm^3) was added to precipitate a dark brown solid, which was isolated by filtration. Yield 310 mg, 80 %. Microanalysis: Found (calculated for $C_{27}H_{30}N_3PSCl_2Ru$) C 50.88 (51.34), H 4.41 (4.79), N 6.46 (6.66). δ_p ($CDCl_3$) 81.1 ppm. IR (KBr) cm^{-1} υ_{NH} 3448, υ_{NH} 3178, $\upsilon_{CN[py]}$ 1611, υ_{PN} 995, υ_{PS} 635. Mass spec (NOBA Matrix): 559($M-Cl_2$).

[Cu($Ph_2P(S)NHNHpy$-*S*,*N*)$_2$][PF_6] (16): $Ph_2P(S)NHNHpy$ (200 mg, 0.6 mmol) and [$Cu(MeCN)_4$][PF_6] (115 mg, 0.3 mmol) were dissolved together under nitrogen in dry CH_2Cl_2 (20 cm^3). The resulting dark green solution was stirred for two hours before the volume of solvent present was reduced to about 2 cm^3. Dry diethyl ether (15 cm^3) was added to yield a precipitate that was isolated by filtration to yield a green/blue solid. Yield 204 mg, 77 %. Microanalysis: Found (calculated for $C_{34}H_{32}P_3N_6S_2F_6Cu$) C 47.30 (47.55), H 3.66 (3.76), N 9.70 (9.79). δ_p ($CDCl_3$) 65.9 ppm. δ_H (CD_2Cl_2) 7.9-8.1 (m, 8 H, aromatic), 7.4-7.55 (m, 16 H, aromatic), 6.8 (d, 2 H, aromatic), 6.65 (t, 2 H, aromatic), 5.0 (d, 2 H, $^2J\{^{31}P\text{-}^1H\}$ 19 Hz, NH[P]). IR (KBr) cm^{-1} υ_{NH} 3262, $\upsilon_{CN[py]}$ 1611, υ_{PN} 997, υ_{PS} 622. Mass spec (NOBA Matrix): 713($M-PF_6^-$).

References.

1. For reviews, see: K. N. Gavrilov and A. I. Polosukhin, *Russ. Chem. Rev.*, 2000, **69**, 661; P. J. Guiry, M. McCarthy, P. M. Lacey, C. P. Saunders, S. Kelly and D. J. Connolly, *Curr. Org. Chem.*, 2000, **4**, 821; P. Espinet and J. K. Soulantica, *Coord. Chem. Rev.*, 1999, **193**, 499.
2. J. M. Brown, D. I. Hulmes and T. P. Layzell, *J. Chem. Soc., Chem. Commun.*, 1993, 1673; I. Beletskaya and A. Pelter, *Tetrahedron*, 1997, **35**, 4957.
3. E. Drent, P. Arnoldy and P. H. M. Budzelaar, *J. Organomet. Chem.*, 1993, **455**, 247 and references therein; A. Dervisi, P. G. Edwards, P. D. Newman and R. P. Tooze, *J. Chem. Soc., Dalton Trans.*, 2000, 523.
4. H. Yoshida, E. Shirakawa, T. Kurahashi, Y. Nakao and T. Hiyama, *Organometallics*, 2000, **19**, 5671 and references therein.
5. A. Lightfoot, P. Schnider and A. Pfaltz, *Angew. Chem., Int. Ed.*, 1998, **37**, 2897.
6. For a review, see: H. Cheng and Z. Zhang, *Coord. Chem. Rev.*, 1996, **147**, 1; see also: J. P. Farr, M. M. Olmstead and A. L. Balch, *Inorg. Chem.*, 1983, **22**, 1229.
7. G. R. Newkome, *Chem. Rev.*, 1993, **93**, 2067.
8. E. Uhlig and M. Schäfer, *Z. Anorg. Allg. Chem.*, 1968, **359**, 67.
9. W. J. Knebel and R. J. Anjelici, *Inorg. Chim. Acta*, 1973, **7**, 713.
10. H. T. Dieck and G. Hahn, *Z. Anorg. Allg. Chem.*, 1989, **577**, 74.
11. M. Alvarez, N. Lugan and R. Mathieu, *J. Chem. Soc., Dalton Trans.*, 1994, 2755.

12. H. Yang, M. Alvarez, N. Lugan and R. Mathieu, *J. Chem. Soc., Chem. Commun.*, 1995, 1721.

13. W. V. Dahlhoff, T. R. Dick, G. H. Ford, W. S. J. Kelly and M. S. Nelson, *J. Chem. Soc., A*, 1971, 3495.

14. M. P. Anderson, B. M. Mattson and L. H. Pignolet, *Inorg. Chem.*, 1983, **22**, 2644.

15. M. P. Anderson, C. T. Bruce, B. M. Mattson and L. H. Pignolet, *Inorg. Chem.*, 1983, **22**, 3267.

16. R. J. McNair, P. V. Nilsson and L. H. Pignolet, *Inorg. Chem.*, 1985, **24**, 1935.

17. R. J. McNair and L. H. Pignolet, *Inorg. Chem.*, 1986, **25**, 4717.

18. E. Uhlig and M. Maaser, *Z. Anorg. Allg. Chem.*, 1966, **334**, 20515.

19. E. Uhlig and S. Keiser, *Z. Anorg. Allg. Chem.*, 1974, **406**, 1.

20. P. Rigo and M. Bressan, *Inorg. Chem.*, 1975, **14**, 1491.

21. M. P. Anderson, A. L. Casalnuovo, B. J. Johnson, A. M. Mueting and L. H. Pignolet, *Inorg. Chem.*, 1988, **27**, 325.

22. L. Costella, A. D. Zotto, A. Mezzetti and P. Rigo, *J. Chem. Soc., Dalton Trans.*, 1994, 2257.

23. A. D. Zotto, G. Nardin and P. Rigo, *J. Chem. Soc., Dalton Trans.*, 1995, 3343.

24. J. A. Casares, P. Espinet and K. Soulantica, *Inorg. Chem.*, 1997, **36**, 5251.

25. W. Seidel and H. Scholer, *Z. Chem.*, 1967, **11**, 431.

26. E. Lindner, H. Rauleder and W. Hiller, *Z. Naturforsch., Teil B*, 1983, **38**, 417.

27. S. M. Aucott, A. M. Z. Slawin and J. D. Woollins, *J. Chem. Soc., Dalton Trans.*, 2000, 2559.

28. K. V. Katti, V. S. Reddy and P. R. Singh, *Chem. Soc. Rev.*, 1995, 97.

29. K. V. Katti, P. R. Singh and C. L. Barnes, *Inorg. Chem.*, 1992, **31**, 4588.

30. M. L. Clarke, A. M. Z.Slawin, M. V. Wheatley, J. D. Woollins, *J. Chem. Soc. Dalton Trans.*, 2001, 3421.

31. TeXsan, Molecular Structure Corporation, The Woodlands 1994.

32. SHELXTL Bruker AXS Madison 1999.

33. D. Drew; J. R. Doyle, *Inorg. Synth.*, 1991, **28**, 346.

34. J. X. McDermott; J. F. White; G. M. Whiteside, *J. Am. Chem. Soc.*, 1976, **60**, 6521.

35. H. C. Clark; L. E. Manzer, *J. Organomet. Chem.*, 1973, **59**, 411.

36. Y. Tatsuno; T. Yoshida; Seiotsuka, *Inorg. Synth.*, 1979, **19**, 220.

37. G. Giordano; R. H. Crabbtree, *Inorg. Synth.*, 1979, **19**, 218.

38. L. Porri; M. C. Gallazzi; A. Colombo; G. Allegra, *Tetrahedron Lett.*, 1965, **47**, 4187.

39. M. A. Bennett; T. N. Huang; T. W. Matheson; A. R. Smith, *Inorg. Synth.*, 1982, **21**, 74.

40. C. White; A. Yates; P. M. Maitlis, *Inorg. Synth.*, 1979, **19**, 218.

41. G. J. Kubas, *Inorg. Synth.*, 1979, **19**, 90.

CHAPTER 2.2: PREPARATION AND COORDINATION CHEMISTRY OF p- (XYLYLENEDIAMINODIPHENYL) PHOSPHINE

2.2.1 *Introduction*

Bridging ligands have received a lot of interest in recent years as they can potentially form a number of bi-, tri- and tetranuclear species. There are a variety of different ligands that can have bridging properties and these include *o*-, *m*- and *p*- derivatives of benzene or pyridine.

An example of an *o*-phenyl ligand, $Ph_2PNHC_6H_4PPh_2$[1], was prepared by the treatment of 2-(diphenylphosphino)aniline[2], (**A**), with ^{n}BuLi at –78 °C and chlorodiphenylphosphine. Other examples include $(Et_2PN(Me)C_6H_4PEt_2)$[3], (**B**), and 1-(diphenylphosphany)naphtha-2-oxydiphenylphosphane[4], (**C**).

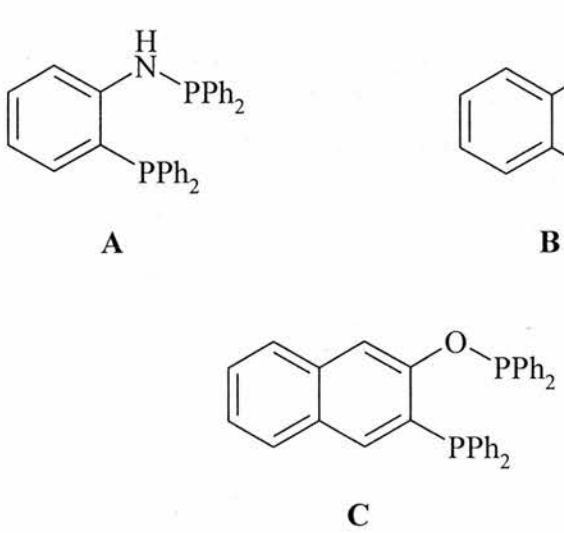

A **B**

C

Figure 2.2.1. Examples of *o*-phenyl derivative ligands.

2,6-bis(diphenylphosphino)pyridine, ($\{Ph_2P\}_2py$), a *m*-bidentate pyridine, has the potential to act as a tridentate ligand containing PNP.[5, 6] $(Ph_2P)_2py$ was shown to react with a variety of platinum and palladium starting materials to give four different complexes (Scheme 2.2.1).

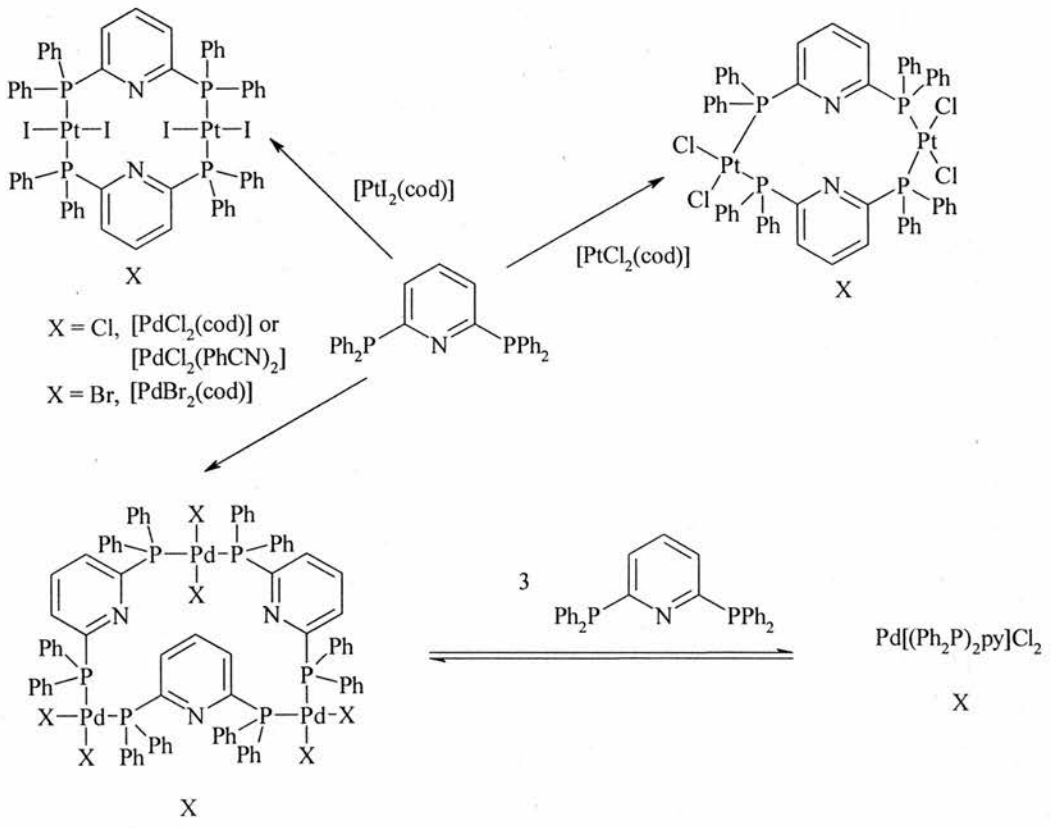

Scheme 2.2.1. Palladium and platinum complexes of $(Ph_2P)_2py$.

p-phenyl ligands have been used in recent years to prepare bridging complexes between two metal centres. Typically these ligands have the property to coordinate different metal centres to form bimetallic species.

Gaw *et al*[7] reported the preparation of the tetradentate (phosphine)amine 1,4-$\{(Ph_2P)_2NCH_2\}_2C_6H_4$ in 2002. They showed the formation of a binuclear *P*, *P'*-ligated complex containing two *cis* $[Mo(CO)_4]$ metal fragments.

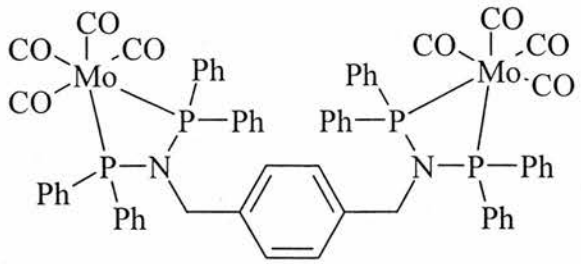

Figure 2.2.2. Structure of 1,4-$\{(OC)_4Mo(Ph_2P)_2NCH_2\}_2C_6H_4$.

In this work we report the preparation of a new phosphine that has a rigid backbone and has the potential to act as a bidentate bridging ligand. Illustrative coordination complexes have been prepared.

Results and Discussion

2.2.2 *Synthesis and chalcogen derivatives of p-$Ph_2PNHCH_2(C_6H_4)CH_2NHPPh_2$* (**17**)

Reaction of *p*-xylene diamine with two equivalents of Ph_2PCl in the presence of NEt_3, proceeds in thf to give **17** which was isolated in very good yield (89 %) after filtration from $Et_3NH^+Cl^-$ as a colourless crystalline solid and recrystallisation from dichloromethane and hexane. The $^{31}P\{^1H\}$ NMR spectrum of **17** consists of a singlet at δ_P 43.3 ppm. The IR spectrum has bands at 3303, 1432 and 997 cm^{-1} that are assigned to ν_{NH}, ν_{PPh} and ν_{PN} respectively. The mass spectrum gave the expected parent ion and fragmentation pattern and microanalysis gave good results.

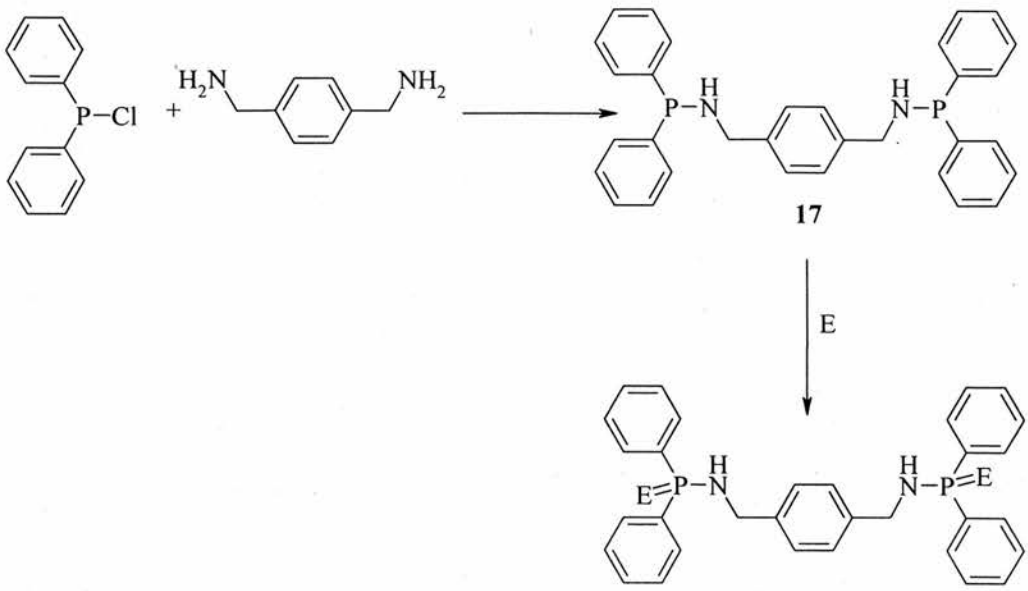

Scheme 2.2.2. Formation of *p*-$Ph_2PNHCH_2(C_6H_4)CH_2NHPPh_2$ and *p*-$Ph_2P(E)NHCH_2(C_6H_4)CH_2NHP(E)Ph_2$ ligands (E = O (**18**), S (**19**), Se (**20**)).

The oxide (**18**) *p*-$Ph_2P(O)NHCH_2(C_6H_4)CH_2NHP(O)Ph_2$ was easily prepared by addition of excess aqueous hydrogen peroxide to **17** in thf whilst the sulfur (**19**) and selenide (**20**) analogues were prepared by the addition of elemental S or Se to the ligand in toluene. Microanalysis for **19** and **20** were satisfactory. The EI^+ mass spectral data obtained for these chalcogens gave the expected parent ions and fragmentation patterns. $^{31}P\{^1H\}$ NMR showed single resonances ($CDCl_3$) at δ_P 24.5 and 60.5 ppm for the oxide and sulfide respectively. The seleno analogue exhibited a single $^{31}P\{^1H\}$ NMR resonance ($CDCl_3$) at δ_P 58.6 ppm with selenium satellites $^1J(^{31}P\text{-}^{77}Se)$ 756 Hz which is typical for a P=Se group[8].

Crystals of $Ph_2P(S)NHCH_2(C_6H_4)CH_2NHP(S)Ph_2$ suitable for X-ray crystallography were obtained by slow diffusion of a $CDCl_3$/hexane solution (Figure 2.2.3). Selected structural data are also given (Table 2.2.1). In the solid

state the molecule exists as two half molecules with a P(1)-S(1) bond length of 1.9523(11) Å and a P(1)-N(2) bond length of 1.654(3) Å.

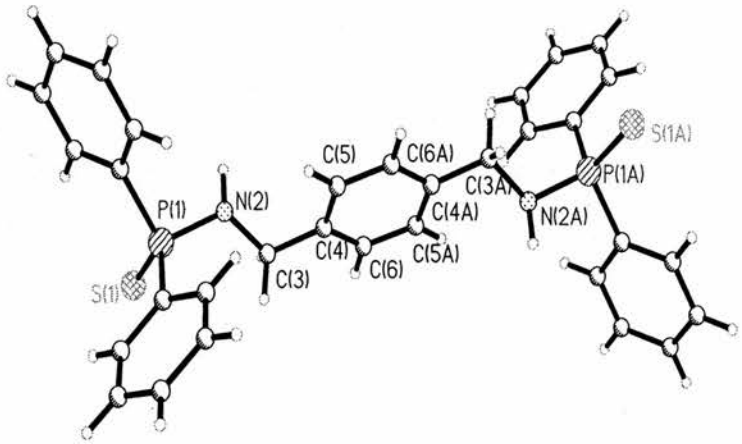

Figure 2.2.3. X-ray structure of *p*-$Ph_2P(S)NHCH_2(C_6H_4)CH_2NHP(S)Ph_2$ (**19**)

Crystals of *p*-$Ph_2P(Se)NHCH_2(C_6H_4)CH_2NHP(Se)Ph_2$ suitable for X-ray crystallography were obtained by slow diffusion of a chloroform solution with ether (Figure 2.2.4). Selected structural data are also given (Table 2.2.1). In the solid state the sulfur and selenide analogues are isomorphorus, The P(1)-N(2) bond length is shown to be 1.654(5) Å and the P(1)-Se(1) bond length is 2.1198(10) Å which is equivalent to previously reported bond lengths for P-N and P-Se[8].

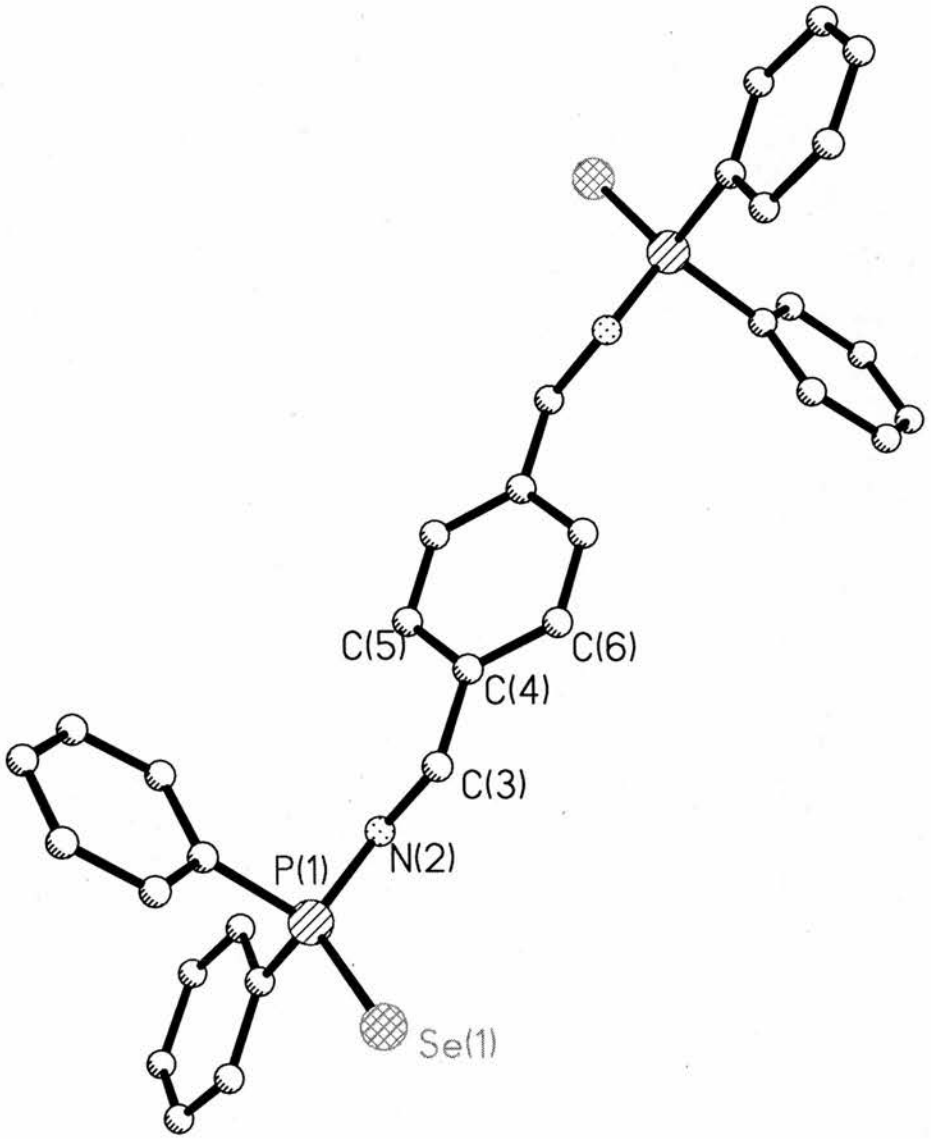

Figure 2.2.4. The X-ray structure of *p*-$Ph_2P(Se)NHCH_2(C_6H_4)CH_2NHP(Se)Ph_2$ (**20**)

Table 2.2.1. Selected bond length (Å) and angles (°) for *p*-$Ph_2P(S)NHCH_2(C_6H_4)CH_2NHP(S)Ph_2$ (**19**) and *p*-$Ph_2P(Se)NHCH_2(C_6H_4)CH_2NHP(Se)Ph_2$ (**20**)

Selected bond lengths (Å) and angles (°)	***(19)***	***(20)***
P(1)-N(2)	1.654(3)	1.654(5)
Se(1)-P(1)	-	2.1198(10)
S(1)-P(1)	1.9523(11)	-
N(2)-C(3)	1.471(4)	1.485(7)
P(1)-C(11)	1.811(3)	1.797(6)
P(1)-C(17)	1.812(3)	1.817(6)
N(2)-H(2)	0.9798(11)	0.979(3)
N(2)-P(1)-C(11)	103.43(13)	104.8(3)
N(2)-P(1)-C(17)	101.72(13)	104.0(3)
C(11)-P(1)-C(17)	106.39(14)	104.5(3)
N(2)-P(1)-Se(1)	-	116.79(19)
N(2)-P(1)-S(1)	117.60(10)	-
C(11)-P(1)-Se(1)	-	113.7(2)
C(11)-P(1)-S(1)	112.64(11)	-
C(17)-P(1)-Se(1)	-	111.8(2)
C(17)-P(1)-S(1)	113.74(10)	-
P(1)-N(2)-H(2)	109.1(18)	110(3)

2.2.3 *Coordination chemistry of p-*$Ph_2PNHCH_2(C_6H_4)CH_2NHPPh_2$

Reaction of $[\{PtCl(\mu\text{-}Cl)(PEt_3)\}_2]$ with *p*-$Ph_2PNHCH_2(C_6H_4)CH_2NHPPh_2$ gives $[((PEt_3)PtCl_2(Ph_2PNHCH_2))_2C_6H_4]$ (**21**) in satisfactory yield (69 %). The

EI^+ mass spectrum of (**21**) contains the expected parent ion and fragmentation pattern and the complex displays resonances with platinum satellites in the $^{31}P\{^1H\}$ NMR spectrum (δ_{PA} 34.0 ppm, $^1J\{^{31}P_A\text{-}^{195}Pt\}$ 1984 Hz, δ_{PX} 7.5 ppm, $^1J\{^{31}P_X\text{-}^{195}Pt\}$ 1715 Hz $^2J\{^{31}P_A\text{-}^{31}P_X\}$ 18 Hz). The IR spectrum has ν_{NH} at 3289 cm^{-1}, ν_{PPh} and ν_{PN} at 1435 and 997 cm^{-1} respectively and two ν_{PtCl} bands at 340, 310 cm^{-1}. $[((PPhMe_2)PtCl_2(Ph_2PNHCH_2))_2C_6H_4]$ (**22**) was prepared in a similar way to (**21**). The complex was isolated by suction filtration in a yield of 60 % and its microanalysis gave satisfactory results. The expected fragmentation pattern and parent ion was observed in the EI^+ mass spectrum. The $^{31}P\{^1H\}$ NMR spectrum revealed resonances with platinum satellites, (δ_{PA} 35.1 ppm, $^1J\{^{31}P_A\text{-}^{195}Pt\}$ 1956 Hz, δ_{PX} –14.2 ppm, $^1J\{^{31}P_X\text{-}^{195}Pt\}$ 1820 Hz $^2J\{^{31}P_A\text{-}^{31}P_X\}$ 19 Hz). The IR bands observed at 3300, 1435, 998, and 311 cm^{-1} represent ν_{NH}, ν_{PPh}, ν_{PN} and two ν_{PtCl} respectively.

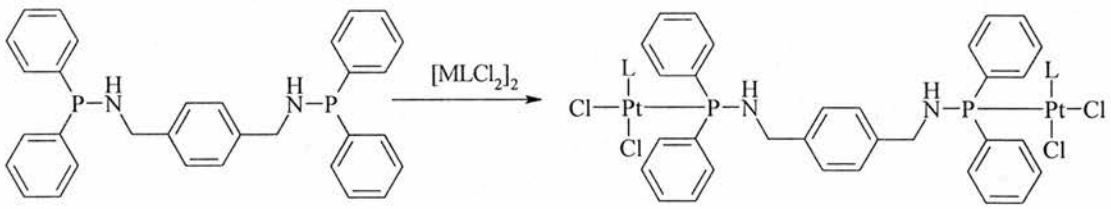

Scheme 2.2.3. Reaction of *p*-$Ph_2PNHCH_2(C_6H_4)CH_2NHPPh_2$ with $[\{MLCl_2\}_2]$ $\{L = PEt_3$ (**21**), $PPhMe_2$ (**22**)$\}$.

The reaction of *p*-$Ph_2PNHCH_2(C_6H_4)CH_2NHPPh_2$ with $[IrCl(\mu\text{-}Cl)(\eta^5\text{-}C_5Me_5)]_2$ gave the expected product $[\{IrCl(\mu\text{-}Cl)(\eta^5\text{-}C_5Me_5)(Ph_2PNHCH_2)\}_2C_6H_4]$ (**23**) in good yield (73 %). The microanalysis found indicated that a 2:1 complex had been formed with the *p*-

$Ph_2PNHCH_2(C_6H_4)CH_2NHPPh_2$ linking the two iridium atoms from the starting material. The ^{31}P NMR ($CDCl_3$) is a single peak at δ_P 34.4 ppm indicating that the two phosphorus atoms have the same environment making the complex symmetrical. The IR spectrum has the ν_{NH}, ν_{PPh}, ν_{PN} and two ν_{MCl} bands at 3309, 1434, 997, 289 and 268 cm^{-1} respectively. EI^+ mass spectral analysis gave the expected parent ion and fragmentation pattern. Similarly the rhodium analogue [{RhCl(μ-Cl)(η^5-C_5Me_5)(Ph_2PNHCH_2)}$_2C_6H_4$] (**24**) was prepared by addition of [RhCl(μ-Cl)(η^5-C_5Me_5)]$_2$ and *p*-$Ph_2PNHCH_2(C_6H_4)CH_2NHPPh_2$ to dichloromethane. The yield obtained from the reaction was again good (78 %) and the micro analytical data obtained again showed the formation of a 2:1 complex. This was further supported by the ^{31}P NMR ($CDCl_3$), which constituted of a single peak at δ_P 66.4 ppm with a coupling constant of $^1J(^{31}P$-$^{103}Rh)$ of 148 Hz. The EI^+ mass spectrum shows the expected fragmentation pattern and parent ion and the IR spectrum showed bands at 3300, 1434, , 282, 245 cm^{-1} which are assigned as ν_{NH}, ν_{PPh}, ν_{PN} and two ν_{RhCl} vibrations respectively.

Complex (**25**), [(RuCl(μ-Cl)(η^6-*p*-$MeC_6H_4{}^iPr$)(Ph_2PNHCH_2))$_2C_6H_4$], was prepared by dissolving molar equivalents of [RuCl(μ-Cl)(η^6-*p*-$MeC_6H_4{}^iPr$)]$_2$ and *p*-$Ph_2PNHCH_2(C_6H_4)CH_2NHPPh_2$ in dichloromethane and stirring at room temperature for 1 hour. After precipitation with diethyl ether the orange microcrystalline product (72 %) was found to contain a 2:1 complex as shown previously with the iridium and rhodium complexes. A single peak was observed in the ^{31}P NMR ($CDCl_3$) at δ_P 61.1 ppm that again indicated that the two phosphorus atoms were in the same environment. The IR spectrum showed

characteristic bands of ν_{NH}, ν_{PPh} and ν_{PN} at 3367, 1434 and cm^{-1} respectively with bands at 281, 249 cm^{-1} corresponding to the presence of two ν_{RuCl} vibrations. Microanalysis and EI^+ mass spectral data gave satisfactory results for the suggested structure. Scheme 2.2.4 illustrates the formation of these complexes.

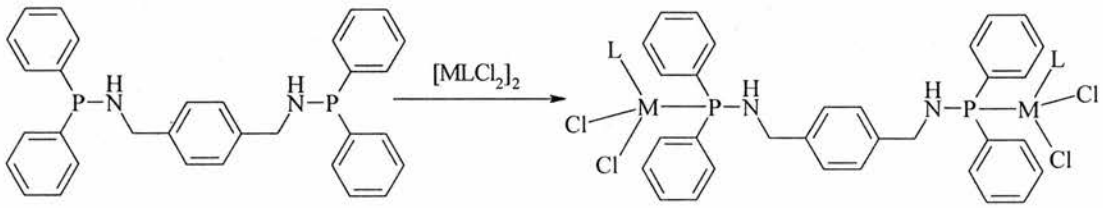

Scheme 2.2.4. Reaction of *p*-$Ph_2PNHCH_2(C_6H_4)CH_2NHPPh_2$ with [{$MLCl_2$}$_2$] {M = Rh (**24**), Ir (**23**); L = η^5-C_5Me_5, M = Ru; η^6-*p*-$MeC_6H_4{}^iPr$ (**25**)}.

[($Pd(\eta^3$-$C_3H_5)Cl(Ph_2PNHCH_2))_2C_6H_4$] (**26**) was prepared (68 %) by dissolving [{$Pd(\mu$-$Cl)(\eta^3$-$C_3H_5)$}$_2$] and **17** in dichloromethane. The microanalysis obtained was satisfactory for the suggested structure and EI^+ mass spectral data gave the expected parent ion and fragmentation pattern. The IR spectrum has bands at 3246, 1433, 998, 276 cm^{-1} that correspond to the ν_{NH}, ν_{PPh}, ν_{PN} and ν_{PdCl} vibrations. The ^{31}P NMR ($CDCl_3$) is a single peak at δ_P 58.1 ppm. Similarly complex (**27**) was prepared by addition of [{$Rh(\mu$-$Cl)(cod)$}$_2$] and **17** to a toluene solution. The yield obtained was found to be acceptable (57 %) and a doublet was shown in the ^{31}P NMR ($CDCl_3$) spectrum at δ_P 62.3 ppm with a coupling constant of $^1J(^{31}P$-$^{103}Rh)$ 157 Hz. The IR spectrum has bands at 3289, 1434, 995, 279 cm^{-1} that correspond to the ν_{NH}, ν_{PPh}, ν_{PN} and ν_{RhCl} vibrations and the EI^+ mass spectrum contains the expected fragmentation pattern and parent ion. Scheme 2.2.5 illustrates the formation of the expected

products obtained by reaction of [{Pd(μ-Cl)(η^3-C_3H_5)}$_2$] and [{Rh(μ-Cl)(cod)}$_2$].

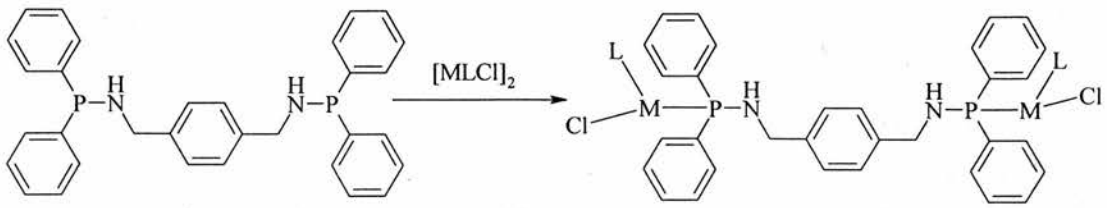

Scheme 2.2.5. Reaction of *p*-$Ph_2PNHCH_2(C_6H_4)CH_2NHPPh_2$ with [{MLCl}$_2$] {M = Pd (**26**), Rh (**27**); L = η^3-C_3H_5, C_8H_{12}}.

The final complex prepared for this ligand was the AuCl complex **28** isolated in 43 % yield. The ^{31}P NMR ($CDCl_3$) showed a single peak at δ_P 61.1 ppm that indicated that a single phosphorus environment existed within the complex. Microanalysis gave satisfactory results for the suggested structure and the EI^+ mass spectrum indicates the expected parent ion and fragmentation pattern.

Table 2.2.2. Characterisation data for $Ph_2PNHCH_2C_6H_4CH_2NHPPh_2$ and its derivatives. ([a] $^1J\{^{31}P\text{-}^{77}Se\}$ 756 Hz.). ([b] $^1J\{^{31}P_A\text{-}^{195}Pt\}$ 1984 Hz, $^1J\{^{31}P_X\text{-}^{195}Pt\}$ 1715 Hz, $^2J\{^{31}P_A\text{-}^{31}P_X\}$ 18 Hz), ([c] $^1J\{^{31}P_A\text{-}^{195}Pt\}$ 1956 Hz, $^1J\{^{31}P_X\text{-}^{195}Pt\}$ 1820 Hz, $^2J\{^{31}P_A\text{-}^{31}P_X\}$ 19 Hz), ([d] $^1J\{^{31}P\text{-}^{103}Rh\}$ 148 Hz), ([e] $^1J\{^{31}P\text{-}^{103}Rh\}$ 157 Hz)

Compound	*$^{31}P\text{-}\{^1H\}$ NMR*	*IR/cm^{-1}*					*Microanalysis/ % Found (calc.)*		
	δ_p/ppm	ν_{PN}	ν_{NH}	ν_{PPh}	$\nu_{P=E}$	ν_{MCl}	C	H	N
$Ph_2PNHCH_2C_6H_4CH_2NHPPh_2$ (17)	43.3	997	3303	1432	-	-	73.43 (73.55)	6.39 (6.17)	5.64 (5.36)
$Ph_2P(O)NHCH_2C_6H_4CH_2NHP(O)Ph_2$ (18)	24.5	998	3097	1437	1357	-	69.37 (69.31)	5.93 (5.82)	5.38 (5.05)
$Ph_2P(S)NHCH_2C_6H_4CH_2NHP(S)Ph_2$ (19)	60.5	997	3180	1437	625	-	65.27 (67.59)	5.35 (5.32)	5.11 (4.93)
$Ph_2P(Se)NHCH_2C_6H_4CH_2NHP(Se)Ph_2$ (20)[a]	58.6[a]	996	3177	1435	551	-	57.53 (58.02)	5.14 (4.56)	4.24 (4.23)

Table continued									
[((PEt$_3$)PtCl(Ph$_2$PNHCH$_2$))$_2$C$_6$H$_4$] (21)	34.0, 7.5[b]	997	3289	1435	-	340, 310	41.36 (41.52)	5.12 (4.75)	2.36 (2.20)
[((PPhMe$_2$)PtCl(Ph$_2$PNHCH$_2$))$_2$C$_6$H$_4$] (22)	35.1, –14.2[c]	998	3300	1435	-	334, 311	44.05 (43.92)	4.17 (3.99)	2.61 (2.13)
[{IrCl(μ-Cl)(η^5-C$_5$Me$_5$)(Ph$_2$PNHCH$_2$)}$_2$C$_6$H$_4$] (23)	34.4	997	3309	1434	-	289, 268	47.64 (48.00)	4.64 (4.65)	2.35 (2.15)
[{RhCl(μ-Cl)(η^5-C$_5$Me$_5$)(Ph$_2$PNHCH$_2$)}$_2$C$_6$H$_4$] (24)	66.4[d]	996	3300	1434	-	282, 267	54.76 (54.86)	5.31 (5.33)	2.41 (2.45)
[(RuCl(μ-Cl)(η^6-*p*-MeC$_6$H$_4$^{i}Pr)(Ph$_2$PNHCH$_2$))$_2$C$_6$H$_4$] (25)	61.1	996	3367	1434	-	291, 281	55.53 (55.92)	4.73 (5.23)	2.46 (2.51)
[(Pd(η^3-C$_3$H$_5$)Cl(Ph$_2$PNHCH$_2$))$_2$C$_6$H$_4$] (26)	58.1	998	3246	1433	-	276	52.34 (52.44)	4.78 (4.63)	3.45 (3.22)

Table continued									
[(RhCl(C_8H_{12})(Ph_2PNHCH_2))$_2C_6H_4$] (27)	62.3[e]	995	3289	1434	-	279	54.66	5.32	2.89
							(54.37)	(5.21)	(2.59)
[(AuCl(Ph_2PNHCH_2))$_2C_4H_6$] (28)	61.1	997	3279	1435	-	323	39.98	3.28	2.94
							(39.65)	(3.12)	(2.89)

Experimental

General experimental conditions and instruments were as set out on page xvii. Unless otherwise stated, all reactions were carried out under an oxygen-free nitrogen atmosphere using standard Schlenk techniques. Diethyl ether and thf were purified by reflux over sodium-benzophenone and distillation under nitrogen. Dichloromethane was heated to reflux over calcium hydride and distilled under nitrogen. Toluene and hexane were heated to reflux over sodium and distilled under nitrogen. The complexes [AuCl(tht)] (tht = tetrahydrothiophene)[9], $[MCl_2(cod)]$ (M = Pt or Pd; cod = cycloocta-1,5-diene)[10, 11], $[\{RuCl(\mu\text{-}Cl)(\eta^6\text{-}p\text{-}MeC_6H_4{}^iPr)\}_2]$[12], $[\{Rh(\mu\text{-}Cl)(cod)\}_2]$[13], $[\{Pd(\mu\text{-}Cl)(\eta^3\text{-}C_3H_5)\}_2]$ $[\{MCl(\mu\text{-}Cl)(\eta^5\text{-}C_5Me_5)\}_2]$ (M = Rh or Ir)[14] $[\{PtCl(\mu\text{-}Cl)(PMe_2Ph)\}_2]$[15] and $[\{PtCl(\mu\text{-}Cl)(PEt_3)\}_2]$[16] were prepared using literature procedures. Chlorodiphenylphopshine was distilled prior to use. NEt_3 (99 % purity), ^tBuOK (95 % purity), H_2O_2 (30 wt. % in H_2O), *p*-xylylene diamine and reagent grade KBr were used without further purification. Infra-red spectra were recorded as KBr discs in the range 4000-200 cm^{-1} on a Perkin-Elmer 2000 FTIR/RAMAN spectrometer. NMR spectra were recorded on a Gemini 2000 spectrometer (operating at 121.4 MHz for ^{31}P and 300 MHz for ^1H). Microanalyses were performed by the St. Andrews University service and mass spectra by the Swansea Mass Spectrometer Service.

$Ph_2PNHCH_2C_6H_4CH_2NHPPh_2$. (17): To a stirring solution of triethylamine (2.26 g, 22.29 mmol) in thf (100 cm^3) at room temperature was added a thf (50 cm^3) solution of chlorodiphenylphosphine (4.92 g, 22.29 mmol) over 2 hours and simultaneously a thf solution of *p*-xylylene diamine (1.52 g, 11.14 mmol) over 2 hours. The stirring was continued for a further hour before removing the colourless precipitate that had

formed by filtration and the solvent removed to yield a colourless solid which was recrystallised from dichloromethane and hexane to give the desired product as a fine colourless solid that was collected by suction filtration and dried *in vacuo*. Yield 4.99 g, 89 %. Microanalysis: Found (calculated for $C_{32}H_{30}P_2N_2.H_2O$) C 73.43 (73.55), H 6.39 (6.17), N 5.64 (5.36) %. $^{31}P\{^1H\}(CDCl_3)$ 43.3 ppm. ^1H ($CDCl_3$) δ 1.4 (m, 4 H, CH_2), 4.1 (br s, 2 H, NH), 7.3-7.9 (m, 24 H, aromatics). IR (KBr disc): 3303, 1432, 997 cm^{-1}. EI^+ MS: *m/z* 504 $[M]^+$.

$Ph_2P(O)NHCH_2C_6H_4CH_2NHP(O)Ph_2$. (18): Aqueous hydrogen peroxide (30 % w/w, 0.1 cm^3, 0.9 mmol) was added drop wise to a suspension of $Ph_2PNHCH_2C_6H_4CH_2NHPPh_2$ (223 mg, 0.4 mmol) in thf (10 cm^3) and the mixture was stirred for 30 minutes. The solution was filtered through Celite to remove a small amount of insoluble material and the solvent was removed *in vacuo* to give viscous oil, which was dissolved in dichloromethane (0.5 cm^3) before precipitating a colourless solid upon addition of diethyl ether (6 cm^3). The product was collected by suction filtration and dried *in vacuo*. Yield 188 mg, 79 %. Microanalysis: Found (calculated for $C_{32}H_{30}P_2N_2O_2.H_2O$) C 69.37 (69.31), H 5.93 (5.82), N 5.38 (5.05) %. ^{31}P-$\{^1H\}$ NMR ($CDCl_3$) 24.5 ppm. ^1H NMR ($CDCl_3$): δ 1.4 (m, 4 H, CH_2), 4.1 (br s, 2 H, NH), 7.3-7.9 (m, 24 H, aromatics) ppm. IR (KBr): 3097, 1437, 1357, 998 cm^{-1}. ES^+ MS: *m/z* 559 $[M + Na]^+$.

$Ph_2P(S)NHCH_2C_6H_4CH_2NHP(S)Ph_2$. (19): $Ph_2PNHCH_2C_6H_4CH_2NHPPh_2$ (214 mg, 0.4 mmol) and grey selenium (27 mg, 0.8 mmol) were heated to reflux in toluene (15 cm^3) for 4 hours. The reaction mixture was filtered through Celite to remove any insoluble material remaining befpre reducing the solvent to yield an off-white solid that was washed with $CHCl_3$ (5 cm^3) and dried *in vacuo*. Yield 106 mg, 44 %.

Microanalysis: Found (calculated for $C_{32}H_{30}P_2N_2S_2$) C 65.27 (67.59). H 5.35 (5.32), N 5.11 (4.93) %. ^{31}P-{^1H} NMR ($CDCl_3$) 60.5 ppm. ^1H NMR ($CDCl_3$): δ 1.4 (m, 4 H, CH_2), 4.1 (d, 2 H, $^2J(^{31}P$-$^1H)$ 8 Hz, NH), 7.2-8.0 (m, 24 H, aromatics) ppm. IR (KBr): 3180, 1437, 997, 625 cm^{-1}. ES^+ MS: *m/z* 681 $[M + Na]^+$.

$Ph_2P(Se)NHCH_2C_6H_4CH_2NHP(Se)Ph_2$. (20): $Ph_2PNHCH_2C_6H_4CH_2NHPPh_2$ (198 mg, 0.4 mmol) and grey selenium (62 mg, 0.8 mmol) were heated to reflux in toluene (10 cm^3) for 5 hours. The solvent was removed *in vacuo* and the crude product was taken up in dcm (5 cm^3) and filtered through Celite to remove a trace of unreacted selenium. The filtrate was evaporated to dryness to yield an off-white solid, which was dried *in vacuo* overnight. Yield 189 mg, 73 %. Microanalysis: Found (calculated for $C_{32}H_{30}P_2N_2Se_2$) C 57.53 (58.02). H 5.14 (4.56), N 4.24 (4.23) %. ^{31}P-{^1H} NMR ($CDCl_3$) 58.6 ppm, $^1J(^{31}P$-$^{77}Se)$ 756 Hz. ^1H NMR ($CDCl_3$): δ 1.4 (m, 4 H, CH_2), 4.1 (d, 2 H, $^2J(^{31}P$-$^1H)$ 8 Hz, NH), 7.2-8.0 (m, 24 H, aromatics) ppm. IR (KBr): 3177, 1435, 996, 551 cm^{-1}. ES^+ MS: *m/z* 681 $[M + Na]^+$.

$[((PEt_3)PtCl(Ph_2PNHCH_2))_2C_6H_4]$. (21): $[\{PtCl(\mu\text{-}Cl)(PEt_3)\}_2]$ (39 mg, 0.05 mmol) and ligand (26 mg, 0.05 mmol) were dissolved in dichloromethane (5 cm^3) and stirred overnight. The reaction mixture was filtered through Celite to remove any insoluble material and then reduced to 0.5 cm^3 before addition of diethyl ether (10 cm^3) to precipitate a colourless solid that was isolated by filtration and dried *in vacuo*. Yield 45 mg, 69 %. Microanalysis: Found (calculated for $C_{44}H_{60}P_4N_2Pt_2Cl_4$) C 41.36 (41.52), H 5.12 (4.75), N 2.36 (2.20) %. $^{31}P\{^1H\}$ NMR ($CDCl_3$) δ_{PA} 34.0 ppm, $^1J\{^{31}P_A$-$^{195}Pt\}$ 1984 Hz, δ_{PX} 7.5 ppm, $^1J\{^{31}P_X$-$^{195}Pt\}$ 1715 Hz $^2J\{^{31}P_A$-$^{31}P_X\}$ 18 Hz ppm. ^1H ($CDCl_3$) δ 1.0 (m, 18 H, CH_3), 1.2 (m, 12 H, CH_2), 1.4 (m, 4 H, CH_2N), 4.1 (d, 2 H, $^2J(^{31}P$-$^1H)$ 8 Hz, NH), 7.2-8.0 (m, 24 H, aromatics) ppm. IR (KBr): 3289,

1435, 997, 340, 310 cm^{-1}. EI^+ MS: *m/z* 1293 $[M + Na]^+$, 1235 $[M - Cl]^+$, 1200 $[M - 2Cl]^+$.

$[((PPhMe_2)PtCl(Ph_2PNHCH_2))_2C_6H_4]$. (22): $[\{PtCl(\mu\text{-}Cl)(PMe_2Ph)\}_2]$ (41 mg, 0.05 mmol) and $Ph_2PNHCH_2C_6H_4CH_2NHPPh_2$ (26 mg, 0.05 mmol) were dissolved in dry CH_2Cl_2 (5 cm^3) and stirred overnight. The pale yellow solution formed was filtered through Celite to remove any inorganic impurities before reducing the solvent volume to 0.5 cm^3 and addition of diethyl ether (10 cm^3) to precipitate a colourless solid that was isolated by suction filtration and dried *in vacuo*. Yield 40 mg, 60 %. Microanalysis: Found (calculated for $C_{48}H_{52}P_4N_2Pt_2Cl_4$) C 44.05 (43.92), H 4.17 (3.99), N 2.61 (2.13) %. $^{31}P\{^1H\}$ NMR ($CDCl_3$) δ_{PA} 35.1 ppm, $^1J\{^{31}P_A\text{-}^{195}Pt\}$ 1956 Hz, δ_{PX} –14.2 ppm, $^1J\{^{31}P_X\text{-}^{195}Pt\}$ 1820 Hz $^2J\{^{31}P_A\text{-}^{31}P_X\}$ 19 Hz ppm. ^1H ($CDCl_3$) δ 1.2 (m, 12 H, CH_2), 1.4 (m, 4 H, CH_2N), 4.1 (d, 2 H, $^2J(^{31}P\text{-}^1H)$ 8 Hz, NH), 7.2-8.0 (m, 34 H, aromatics) ppm. IR (KBr): 3300, 1435, 998, 334, 310 cm^{-1}. EI^+ MS: *m/z* 1333 $[M + Na]^+$, 1275 $[M - Cl]^+$, 1239 $[M - 2Cl]^+$.

$[\{IrCl(\mu\text{-}Cl)(\eta^5\text{-}C_5Me_5)(Ph_2PNHCH_2)\}_2C_6H_4]$ (23): $[\{IrCl(\mu\text{-}Cl)(\eta^5\text{-}C_5Me_5)\}_2]$ (50 mg, 0.06 mmol) and $Ph_2PNHCH_2C_6H_4CH_2NHPPh_2$ (32 mg, 0.06 mmol) were dissolved in dry CH_2Cl_2 (5 cm^3) and stirred for 2 hours. The orange solution was filtered through Celite to remove a small amount of insoluble material before reducing the volume to 0.5 cm^3 and addition of diethyl ether (20 cm^3) to precipitate an orange solid that was isolated by filtration and dried *in vacuo*. Yield 60 mg, 73 %. Microanalysis: Found (calculated for $C_{52}H_{60}N_2P_2Ir_2Cl_4$) C 47.64 (48.00), H 4.64 (4.65), N 2.35 (2.15) %. $^{31}P\{^1H\}$ NMR ($CDCl_3$) 34.4 ppm. ^1H ($CDCl_3$) δ 1.3 (s, 30 H, CH_3), 1.5 (m, 4 H, CH_2N), 4.1 (d, 2 H, $^2J(^{31}P\text{-}^1H)$ 8 Hz, NH), 7.2-8.0 (m, 24 H,

aromatics) ppm. IR (KBr): 3309, 1434, 997, 289, 268 cm^{-1}. EI^+ MS: *m/z* 1323 $[M + Na]^+$, 1158 $[M - 4Cl]^+$.

$[\{RhCl(\mu\text{-}Cl)(\eta^5\text{-}C_5Me_5)(Ph_2PNHCH_2)\}_2C_6H_4]$. (24): $[\{RhCl(\mu\text{-}Cl)(\eta^5\text{-}C_5Me_5)\}_2]$ (48 mg, 0.08 mmol) and $Ph_2PNHCH_2C_6H_4CH_2NHPPh_2$ (39 mg, 0.08 mmol) were dissolved in dry CH_2Cl_2 (5 cm^3) and stirred for 2 hours. The orange solution was filtered through Celite to remove a small amount of insoluble material before reducing the volume to 0.5 cm^3 and addition of diethyl ether (10 cm^3) to precipitate an orange solid that was isolated by filtration and dried *in vacuo*. Yield 68 mg, 78 %. Microanalysis: Found (calculated for $C_{52}H_{60}N_2P_2Rh_2Cl_4.0.25CH_2Cl_2$) C 54.76 (54.86), H 5.31 (5.33), N 2.41 (2.45) %. $^{31}P\{^1H\}$ NMR ($CDCl_3$) 66.4 ppm $^1J(^{31}P\text{-}^{103}Rh)$ 148 Hz. ^1H ($CDCl_3$) δ 1.3 (s, 30 H, CH_3), 1.5 (m, 4 H, CH_2N), 4.1 (d, 2 H, $^2J(^{31}P\text{-}^1H)$ 8 Hz, NH), 7.2-8.0 (m, 24 H, aromatics) ppm. IR (KBr): 3300, 1434, 996, 282, 245 cm^{-1}. EI^+ MS: *m/z* 1145 $[M + Na]^+$, 1087 $[M - Cl]^+$, 1049 $[M - 2Cl]^+$.

$[(RuCl(\mu\text{-}Cl)(\eta^6\text{-}p\text{-}MeC_6H_4{}^iPr)(Ph_2PNHCH_2))_2C_6H_4]$. (25): $[\{RuCl(\mu\text{-}Cl)(\eta^6\text{-}p\text{-}MeC_6H_4{}^iPr)\}_2]$ (47 mg, 0.08 mmol) and $Ph_2PNHCH_2C_6H_4CH_2NHPPh_2$ (39 mg, 0.08 mmol) were dissolved in dry CH_2Cl_2 (5 cm^3) and stirred for 1 hour. The orange solution was filtered through Celite to remove a small amount of insoluble material before reducing the volume to 0.5 cm^3 and addition of diethyl ether (10 cm^3) to precipitate an orange solid that was isolated by filtration and dried *in vacuo*. Yield 62 mg, 72 %. Microanalysis: Found (calculated for $C_{52}H_{58}N_2P_2Ru_2Cl_4$) C 55.53 (55.92), H 4.73 (5.23), N 2.46 (2.51) %. $^{31}P\{^1H\}$ NMR ($CDCl_3$) 61.1 ppm. ^1H ($CDCl_3$) δ 0.8 (m, 12 H, CH_3), 1.2 (m, 6 H, CH_3), 1.9 (m, 4 H, CH_2N), 2.5 (m, 2 H, CH), 4.1 (d, 2 H, $^2J(^{31}P\text{-}^1H)$ 8 Hz, NH), 7.2-8.0 (m, 32 H, aromatics) ppm. IR (KBr): 3367, 1434, 996, 281, 249 cm^{-1}. EI^+ MS: *m/z* 1139 $[M + Na]^+$.

[(Pd(η^3-C_3H_5)Cl(Ph_2PNHCH_2))$_2C_6H_4$]. (26): [{Pd(μ-Cl)(η^3-C_3H_5)}$_2$] (61 mg, 0.2 mmol) and $Ph_2PNHCH_2C_6H_4CH_2NHPPh_2$ (84 mg, 0.2 mmol) were dissolved in dry CH_2Cl_2 (5 cm^3) and stirred overnight. The reaction mixture was filtered through Celite to remove any insoluble inorganic material before reducing the solvent to 0.5 cm^3 and addition of diethyl ether (10 cm^3) to precipitate a yellow microcrystalline solid that was isolated by suction filtration. Yield 98 mg, 68 %. Microanalysis: Found (calculated for $C_{38}H_{40}N_2P_2Pd_2Cl_2$) C 52.34 (52.44), H 4.78 (4.63), N 3.45 (3.22) %. $^{31}P\{^1H\}$ NMR ($CDCl_3$) 58.1 ppm. ^1H ($CDCl_3$) δ 1.3 (m, 8 H, CH_2), 1.9 (m, 4 H, CH_2N), 2.5 (m, 2 H, CH), 4.1 (d, 2 H, $^2J(^{31}P\text{-}^1H)$ 8 Hz, NH), 7.2-8.0 (m, 24 H, aromatics) ppm. IR (KBr): 3246, 1433, 998, 276 cm^{-1}. EI^+ MS: *m/z* 835 $[M - Cl]^+$.

[(RhCl(C_8H_{12})(Ph_2PNHCH_2))$_2C_6H_4$]. (27): [{Rh(cod)Cl}$_2$] (49 mg, 0.1 mmol) and $Ph_2PNHCH_2C_6H_4CH_2NHPPh_2$ (50 mg, 0.1 mmol) were dissolved in dry toluene (5 cm^3) and stirred for 2 hour. The solution was filtered through Celite to remove a small amount of insoluble material before reducing the volume to 0.5 cm^3 and addition of hexane (20 cm^3) to precipitate a yellow solid that was isolated by filtration and dried *in vacuo*. Yield 56 mg, 57 %. Microanalysis: Found (calculated for $C_{48}H_{54}N_2P_2Rh_2Cl_2.CH_2Cl_2.CH_2Cl_2$) C 54.66 (54.37), H 5.32 (5.21), N 2.89 (2.59) %. $^{31}P\{^1H\}$ NMR ($CDCl_3$) 62.3 ppm, $^1J(^{31}P\text{-}^{103}Rh)$ 157 Hz. ^1H ($CDCl_3$) δ 1.8 (m, 24 H, C_8H_{12}), 1.9 (m, 4 H, CH_2N), 4.1 (d, 2 H, $^2J(^{31}P\text{-}^1H)$ 8 Hz, NH), 7.2-8.0 (m, 24 H, aromatics) ppm. IR (KBr): 3289, 1434, 995, 279 cm^{-1}. EI^+ MS: *m/z* 961 $[M - Cl]^+$.

[(AuCl(Ph_2PNHCH_2))$_2C_4H_6$]. (28): [AuCl(tht)] (116 mg, 0.4 mmol) was dissolved in dry CH_2Cl_2 (5 cm^3) and $Ph_2PNHCH_2C_6H_4CH_2NHPPh_2$ (91 mg, 0.2 mmol) was added in one portion before stirring for 30 minutes. The colourless solution was filtered through Celite to remove a small amount of insoluble material before reducing

the volume to 2 cm^3 precipitate a colourless solid that was isolated by suction filtration and dried *in vacuo*. Yield 88 mg, 43 %. Microanalysis: Found (calculated for $C_{32}H_{30}N_2P_2Au_2Cl_2$) C 39.98 (39.65), H 3.28 (3.12), N 2.94 (2.89) %. $^{31}P\{^1H\}$ NMR ($CDCl_3$) 61.1 ppm. ^1H ($CDCl_3$) δ 1.6 (s, 4 H, CH_2N), 4.2 (d, 2 H, $^2J(^{31}P\text{-}^1H)$ 10 Hz, NH), 7.2-8.0 (m, 24 H, aromatics) ppm. IR (KBr): 3279, 1435, 997, 323 cm^{-1}. EI^+ MS: *m/z* 991 $[M + Na]^+$, 933 $[M - Cl]^+$.

References.

1. S. M. Aucott, *Coordination Chemistry of Aminophosphine Ligands, Ph. D. Thesis, University of Loughborough*, 1999.
2. M. K. Copper; J. M. Downes; P. A. Duckworth; E. R. T. Tiekink, *Aust. J. Chem.*, 1992, **45**, 595.
3. J. Heinicke; A. Tzschach, *J. Pract. Chem.*, 1983, **325**, 232.
4. J. Heinicke; R. Kadryov; M. K. Kindermann; M. Kloss; A. Fischer; P. G. Jones, *Chem. Ber.*, 1996, **129**, 1061.
5. F. E. Wood; M. M. Olmstead; A. L. Balch, *J. Am. Chem. Soc.*, 1983, **105**, 6332.
6. F. E. Wood; J. Hvoslef; H. Hope; A. L. Balch, *Inorg. Chem.*, 1984, **23**, 4309.
7. K. G. Gaw; M. B. Smith; J. W. Steed, *J. Organomet. Chem.*, 2002, **664**, 294.
8. A. M. Z. Slawin; J. Wheatley; M. V. Wheatley; J. D. Woollins, *Polyhedron*, 2003, **22**, 1397.
9. R. Uson; A. Laguna; M. Laguna, *Inorg. Synth.*, 1991, **28**, 346.
10. D. Drew; J. R. Doyle, *Inorg. Synth.*, 1991, **28**, 346.
11. J. X. McDermott; J. F. White; G. M. Whiteside, *J. Am. Chem. Soc.*, 1976, **60**, 6521.

12. M. A. Bennett; T. N. Huang; T. W. Matheson, *Inorg. Synth.*, 1982, **21**, 74.

13. G. Giordano; R. H. Crabtree, *Inorg. Synth.*, 1979, **19**, 218.

14. C. White; A. Yates; P. M. Maitlis, *Inorg. Synth.*, 1992, **29**, 228.

15. W. Baratta; P. S. Pregosin, *Inorg. Chim. Acta.*, 1993, **209**, 85.

16. J. Chatt; R. G. Wilkins, *J. Chem. Soc.*, 1952, 273.

CHAPTER 3.1: PREPARATION AND COORDINATION CHEMISTRY OF N-ALLYLAMINOPHOSPHINE

3.1.1 Introduction

Phospho-alkenes have the potential to coordinate via the phosphorus atom or the through the olefin. Coutinho *et al*[1] reacted a variety of phosphido-bridged complexes, $(OC)_4M(\mu\text{-}PPh_2)_2RhH(CO)(PPh_3)$, with the phosphinoalkenes $Ph_2P(CH_2)_nCH{=}CH_2$ where M = Cr, Mo or W and n = 1-3. In these reactions the olefin undergoes hydroformylation, which is of great interest today in commercial processes including the Rhone-Poulenc/Ruhrchemie aqueous-based system[2]. Furthermore as work continues to prepare ligands that lead to greater regioselectivity[3], ease of catalyst recovery[4] and enantioselectivity[5] it is necessary to investigate other potentially hemilabile ligands to increase the success and efficiency of current processes.

In this work we report the preparation of a new phosphine that contains an olefinic side chain and the potential to act as a hemilabile ligand. Illustrative coordination complexes have been prepared.

Results and Discussion

3.1.2 *Synthesis and chalcogen derivatives of $(C_3H_5)NHPPh_2$* ***29***

Reaction of allylamine with one equivalent of Ph_2PCl in the presence of NEt_3, proceeds in thf to give **29** which was isolated (41 %) by filtration from $Et_3NH^+Cl^-$ as a colourless oil that was purified by distillation (132 °C, 0.2 mmHg). After storing under nitrogen at –18 °C a colourless waxy solid formed

(41 % yield). The $^{31}P\{^{1}H\}$ NMR spectrum of (**29**) consists of a singlet at δ_P 42.5 ppm. The EI^+ mass spectrum gave the expected fragmentation pattern and parent ion observed at *m/z* 242. The microanalysis gave satisfactory results for the suggested structure. The chalcogenides of $Ph_2PNH(C_3H_5)$ were prepared easily.

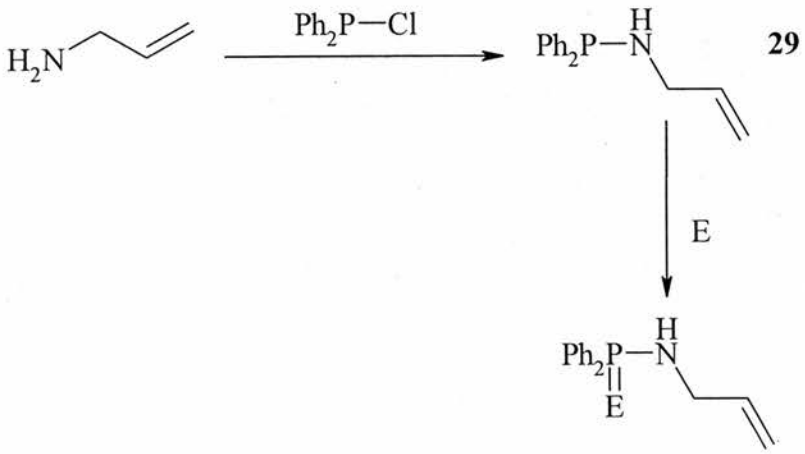

Scheme 3.1.1. Formation of $Ph_2PNH(C_3H_5)$ and $Ph_2P(E)NH(C_3H_5)$ {E = O (**30**), S (**31**), Se (**32**)}.

The oxide $Ph_2P(O)NH(C_3H_5)$ (**30**) was prepared by addition of urea hydrogen peroxide to a dichloromethane solution of **29** whilst the sulfur (**31**) and selenide (**32**) analogues were prepared by the addition of elemental S or Se to the ligand in toluene. Microanalysis obtained for all the chalcogens prepared were satisfactory for the composition suggested for each compound. The EI^+ mass spectral data obtained for each chalcogen gave the expected parent ion and fragment pattern and the $^{31}P\{^{1}H\}$ NMR showed single resonances ($CDCl_3$) at δ_P 24.4 and 60.5 ppm for the oxide and sulfide respectively. The seleno analogue exhibited a single $^{31}P\{^{1}H\}$ NMR resonance ($CDCl_3$) at δ_P 58.1 ppm with selenium satellites $^{1}J(^{31}P\text{-}^{77}Se)$ 756 Hz which is typical for a P=Se group[6].

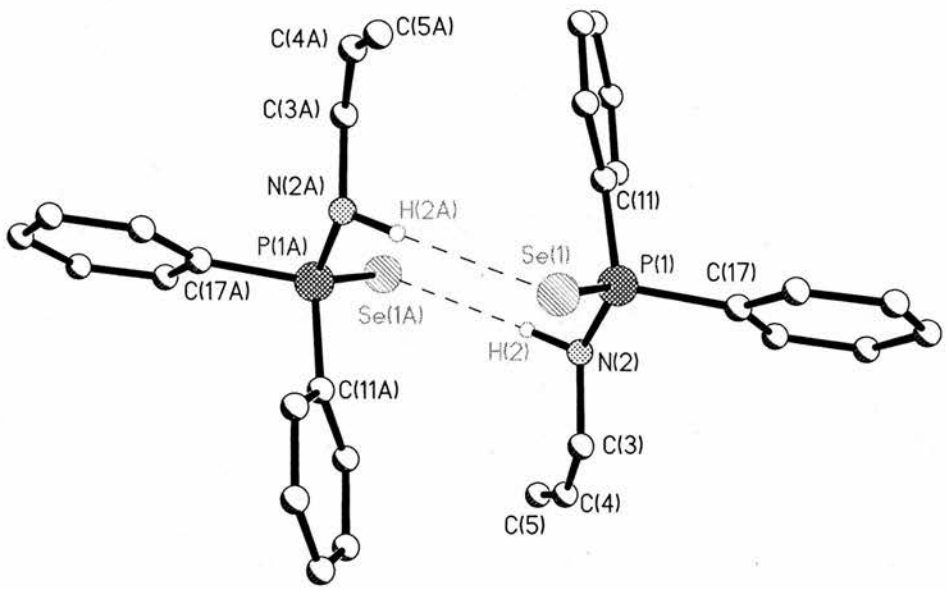

Figure 3.1.1. The X-ray structure of $Ph_2P(Se)NH(C_3H_5)$ (**32**) showing hydrogen-bonding.

Crystals of $Ph_2P(Se)NH(C_3H_5)$ suitable for X-ray crystallography were obtained by slow diffusion of a $CDCl_3$ solution with ether (Figure 3.1.1). Selected structural data are also given (Table 3.1.1). The crystal structure shows that in the solid state the molecule occurs as hydrogen-bonded dimers. The NH proton of one molecule is hydrogen-bonded to the selenium atom of a second and the selenium of the second interacts with the NH proton of the first, leading to a head to tail type arrangement of the molecules. The H(2)---Se(1A) distance is 2.63 Å with an intermolecular N(2)....Se(1A) separation of 3.61 Å and an N(2)-H(2)....Se(1A) angle of 174 °.

Table.3.1.1 Selected bond lengths (Å) and angles (°) for $Ph_2P(Se)NH(C_3H_5)$.

Selected bond lengths (Å) and angles (°)	*(32)*
P(1)-N(2)	1.657(4)
Se(1)-P(1)	2.1082(12)
P(1)-C(11)	1.806(4)
P(1)-C(17)	1.814(4)
N(2)-H(2)	0.9799(11)
N(2)-P(1)-C(11)	103.30(19)
N(2)-P(1)-C(17)	103.49(18)
C(11)-P(1)-C(17)	105.86(18)
C(11)-P(1)-Se(1)	113.32(13)
C(17)-P(1)-Se(1)	112.20(14)
N(2)-P(1)-Se(1)	117.48(15)
P(1)-N(2)-H(2)	116(3)

3.1.3 *Coordination chemistry of $Ph_2PNH(C_3H_5)$*

Reaction of $[PtCl_2(cod)]$ with $Ph_2PNH(C_3H_5)$ gives $[PtCl_2\{Ph_2PNH(C_3H_5)\}_2]$ (**33**) in very good yield (90 %). The FAB mass spectrum showed the expected parent ion and fragmentation pattern and the complex displays a single resonance with platinum satellites in the $^{31}P\{^1H\}$ NMR spectrum (δ_P 34.8 ppm, $^1J\{^{31}P\text{-}^{195}Pt\}$ 3949 Hz) which indicates the presence of Cl^- *trans* to P. The IR spectrum has ν_{NH} at 3054 cm^{-1}, $\nu_{C=C}$ and ν_{PN} at 1642 and 1000 cm^{-1} respectively and two ν_{PtCl} bands at 305 and 288 cm^{-1} which support the *cis* geometry.

Crystals of $[PtCl_2\{Ph_2PNH(C_3H_5)\}_2]$ suitable for X-ray crystallography were obtained by slow evaporation of a concentrated $CDCl_3$ solution (Figure 3.1.2). Selected structural data are also given (Table 3.1.2). The crystal structure of *cis*-$[PtCl_2\{Ph_2PNH(C_3H_5)\}_2]$ shows that the molecule is square planar at platinum. The angles, *cis* P(21)-Pt(1)-P(1) [98.81(4)°] and *cis* Cl(1)-Pt(1)-Cl(2) [84.53(4)°], are significantly larger and smaller respectively than the ideal 90° due to the existence of bulky R groups on the phosphorus. The platinum-phosphorus bond lengths are shown to be 2.263(10) Å for Pt(1)-P(1) and 2.251(9) Å for Pt(1)-P(2) which are consistent with other similar platinum complexes containing two ligands[7]. In the solid state the X-ray structure displays two intramolecular N-H…Cl H-bonds that form two five-membered rings. The N(13)-H(13)….Cl(1) distance is 2.34(4) Å with an N(13)-H(13)….Cl(1) angle of 127(4) °. The N(33)-H(33)….Cl(2) distance is equivalent at 2.34(4) Å and an N(33)-H(33)….Cl(2) angle of 128(4) °.

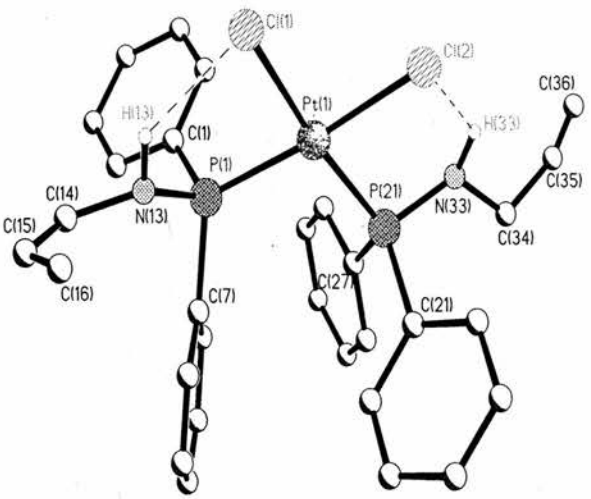

Figure 3.1.2. The X-ray structure of $[PtCl_2\{Ph_2PNH(C_3H_5)\}_2]$ (**33**).

Table 3.1.2. Selected bond lengths (Å) and angles (°) for

$[PtCl_2\{Ph_2PNH(C_3H_5)\}_2]$

Selected bond lengths (Å) and angles (°)	*(33)*
M(1)-Cl(1)	2.364(10)
M(1)-Cl(2)	2.365(12)
M(1)-P(1)	2.263(10)
M(1)-P(21)	2.251(9)
P(1)-N(13)	1.663(3)
P(21)-N(33)	1.660(4)
N(13)-C(14)	1.457(5)
N(33)-C(34)	1.463(6)
N(13)-H(13)----Cl(1)	3.039(3)
N(33)-H(33)----Cl(2)	3.050(4)
P(1)-M(1)-Cl(1)	88.22(4)
Cl(1)-M(1)-Cl(2)	84.53(4)
N(13)-P(1)-M(1)	108.03(12)
P(21)-M(1)-P(1)	98.81(4)
P(21)-M(1)-Cl(1)	172.97(3)
P(21)-M(1)-Cl(2)	88.45(4)
P(1)-M(1)-Cl(2)	172.59(4)
C(14)-N(13)-P(1)	125.3(3)
N(33)-P(21)-M(1)	109.64(13)
C(34)-N(33)-P(21)	123.0(3)

$[PdCl_2\{Ph_2PNH(C_3H_5)\}_2]$ (**34**) is prepared in a similar way to (**33**). The complex was isolated by suction filtration in a yield of 91 % and microanalysis gave satisfactory results. The expected fragmentation pattern and parent ion was observed in the FAB mass spectrum and contains M – Cl^- at 624 whilst the $^{31}P\{^1H\}$ NMR spectrum showed two peaks at 58.8 and 46.2 ppm which is indicative of *cis* and *trans* isomers. The IR bands observed at 3054, 1643 and 997 cm^{-1} represent ν_{NH}, $\nu_{C=C}$ and ν_{PN} with two ν_{PdCl} bands at 297 and 277 cm^{-1} respectively.

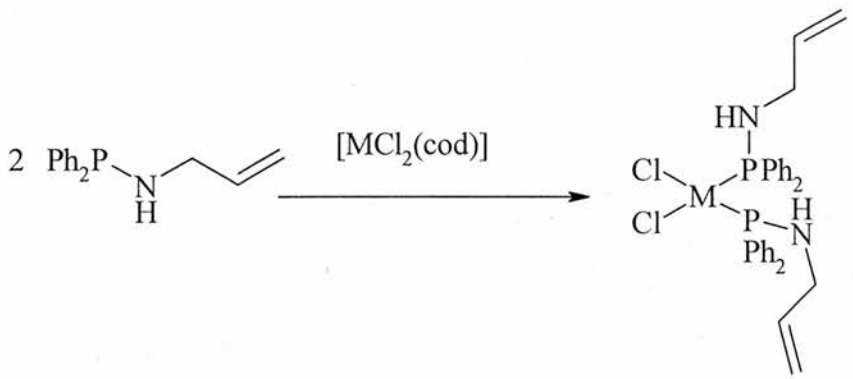

M = Pt (**33**), Pd (**34**)
cod = 1,5-cyclooctadiene

Scheme 3.1.2. Reaction of 2 $Ph_2PNH(C_3H_5)$ with $[MCl_2(cod)]$ (M = Pt, Pd; cod = C_8H_{12})).

The reaction of $Ph_2PNH(C_3H_5)$ with one equivalent of $[MCl_2(cod)]$ gave the expected chelated complexes **35** and **36** (where M = Pd and Pt respectively). $[PdCl_2\{Ph_2PNH(C_3H_5)\}]$ (**35**) is prepared in good yield and the $^{31}P\{^1H\}$ NMR showed a single peak (CD_2Cl_2) at δ_P 93.6 ppm. The FAB mass spectrum shows the expected parent ion and fragmentation pattern for the suggested structure and in the IR spectrum ν_{NH}, ν_{PN} and two ν_{PdCl} vibrations were observed at 3054, 996,

318 and 281 cm^{-1} respectively which indicated that olefinic bond forms a chelate on the metal centre. The $^{31}P\{^{1}H\}$ NMR (CD_2Cl_2) showed a single resonance at δ_P 63.5 ppm with platinum satellites, $^{1}J(^{31}P\text{-}^{195}Pt)$ 3481 Hz for **36**. The IR spectrum again shows that the olefinic bond is used in coordination on the Pt centre. The vibrations for ν_{NH}, ν_{PN} and two ν_{PtCl} are observed at 3055, 998, 328 and 289 cm^{-1} respectively. The FAB mass spectrum shows the expected parent ion and fragmentation pattern for the suggested structure.

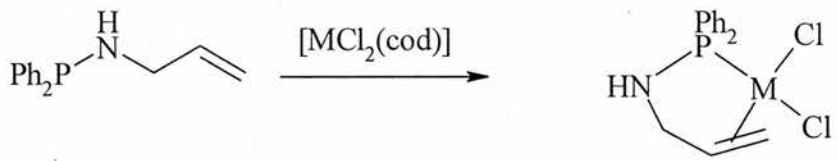

M = Pt (**36**), Pd (**35**)
cod = 1,5-cyclooctadiene

Scheme 3.1.3. Reaction of $Ph_2PNH(C_3H_5)$ with $[MCl_2(cod)]$ (M = Pt, Pd; cod = C_8H_{12})).

The reaction of [AuCl(tht)] with $Ph_2PNH(C_3H_5)$ gave the expected product $[AuCl\{Ph_2PNH(C_3H_5)\}]$ (**37**) in poor yield (29 %). The $^{31}P\{^{1}H\}$ NMR ($CDCl_3$) showed a single peak at δ_P 64.9 ppm and the microanalysis gave good results for the suggested structure. The IR spectrum showed the presence of bands at 3069, 1643, 996 and 323 cm^{-1} which correspond to ν_{NH}, $\nu_{C=C}$, ν_{PN} and ν_{AuCl} respectively and the FAB mass spectrum gave the expected fragmentation pattern and parent ion.

$[RuCl(\mu\text{-}Cl)(\eta^6\text{-}p\text{-}MeC_6H_4{}^{i}Pr)\{Ph_2PNH(C_3H_5)\}]$ (**38**) is prepared by dissolving $[\{RuCl(\mu\text{-}Cl)(\eta^6\text{-}p\text{-}MeC_6H_4{}^{i}Pr)\}_2]$ and $Ph_2PNH(C_3H_5)$ in dichloromethane in good yield (85 %). The microanalysis gave satisfactory

results for the suggested structure and the $^{31}P\{^{1}H\}$ NMR ($CDCl_3$) showed a single resonance at δ_P 61.3 ppm. The FAB mass spectrum showed the expected parent ion and fragmentation pattern with [M^+] at 547/9. In the IR spectrum vibrations at 3051, 1642, 996, 283 and 245 cm^{-1} correspond to ν_{NH}, $\nu_{C=C}$, ν_{PN} and two ν_{RuCl} respectively.

Crystals of [RuCl(μ-Cl)(η^6-*p*-$MeC_6H_4{}^iPr$){$Ph_2PNH(C_3H_5)$}] suitable for X-ray crystallography were obtained by slow diffusion of a $CDCl_3$/ether solution (Figure 3.1.3). Selected structural data are also given (Table 3.1.3). The molecular structure of [RuCl(μ-Cl)(η^6-*p*-$MeC_6H_4{}^iPr$){$Ph_2PNH(C_3H_5)$}] contains one ligand and is bound to the ruthenium metal via phosphorus with a P(1)-Ru(1) bond length of 2.3404(11). The NH proton interacts with two chlorine atoms as shown in Figure 3.1.3. The N(2)-H(2)....Cl(2) distance is 2.74(4) Å and an N(2)-H(2)....Cl(2) angle of 110(3) °.

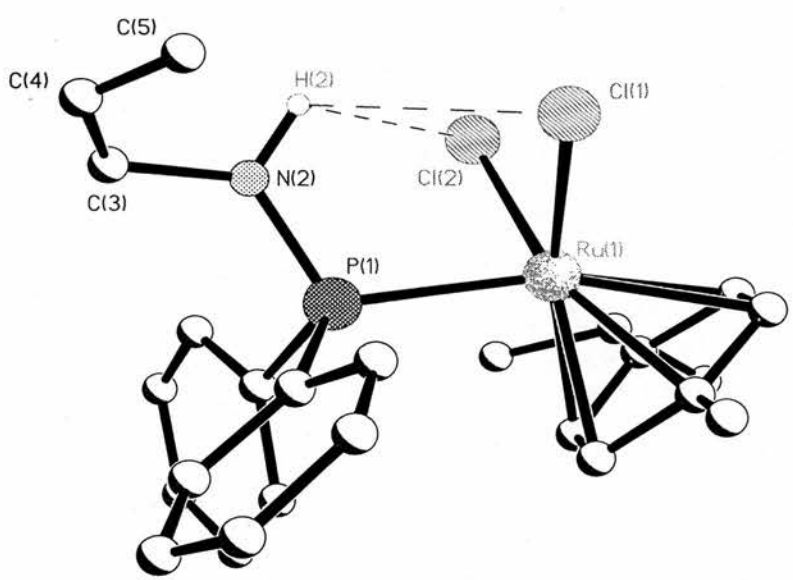

Figure. 3.1.3. The X-ray structure of [RuCl(μ-Cl)(η^6-*p*-$MeC_6H_4{}^iPr$){$Ph_2PNH(C_3H_5)$}] (**38**) showing hydrogen-bonding.

Table 3.1.3. Selected bond lengths (Å) and angles (°) for [RuCl(μ-Cl)(η^6-*p*-$MeC_6H_4{}^iPr$){$Ph_2PNH(C_3H_5)$}]

Selected bond lengths (Å) and angles (°)	*(38)*
M(1)-Cl(1)	2.4314(11)
M(1)-Cl(2)	2.4037(12)
M(1)-P(1)	2.3404(11)
P(1)-N(2)	1.657(3)
P(1)-C(11)	1.823(4)
P(1)-C(17)	1.827(4)
N(2)-H(2)	0.9799(11)
N(2)-H(2)----Cl(2)	3.202(3)
P(1)-M(1)-Cl(1)	88.54(4)
P(1)-M(1)-Cl(2)	85.35(4)
Cl(2)-M(1)-Cl(1)	87.06(4)
N(2)-P(1)-C(11)	105.94(18)
N(2)-P(1)-C(17)	106.69(17)
C(11)-P(1)-C(17)	104.36(18)
N(2)-P(1)-M(1)	112.64(12)
C(11)-P(1)-M(1)	111.88(12)
C(17)-P(1)-M(1)	114.61(13)
P(1)-N(2)-H(2)	118(3)
N(2)-H(2)----Cl(2)	110(3)

The complex, [Pt{$Ph_2PNH(C_3H_8O)$}$_2$] (**39**), was prepared by reaction of K^{t}BuO in methanol with complex **33** in good yield (51 %). The $^{31}P\{^1H\}$ NMR

showed a single peak at δ_P 91.4 ppm with platinum satellites at $^1J(^{31}P\text{-}^{195}Pt)$ 2294 Hz. The IR spectrum shows typical vibrations at 2873-2809 cm^{-1}, which correspond to ν_{OMe} stretches along with vibrations at 3069 and 997, which are assigned to ν_{NH} and ν_{PN} respectively. The FAB mass spectral analysis gave the expected parent ion and fragmentation pattern and the microanalysis shows good results for the suggested structure. The absence of the $\nu_{C=C}$ vibration in the IR spectrum suggests that the double bond is used in coordination to the metal centre.

Crystals of $[Pt\{Ph_2PNH(C_3H_8O)\}_2]$ (**39**) suitable for X-ray crystallography were obtained by slow diffusion of a $CDCl_3$/ether solution (Figure 3.1.4). Selected structural data are also given (Table 3.1.4). The crystal structure shows that in the solid state the molecule occurs as hydrogen-bonded dimers. The NH proton of one molecule is hydrogen-bonded to the oxygen atom of a second and the oxygen of the second interacts with the NH proton of the first, leading to a head to tail type arrangement of the molecules. The H(1N)---O(5) distance is 2.241(19) Å with an intermolecular N(1)….O(5) separation of 3.164(4) Å and an N(1)-H(1N)….O(5) angle of 157(4) °.

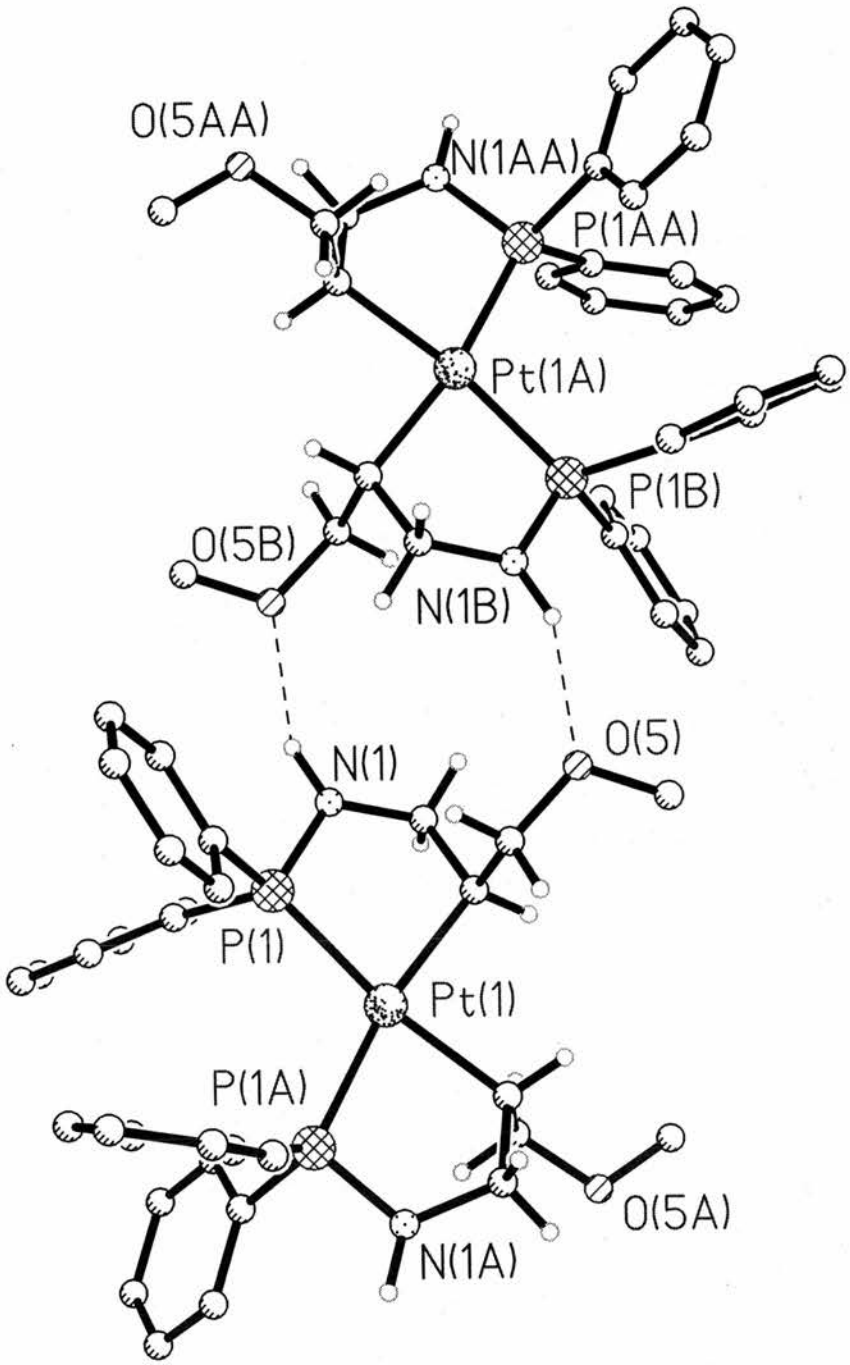

Figure. 3.1.4. The X-ray structure of [Pt{$Ph_2PNH(C_3H_5OMe)_2$}] (**39**) showing hydrogen bonding.

Table 3.1.4. Selected bond lengths (Å) and angles (°) for

$[Pt\{Ph_2PNH(C_3H_5OMe)_2\}]$

Selected bond lengths (Å) and angles (°)	*(39)*
M(1)-C(3)	2.113(4)
M(1)-P(1)	2.2743(9)
P(1)-N(1)	1.664(3)
P(1)-C(7)	1.832(4)
P(1)-C(13)	1.827(4)
N(1)-C(2)	1.451(5)
C(3)-M(1)-P(1)	81.56(11)
N(1)-P(1)-C(13)	105.68(18)
N(1)-P(1)-C(7)	106.47(18)
C(13)-P(1)-C(7)	102.15(17)
N(1)-P(1)-M(1)	104.19(12)
C(13)-P(1)-M(1)	119.72(11)
C(7)-P(1)-M(1)	117.51(12)
C(2)-N(1)-P(1)	117.6(3)

The reaction of $Ph_2PNH(C_3H_5)$ with $[\{RhCl(\mu\text{-}Cl)(\eta^5\text{-}C_5Me_5)\}_2]$ and $[\{IrCl(\mu\text{-}Cl)(\eta^5\text{-}C_5Me_5)\}_2]$ proceeded in similar fashion to the reaction with $[\{RuCl(\mu\text{-}Cl)(\eta^6\text{-}p\text{-}MeC_6H_4{}^iPr)\}_2]$ to prepare the complexes $[RhCl(\mu\text{-}Cl)(\eta^5\text{-}C_5Me_5)\{Ph_2PNH(C_3H_5)\}]$ (**40**) and $[IrCl(\mu\text{-}Cl)(\eta^5\text{-}C_5Me_5)\{Ph_2PNH(C_3H_5)\}]$ (**41**) in good yields (67 % and 65 % respectively). The microanalytical data obtained for each complex was satisfactory for the suggested structure and the FAB mass spectral data obtained showed the expected parent ions and

fragmentation patterns for each complex. The $^{31}P\{^{1}H\}$ NMR ($CDCl_3$) for **40** shows a single resonance at δ_P 66.4 ppm with rhodium satellites at $^{1}J(^{31}P\text{-}^{103}Rh)$ 148 Hz. In **41** a single resonance in the $^{31}P\{^{1}H\}$ NMR ($CDCl_3$) is observed at δ_P 34.5 ppm. The IR spectrum for both **40** and **41** show the expected identification peaks for the ν_{NH}, $\nu_{C=C}$, ν_{PN} and two ν_{MCl} vibrations.

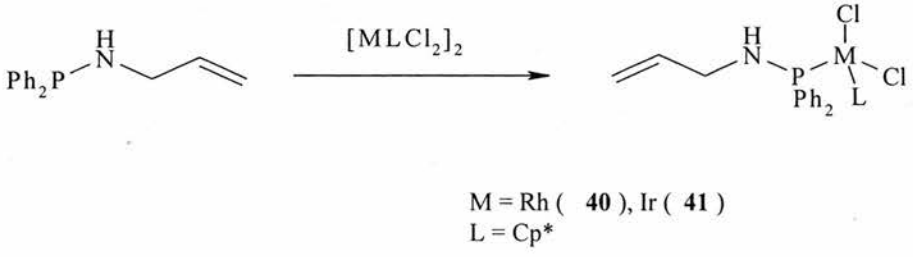

Scheme 3.1.4. Reaction of $Ph_2PNH(C_3H_5)$ with $[\{MLCl_2\}_2]$ (M = Rh, Ir; L = η^5-C_5Me_5).

Upon slow addition of $[\{Pt(PEt_3)Cl_2\}_2]$ to $Ph_2PNH(C_3H_5)$, $[Pt(PEt_3)Cl_2\{Ph_2PNH(C_3H_5)\}]$ (**42**) was obtained in a yield of 59 %. Microanalysis gave satisfactory results with the $^{31}P\{^{1}H\}$ NMR ($CDCl_3$) displaying two phosphorus environments at δ_{PA} 34.2 ppm and δ_{PX} 7.3 ppm with platinum satellites at $^{1}J(^{31}P_A\text{-}^{195}Pt)$ 3979 Hz and $^{1}J(^{31}P_X\text{-}^{195}Pt)$ 3479 Hz. The phosphorus coupling in this complex was shown at $^{2}J(^{31}P_A\text{-}^{31}P_X)$ 19 Hz, which is typical for complexes of this type. The IR spectrum contains bands at 3072, 1641, 1002, 309 and 283 cm^{-1} which represent the ν_{NH}, $\nu_{C=C}$, ν_{PN} and two ν_{PtCl} respectively. Crystals of $[PtPEt_3Cl_2\{Ph_2PNH(C_3H_5)\}]$ suitable for X-ray crystallography were obtained by slow diffusion of a $CDCl_3$/ether solution (Figure 3.1.5). Selected structural data are also given (Table 3.1.5).

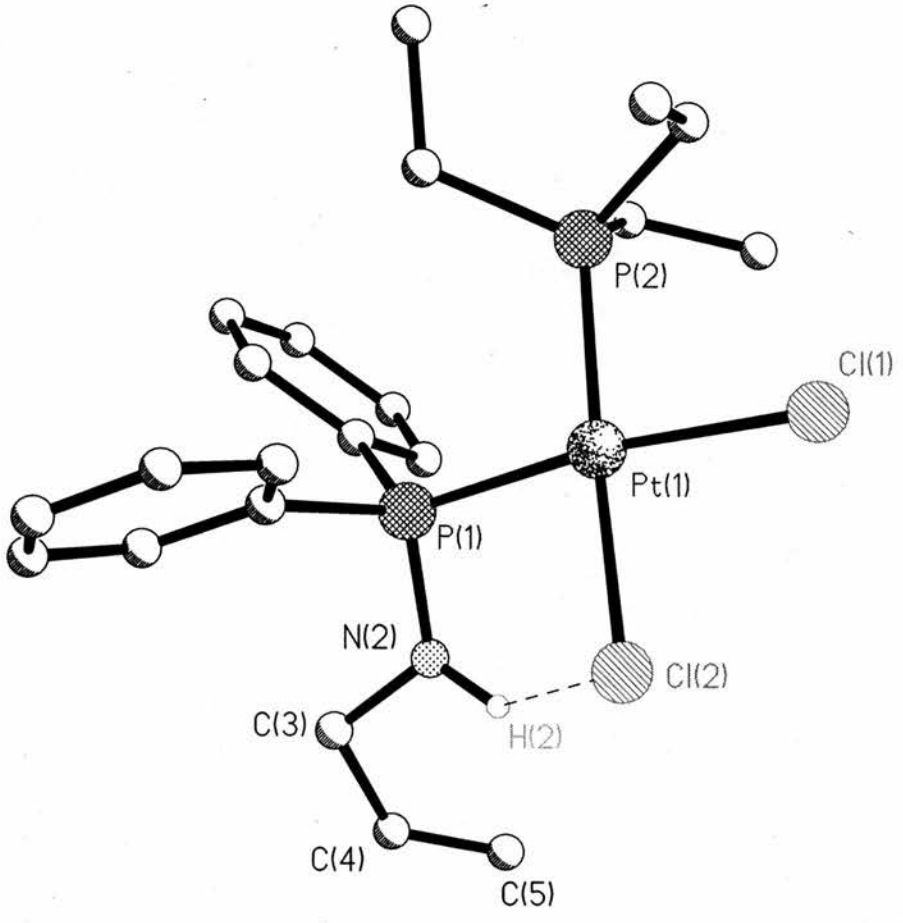

Figure. 3.1.5. The X-ray structure of [Pt(PEt_3)Cl_2{$Ph_2PNH(C_3H_5)$}] (**42**).

The crystal structure of [Pt(PEt_3)Cl_2{$Ph_2PNH(C_3H_5)$}] (**42**) shows that the molecule is square planar at platinum. The molecular structure contains one ligand and is bound to the platinum metal via phosphorus with a P(1)-Pt(1) bond length of 2.3404(11). The NH proton interacts with the chlorine atom as shown in Figure 3.1.5. The N(2)-H(2)….Cl(2) distance is 2.74(4) Å and an N(2)-H(2)….Cl(2) angle of 110(3) ^{o}.

Table 3.1.5. Selected bond lengths (Å) and angles (°) for

$[Pt(PEt_3)Cl_2\{Ph_2PNH(C_3H_5)\}]$

Selected bond lengths (Å) and angles (°)	*(42)*
M(1)-Cl(1)	2.4314(11)
M(1)-Cl(2)	2.4037(12)
M(1)-P(1)	2.3404(11)
P(1)-N(2)	1.657(3)
P(1)-C(11)	1.823(4)
P(1)-C(17)	1.827(4)
N(2)-H(2)	0.9799(11)
N(2)-H(2)----Cl(2)	2.74(4)
P(1)-M(1)-Cl(1)	88.54(4)
P(1)-M(1)-Cl(2)	85.35(4)
Cl(2)-M(1)-Cl(1)	87.06(4)
N(2)-P(1)-C(11)	105.94(18)
N(2)-P(1)-C(17)	106.69(17)
C(11)-P(1)-C(17)	104.36(18)
N(2)-P(1)-M(1)	112.64(12)
C(11)-P(1)-M(1)	111.88(12)
C(17)-P(1)-M(1)	114.61(13)
P(1)-N(2)-H(2)	118(3)
N(2)-H(2)----Cl(2)	110(3)

$[Pt(PPhMe_2)Cl_2\{Ph_2PNH(C_3H_5)\}]$ (**43**) is prepared in a similar way to **42** in good yield (62 %). The $^{31}P\{^1H\}$ NMR ($CDCl_3$) showed two phosphorus

signals at δ_{PA} 35.3 ppm and δ_{PX} −14.2 ppm with platinum satellites at $^{1}J(^{31}P_{A}$-$^{195}Pt)$ 3878 Hz and $^{1}J(^{31}P_{X}$-$^{195}Pt)$ 3625 Hz. There is again splitting of the signals due to the presence of two phosphorus atoms and this is found at $^{2}J(^{31}P_{A}$-$^{31}P_{X})$ 19 Hz. This is similar to the splitting observed in complex **42**. In the IR spectrum bands are observed at 3053, 1642, 1000, 313 and 283 cm^{-1} which correspond to ν_{NH}, $\nu_{C=C}$, ν_{PN} and two ν_{PtCl} vibrations.

Crystals of $[Pt(PPhMe_2)Cl_2\{Ph_2PNH(C_3H_5)\}]$ suitable for X-ray crystallography were obtained by slow diffusion of a $CDCl_3$/ether solution (Figure 3.1.6). Selected structural data are also given (Table 3.1.6).

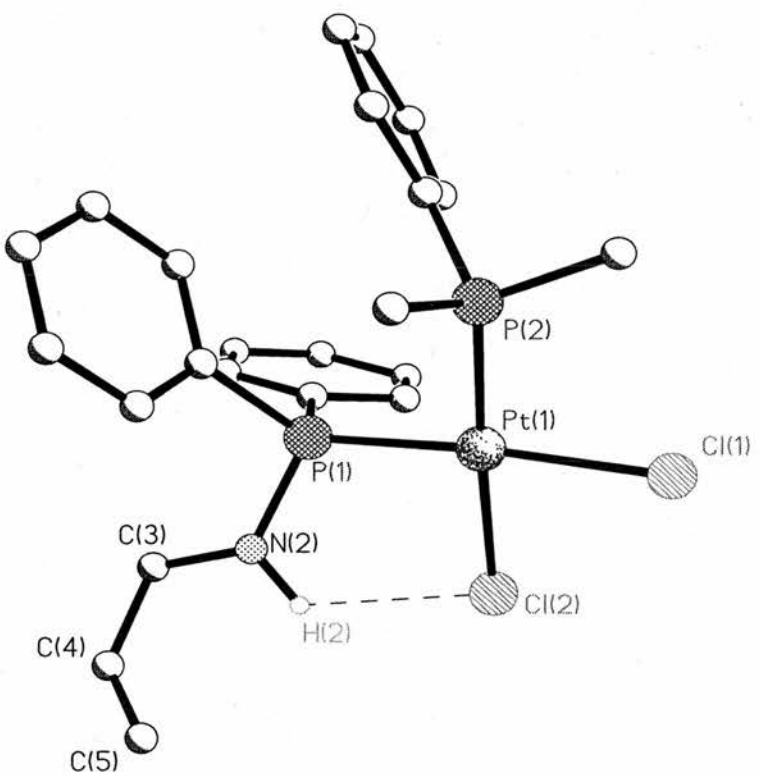

Figure. 3.1.6. The X-ray structure of $[Pt(PPhMe_2)Cl_2\{Ph_2PNH(C_3H_5)\}]$ (**43**).

The crystal structure of [Pt(PPhMe$_2$)Cl$_2${Ph$_2$PNH(C$_3$H$_5$)}] (**43**) shows that the molecule is square planar at platinum. The molecular structure contains one ligand and is bound to the platinum metal via phosphorus with a P(1)-Pt(1) bond length of 2.3404(11). The NH proton interacts with the chlorine atom as shown in Figure 3.1.6. The N(2)-H(2)....Cl(2) distance is 2.74(4) Å and an N(2)-H(2)....Cl(2) angle of 110(3) °.

Table 3.1.6. Selected bond lengths (Å) and angles (°) for

$[Pt(PPhMe_2)Cl_2\{Ph_2PNH(C_3H_5)\}]$

Selected bond lengths (Å) and angles (°)	*(43)*
M(1)-Cl(1)	2.4314(11)
M(1)-Cl(2)	2.4037(12)
M(1)-P(1)	2.3404(11)
P(1)-N(2)	1.657(3)
P(1)-C(11)	1.823(4)
P(1)-C(17)	1.827(4)
N(2)-H(2)	0.9799(11)
N(2)-H(2)----Cl(2)	2.74(4)
P(1)-M(1)-Cl(1)	88.54(4)
P(1)-M(1)-Cl(2)	85.35(4)
Cl(2)-M(1)-Cl(1)	87.06(4)
N(2)-P(1)-C(11)	105.94(18)
N(2)-P(1)-C(17)	106.69(17)
C(11)-P(1)-C(17)	104.36(18)
N(2)-P(1)-M(1)	112.64(12)
C(11)-P(1)-M(1)	111.88(12)
C(17)-P(1)-M(1)	114.61(13)
P(1)-N(2)-H(2)	118(3)
N(2)-H(2)----Cl(2)	110(3)

$[PdCl(C_{10}H_8N)\{Ph_2PNH(C_3H_5)\}]$ (**44**) was prepared by dropwise addition of $Ph_2PNH(C_3H_5)$ to a dichloromethane suspension of

[{PdCl($C_{10}H_8N$)}$_2$]. The microanalysis obtained gave satisfactory results for the structure suggested and the $^{31}P\{^1H\}$ NMR ($CDCl_3$) showed a single resonance at δ_P 65.0 ppm. The FAB mass spectrum gave the expected parent ion and fragmentation pattern and the IR spectrum showed bands at 3049, 1639, 993 and 289 cm^{-1}, which were assigned to ν_{NH}, $\nu_{C=C}$, ν_{PN} and ν_{PdCl} vibrations.

Table 3.1.7. Characterisation data for $Ph_2PNH(C_3H_5)$ and its derivatives. ([a] $^1J\{^{31}P\text{-}^{77}Se\}$ 756 Hz.). ([b] $^1J\{^{31}P\text{-}^{195}Pt\}$ 3949 Hz), ([c] $^1J\{^{31}P\text{-}^{195}Pt\}$ 3481 Hz), ([d] $^1J\{^{31}P\text{-}^{195}Pt\}$ 2294 Hz), ([e] $^1J\{^{31}P\text{-}^{103}Rh\}$ 148 Hz), ([f] $^1J\{^{31}P_A\text{-}^{195}Pt\}$ 3979 Hz, $^1J\{^{31}P_X\text{-}^{195}Pt\}$ 3479 Hz, $^2J(^{31}P_A\text{-}^{31}P_X)$ 19 Hz, ([g] $^1J\{^{31}P_A\text{-}^{195}Pt\}$ 3878 Hz, $^1J\{^{31}P_X\text{-}^{195}Pt\}$ 3625 Hz, $^2J(^{31}P_A\text{-}^{31}P_X)$ 19 Hz

Compound	*$^{31}P\text{-}\{^1H\}$ NMR*	*IR/cm^{-1}*					*Microanalysis/ % Found (calc.)*		
	δ_p/ppm	ν_{PN}	ν_{NH}	$\nu_{C=C}$	$\nu_{P=E}$	ν_{MCl}	C	H	N
$Ph_2PNH(C_3H_5)$ (29)	42.5				-	-	72.27 (74.67)	7.37 (6.68)	5.58 (5.81)
$Ph_2P(O)NH(C_3H_5)$ (30)	24.4	993	3189	1641	1181	-	69.74 (70.03)	6.22 (6.27)	5.15 (5.44)
$Ph_2P(S)NH(C_3H_5)$ (31)	60.5	997	3170	1642	689	-	66.01 (65.91)	6.09 (5.90)	5.11 (5.12)

Table continue. Characterisation data for $Ph_2PNH(C_3H_5)$ and its derivatives.									
$Ph_2P(Se)NH(C_3H_5)$ (32)	58.1[a]	991	3177	1644	573	-	55.97	5.25	4.43
							(56.07)	(5.02)	(4.36)
$[PtCl_2\{Ph_2PNH(C_3H_5)\}_2]$ (33)	34.8[b]	1000	3054	1642	-	305,	48.23	4.10	3.65
						288	(48.14)	(4.31)	(3.74)
$[PdCl_2\{Ph_2PNH(C_3H_5)\}_2]$ (34)	58.8, 46.2	997	3054	1643	-	297,	54.80	4.67	4.06
						277	(54.61)	(4.89)	(4.25)
$[PdCl_2\{Ph_2PNH(C_3H_5)\}]$ (35)	93.6	996	3054	-	-	318,	43.95	4.26	2.70
						281	(43.04)	(3.85)	(3.35)
$[PtCl_2\{Ph_2PNH(C_3H_5)\}]$ (36)	63.5[c]	998	3055	3051	-	328,	36.53	2.99	2.60
						289	(35.52)	(3.18)	(2.76)
$[AuCl\{Ph_2PNH(C_3H_5)\}]$ (37)	64.9	996	3069	1643	-	323	37.98	2.76	3.07
							(38.03)	(3.40)	(2.96)
$[RuCl(\mu\text{-}Cl)(\eta^6\text{-}p\text{-}MeC_6H_4{}^iPr)\{(Ph_2PNH(C_3H_5)\}]$ (38)	61.3	996	3051	1642	-	290,	55.71	5.62	2.71
						283	(54.85)	(5.52)	(2.56)

Table continue. Characterisation data for $Ph_2PNH(C_3H_5)$ and its derivatives.									
$[Pt\{Ph_2PNH(C_4H_8O)\}_2]$ (39)	91.4[d]	997	3069	-	-	-	52.06	4.60	3.70
							(51.96)	(5.18)	(3.79)
$[RhCl(\mu\text{-}Cl)(\eta^5\text{-}C_5Me_5)\{(Ph_2PNH(C_3H_5)\}]$ (40)	66.4[e]	995	3063	1642	-	279, 267	54.32 (54.56)	5.78 (5.68)	2.44 (2.55)
$[IrCl(\mu\text{-}Cl)(\eta^5\text{-}C_5Me_5)\{(Ph_2PNH(C_3H_5)\}]$ (41)	34.5	994	3058	1640	-	291, 280	47.07 (46.95)	4.85 (4.89)	2.13 (2.19)
$[Pt(PEt_3Cl_2\{Ph_2PNH(C_3H_5)\}]$ (42)	34.2, 7.3[f]	1002	3072	1641	-	309, 283	40.61 (40.38)	4.38 (5.01)	2.49 (2.24)
$[Pt(PMe_2Ph)Cl_2\{Ph_2PNH(C_3H_5)\}]$ (43)	35.3, -14.2[g]	1000	3053	1642	-	313, 283	42.99 (42.85)	2.26 (4.22)	2.08 (2.17)
$[PdCl(C_{10}H_8N)\{Ph_2PNH(C_3H_5)\}]$ (44)	65.0	993	3049	1639	-	289	56.93 (57.16)	3.93 (4.60)	5.24 (5.33)

Experimental

General experimental conditions and instruments were as set out on page xvii. Unless otherwise stated, all reactions were carried out under an oxygen-free nitrogen atmosphere using standard Schlenk techniques. Diethyl ether and thf were purified by reflux over sodium-benzophenone and distillation under nitrogen. Dichloromethane was heated to reflux over calcium hydride and distilled under nitrogen. Toluene and hexane were heated to reflux over sodium and distilled under nitrogen. The complexes [PtMeX(cod)] (X = Cl or Me)[8], $[\{Pd(\mu\text{-}Cl)(\eta^3\text{-}C_3H_5)\}_2]$[9], $[Cu(MeCN)_4][PF_6]$[10], [AuCl(tht)] (tht = tetrahydrothiophene)[11], $[MCl_2(cod)]$ (M = Pt or Pd; cod = cycloocta-1,5-diene)[12, 13], $[\{RuCl(\mu\text{-}Cl)(\eta^6\text{-}p\text{-}MeC_6H_4{}^iPr)_2\}]$[14], $[\{Rh(\mu\text{-}Cl)(cod)\}_2]$[15], $[\{MCl(\mu\text{-}Cl)(\eta^5\text{-}C_5Me_5)\}_2]$ (M = Rh or Ir)[16], $[\{PtCl(\mu\text{-}Cl)(PMe_2Ph)\}_2]$[17], $[\{PtCl(\mu\text{-}Cl)(PMe_2Ph)\}_2]$[18] and $[\{Pd(\mu\text{-}Cl)(C_{10}H_8N)\}_2]$[19] were prepared using literature procedures. Chlorodiphenylphopshine and allylamine were distilled prior to use. NEt_3 (99 % purity), ^tBuOK (95 % purity), H_2O_2 (30 wt. % in H_2O) and reagent grade KBr were used without further purification. Infra-red spectra were recorded as KBr discs in the range 4000-200 cm^{-1} on a Perkin-Elmer 2000 FTIR/RAMAN spectrometer. NMR spectra were recorded on a Gemini 2000 spectrometer (operating at 121.4 MHz for ^{31}P and 300 MHz for ^1H). Microanalyses were performed by the St. Andrews University service and mass spectra by the Swansea Mass Spectrometer Service.

$Ph_2PNH(C_3H_5)$. (29): Allylamine (3.671 g, 64.3 mmol) and triethylamine (6.831 g, 67.5 mmol) were added together in dry thf (50 cm^3). Chlorodiphenylphosphine (14.894 g, 67.5 mmol) in dry thf (50 cm^3) was added

dropwise with stirring overnight. Triethylamine hydrochloride was removed by filtration under nitrogen and the solvent removed in vacuo to yield a colourless oil which was purified by distillation (132 °C, 0.2 mmHg) and storing under nitrogen in the freezer which yielded a colourless waxy solid. Yield 6.283 g, 41 %. Microanalysis: Found (calculated for $C_{15}H_{16}NP$) C 72.27 (74.67), H 7.37 (6.68), N 5.58 (5.81) %. $^{31}P\{^{1}H\}$ NMR ($CDCl_3$): 42.5 ppm. ^{1}H NMR ($CDCl_3$) δ 7.4-7.2 (m, 10 H, aromatic), 5.8 (m, 1 H, CH), 5.2 (q, 1 H, CH_2), 5.1 (q, 1 H, CH_2), 3.5 (m, 2 H, NCH_2) and 1.9 (s, 1 H, NH) ppm. EI^+ MS: m/z 242 $[M]^+$.

$Ph_2P(O)NH(C_3H_5)$. (30): $Ph_2PNH(C_3H_5)$ (461 mg, 1.9 mmol) was dissolved in dichloromethane (10 cm^3). Urea hydrogen peroxide (180 mg, 1.9 mmol) was added and the reaction mixture was stirred overnight. The product was extracted from the CH_2Cl_2 by addition of distilled water, washed with CH_2Cl_2 (3x 5 cm^3), dried over magnesium sulfate and evaporated to dryness to yield a colourless solid. Yield 338 mg, 67 %. Microanalysis: Found (calculated for $C_{15}H_{16}NOP$) C 69. 74 (70.03), H 6.22 (6.27), N 5.15 (5.44) %. $^{31}P\{^{1}H\}$ NMR ($CDCl_3$): 24.4 ppm. ^{1}H ($CDCl_3$) δ 7.4-7.2 (m, 10 H, aromatic), 5.9 (m, 1 H, CH), 5.3 (q, 1 H, CH_2), 5.1 (q, 1 H, CH_2), 3.5 (m, 2 H, NCH_2) and 2.9 (br s, 1 H, NH) ppm. EI^+ MS: *m/z* 257 [M]. IR(KBr disc): 3189, 1641, 1181, 993 cm^{-1}.

$Ph_2P(S)NH(C_3H_5)$. (31): $Ph_2PNH(C_3H_5)$ (420 mg, 1.7 mmol) and elemental sulfur (56 mg, 1.7 mmol) were dissolved in dry toluene (10 cm^3) to yield a yellow solution which was stirred overnight. The solvent was reduced to 1 cm^3 before addition of hexane (10 cm^3) to precipitate a colourless solid that was isolated by filtration. Yield 246 mg, 52 %. Microanalysis: Found (calculated for $C_{15}H_{16}NPS$) C 66.01 (65.91), H 6.09 (5. 90), N 5.11 (5.12) %. $^{31}P\{^{1}H\}$ NMR

($CDCl_3$): 60.5 ppm. ^1H NMR ($CDCl_3$) δ 7.4-7.2 (m, 10 H, aromatic), 5.9 (m, 1 H, CH), 5.2 (q, 1 H, CH_2), 5.1 (q, 1 H, CH_2), 3.5 (m, 2 H, NCH_2) and 2.4 (br s, 1 H, NH) ppm. EI^+ MS: *m/z* 273 [M]. IR(KBr disc): 3170, 1642, 997, 689 cm^{-1}.

$Ph_2P(Se)NH(C_3H_5)$. (32): $Ph_2PNH(C_3H_5)$ (235 mg, 1.0 mmol) and grey selenium (77 mg, 1.0 mmol) were refluxed in dry toluene (10 cm^3) for 1 hour before cooling to room temperature and filtering through a Celite plug to remove any insoluble material. The solvent was reduced to 1 cm^3 to yield a colourless solid that was isolated by suction filtration and dried *in vacuo*. Yield 269 mg, 86 %. Microanalysis: Found (calculated for $C_{15}H_{16}NPSe$) C 55.97 (56.07), H 5.25 (5.02), N 4.43 (4.36) %. $^{31}P\{^1H\}$ NMR ($CDCl_3$): 58.1 ppm $^1J(^{31}P\text{-}^{77}Se)$ 756 Hz. ^1H NMR ($CDCl_3$) δ 7.4-7.2 (m, 10 H, aromatic), 5.9 (m, 1 H, CH), 5.3 (q, 1 H, CH_2), 5.1 (q, 1 H, CH_2), 3.5 (m, 2 H, NCH_2) and 2.3 (br s, 1 H, NH) ppm. EI^+ MS: *m/z* 322 [M + H]. IR(KBr disc): 3177, 1644, 991, 573 cm^{-1}.

$[PtCl_2\{Ph_2PNH(C_3H_5)\}_2]$. (33): $Ph_2PNH(C_3H_5)$ (161 mg, 0.7 mmol) and $[PtCl_2(cod)]$ (125 mg, 0.3 mmol) were dissolved in dry CH_2Cl_2 (10 cm^3) to yield a colourless solution which was stirred overnight before reducing the solvent volume to 0.5 cm^3 and addition of diethyl ether (20 cm^3) to precipitate a colourless solid which was isolated by suction filtration and dried *in vacuo*. Yield 226 mg, 90 %. Microanalysis: Found (calculated for $C_{30}H_{32}P_2N_2PtCl_2$) C 48.23 (48.14), H 4.10 (4.31), N 3.65 (3.74) %. $^{31}P\{^1H\}$ NMR ($CDCl_3$): 34.8 ppm $^1J(^{31}P\text{-}^{195}Pt)$ 3949 Hz. ^1H NMR ($CDCl_3$) δ 7.5-7.3 (m, 20 H, aromatic), 5.5 (m, 2 H, CH), 5.0 (q, 2 H, CH_2), 4.9 (q, 2 H, CH_2), 4.1 (br s, 2 H, NH) and 3.5 (m, 4 H, NCH_2) ppm. FAB^+ MS: *m/z* 713 $[M - Cl]^+$, 677 $[M - 2Cl]^{2+}$. IR(KBr disc): 3054, 1642, 1000, 305, 288 cm^{-1}.

$[PdCl_2\{Ph_2PNH(C_3H_5)\}_2]$. (34): $Ph_2PNH(C_3H_5)$ (179 mg, 0.7 mmol) and $[PdCl_2(cod)]$ (106 mg, 0.4 mmol) were dissolved in CH_2Cl_2 (10 cm^3) and stirred overnight. The solvent volume was reduced to 0.5 cm^3 before addition of hexane (20 cm^3) to precipitate a yellow solid that was isolated by filtration and dried *in vacuo*. Yield 224 mg, 91 %. Microanalysis: Found (calculated for $C_{30}H_{32}P_2N_2PdCl_2$) C 54.80 (54.61), H 4.67 (4.89), N 4.06 (4.25) %. $^{31}P\{^1H\}$ NMR ($CDCl_3$): 58.8 and 46.2 ppm. ^1H NMR ($CDCl_3$) δ 7.5-7.2 (m, 20 H, aromatic), 5.6 (m, 2 H, CH), 5.2 (q, 2 H, CH_2), 5.1 (q, 2 H, CH_2), 3.5 (m, 4 H, NCH_2) and 4.1 (br s, 2 H, NH) ppm. FAB^+ MS: *m/z* 624 $[M - Cl]^+$, 588 $[M - 2Cl]^{2+}$. IR (KBr disc): 3054, 1643, 997, 297, 277 cm^{-1}.

$[PdCl_2\{Ph_2PNH(C_3H_5)\}]$. (35): $Ph_2PNH(C_3H_5)$ (52 mg, 0.2 mmol) in CH_2Cl_2 (5 cm^3) was added dropwise to CH_2Cl_2 (5 cm^3) solution of $[PdCl_2(cod)]$ (53 mg, 0.2 mmol). After stirring for 30 minutes the solvent was reduced *in vacuo* to 0.5 cm^3 before precipitating a yellow microcrystalline solid upon addition of hexane (10 cm^3) and isolation by suction filtration. Yield 65 mg, 83 %. Microanalysis: Found (calculated for $C_{15}H_{16}PNPdCl_2$) C 43.95 (43.04), H 4.26 (3.85), N 2.70 (3.35) %. $^{31}P\{^1H\}$ NMR (CD_2Cl_2): 93.6 ppm. ^1H NMR (CD_2Cl_2) δ 7.5-7.2 (m, 10 H, aromatic), 5.6 (m, 1 H, CH), 5.2 (q, 1 H, CH_2), 5.1 (q, 1 H, CH_2), 3.5 (m, 2 H, NCH_2) and 4.1 (br s, 1 H, NH) ppm. FAB^+ MS: *m/z* 382/4 $[M - Cl]^+$, 347 $[M - 2Cl]^{2+}$. IR (KBr disc): 3054, 996, 318, 281 cm^{-1}.

$[PtCl_2\{Ph_2PNH(C_3H_5)\}]$. (36): $Ph_2PNH(C_3H_5)$ (43 mg, 0.2 mmol) in CH_2Cl_2 (5 cm^3) was added dropwise to a CH_2Cl_2 (5 cm^3) solution of $[PtCl_2(cod)]$ (58 mg, 0.2 mmol) over 2.5 hours. The solvent was reduced to 1 cm^3 before addition of hexane (10 cm^3) to yield an off white sticky solid on reduction of solvent. The

sticky solid was subsequently dissolved in CH_2Cl_2 (0.5 cm^3) before addition of petroleum ether (40-60) (10 cm^3) to yield a colourless solid that was isolated by suction filtration. Yield 51 mg, 65 %. Microanalysis: Found (calculated for $C_{15}H_{16}NPPtCl_2$) C 36.53 (35.52), H 2.99 (3.18), N 2.60 (2.76) %. $^{31}P\{^1H\}$ NMR (CD_2Cl_2): 63.5 ppm $^1J(^{31}P\text{-}^{195}Pt)$ 3481 Hz. ^1H NMR (CD_2Cl_2) δ 7.5-7.2 (m, 10 H, aromatic), 5.6 (m, 1 H, CH), 5.2 (q, 1 H, CH_2), 5.1 (q, 1 H, CH_2), 3.5 (m, 2 H, NCH_2) and 4.1 (br s, 1 H, NH) ppm. FAB^+ MS: *m/z* 472 $[M - Cl]^+$, 436 $[M - 2Cl]^{2+}$. IR (KBr disc): 3055, 998, 328, 289 cm^{-1}.

[AuCl{$Ph_2PNH(C_3H_5)$}]. (37): $Ph_2PNH(C_3H_5)$ (78 mg, 0.3 mmol) and [AuCl(tht)] (103 mg, 0.3 mmol) were dissolved in CH_2Cl_2 (5 cm^3) and stirred overnight in the dark. Hexane (20 cm^3) was added to precipitate a colourless solid that was isolated by suction filtration. Yield 44 mg, 29 %. Microanalysis: Found (calculated for $C_{15}H_{16}PNAuCl$) C 37.98 (38.03), H 2.76 (3.40), N 3.07 (2.96) %. $^{31}P\{^1H\}$ NMR ($CDCl_3$): 64.9 ppm. ^1H NMR ($CDCl_3$) δ 7.6-7.2 (m, 10 H, aromatic), 5.9 (m, 1 H, CH), 5.2 (q, 1 H, CH_2), 5.1 (q, 1 H, CH_2), 3.6 (m, 2 H, NCH_2), 2.5 (br s, 1 H, NH) ppm. FAB^+ MS: *m/z* 496 $[M + Na]^+$, 473 $[M]^+$, 438 $[M - Cl]^+$. IR (KBr disc): 3069, 1643, 996, 323 cm^{-1}.

[RuCl(μ-Cl)(η^6-*p*-$MeC_6H_4{}^iPr$){$Ph_2PNH(C_3H_5)$}]. (38): $Ph_2PNH(C_3H_5)$ (170 mg, 0.7 mmol) and [{RuCl(μ-Cl)(η^6-*p*-$MeC_6H_4{}^iPr$)}$_2$] (54 mg, 0.1 mmol) were dissolved in CH_2Cl_2 (5 cm^3) to yield a dark red solution that was stirred for 30 minutes. The solvent was reduced to 0.5 cm^3 before addition of hexane (10 cm^3 to precipitate an orange microcrystalline solid that was isolated by suction filtration and dried *in vacuo*. Yield 82 mg, 85 %. Microanalysis: Found (calculated for $C_{25}H_{30}PNRuCl_2$) C 55.71 (54.85), H 5.62 (5.52), N 2.71 (2.56) %.

$^{31}P\{^{1}H\}$ NMR ($CDCl_3$): 61.3 ppm. ^{1}H NMR δ 7.4-7.2 (m, 14 H, aromatic), 5.5 (m, 1 H, CH), 5.2 (q, 1 H, CH_2), 5.1 (q, 1 H, CH_2), 3.5 (m, 2 H, NCH_2), 2.9 (br s, 1 H, NH), 2.6 (m, 1 H, CH), 1.2 (m, 3 H, CH_3), 0.8 (m, 6 H, CH_3). FAB^+ MS: *m/z* 570/2 $[M + Na]^+$, 547/9 $[M]^+$, 512 $[M - Cl]^+$, 476 $[M - 2Cl]^{2+}$. IR (KBr disc): 3051, 1642, 996, 290, 283 cm^{-1}.

$[Pt\{Ph_2PNH(C_4H_8O)\}_2]$. (39): To a CH_3OH (10 cm^3 suspension of $[PtCl_2(Ph_2PNH(C_3H_5))_2]$ (100 mg, 0.1 mmol) was added potassium *tert*-butoxide (30 mg, 0.2 mmol) with stirring to yield a colourless precipitate after 1 hour. This microcrystalline solid was subsequently isolated by suction filtration and dried *in vacuo*. Yield 46 mg, 51 %. Microanalysis: Found (calculated for $C_{32}H_{38}P_2N_2Opt$) C 52.06 (51.96), H 4.60 (5.18), N 3.70 (3.79) %. $^{31}P\{^{1}H\}$ NMR ($CDCl_3$): 91.4 ppm $^{1}J(^{31}P\text{-}^{195}Pt)$ 2294 Hz. ^{1}H NMR ($CDCl_3$) δ 7.6-7.2 (m, 20 H, aromatic), 5.9 (m, 2 H, CH), 5.2 (q, 2 H, CH_2), 5.1 (q, 2 H, CH_2), 3.6 (m, 4 H, NCH_2), 2.5 (br s, 2 H, NH), 1.5 (s, 6 H, MeO) ppm. FAB^+ MS: 678 $[M + H]^+$. IR (KBr disc): 3069, 3045, 2873-2809 (m), 997 cm^{-1}.

$[RhCl(\mu\text{-}Cl)(\eta^5\text{-}C_5Me_5)\{Ph_2PNH(C_3H_5)\}]$. (40): $Ph_2PNH(C_3H_5)$ (45 mg, 0.2 mmol) and $[\{RhCl(\mu\text{-}Cl)(\eta^5\text{-}C_5Me_5)\}_2]$ (58 mg, 0.1 mmol) were dissolved in CH_2Cl_2 (10 cm^3) to yield a blood red solution that stirred for 30 minutes before reducing the solvent to 1 cm^3 and addition of diethyl ether (20 cm^3) to precipitate a red microcrystalline solid that was isolated by suction filtration and dried *in vacuo*. Yield 69 mg, 67 %. Microanalysis: Found (calculated for $C_{25}H_{31}PNRhCl_2$) C 54.32 (54.56), H 5.78 (5.68), N 2.44 (2.55) %. $^{31}P\{^{1}H\}$ NMR ($CDCl_3$): 66.4 ppm $^{1}J(^{31}P\text{-}^{103}Rh)$ 148 Hz. ^{1}H NMR ($CDCl_3$) δ 7.4-7.2 (m, 10 H, aromatic), 5.6 (m, 1 H, CH), 5.2 (q, 1 H, CH_2), 5.1 (q, 1 H, CH_2), 3.3 (m, 2

H, NCH_2), 3.2 (br s, 1 H, NH), 1.3 (s, 15 H, CH_3) ppm. FAB^+ MS: *m/z* 572/4 $[M + Na]^+$, 514 $[M - Cl]^+$, 474 $[M - 2Cl]^{2+}$. IR (KBr disc): 3063, 1642, 995, 279, 267 cm^{-1}.

$[IrCl(\mu\text{-}Cl)(\eta^5\text{-}C_5Me_5)\{Ph_2PNH(C_3H_5)\}]$. (41): $Ph_2PNH(C_3H_5)$ (42 mg, 0.2 mmol) and $[\{IrCl(\mu\text{-}Cl)(\eta^5\text{-}C_5Me_5)\}_2]$ (69 mg, 0.1 mmol) were dissolved in CH_2Cl_2 (10 cm^3) to yield an orange solution. The solvent was reduced to 1 cm^3 before diethyl ether was added to precipitate a yellow microcrystalline solid that was isolated by filtration and dried *in vacuo*. Yield 72 mg, 65 %. Microanalysis: Found (calculated for $C_{25}H_{31}PNIrCl_2$) C 47.07 (46.95), H 4.85 (4.89), N 2.13 (2.19) %. $^{31}P\{^1H\}$ NMR ($CDCl_3$): 34.5 ppm. ^1H NMR ($CDCl_3$) δ 7.4-7.2 (m, 10 H, aromatic), 5.6 (m, 1 H, CH), 5.2 (q, 1 H, CH_2), 5.1 (q, 1 H, CH_2), 3.5 (m, 2 H, NCH_2), 3.2 (br s, 1 H, NH), 1.3 (s, 15 H, CH_3) ppm. FAB^+ MS: *m/z* 604 $[M - Cl]^+$, 568 $[M - 2Cl]^{2+}$. IR (KBr disc): 3058, 1640, 994, 291, 280 cm^{-1}.

$[Pt(PEt_3)Cl_2\{Ph_2PNH(C_3H_5)\}]$. (42): To a CH_2Cl_2 (10 cm^3) solution of $[\{PtCl(\mu\text{-}Cl)(PEt_3)\}_2]$ (56 mg, 0.07 mmol) was added dropwise a CH_2Cl_2 (10 cm^3) solution of $Ph_2PNH(C_3H_5)$ (35 mg, 0.1 mmol) with stirring to yield a pale yellow solution. After 30 minutes the solvent was reduced to 1 cm^3 before addition of diethyl ether (20 cm^3) to precipitate a colourless solid that was isolated by suction filtration. Yield 54 mg, 59 %. Microanalysis: Found (calculated for $C_{21}H_{31}P_2NPtCl_2$) C 40.61 (40.38), H 4.38 (5.01), N 2.49 (2.24) %. $^{31}P\{^1H\}$ NMR ($CDCl_3$): $\delta(P_A)$ 34.2 (d) ppm, $^1J(^{31}P_A\text{-}^{195}Pt)$ 3979 Hz. $\delta(P_X)$ 7.3 (d) ppm, $^1J(^{31}P_X\text{-}^{195}Pt)$ 3479 Hz. $^2J(^{31}P_A\text{-}^{31}P_X)$ 19 Hz. ^1H NMR ($CDCl_3$) δ 7.4-7.2 (m, 10 H, aromatic), 5.7 (m, 1 H, CH), 5.2 (q, 1 H, CH_2), 5.0 (q, 1 H, CH_2),

3.5 (m, 2 H, NCH_2), 3.2 (br s, 1 H, NH), 1.5 (m, 6 H, PCH_2) and 0.9 (m, 9 H, Me) ppm. ES^+ MS: *m/z* 590 $[M - Cl]^+$. IR (KBr disc): 3072, 1641, 1002, 309, 283 cm^{-1}.

$[Pt(PMe_2Ph)Cl_2\{Ph_2PNH(C_3H_5)\}]$. (43): $Ph_2PNH(C_3H_5)$ (33 mg, 0.1 mmol) in CH_2Cl_2 (10 cm^3) was added dropwise to a CH_2Cl_2 (10 cm^3) solution of $[\{PtCl(\mu\text{-}Cl)(PMe_2Ph)\}_2]$ 56 mg, 0.07 mmol) over 10 minutes with stirring. The solution was stirred for a further 30 minutes before reduction of the solvent to 1 cm^3 and addition of diethyl ether (20 cm^3) to precipitate a colourless solid that was isolated by suction filtration and dried *in vacuo*. Yield 55 mg, 62 %. Microanalysis: Found (calculated for $C_{23}H_{27}P_2NPtCl_2$) C 42.99 (42.85), H 2.26 (4.22), N 2.08 (2.17) %. $^{31}P\{^1H\}$ NMR ($CDCl_3$): $\delta(P_A)$ 35.3 (d) ppm, $^1J(^{31}P_A\text{-}^{195}Pt)$ 3878 Hz. $\delta(P_X)$ –14.2 (d) ppm, $^1J(^{31}P_X\text{-}^{195}Pt)$ 3625 Hz. $^2J(^{31}P_A\text{-}^{31}P_X)$ 19 Hz. ^1H NMR ($CDCl_3$) δ 7.6-7.2 (m, 15 H, aromatic), 5.6 (m, 1 H, CH), 5.1 (q, 1 H, CH_2), 4.9 (q, 1 H, CH_2), 4.5 (br s, 1 H, NH), 3.1 (m, 2 H, NCH_2) and 1.7 (d, 6H, $^3J(^{195}Pt\text{-}^1H)$ 32 Hz, $^2J(^{31}P\text{-}^1H)$ 11 Hz, PMe) ppm. ES^+ MS: *m/z* 645 $[M + H]^+$, 610 $[M - Cl]^+$, 575 $[M - 2Cl]^{2+}$. IR (KBr disc): 3053, 1642, 1000, 313, 283 cm^{-1}.

$[PdCl(C_{10}H_8N)\{Ph_2PNH(C_3H_5)\}]$. (44): To a CH_2Cl_2 (10 cm^3) suspension of $[\{PdCl(C_{10}H_8N)\}_2]$ (61 mg, 0.1 mmol) was added dropwise a CH_2Cl_2 solution of $Ph_2PNH(C_3H_5)$ (52 mg, 0.2 mmol) over 10 minutes to yield a colourless solution. After stirring for a further 30 minutes the solution was filtered through a Celite plug to remove any insoluble material remaining before reducing the solvent volume to 1 cm^3 and addition of diethyl ether (20 cm^3) to precipitate a tan coloured microcrystalline solid that was isolated by filtration. Yield 78 mg, 69

%. Microanalysis: Found (calculated for $C_{25}H_{24}PN_2PdCl$) C 56.93 (57.16), H 3.93 (4.60), N 5.24 (5.33) %. $^{31}P\{^1H\}$ NMR ($CDCl_3$): 65.0 ppm. ^1H NMR ($CDCl_3$) δ 9.6-7.8 (m, 6 H, naphthalene aromatic), 7.4-7.2 (m, 10 H, aromatic), 5.7 (m, 1 H, CH), 5.2 (q, 1 H, CH_2), 5.0 (q, 1 H, CH_2), 4.5 (br s, 1 H, NH), 3.4 (m, 2 H, NCH_2), 2.8 (d, 2 H, $^2J(^{31}P\text{-}^1H)$ 5 Hz, CH_2) ppm. ES^+ MS: *m/z* 489 $[M - Cl]^+$. IR (KBr disc): 3049, 1639, 993, 289 cm^{-1}.

References.

1. K. J. Coutinho; R. S. Dickson; G. D. Fallon; W. R. Jackson; T. De Simone; B. W. Skelton; A. H. White, *J. Chem. Soc. Dalton Trans.*, 1997, 3193.
2. B. Cornils; E. Wilbus, *Chem. Tech.*, 1995, 33. B. Cornils, *Angew. Chem. Int. Ed. Engl.*, 1995, **34**, 1575.
3. E. Billig; A. G. Abatjoghe; D. R. Bryant, *US Pat.*, 4668651,1987, 4769498, 1988. G. D. Cuny; S. L. Buckwald, *J. Am. Chem. Soc.*, 1993, **115**, 2066.
4. M. E. Davis, *Chem. Tech.*, 1992, 498. W. A. Herrmann; C. W. Kohlpaintner, *Angew. Chem. Int. Ed. Engl.*, 1993, **32**, 1524.
5. T. Higashizima; N. Sakai; K. Nozaki; H. Takaya, *Tetrahedron Lett.*, 1994, **35**, 2023.
6. A. M. Z. Slawin; J. Wheatley; M. V. Wheatley; J. D. Woollins, *Polyhedron*, 2003, **22**, 1397.
7. S. M. Aucott; A. M. Z. Slawin; J. D. Woollins, *J. Chem. Soc. Dalton Trans.*, 2000, 2559.
8. H. C. Clark; L. E. Manzer, *J. Organomet. Chem.*, 1973, **59**, 411.

9. Y. Tatsuno; T. Yoshida; Seiotsuka, *Inorg. Synth.*, 1979, **19**, 220.

10. G. J. Kubas, *Inorg. Synth.*, 1979, **19**, 90.

11. R. Uson; A. Laguna; M. Laguna, *Inorg. Synth.*, 1989, **26**, 85.

12. D. Drew; J. R. Doyle, *Inorg. Synth.*, 1991, **28**, 346.

13. J. X. McDermott; J. F. White; G. M. Whiteside, *J. Am. Chem. Soc.*, 1976, **60**, 6521.

14. M. A. Bennett; T. N. Huang; T. W. Matheson; A. R. Smith, *Inorg. Synth.*, 1982, **21**, 74.

15. G. Giordano; R. H. Crabtree, *Inorg. Synth.*, 1979, **19**, 218.

16. C. White; A. Yates; P. M. Maitlis, *Inorg. Synth.*, 1992, **29**, 228.

17. W. Baratta; P. S. Pregosin, *Inorg. Chim. Acta.*, 1993, **209**, 85.

18. J. Chatt; R. G. Wilkins, *J. Chem. Soc.*, 1952, 273.

19. J. W. Suggs; K. S. Lee, *J. Organomet. Chem.*, 1986, **299**, 297.

CHAPTER 3.2: PREPARATION AND COORDINATION CHEMISTRY OF N-ALLYLAMINOBISPHOSPHINE

3.2.1 *Introduction*

Bis(diphenylphosphino)amines[1] have received a vast amount of interest in recent years, the most common of which is bis(diphenylphosphino)ethane, $Ph_2PCH_2CH_2PPh_2$ (dppe). More recently bis(diphenylphosphino)methane, $Ph_2PCH_2PPh_2$ (dppm), has become a ligand that has seen its use increase[2-4]. Coordination of dppm to metal centres can occur through the lone pair of electrons at one or both of the phosphorus centres as well as deprotonation, by strong bases, of the methylene group to form a tridentate ligand.

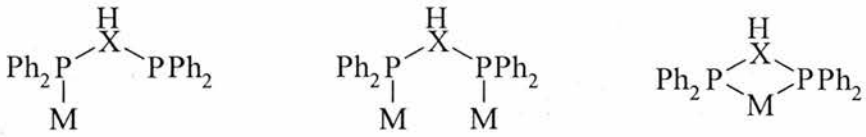

Figure 3.2.1. Coordination modes of dppm and its anion (X = CH or C).

However, diphosphinoamines have received significantly less coverage[4, 6]. Bis(diphenylphosphino)amine, $Ph_2PNHPPh_2$ (dppa) demonstrates similar coordination to dppm in both its neutral and anionic forms. Participation in cyclocondensations that lead to heterocycle formation and oxidation of the phosphorus atoms to prepare new ligands are two ways in which dppa and dppm are similar.

In this work a new disphosphine has been prepared containing an olefinic side chain that has the potential to add a fourth coordination mode. Illustrative coordination complexes have been prepared.

Results and Discussion

3.2.2 *Synthesis of* $(Ph_2P)_2N(C_3H_5)$ ***45***

Reaction of allylamine with two equivalents of Ph_2PCl in the presence of NEt_3 proceeds in thf to give **45,** which was isolated in a good yield (78 %) by filtration from $Et_3NH^+Cl^-$ as a colourless solid. The microanalysis gave fairly satisfactory results and the $^{31}P\{^1H\}$ NMR spectrum consists of a singlet observed at δ_P 62.9 ppm. The IR spectrum has bands observed at 1635, 1434 and 993 cm^{-1}, which are assigned to $\nu_{C=C}$, ν_{PPh} and ν_{PN} respectively. The mass spectrum gave the expected parent ion, observed at *m/z* 424 corresponding to M^+, and fragmentation pattern.

45

Scheme 3.2.1. Formation of $(C_3H_5)N(Ph_2P)_2$.

Formation of the chalcogen derivatives of **45** proved difficult due to the absence of any hydrogen bonding which had been shown for $(C_3H_5)NHPPh_2$ (**29**). When prepared the chalcogens formed sticky oils which were difficult to isolate and characterise though it was possible to show the formation of these ligands by $^{31}P\{^1H\}$ NMR. The dioxide, $(C_3H_5)N(P(O)Ph_2)_2$, showed a single resonance at δ_P 30.4 ppm, the disulfide, $(C_3H_5)N(P(S)Ph_2)_2$, showed a single peak observed at δ_P 71.0 ppm and the diselenide, $(C_3H_5)N(P(Se)Ph_2)_2$, was observed at δ_P 70.3 ppm with selenium satellites $^1J(^{31}P\text{-}^{77}Se)$ 786 Hz.

3.2.3 *Coordination chemistry of* $(C_3H_5)N(PPh_2)_2$

Reaction of $[PtCl_2(cod)]$ with $(C_3H_5)N(PPh_2)_2$ gives $[PtCl_2\{(C_3H_5)N(PPh_2)_2\}]$ (**46**) in good yield (71 %). The FAB^+ mass spectrum showed the expected parent ion and fragmentation pattern and the complex displays a resonance with platinum satellites in the $^{31}P\{^1H\}$ NMR spectrum at δ_P 19.1 ppm, $^1J(^{31}P\text{-}^{195}Pt)$ 3296 Hz. The IR spectrum showed bands at 1635, 1435, 995, 291 and 245 cm^{-1}, which are assigned to $\nu_{C=C}$, ν_{PPh}, ν_{PN} and two ν_{PtCl} vibrations respectively.

Crystals of $[PtCl_2\{(C_3H_5)N(PPh_2)_2\}]$ (**46**) suitable for X-ray crystallography were grown overnight by layering a chloroform solution with diethyl ether. The crystal structure of the complex (Figure 3.2.2) and selected bond lengths and angles (Table 3.2.1) are shown below and confirm the proposed *cis* chelate geometry. The crystal structure shows that the $[PtCl_2\{(C_3H_5)N(PPh_2)_2\}]$ (**46**) molecule is approximately square planar at platinum. The bite angle of the chelating phosphine is significantly lower than the ideal 90 ° {P(2)-Pt(1)-P(1) 72.03(8) °}.

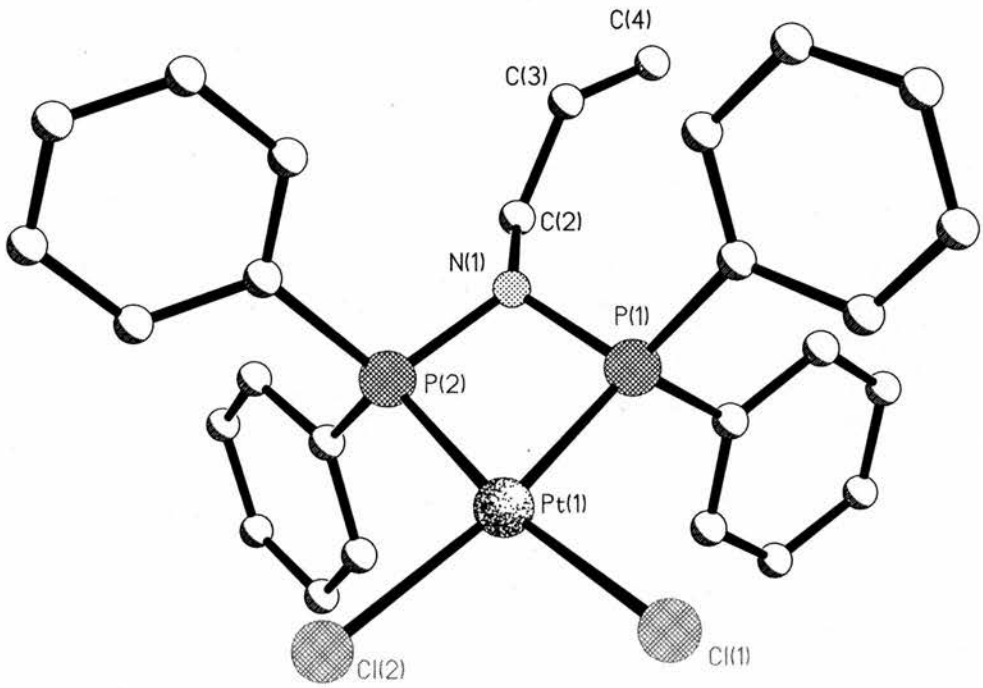

Figure. 3.2.2. The X-ray structure of $[PtCl_2\{(C_3H_5)N(PPh_2)_2\}]$ (**46**).

Table 3.2.1. Selected bond lengths (Å) and angles (°) for

$[PtCl_2\{(C_3H_5)N(PPh_2)_2\}]$

Selected bond lengths (Å)	*(46)*	*Selected bond angles (°)*	*(46)*
M(1)-Cl(1)	2.344(2)	**P(2)-M(1)-P(1)**	72.03(8)
M(1)-Cl(2)	2.355(2)	**P(2)-M(1)-Cl(1)**	170.10(9)
M(1)-P(1)	2.200(2)	**P(1)-M(1)-Cl(1)**	98.88(9)
M(1)-P(2)	2.198(2)	**P(2)-M(1)-Cl(2)**	97.45(9)
P(1)-N(1)	1.695(7)	**P(1)-M(1)-Cl(2)**	169.43(8)
P(2)-N(1)	1.696(7)	**Cl(2)-M(1)-Cl(1)**	91.69(9)
P(1)-C(11)	1.806(9)	**P(2)-N(1)-P(1)**	99.4(4)
P(1)-C(17)	1.806(9)	**N(1)-P(1)-C(11)**	111.2(4)
P(2)-C(23)	1.793(8)	**N(1)-P(1)-C(17)**	108.8(4)
P(2)-C(29)	1.796(8)	**C(11)-P(1)-C(17)**	105.2(4)
		N(1)-P(1)-M(1)	94.0(3)
		C(11)-P(1)-M(1)	117.1(3)
		C(17)-P(1)-M(1)	119.9(3)
		N(1)-P(2)-C(23)	109.2(4)
		N(1)-P(2)-C(29)	108.4(4)
		C(23)-P(2)-C(29)	107.1(4)
		N(1)-P(2)-M(1)	94.1(2)
		C(23)-P(2)-M(1)	118.2(3)
		C(29)-P(2)-M(1)	118.5(3)

$[PdCl_2\{(C_3H_5)N(PPh_2)_2\}]$ (**47**) is prepared in a similar way to **46** in good yield (85 %). The $^{31}P\{^1H\}$ NMR ($CDCl_3$) spectrum exhibited a single peak

observed at δ_P 33.1 ppm and the FAB^+ mass spectrum gave the expected parent ion and fragmentation pattern for the suggested structure. The microanalysis gave satisfactory results and the IR spectrum gave bands at 1638, 1435, 995, 286 and 245 cm^{-1} which are attributed to $\nu_{C=C}$, ν_{PPh}, ν_{PN} and two ν_{PdCl} respectively.

Upon slow addition of $[Mo(CO)_4(nbd)]$ to $(C_3H_5)N(PPh_2)_2$, $[Mo(CO)_4\{(Ph_2P)_2N(C_3H_5)\}]$ (**48**) is obtained in a yield of 60 %. Microanalysis gave satisfactory results for the replacement of nbd with $(Ph_2P)_2N(C_3H_5)$ to retain the 6 coordinate Mo species. The $^{31}P\{^1H\}$ NMR ($CDCl_3$) displayed a single peak as expected at δ_P 92.1 ppm and the FAB^+ mass spectral analysis gave the expected parent ion and fragmentation pattern. The IR spectrum showed the presence of υ_{CO} vibrations indicating the retention of the CO groups in the final complex. Also present in the IR spectrum was the presence of ν_{PPh} and ν_{PN} vibrations at 1434 and 999 cm^{-1} though the presence of the $\nu_{C=C}$ vibration is masked by the ν_{CO} vibrations previously shown.

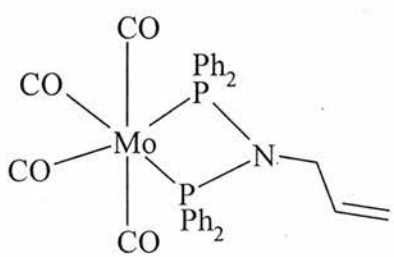

48

Figure 3.2.3. Suggested structure for $[Mo(CO)_4\{(Ph_2P)_2N(C_3H_5)\}]$.

The formation of $[Cu\{(Ph_2P)_2N(C_3H_5)\}_2][PF_6]$ (**49**) proceeds by dropwise addition of a dichloromethane solution of $(C_3H_5)N(Ph_2P)_2$ to $[Cu(MeCN)_4][PF_6]$ and subsequent precipitation of a colourless solid upon addition of diethyl ether.

$[Cu\{(Ph_2P)_2N(C_3H_5)\}_2][PF_6]$ (**49**) is obtained in a yield of 63 % and microanalysis gave satisfactory results for the replacement of the four MeCN groups by the two ligands which act as a bidentate ligand. The FAB^+ mass spectrum gives the expected parent ion of $[M - PF_6]$ at 913 and the IR spectrum shows vibrations for $\nu_{C=C}$, ν_{PPh} and ν_{PN} at 1635, 1437 and 996 cm^{-1} respectively.

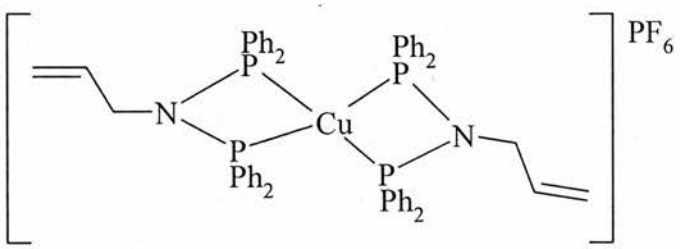

49

Figure 3.2.4. Suggested structure of $[Cu\{(Ph_2P)_2N(C_3H_5)\}_2][PF_6]$.

Reaction of [AuCl(tht)] with $(C_3H_5)N(PPh_2)_2$ proceeds to yield $[\{(C_3H_5)N(PPh_2)_2\}(AuCl)_2]$ (**50**) in a yield of 45 %. The microanalysis obtained gave good results for the coordination of two gold atoms onto the phosphorus atoms. The structure obtained is linear as has been shown previously with other Au(I) complexes and the FAB^+ mass spectrum gave the expected fragmentation pattern and parent ion. The $^{31}P\{^1H\}$ NMR ($CDCl_3$) spectrum gave a single peak observed at δ_P 83.8 ppm and the IR spectrum gave the expected vibrations.

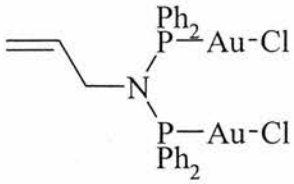

50

Figure 3.2.5. Suggested structure of $[\{(C_3H_5)N(PPh_2)_2\}(AuCl)_2]$

The reaction of $[\{RuCl(\mu\text{-}Cl)(\eta^6\text{-}p\text{-}MeC_6H_4{}^iPr)\}_2]$ with $(C_3H_5)N(Ph_2P)_2$ proceeds in a similar way to the reaction of $[Cu(MeCN)_4][PF_6]$ to form $[RuCl_2\{(Ph_2P)_2N(C_3H_5)\}_2]$ (**51**) in a yield of 63 %. Again it was observed that the $(\eta^6\text{-}p\text{-}MeC_6H_4{}^iPr)$ group of the starting complex was replaced with two equivalents of the ligand to form a bidentate complex. The microanalysis obtained for the suggested structure gave fairly satisfactory results and the FAB^+ mass spectrum gave the expected parent ion and fragmentation pattern. The $^{31}P\{^1H\}$ NMR ($CDCl_3$) displayed a single peak observed at δ_P 79.7 ppm and the IR spectrum showed the expected vibrations for $\nu_{C=C}$, ν_{PPh} ν_{PN} and two ν_{RuCl} at 1637, 1434, 998, 254 and 233 cm^{-1} respectively.

Crystals of $[RuCl_2\{(Ph_2P)_2N(C_3H_5)\}_2]$ (**51**) suitable for X-ray crystallography were grown overnight by layering a chloroform solution with diethyl ether. The crystal structure of the complex (Figure 3.2.6) and selected bond lengths and angles (Table 3.2.2) are shown below. As can be seen from the X-ray structure the $(\eta^6\text{-}p\text{-}MeC_6H_4{}^iPr)$ ligand of the ruthenium complex is displaced by the bidentate phosphine ligand and in the solid state forms a symmetrical structure. The bite angle of the chelating phosphine is significantly lower than the ideal 90 ° {P(2)-Pt(1)-P(1) 69.10(3) °}.

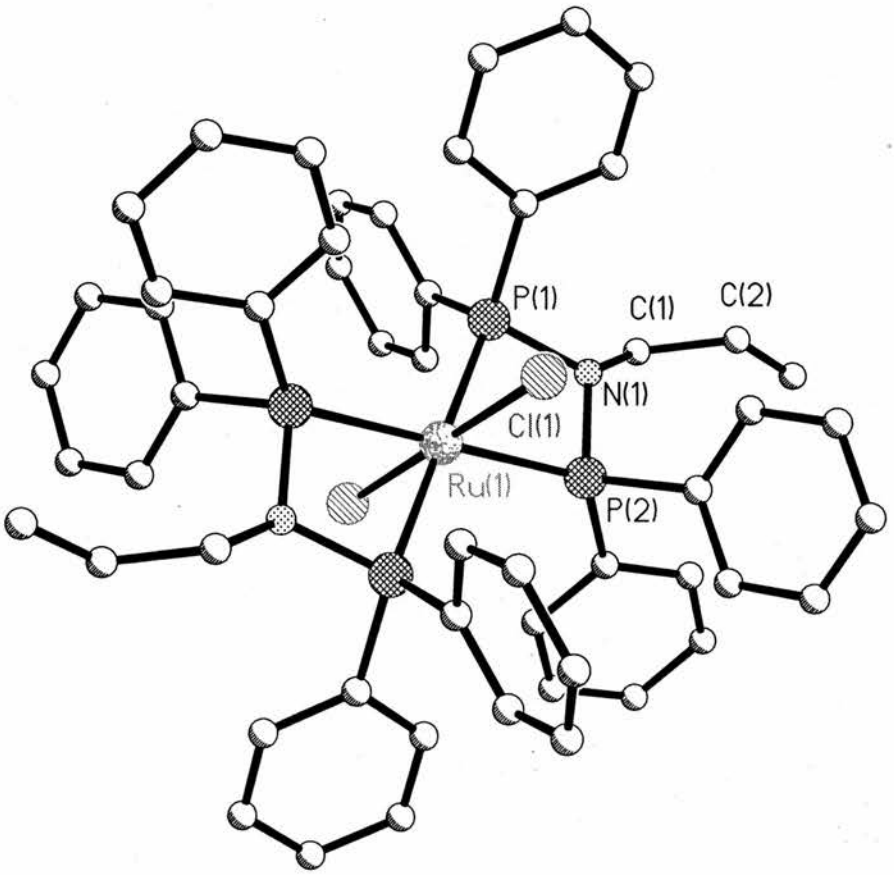

Figure. 3.2.6. The X-ray structure of $[RuCl_2\{(Ph_2P)_2N(C_3H_5)\}_2]$ (**51**).

Table 3.2.2. Selected bond lengths (Å) and angles (°) for

$[RuCl_2\{(Ph_2P)_2N(C_3H_5)\}_2]$

Selected bond lengths (Å) and angles (°)	*(51)*
M(1)-Cl(1)	2.4189(7)
M(1)-P(2)	2.3585(8)
M(1)-P(1)	2.3356(7)
P(2)-N(1)	1.721(2)
P(1)-N(1)	1.710(2)
N(1)-C(1)	1.474(3)
P(1)-C(11)	1.831(3)
P(1)-C(17)	1.831(3)
P(2)-C(21)	1.833(3)
P(2)-C(27)	1.834(3)
P(2)-M(1)-P(1)	69.10(3)
P(2)-M(1)-Cl(1)	85.65(2)
P(1)-M(1)-Cl(1)	89.65(2)
P(2)-N(1)-P(1)	101.78(12)
N(1)-P(1)-C(11)	104.88(12)
N(1)-P(1)-C(17)	106.56(12)
C(11)-P(1)-C(17)	103.34(12)
N(1)-P(1)-M(1)	95.12(8)
C(11)-P(1)-M(1)	122.52(9)
C(17)-P(1)-M(1)	121.69(9)
N(1)-P(2)-C(21)	107.61(12)
N(1)-P(2)-C(27)	106.51(11)
C(21)-P(2)-C(27)	99.46(13)
N(1)-P(2)-M(1)	94.00(8)
C(21)-P(2)-M(1)	118.95(9)
C(27)-P(2)-M(1)	128.33(9)

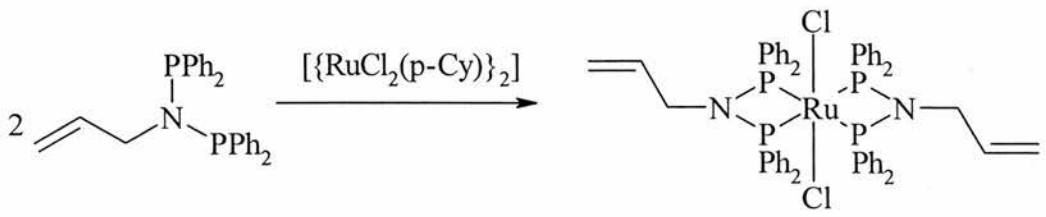

51

Scheme 3.2.2. Reaction of $(Ph_2P)_2N(C_3H_5)$ with $[\{RuCl(\mu\text{-}Cl)(\eta^6\text{-}p\text{-}MeC_6H_4{}^iPr)\}_2]$.

The complexes $[RhCl(\mu\text{-}Cl)(\eta^5\text{-}C_5Me_5)\{(Ph_2P)_2N(C_3H_5)\}]$ (**52**) and $[IrCl(\mu\text{-}Cl)(\eta^5\text{-}C_5Me_5)\{(Ph_2P)_2N(C_3H_5)\}]$ (**53**) were both prepared similarly in good yield (84 % and 72 % respectively). The FAB^+ mass spectral analysis for each complex gave the expected fragmentation pattern and parent ions and the IR spectra gave the expected vibrations corresponding to $\upsilon_{C=C}$, υ_{PPh} υ_{PN} and two υ_{MCl}. In the $^{31}P\{^1H\}$ NMR spectrum of **52** the expected peak was displayed at δ_P 70.9 ppm with a coupling constant of $^1J(^{31}P\text{-}^{103}Rh)$ of 120 Hz. For complex **53** the $^{31}P\{^1H\}$ NMR spectrum showed a single peak at 37.3 ppm. Microanalysis for complexes **52** and **53** gave satisfactory results for the structures suggested.

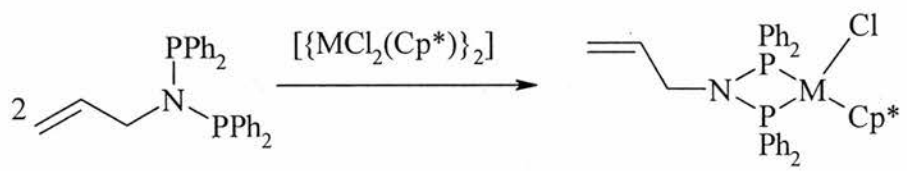

M = Rh (**52**), Ir (**53**)

Scheme 3.2.3. Reaction of $(Ph_2P)_2N(C_3H_5)$ with $[\{MCl(\mu\text{-}Cl)(\eta^5\text{-}C_5Me_5)\}_2]$ {M = Rh (**52**), Ir (**53**)}.

Table 3.2.3. Characterisation data for $(Ph_2P)_2N(C_3H_5)$ and its derivatives. ([a] $^1J\{^{31}P\text{-}^{195}Pt\}$ 3296 Hz), ([b] $^1J\{^{31}P\text{-}^{103}Rh\}$ 120 Hz).

Compound	*$^{31}P\{^1H\}$ NMR*	*IR/cm^{-1}*					*Microanalysis/ % Found (calc.)*		
	δ_P/ppm	ν_{PN}	ν_{PPh}	$\nu_{C=C}$	$\nu_{P=E}$	ν_{MCl}	C	H	N
$(Ph_2P)_2N(C_3H_5)$ (45)	62.9	993	1434	1635	-	-	75.19 (76.22)	6.20 (5.92)	3.34 (3.29)
$[PtCl_2\{(Ph_2P)_2N(C_3H_5)\}]$ (46)	19.1[a]	995	1435	1635	-	302, 291	47.81 (46.90)	2.53 (3.64)	1.56 (2.03)
$[PdCl_2\{(Ph_2P)_2N(C_3H_5)\}]$ (47)	33.1	995	1435	1638	-	329, 286	52.65 (53.80)	4.11 (4.18)	2.15 (2.32)
$[Mo(CO)_4\{(Ph_2P)_2N(C_3H_5)\}]$ (48)	92.1	999	1434	-	-	-	58.44 (58.78)	3.83 (3.98)	2.18 (2.21)

Table continue. Characterisation data for $Ph_2PNH(C_3H_5)$ and its derivatives.									
$[Cu\{(Ph_2P)_2N(C_3H_5)\}_2][PF_6]$ (49)	85.8	996	1437	1635	-	-	61.57 (61.22)	4.87 (4.76)	2.72 (2.64)
$[(AuCl)_2\{(Ph_2P)_2N(C_3H_5)\}]$ (50)	83.8	997	1436	1655	-	282	36.22 (36.43)	2.67 (2.83)	1.55 (1.57)
$[RuCl_2\{(Ph_2P)_2N(C_3H_5)\}_2]$ (51)	79.7	998	1434	1637	-	289, 273	62.64 (63.41)	5.39 (4.93)	2.90 (2.74)
$[RhCl(\mu\text{-}Cl)(\eta^5\text{-}C_5Me_5)\{(Ph_2P)_2N(C_3H_5)\}]$ (52)	70.9[b]	997	1434	1629	-	297, 273	58.71 (59.20)	5.36 (5.40)	1.90 (1.85)
$[IrCl(\mu\text{-}Cl)(\eta^5\text{-}C_5Me_5)\{(Ph_2P)_2N(C_3H_5)\}]$ (53)	37.3	997	1434	1629	-	310, 304	51.64 (51.99)	4.54 (4.77)	1.59 (1.62)

Experimental

General experimental conditions and instruments were as set out on page xvii. Unless otherwise stated, all reactions were carried out under an oxygen-free nitrogen atmosphere using standard Schlenk techniques. Diethyl ether and thf were purified by reflux over sodium-benzophenone and distillation under nitrogen. Dichloromethane was heated to reflux over calcium hydride and distilled under nitrogen. Toluene and hexane were heated to reflux over sodium and distilled under nitrogen. The complexes [PtMeX(cod)] (X = Cl or Me)[6], $[Pd(\mu Cl)(\eta^3\text{-}C_3H_5)]_2$[7], $[Cu(MeCN)_4][PF_6]$[8], [AuCl(tht)] (tht = tetrahydrothiophene)[9], $[MCl_2(cod)]$ (M = Pt or Pd; cod = cycloocta-1,5-diene)[10, 11], $[\{RuCl(\mu\text{-}Cl)(\eta^6\text{-}p\text{-}MeC_6H_4{}^iPr)_2\}]$[12], $[\{Rh(\mu\text{-}Cl)(cod)\}_2]$[13], $[\{MCl(\mu\text{-}Cl)(\eta^5\text{-}C_5Me_5)\}_2]$ (M = Rh or Ir)[14] were prepared using literature procedures. Chlorodiphenylphopshine and allylamine were distilled prior to use. NEt_3 (99 % purity), ^tBuOK (95 % purity), H_2O_2 (30 wt. % in H_2O) and reagent grade KBr were used without further purification. Infra-red spectra were recorded as KBr discs in the range 4000-200 cm^{-1} on a Perkin-Elmer 2000 FTIR/RAMAN spectrometer. NMR spectra were recorded on a Gemini 2000 spectrometer (operating at 121.4 MHz for ^{31}P and 300 MHz for ^1H). Microanalyses were performed by the St. Andrews University service and mass spectra by the Swansea Mass Spectrometer Service.

$(Ph_2P)_2N(C_3H_5)$. (45): Allylamine (2.319 g, 40.6 mmol) and triethylamine (8.219 g, 81.2 mmol) were dissolved in thf (50 cm^3). Chlorodiphenylphosphine (17.922 g, 81.2 mmol) in thf (50 cm^3) was added dropwise with stirring overnight to yield triethylamine hydrochloride that was isolated by filtration.

The solvent was removed *in vacuo* to yield a colourless solid that was dried *in vacuo*. Yield 13.434 g, 78 %. Microanalysis: Found (calculated for $C_{27}H_{25}P_2N$) C 75.19 (76.22), H 6.20 (5.92), N 3.34 (3.29) %. $^{31}P\{^1H\}$ NMR ($CDCl_3$): 62.9 ppm. ^1H NMR ($CDCl_3$) δ 7.4-7.2 (m, 20 H, aromatic), 5.3 (m, 1 H, CH), 4.8 (m, 2 H, CH_2), 3.9 (m, 2 H, NCH_2) ppm. EI^+ MS: *m/z* 424 $[M]^+$. IR (KBr disc): 1635, 1434, 993 cm^{-1}.

$[PtCl_2\{(Ph_2P)_2N(C_3H_5)\}]$. (46): $(Ph_2P)_2N(C_3H_5)$ (88 mg, 0.2 mmol) and $[PtCl_2(cod)]$ (77 mg, 0.2 mmol) were dissolved in CH_2Cl_2 (10 cm^3) to yield a pale yellow solution that was stirred for 30 minutes. The solvent was reduced to 1 cm^3 before precipitating a colourless solid upon addition of diethyl ether (20 cm^3) that was isolated by suction filtration. Yield 101 mg, 71 %. Microanalysis: Found (calculated for $C_{27}H_{25}P_2NPtCl_2$) C 47.81 (46.90), H 2.53 (3.64), N 1.56 (2.03) %. $^{31}P\{^1H\}$ NMR ($CDCl_3$): 19.1 ppm, $^1J(^{31}P\text{-}^{195}Pt)$ 3296 Hz. ^1H NMR ($CDCl_3$) δ 7.4-7.2 (m, 20 H, aromatic), 5.3 (m, 1 H, CH), 4.9 (m, 2 H, CH_2), 3.5 (m, 2 H, NCH_2) ppm. FAB^+ MS: *m/z* 713/4 $[M + Na]^+$, 691 $[M]^+$, 656 $[M - Cl]^+$, 621 $[M - 2Cl]^{2+}$. IR(KBr disc): 1635, 1435, 995, 302, 291 cm^{-1}.

$[PdCl_2\{(Ph_2P)_2N(C_3H_5)\}]$. (47): $(Ph_2P)_2N(C_3H_5)$ (104 mg, 0.2 mmol) and $[PdCl_2(cod)]$ (70 mg, 0.2 mmol) were dissolved in CH_2Cl_2 (10 cm^3) to yield an orange solution that was stirred for 30 minutes. The solvent was reduced to 1 cm^3 before precipitating a pale yellow solid upon addition of diethyl ether (20 cm^3) that was isolated by suction filtration. Yield 125 mg, 85 %. Microanalysis: Found (calculated for $C_{27}H_{25}P_2NPdCl_2$) C 52.65 (53.80), H 4.11 (4.18), N 2.15 (2.32) %. $^{31}P\{^1H\}$ NMR ($CDCl_3$): 33.1 ppm. ^1H NMR ($CDCl_3$) δ 7.4-7.2 (m, 20 H, aromatic), 5.3 (m, 1 H, CH), 4.9 (m, 2 H, CH_2), 3.6 (m, 2 H, NCH_2) ppm.

FAB^+ MS: *m/z* 568 $[M - Cl]^+$, 531 $[M - 2Cl]^{2+}$. IR(KBr disc): 1638, 1435, 995, 329, 286 cm^{-1}.

$[Mo(CO)_4\{(Ph_2P)_2N(C_3H_5)\}]$. (48): To a CH_2Cl_2 (10 cm^3) solution of $[Mo(CO)_4(nbd)]$ (100 mg, 0.3 mmol) was added dropwise a CH_2Cl_2 (10 cm^3) solution of $(Ph_2P)_2N(C_3H_5)$ (141 mg, 0.3 mmol). After stirring for 30 minutes the solvent was reduced to 2 cm^3 before addition of petroleum ether (bp 40-60) (20 cm^3) and storing overnight at –18 °C. The yellow solid precipitated was isolated by filtration and dried *in vacuo*. Yield 127 mg, 60 %. Microanalysis: Found (calculated for $C_{31}H_{25}P_2NO_4Mo$) C 58.44 (58.78), H 3.83 (3.98), N 2.18 (2.21) %. $^{31}P\{^1H\}$ NMR ($CDCl_3$): 92.1 ppm. ^1H NMR ($CDCl_3$) δ 7.4-7.2 (m, 20 H, aromatic), 5.3 (m, 1 H, CH), 4.7 (m, 2 H, CH_2), 3.5 (m, 2 H, NCH_2) ppm. FAB^+ MS: *m/z* 635 $[M]^+$, 579 $[M - 2CO]^+$, 523 $[M - 4CO]^+$. IR (KBr disc): 1887, 1434, 999 cm^{-1}.

$[Cu\{(Ph_2P)_2N(C_3H_5)\}_2][PF_6]$. (49): To a CH_2Cl_2 (10 cm^3) solution of $[Cu(MeCN)_4]$ (71 mg, 0.2 mmol) was added dropwise a CH_2Cl_2 (10 cm^3) solution of $(Ph_2P)_2N(C_3H_5)$ (162 mg, 0.4 mmol). After stirring for 30 minutes the solvent was reduced to 2 cm^3 before addition of diethyl ether (15 cm^3) to precipitate a colourless solid that was isolated by filtration and dried *in vacuo*. Yield 127 mg, 63 %. Microanalysis: Found (calculated for $C_{54}H_{50}P_5N_2CuF_6$) C 61.57 (61.22), H 4.87 (4.76), N 2.72 (2.64) %. $^{31}P\{^1H\}$ NMR ($CDCl_3$): 85.8 ppm. ^1H NMR ($CDCl_3$) δ 7.4-7.2 (m, 40 H, aromatic), 5.1 (m, 2 H, CH), 4.7 (m, 4 H, CH_2), 3.5 (m, 4 H, NCH_2) ppm. FAB^+ MS: *m/z* 913 $[M-PF_6]^+$. IR (KBr disc): 1635, 1437, 996 cm^{-1}.

[{$(C_3H_5)N(PPh_2)_2$}$(AuCl)_2$]. (50): $(Ph_2P)_2N(C_3H_5)$ (21 mg, 0.05 mmol) and [AuCl(tht)] (32 mg, 0.1 mmol) were dissolved in $CHCl_3$ (2 cm^3) to yield a colourless solution. Diethyl ether (15 cm^3) was added to precipitate a colourless solid that was isolated by suction filtration. Yield 20 mg, 45 %. Microanalysis: Found (calculated for $C_{27}H_{25}P_2NAu_2Cl_2$) C 36.22 (36.43), H 2.67 (2.83), N 1.55 (1.57) %. $^{31}P\{^1H\}$ NMR ($CDCl_3$): 83.8 ppm. ^1H NMR ($CDCl_3$) δ 7.4-7.2 (m, 20 H, aromatic), 5.3 (m, 1 H, CH), 4.8 (m, 2 H, CH_2), 3.9 (m, 2 H, NCH_2), ppm. FAB^+ MS: *m/z* 853 $[M - Cl]^+$, 819 $[M - 2Cl]^{2+}$. IR (KBr disc): 1655, 1436, 997, 282 cm^{-1}.

[$RuCl_2${$(Ph_2P)_2N(C_3H_5)$}$_2$]. (51): $(Ph_2P)_2N(C_3H_5)$ (150 mg, 0.4 mmol) and [RuCl(μ-Cl)(η^6-*p*-$MeC_6H_4{}^iPr$)$_2$] (54 mg, 0.1 mmol) were dissolved in CH_2Cl_2 (5 cm^3) to yield a dark red solution. The solvent was reduced to 1 cm^3 before addition of diethyl ether (10 cm^3) to precipitate a red solid that was isolated by suction filtration. Yield 57 mg, 63 %. Microanalysis: Found (calculated for $C_{54}H_{50}P_4N_2RuCl_2$) C 62.64 (63.41), H 5.39 (4.93), N 2.90 (2.74) %. $^{31}P\{^1H\}$ NMR ($CDCl_3$): 79.7 ppm. ^1H NMR ($CDCl_3$) δ 7.4-7.2 (m, 40 H, aromatic), 5.9 (m, 2 H, CH), 4.8 (m, 4 H, CH_2), 3.5 (m, 4 H, NCH_2) ppm. FAB^+ MS: *m/z* 1022 $[M]^+$, 987 $[M - Cl]^+$, 951 $[M - 2Cl]^{2+}$. IR (KBr disc): 1637, 1434, 998, 289, 273 cm^{-1}.

[$RhCp^*Cl_2${$(Ph_2P)_2N(C_3H_5)$}]. (52): $(Ph_2P)_2N(C_3H_5)$ (67 mg, 0.2 mmol) and [{RhCl(μ-Cl)(η^5-C_5Me_5)}$_2$] (49 mg, 0.1 mmol) were dissolved in CH_2Cl_2 (5 cm^3) to yield a blood red solution. The solvent was reduced to 0.5 cm^3 before addition of diethyl ether (20 cm^3) to precipitate an orange solid that was isolated by suction filtration. Yield 97 mg, 84 %. Microanalysis: Found (calculated for

$C_{37}H_{40}P_2NRhCl_2.0.25CH_2Cl_2$) C 58.71 (59.20), H 5.36 (5.40), N 1.90 (1.85) %. $^{31}P\{^1H\}$ NMR ($CDCl_3$): 70.9 ppm, $^1J(^{31}P\text{-}^{103}Rh)$ 120 Hz. ^1H NMR ($CDCl_3$) δ 7.4-7.2 (m, 20 H, aromatic), 5.5 (m, 1 H, CH), 4.9 (m, 2 H, CH_2), 3.8 (m, 2 H, NCH_2), 1.6 (m, 15 H, Cp*) ppm. FAB^+ MS: *m/z* 733 $[M]^+$, 698 $[M - Cl]^+$. IR (KBr disc): 1629, 1434, 997, 297, 273 cm^{-1}.

[IrCp*Cl$_2${(Ph$_2$P)$_2$N(C$_3$H$_5$)}]. (53): $(Ph_2P)_2N(C_3H_5)$ (54 mg, 0.1 mmol) and $[\{IrCl(\mu\text{-}Cl)(\eta^5\text{-}C_5Me_5)\}_2]$ (51 mg, 0.05 mmol) were dissolved in CH_2Cl_2 (10 cm^3) to yield a yellow solution. The solvent was reduced to 0.5 cm^3 before addition of diethyl ether (20 cm^3) to precipitate a yellow solid that was isolated by suction filtration and dried *in vacuo*. Yield 76 mg, 72 %. Microanalysis: Found (calculated for $C_{37}H_{40}P_2NIrCl_2.0.5CH_2Cl_2$) C 51.64 (51.99), H 4.54 (4.77), N 1.59 (1.62) %. $^{31}P\{^1H\}$ NMR ($CDCl_3$): 37.3 ppm. ^1H NMR ($CDCl_3$) δ 7.4-7.2 (m, 20 H, aromatic), 5.3 (m, 1 H, CH), 4.8 (m, 2 H, CH_2), 3.9 (m, 2 H, NCH_2), 1.6 (m, 15 H, Cp*) ppm. FAB^+ MS: *m/z* 823 $[M]^+$, 788 $[M - Cl]^+$. IR (KBr disc): 1629, 1434, 997, 310, 304 cm^{-1}.

References.

1. P. Bhattacharyya; J. D. Woollins, *Polyhedron*, 1995, **14**, 3367.
2. R. J. Puddephatt, *Chem. Soc. Rev.*, 1983, 99.
3. I. Haiduc; I. Silaghi-Dumitrescu, *Coord. Chem. Rev.*, 1986, **74**, 127.
4. B. Chaudret; B. Delavaux; R. Poilblanc, *Coord. Chem. Rev.*, 1988, **86**, 191.
5. M. S. Balakrishna; V. Sreenivasa Reddy; S. S. Krishnamurthy; J. F. Nixon; J. C. T. R. Burckett St Laurent, *Coord. Chem. Rev.*, 1994, **129**, 1.
6. H. C. Clark; L. E. Manzer, *J. Organomet. Chem.*, 1973, **59**, 411.

7. Y. Tatsuno; T. Yoshida; Seiotsuka, *Inorg. Synth.*, 1979, **19**, 220.

8. G. J. Kubas, *Inorg. Synth.*, 1979, **19**, 90.

9. R. Uson; A. Laguna; M. Laguna, *Inorg. Synth.*, 1989, **26**, 85.

10. D. Drew; J. R. Doyle, *Inorg. Synth.*, 1991, **28**, 346.

11. J. X. McDermott; J. F. White; G. M. Whiteside, *J. Am. Chem. Soc.*, 1976, **60**, 6521.

12. M. A. Bennett; T. N. Huang; T. W. Matheson; A. R. Smith, *Inorg. Synth.*, 1982, **21**, 74.

13. G. Giordano; R. H. Crabtree, *Inorg. Synth.*, 1979, **19**, 218.

14. C. White; A. Yates; P. M. Maitlis, *Inorg. Synth.*, 1992, **29**, 228.

CHAPTER 3.3: PREPARATION AND COORDINATION CHEMISTRY OF N-DIALLYLAMINOPHOSPHINE

3.3.1 *Introduction*

Diallylamine has been used as a ligand in a variety of interesting reactions. Due to the presence of the two-allyl arms it can bind through one or both depending on the metal present in the co-ordination reaction. Andreu and co-workers[1] demonstrated this binding mode when they reacted (tmeda)Pd(CH_3)$_2$ with diallylamine and PR_3. They used the prepared palladium (0) monophosphine complexes as catalysts in Suzuki coupling reactions and they were shown to be efficient cross-coupling catalysts for aryl chlorides and phenylboronic acid compared with the traditional palladium (II)-PR_3 catalysts previously used.

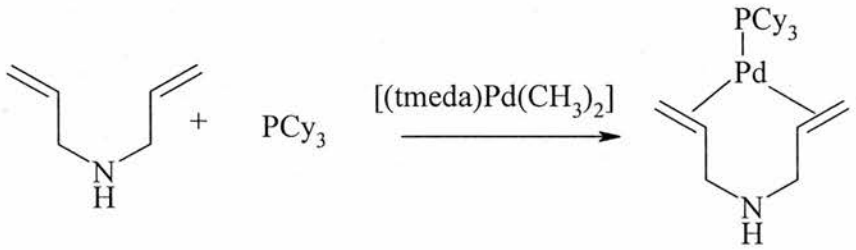

Scheme 3.3.1. Reaction of $(C_3H_5)_2NH$ with PR_3.

Wu *et al* in 2001[2] prepared complexes that showed the nitrogen being used in coordination. Wu reacted pentacarbonyl[3-(cyclopent-1-enyl)-1-ethoxy-2-propyn-1-ylidene]tungsten with diallylamine. The product obtained showed that the N atom had bound to the metal complex through the propyne moiety. Figure 3.3.1 shows this coordination.

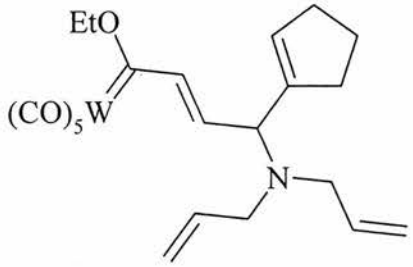

Figure 3.3.1. Coordination of diallylamine to a $(CO)_5W$ complex.

A third binding motif occurs when diallylamine binds through one of the allyl chains and through the N atom as shown by Hiraki *et al* in 1994[3]. Hiraki performed reactions of $[RuClH(CO)(PPh_3)]$ with both primary and secondary allylamines to yield olefin-insertion products. Diallylamine has also recently been used to investigate the reaction of different mono-, di-, and triamino alkynyl metal carbene systems. The results obtained by Moretó and Ricart[4] showed fairly good stability of the complexes formed by addition of secondary amines compared with the corresponding primary amines. The work performed by Moretó *et al* concentrated on the use of tungsten carbene complexes prepared by Pares *et al*[5] and Moretó *et al*[6]. The results obtained showed that in all the experiments performed the addition of the secondary amine was stereo- and regioselective to give the *E* isomer, which was shown previously by Aumann[7] for additions of similar amines and alkoxy systems.

Cyclopentadienyl complexes can undergo base-induced migration reactions. Baya *et al*[8] reported the reaction of $[OsH(\eta^5\text{-}C_5H_5)Cl(GePh_3)(P^iPr_3)]$ **A** with $LiN(C_3H_5)_2$ and showed that the cyclopentadienyl group contains a nitrogen atom. The formation of this complex is rationalised by the initial replacement of the chlorine ligand of **A** by the amide followed by exchange of the $N(C_3H_5)_2(Os)/H(C_5H_5)$.

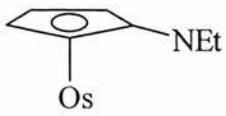

A

Diallylamine has been shown to react with Ni (II) complexes containing furanyl rings. Eilmes *et al*[9] prepared the di- and mono-substituted succinyl dichloride products of 5,14-dihydro-6,8,15,17-tetramethyldibenzo [b,I][1,4,8,11]tetraazacyclotetradecine which were subsequently reacted with the appropriate amine to yield the desired amino complex in good yields. The amino complexes formed are explained in terms of nucleophilic attack of the amine on the carbonyl carbon within the *meso* substituents of the macrocycle. Reactions of diallylamine with [Cp*W(NO)(η^2-CPhCH$_2$)Cl] yielded an unusual product where the vinyl group coupled with the amine fragment in very good yield[10]. X-ray analysis performed on this complex showed that a dative bond was formed between the diallylamine and W and a single N-C bond through the vinyl fragment.

In this work the preparation of a new phosphine that contains the diallyl backbone with the potential to act as a hemilabile ligand. Coordination complexes have also been prepared.

Results and Discussion

3.3.2 *Synthesis and chalogen derivatives of $Ph_2PN(C_3H_5)_2$*

Reaction of diallylamine with one equivalent of Ph_2PCl in the presence of NEt_3 proceeds in thf to give **54** that was isolated (83 % yield) by filtration from $Et_3NH^+Cl^-$ as a colourless oil. The $^{31}P\{^1H\}$ NMR spectrum of **54** consists of a singlet at δ_P 64.3 ppm. In the IR spectrum bands are observed at 1638, 1433 and

993 cm^{-1}, which are assigned to $\nu_{C=C}$, ν_{PPh2} and ν_{PN} respectively. The microanalysis gave satisfactory results.

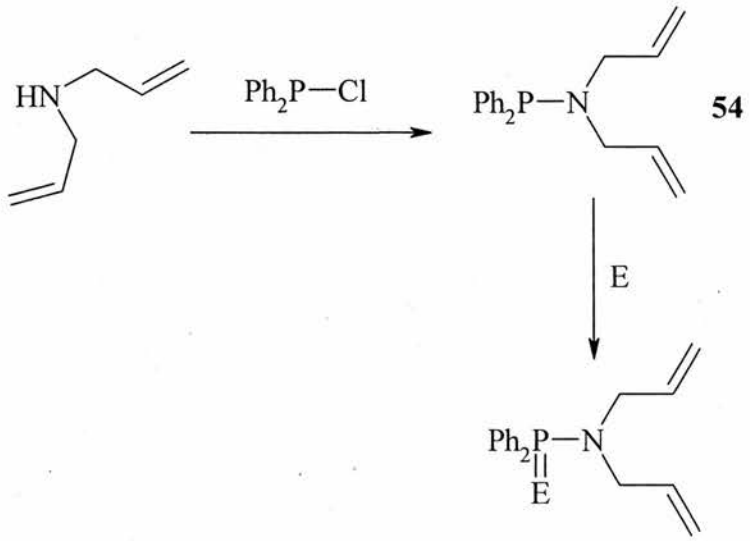

Scheme 3.3.2. Formation of $Ph_2PN(C_3H_5)_2$ and $Ph_2P(E)N(C_3H_5)_2$ ligands {E = O (**55**), S (**56**), Se (**57**)}.

The oxide (**55**) $Ph_2P(O)N(C_3H_5)_2$ was easily prepared by addition of urea hydrogen peroxide to a dichloromethane solution of **54**, whilst the sulfur (**56**) and seleno (**57**) analogues were prepared by the addition of elemental S or Se to the ligand in toluene. Satisfactory microanalysis was obtained for the **57** though only fairly satisfactory results were obtained for **55** and **56**, possibly due to difficulties in purifying the oily products formed, and the EI^+ mass spectral data gave the expected parent ion and fragmentation patterns. The $^{31}P\{^1H\}$ NMR show single resonances ($CDCl_3$) at δ_P 31.3 and 69.8 ppm for the oxide and sulfide respectively. The seleno analogue exhibits a single $^{31}P\{^1H\}$ NMR resonance ($CDCl_3$) at δ_P 58.1 ppm with selenium satellites $^1J(^{31}P\text{-}^{77}Se)$ 756 Hz which is typical for a P=Se group.

3.3.3 *Coordination chemistry of $Ph_2PN(C_3H_5)_2$*

Reaction of $[PtCl_2(cod)]$ with $Ph_2PN(C_3H_5)_2$ gave interesting results. Initially a 2:1 reaction was carried out as it was thought that two ligands would replace the cod moiety of the starting metal complex. However, after running the $^{31}P\{^1H\}$ NMR two products were identified. From this initial finding a further two experiments were performed to try to isolate each product and determine the coordination chemistry around the platinum centre. Reaction of $[PtCl_2(cod)]$ with three equivalents of $Ph_2PN(C_3H_5)_2$ gives $[Pt\{Ph_2PN(C_3H_5)_2\}_3][Cl_2]$ (**58**) in good yield (64 %). The FAB mass spectrum of **58** contains the expected parent ion and fragmentation pattern and the complex exhibits three different resonances with platinum satellites in the $^{31}P\{^1H\}$ NMR spectrum ($\delta(P_A)$ 83.7 (d) ppm, $^1J(^{31}P_A\text{-}^{195}Pt)$ 4800 Hz; $\delta(P_X)$ 74.5 (d of d) ppm, $^1J(^{31}P_X\text{-}^{195}Pt)$ 2052 Hz, $^2J(^{31}P_A\text{-}^{31}P_X)$ 9 Hz, $^2J(^{31}P_X\text{-}^{31}P_Y)$ 44 Hz; $\delta(P_Y)$ 47.9 (d) ppm, $^2J(^{31}P_Y\text{-}^{195}Pt)$ 281 Hz) which indicates the presence of three phosphorus ligands around the platinum centre. Figure 3.3.2 shows three discrete phosphorus environments each with its own platinum satellites. Scheme 3.3.3 gives a suggested structure that is consistent with these spectral observations. The IR spectrum has bands at 1637, 1356 and 1436 cm^{-1} corresponding to two $\upsilon_{C=C}$ and υ_{PPh2} respectively and a υ_{PN} vibration at 997 cm^{-1}. Reaction of $[PtCl_2(cod)]$ with one equivalent of $Ph_2PN(C_3H_5)_2$ gives the second product observed in the 2:1 reaction, $[PtCl_2\{Ph_2PN(C_3H_5)_2\}]$ (**59**), in good yield (65 %). Microanalysis gave satisfactory results for the formation of the chelated ligand complex and FAB mass spectral analysis gives the expected parent ion and fragmentation pattern. The complex displays a single resonance with platinum satellites in the $^{31}P\{^1H\}$ NMR spectrum (δ_P 70.1 ppm, $^1J(^{31}P\text{-}^{195}Pt)$

3491 Hz) and the IR spectrum has two $\upsilon_{C=C}$, υ_{PPh2} and υ_{PN} vibrations at 1634, 1362, 1434 and 1010 cm^{-1} respectively and two υ_{PtCl} bands at 317 and 295 cm^{-1} which suggest a *cis* geometry.

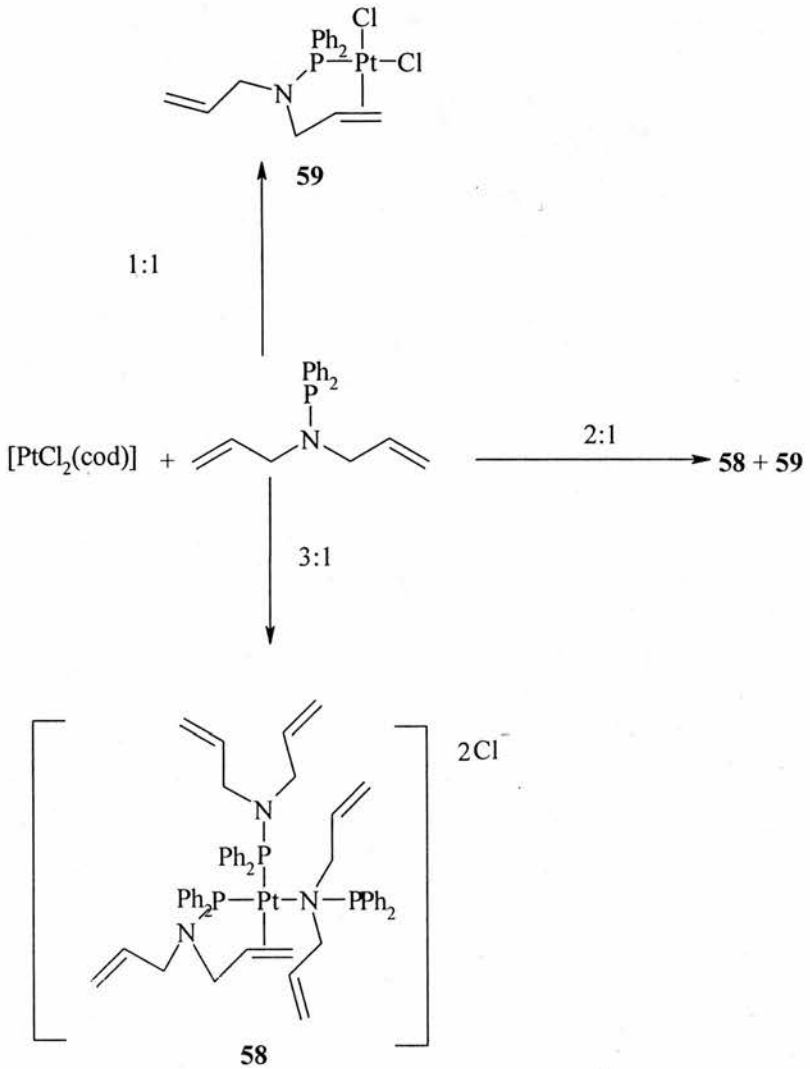

Scheme 3.3.3. Reaction of $Ph_2PN(C_3H_5)_2$ with $[PtCl_2(cod)]$.

Figure 3.3.2. ^{31}P NMR of $Ph_2PN(C_3H_5)_2$ with $[PtCl_2(cod)]$.

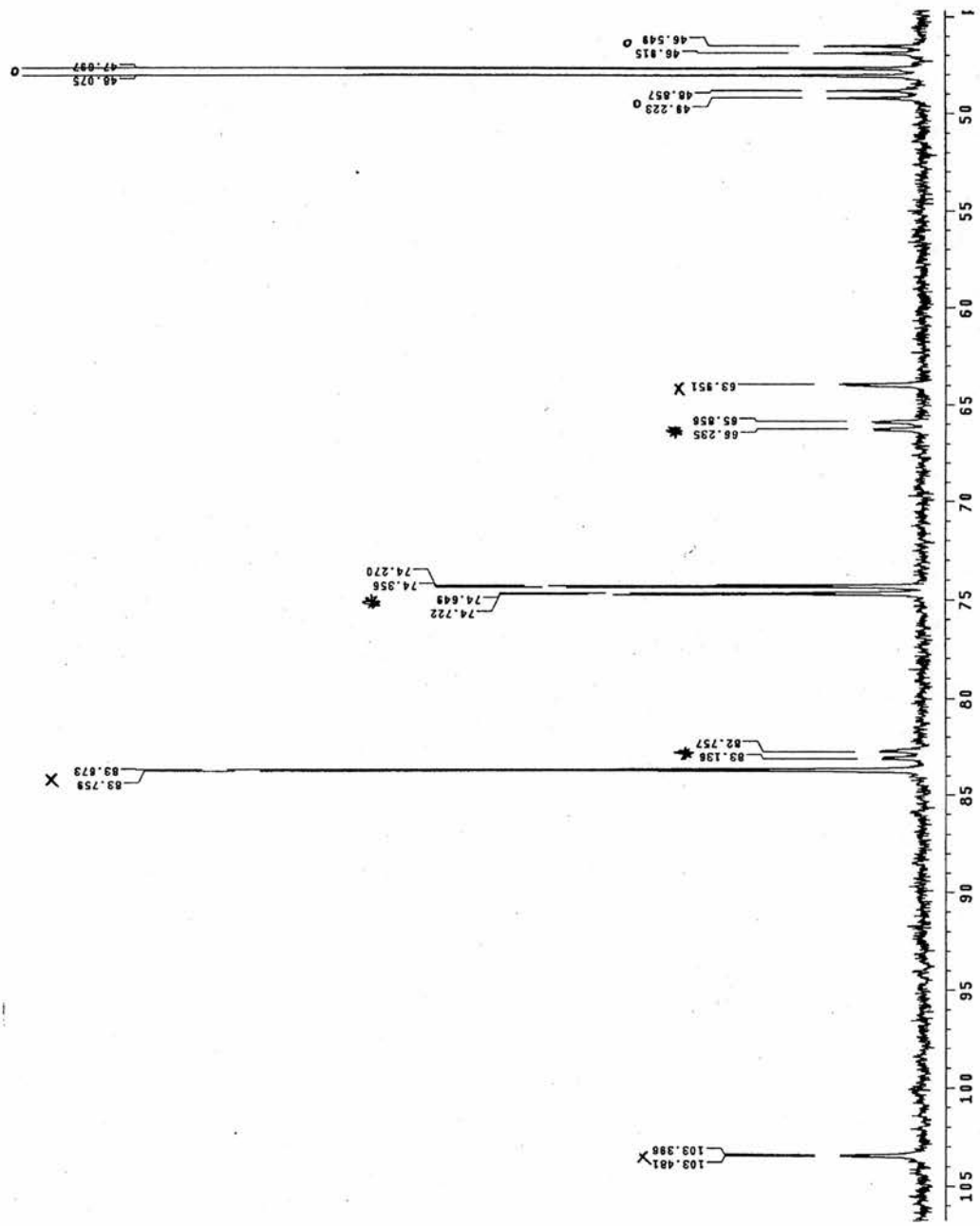

Reaction of $[PdCl_2(cod)]$ with $Ph_2PN(C_3H_5)_2$ behaved similarly in the presence of two equivalents of ligand. The $^{31}P\{^1H\}$ NMR study of the 2:1 reaction revealed that two products were again observed and a similar approach

as discussed previously was performed to isolate the two compounds. However, in the presence of three equivalents of **54** and one equivalent of $[PdCl_2(cod)]$ only the 2:1 complex, $[PdCl_2\{Ph_2PN(C_3H_5)_2\}_2]$ (**60**) is obtained. The $^{31}P\{^1H\}$ NMR shows two signals at δ_P 109.2 and 44.7 ppm ($^2J\{^{31}P_A\text{-}^{31}P_X\}$ 18 Hz) indicating two phosphorus environments within the complex. The FAB mass spectrum gives the expected parent ion and fragmentation pattern and microanalysis is found to be fairly satisfactory. The IR spectrum has bands at 1638, 1356, 1435 and 995 cm^{-1} that correspond to two $\nu_{C=C}$, ν_{PPh2} and ν_{PN} respectively and two ν_{PdCl} bands at 292 and 277 cm^{-1}. The reaction of one equivalent of $Ph_2PN(C_3H_5)_2$ with $[PdCl_2(cod)]$ proceeds in a similar fashion to the reaction of one equivalent of $Ph_2PN(C_3H_5)_2$ and $[PtCl_2(cod)]$ to prepare $[PdCl_2\{Ph_2PN(C_3H_5)_2\}]$ (**61**) in good yield (91 %). The microanalytical data obtained was satisfactory for the suggested structure and the FAB mass spectral data showed the expected parent ion and fragmentation pattern. The $^{31}P\{^1H\}$ NMR ($CDCl_3$) shows a single resonance at δ_P 101.3 ppm. The IR spectrum shows vibrations at 1634, 1361 cm^{-1} that correspond to two $\nu_{C=C}$, and bands at 1435, 999, 317 and 290 cm^{-1} corresponding to ν_{PPh2}, ν_{PN} and two ν_{PdCl} bands respectively.

Crystals of $[PdCl_2\{Ph_2PN(C_3H_5)_2\}]$ (**61**) suitable for X-ray crystallography were grown overnight by layering a chloroform solution with diethyl ether. The crystal structure of the complex (Figure 3.3.2) and selected bond lengths and angles (Table 3.3.1) are shown below. The crystal structure shows that the molecule is square planar at palladium and forms *cis* geometry. The molecular structure contains one ligand and is bound to the palladium metal

via phosphorus with a P(1)-Pd(1) bond length of 2.2247(6) and one of the olefinic arms of the ligand. The angle for P(1)-Pd(1)-C(16) is 90.68(8) ° and for P(1)-Pd(1)-C(15) is 83.25(7) °.

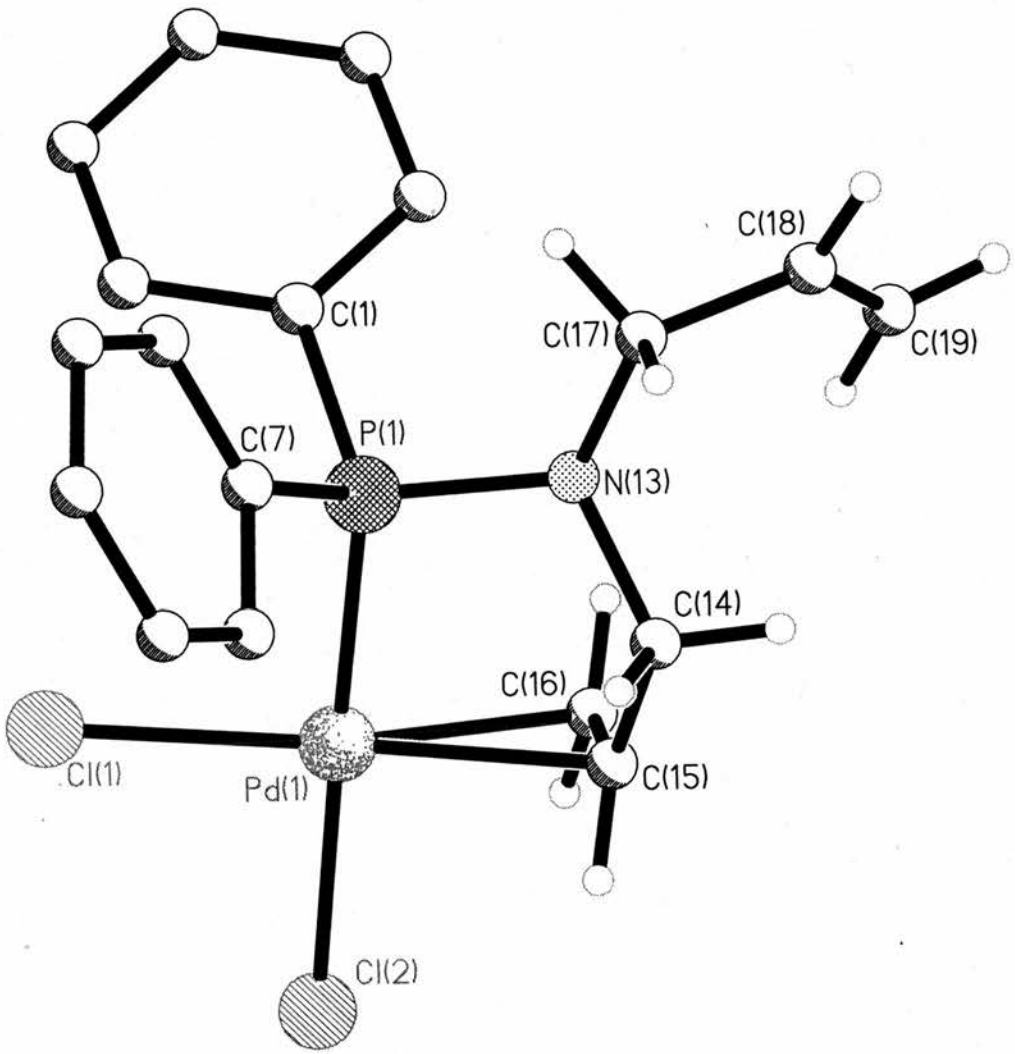

Figure 3.3.3. The X-ray structure of $[PdCl_2\{Ph_2PN(C_3H_5)_2\}]$ (**61**).

Table 3.3.1. Selected bond lengths (Å) and angles (°) for

$[PdCl_2\{Ph_2PN(C_3H_5)_2\}]$

Selected bond lengths (Å) and angles (°)	*(61)*
M(1)-Cl(1)	2.2983(7)
M(1)-Cl(2)	2.3641(7)
M(1)-P(1)	2.2247(6)
M(1)-C(15)	2.192(2)
M(1)-C(16)	2.177(3)
P(1)-N(13)	1.6719(19)
N(13)-C(14)	1.465(3)
N(13)-C(17)	1.466(3)
P(1)-M(1)-Cl(1)	88.07(2)
C(16)-M(1)-C(15)	36.30(10)
C(16)-M(1)-P(1)	90.68(8)
C(15)-M(1)-P(1)	83.25(7)
C(16)-M(1)-Cl(1)	162.80(8)
C(15)-M(1)-Cl(1)	159.63(8)
C(15)-M(1)-Cl(2)	95.46(7)
C(16)-M(1)-Cl(2)	88.46(8)
Cl(1)-M(1)-Cl(2)	93.05(3)
N(13)-P(1)-M(1)	103.54(7)
P(1)-M(1)-Cl(2)	178.67(2)
C(14)-N(13)-P(1)	112.62(15)
C(17)-N(13)-P(1)	120.58(17)

The reaction of $[PtMe_2(cod)]$ with one equivalent of $Ph_2PN(C_3H_5)_2$ gave the expected chelate complex, $[PtMe_2\{Ph_2PN(C_3H_5)_2\}$ (**62**), in average yield (53 %). The FAB mass spectral data obtained gave the expected parent ion and fragmentation pattern and in the IR spectrum $\nu_{C=C}$, ν_{PPh2} and ν_{PN} vibrations were observed at 1636, 1432 and 992 cm^{-1} respectively. The $^{31}P\{^1H\}$ NMR (CD_2Cl_2) showed a single resonance with platinum satellites (δ_P 90.7 ppm, $^1J(^{31}P\text{-}^{195}Pt)$ 1937 Hz).

Reaction of $Ph_2PN(C_3H_5)_2$ with $[Mo(CO)_4(nbd)]$ gives $[Mo(CO)_4\{Ph_2PN(C_3H_5)_2\}]$ (**63**) as a yellow solid in poor yield (32 %). The $^{31}P\{^1H\}$ NMR ($CDCl_3$) displays a single resonance at δ_P 116.2 ppm and the microanalysis gave good results for the suggested structure. The FAB mass spectrum shows the expected fragmentation pattern and parent ion and the IR spectrum shows bands at 1893, 1434 and 987 cm^{-1} that correspond to ν_{CO} ν_{PPh2} and ν_{PN} vibrations respectively with two $\nu_{C=C}$ bands observed at 1637 and 1458 cm^{-1}.

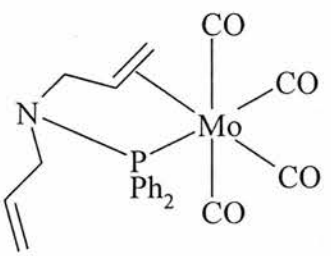

63

Figure 3.3.4. Suggested structure of $[Mo(CO)_4\{Ph_2PN(C_3H_5)_2\}]$.

$[RuCl_2\{Ph_2PN(C_3H_5)_2\}(\eta^6\text{-}p\text{-}MeC_6H_4{}^iPr)]$ (**64**) is prepared easily in good yield (92 %) by dissolving $[\{RuCl(\mu\text{-}Cl)(\eta^6\text{-}p\text{-}MeC_6H_4{}^iPr)_2\}_2]$ and $Ph_2PN(C_3H_5)_2$ in dichloromethane. The microanalysis gave satisfactory results for the suggested structure and the $^{31}P\{^1H\}$ NMR ($CDCl_3$) shows a single resonance at δ_P 74.1 ppm. The FAB mass spectrum shows the expected parent ion and fragmentation pattern with $[M\text{-}Cl]^+$ at 552. In the IR spectrum bands are observed at 1637, 1432, 994, 299 and 278 cm^{-1} corresponding to $\nu_{C=C}$, ν_{PPh2} and ν_{PN} and two ν_{RuCl} vibrations respectively.

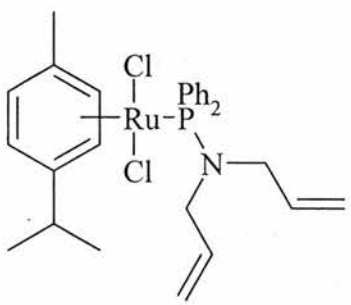

64

Figure 3.3.5. Suggested structure of $[RuCl_2\{Ph_2PN(C_3H_5)_2\}(\eta^6\text{-}p\text{-}MeC_6H_4{}^iPr)]$.

The complex $[RhCl\{Ph_2PN(C_3H_5)_2\}]$ (**65**) is prepared by reaction of $[\{Rh(\mu\text{-}Cl)(cod)\}_2]$ and $Ph_2PN(C_3H_5)_2$ in dichloromethane in good yield (96 %). The $^{31}P\{^1H\}$ NMR ($CDCl_3$) shows a two resonances with rhodium satellites ($\delta(P_A)$ 115.5 (d) ppm, $^1J(^{31}P_A\text{-}^{103}Rh)$ 154 Hz. $\delta(P_X)$ 84.7 (d) ppm, $^1J(^{31}P_X\text{-}^{103}Rh)$ 114 Hz. $^2J(^{31}P_A\text{-}^{31}P_X)$ 25 Hz). The IR spectrum shows bands at 1638, 1433, 990 and 251 cm^{-1} that correspond to $\upsilon_{C=C}$, υ_{PPh2} and υ_{PN} and υ_{RhCl} vibrations respectively. The microanalysis shows fairly satisfactory results and the FAB mass spectrum shows the expected fragmentation pattern and parent ion of $[M\text{-}Cl]^+$ at 665.

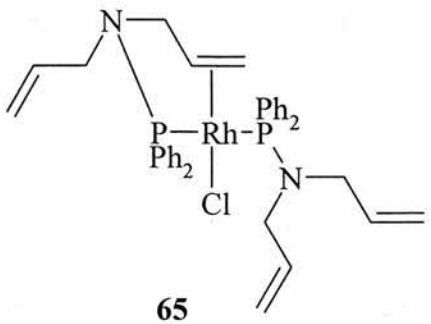

65

Figure 3.3.6. Suggested structure of [RhCl{$Ph_2PN(C_3H_5)_2$}].

[PdCl($C_{14}H_{12}N$){$Ph_2PN(C_3H_5)_2$}] (**66**) is prepared easily in good yield (92 %) by adding a suspension of [{PdCl($C_{14}H_{12}N$)}$_2$] in dichloromethane to a solution of $Ph_2PN(C_3H_5)_2$ in dichloromethane. The microanalysis gave fairly satisfactory results for the suggested structure and the $^{31}P\{^1H\}$ NMR ($CDCl_3$) shows a single resonance at δ_P 97.7 ppm. The FAB mass spectrum shows the expected parent ion and fragmentation pattern with $[M\text{-}Cl]^+$ at 557. In the IR spectrum bands are observed at 1638, 1435, 1003 and 282 cm^{-1} corresponding to $\nu_{C=C}$, ν_{PPh2} and ν_{PN} and ν_{PdCl} vibrations respectively.

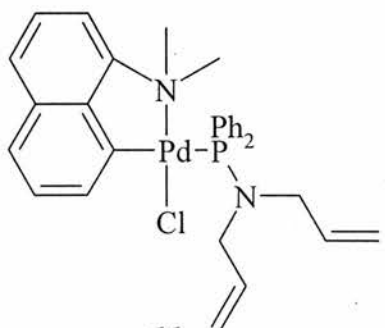

66

Figure 3.3.7. Suggested structure of [PdCl($C_{14}H_{12}N$){$Ph_2PN(C_3H_5)_2$}].

Table 3.3.2. Characterisation data for $Ph_2PN(C_3H_5)_2$ and its derivatives. ([a] $^1J\{^{31}P\text{-}^{77}Se\}$ 756 Hz.). ([b] $^1J\{^{31}P_A\text{-}^{195}Pt\}$ 4800 Hz. $^1J\{^{31}P_X\text{-}^{195}Pt\}$ 2052 Hz. $^2J\{^{31}P_A\text{-}^{195}Pt\}$ 9 Hz, $^2J\{^{31}P_X\text{-}^{31}P_Y\}$ 44 Hz. $^2J\{^{31}P_Y\text{-}^{195}Pt\}$ 281 Hz.). ([c] $^2J\{^{31}P_A\text{-}^{31}P_X\}$ 18 Hz.). ([d] $^1J\{^{31}P\text{-}^{195}Pt\}$ 3491 Hz), ([e] $^1J\{^{31}P\text{-}^{195}Pt\}$ 1937 Hz.). ([f] $^1J\{^{31}P\text{-}^{103}Rh\}$ Hz.). ([g] $^1J\{^{31}P_A\text{-}^{103}Rh\}$ 154 Hz. $^1J\{^{31}P_X\text{-}^{103}Rh\}$ 114 Hz, $^2J\{^{31}P_A\text{-}^{31}P_X\}$ 25 Hz.).

Compound	*$^{31}P\{^1H\}$ NMR*	*IR/cm^{-1}*					*Microanalysis/ % Found (calc.)*		
	δ_P/ppm	ν_{PN}	$\nu_{C=C}$	ν_{PPh2}	$\nu_{P=E]}$	ν_{MCl}	C	H	N
$Ph_2PN(C_3H_5)_2$ (54)	64.3	993	1638	1433	-	-	74.47 (76.85)	7.79 (7.17)	4.72 (4.98)
$Ph_2P(O)N(C_3H_5)_2$ (55)	31.3	992	1635	1433	1181	-	68.61 (72.71)	6.58 (6.78)	4.46 (4.71)

Table continue. Characterisation data for $Ph_2PN(C_3H_5)_2$ and its derivatives.									
$Ph_2P(S)N(C_3H_5)_2$ (56)	69.8	997	1638	1434	689	-	66.03	7.48	4.80
							(68.98)	(6.43)	(4.47)
$Ph_2P(Se)N(C_3H_5)_2$ (57)	58.1[a]	995	1636	1435	573	-	59.93	6.80	4.28
							(60.01)	(5.60)	(3.89)
$[PtCl\{(Ph_2PN(C_3H_5)_2\}_3][Cl^-]$ (58)	83.7,	997	1637	1436	-	296	58.84	5.38	3.73
	74.9,		1356				(58.43)	(5.45)	(3.79)
	47.9 [b]								
$[PtCl_2\{Ph_2PN(C_3H_5)_2\}]$ (59)	70.1[d]	1010	1634	1434	-	317,	40.02	3.50	3.41
			1362			295	(39.50)	(3.68)	(2.56)
$[PdCl_2\{Ph_2PN(C_3H_5)_2\}_2]$ (60)	109.2,	995	1638	1435	-	292,	57.56	5.22	3.40
	44.7[c]		1356			277	(58.43)	(5.45)	(3.79)
$[PdCl_2\{Ph_2PN(C_3H_5)_2\}]$ (61)	101.3	999	1634	1435	-	317,	46.76	4.18	2.70
			1361			290	(47.14)	(4.40)	(3.05)

Table continue. Characterisation data for $Ph_2PN(C_3H_5)_2$ and its derivatives.									
$[PtMe_2\{Ph_2PN(C_3H_5)_2\}]$ (62)	90.7[e]	992	1636	1432	-	-	46.90	4.46	2.35
							(47.42)	(5.18)	(2.77)
$[Mo(CO)_4\{Ph_2PN(C_3H_5)_2\}]$ (63)	116.2	987	1637	1434	-	-	54.04	3.16	2.76
			1458				(54.00)	(4.12)	(2.86)
$[RuCl_2\{Ph_2PN(C_3H_5)_2\}(\eta^6\text{-}p\text{-}MeC_6H_4{}^iPr)]$ (64)	74.1	994	1637	1432	-	299,	57.33	5.65	2.21
						278	(57.24)	(5.83)	(2.38)
$[RhCl\{Ph_2PN(C_3H_5)_2\}_2]$ (65)	115.5,	990	1638	1433	-	251	61.00	6.12	3.83
	84.7[g]						(61.70)	(5.75)	(4.00)
$[PdCl(C_{14}H_{12}N)\{Ph_2PN(C_3H_5)_2\}]$ (66)	97.7	1003	1638	1435	-	282	59.65	5.52	4.42
							(60.72)	(5.44)	(4.72)

Experimental

General experimental conditions and instruments were as set out on page xvii. Unless otherwise stated, all reactions were carried out under an oxygen-free nitrogen atmosphere using standard Schlenk techniques. Diethyl ether and thf were purified by reflux over sodium-benzophenone and distillation under nitrogen. Dichloromethane was heated to reflux over calcium hydride and distilled under nitrogen. Toluene and hexane were heated to reflux over sodium and distilled under nitrogen. The complexes [PtMeX(cod)] (X = Cl or Me)[11], $[Pd(\mu Cl)(\eta^3\text{-}C_3H_5)]_2$[12], $[Cu(MeCN)_4][PF_6]$[13], [AuCl(tht)] (tht = tetrahydrothiophene)[14], $[MCl_2(cod)]$ (M = Pt or Pd; cod = cycloocta-1,5-diene)[15, 16], $[\{RuCl(\mu\text{-}Cl)(\eta^6\text{-}p\text{-}MeC_6H_4{}^iPr)_2\}]$[17], $[\{Rh(\mu\text{-}Cl)(cod)\}_2]$[18], [Mo(CO)4(nbd)][19] and $[\{Pd(\mu\text{-}Cl)(C_{14}H_{12}N)\}_2]$[20] were prepared using literature procedures. Chlorodiphenylphopshine and diallylamine were distilled prior to use. NEt_3 (99 % purity), ^tBuOK (95 % purity), H_2O_2 (30 wt. % in H_2O) and reagent grade KBr were used without further purification. Infra-red spectra were recorded as KBr discs in the range 4000-200 cm^{-1} on a Perkin-Elmer 2000 FTIR/RAMAN spectrometer. NMR spectra were recorded on a Gemini 2000 spectrometer (operating at 121.4 MHz for ^{31}P and 300 MHz for ^1H). Microanalyses were performed by the St. Andrews University service and mass spectra by the Swansea Mass Spectrometer Service.

$[Ph_2PN(C_3H_5)_2]$. (54): Diallylamine (2.841 g, 29.2 mmol) and triethylamine (3.107 g, 30.7 mmol) were added together in dry thf (50 cm^3). Chlorodiphenylphosphine (6.453 g, 29.2 mmol) in dry thf (50 cm^3) was added dropwise with stirring overnight. Triethylamine hydrochloride was removed by filtration under nitrogen and the solvent removed *in vacuo* to yield a colourless oil. Yield 6.840 g, 83 %. Microanalysis:

Found (calculated for $C_{18}H_{20}NP$) C 74.47 (76.85), H 7.79 (7.17), N 4.72 (4.98) %. $^{31}P\{^1H\}$ NMR ($CDCl_3$): 64.3 ppm. ^1H NMR ($CDCl_3$) δ 7.3-7.8 (m, 10 H, Ph), 5.6-5.7 (m, 2 H, $CH=CH_2$), 5.0-5.1 (t, 4 H, CH_2), 3.4-3.5 (m, 4 H, CH_2) ppm. IR (thin film): 1638, 1433, 933 cm^{-1}.

$Ph_2P(O)N(C_3H_5)_2$. (55): $Ph_2PN(C_3H_5)_2$ (256 mg, 0.9 mmol) was dissolved in CH_2Cl_2 (20 cm^3) and cooled to 0 °C before addition of urea hydrogen peroxide (86 mg, 0.9 mmol) was added and the reaction mixture was stirred overnight. The product was extracted from the CH_2Cl_2 by addition of distilled water, washed with CH_2Cl_2 (3x 5 cm^3), dried over magnesium sulfate and evaporated to dryness to yield a colourless oil. Yield 254 mg, 94 %. Microanalysis: Found (calculated for $C_{18}H_{20}NOP$) C 68.61 (72.71), H 6.58 (6.78), N 4.46 (4.71) %. $^{31}P\{^1H\}$ NMR ($CDCl_3$): 31.3 ppm. ^1H ($CDCl_3$) δ 7.3-7.8 (m, 10 H, Ph), 5.6-5.7 (m, 2 H, $CH=CH_2$), 5.0-5.1 (t, 4 H, CH_2), 3.4-3.5 (m, 4 H, CH_2) ppm. EI^+ MS: *m/z* 297 $[M]^+$. IR (thin film): 1635, 1433, 1181, 992 cm^{-1}.

$Ph_2P(S)N(C_3H_5)_2$. (56): $Ph_2PN(C_3H_5)_2$ (766 mg, 2.7 mmol) and elemental sulfur (87 mg, 2.7 mmol) were dissolved in dry toluene (10 cm^3) to yield a yellow solution which was stirred overnight. The reaction mixture was cooled to room temperature and the solvent removed before addition of CH_2Cl_2 (2 cm^3) and filtering through Celite to remove any remaining inorganic solid. After removing the CH_2Cl_2 colourless oil was yielded. Yield 753 mg, 88 %. Microanalysis: Found (calculated for $C_{18}H_{20}NPS$) C 66.03 (68.98), H 7.48 (6. 43), N 4.80 (4.47) %. $^{31}P\{^1H\}$ NMR ($CDCl_3$): 69.8 ppm. ^1H NMR ($CDCl_3$) δ 7.3-7.8 (m, 10 H, Ph), 5.6-5.7 (m, 2 H, $CH=CH_2$), 5.0-5.1 (t, 4 H, CH_2), 3.4-3.5 (m, 4 H, CH_2) ppm. EI^+: *m/z* 273 $[M]^+$. IR(thin film): 1638, 1434, 997, 689 cm^{-1}.

$Ph_2P(Se)N(C_3H_5)_2$. (57): $Ph_2PN(C_3H_5)_2$ (235 mg, 1.0 mmol) and grey selenium (77 mg, 1.0 mmol) were refluxed in dry toluene (10 cm^3) for 1 hour before cooling to room temperature and filtering through a Celite plug to remove any insoluble material. The solvent was reduced to 1 cm^3 to yield a colourless solid that was isolated by suction filtration and dried *in vacuo*. Yield 269 mg, 86 %. Microanalysis: Found (calculated for $C_{18}H_{20}NPSe$) C 59.93 (60.01), H 6.80 (5.60), N 4.28 (3.89) %. $^{31}P\{^1H\}$ NMR ($CDCl_3$): 58.1 ppm $^1J(^{31}P\text{-}^{77}Se)$ 756 Hz. ^1H NMR ($CDCl_3$) δ 7.3-7.8 (m, 10 H, Ph), 5.6-5.7 (m, 2 H, $CH{=}CH_2$), 5.0-5.1 (t, 4 H, CH_2), 3.4-3.5 (m, 4 H, CH_2) ppm. EI^+ MS: *m/z* 361 $[M + H]^+$. IR (KBr disc): 1636, 1435, 995, 573 cm^{-1}.

$[Pt\{Ph_2PN(C_3H_5)_2\}_3][Cl_2^-]$. (58): $Ph_2PN(C_3H_5)_2$ (165 mg, 0.6 mmol) and $[PtCl_2(cod)]$ (73 mg, 0.2 mmol) were dissolved in CH_2Cl_2 (5 cm^3) to yield a pale yellow solution that was stirred for 30 minutes. The solvent was reduced to 1 cm^3 before precipitating a colourless solid upon addition of diethyl ether (cm^3) that was isolated by suction filtration. Yield 140 mg, 64 %. Microanalysis: Found (calculated for $C_{54}H_{60}P_3N_3PtCl_2$) C 58.84 (58.43), H 5.38 (5.45), N 3.73 (3.79) %. $^{31}P\{^1H\}$ NMR ($CDCl_3$): $\delta(P_A)$ 83.7 (d) ppm, $^1J(^{31}P_A\text{-}^{195}Pt)$ 4800 Hz. $\delta(P_X)$ 74.5 (d of d) ppm, $^1J(^{31}P_X\text{-}^{195}Pt)$ 2052 Hz. $^2J(^{31}P_A\text{-}^{31}P_X)$ 9 Hz. $^2J(^{31}P_Y\text{-}^{31}P_X)$ 44 Hz. $\delta(P_Y)$ 47.9 (d) ppm, $^2J(^{31}P_Y\text{-}^{195}Pt)$ 281 Hz. ^1H NMR ($CDCl_3$) δ 7.3-7.8 (m, 30 H, Ph), 5.6-5.7 (m, 4 H, $CH{=}CH_2$), 5.0-5.1 (m, 2 H, chelate $CH{=}CH_2$), 4.8-4.9 (m, 8 H, CH_2), 4.4-4.5 (m, 4 H, chelate CH_2), 3.4-3.5 (m, 12 H, CH_2) ppm. FAB^+ MS: *m/z* 1075 $[M - Cl]^+$. IR(KBr disc): 1637, 1436, 997, 296 cm^{-1}.

$[PtCl_2\{Ph_2PN(C_3H_5)_2\}]$. (59): $Ph_2PN(C_3H_5)_2$ (197 mg, 0.7 mmol) in CH_2Cl_2 (5 cm^3) was added dropwise to a CH_2Cl_2 (5 cm^3) solution of $[PtCl_2(cod)]$ (262 mg, 0.7 mmol) over 2.5 hours. The solvent was reduced to 1 cm^3 before addition of hexane (10 cm^3)

to yield an off white sticky solid on reduction of solvent. The sticky solid was subsequently dissolved in CH_2Cl_2 (0.5 cm^3) before addition of petroleum ether (40-60) (10 cm^3) to yield a colourless solid that was isolated by suction filtration. Yield 248 mg, 65 %. Microanalysis: Found (calculated for $C_{18}H_{20}NPPtCl_2$) C 40.02 (39.50), H 3.50 (3.68), N 3.41 (2.56) %. $^{31}P\{^1H\}$ NMR ($CDCl_3$): 70.1 ppm $^1J(^{31}P\text{-}^{195}Pt)$ 3491 Hz. ^1H NMR ($CDCl_3$) δ 7.8-7.4 (m, 10 H, aromatic), 5.3 (m, 2 H, CH), 5.1 (m, 2 H, CH_2), 4.7 (d, 1 H, $^3J(^{195}Pt\text{-}^1H)$ 54 Hz, $^2J(^{31}P\text{-}^1H)$ 8 Hz, CH_2), 4.1 (d, 1 H, $^3J(^{195}Pt\text{-}^1H)$ 59 Hz, $^2J(^{31}P\text{-}^1H)$ 13 Hz, CH_2) 3.5 (m, 4 H, NCH_2) ppm. FAB^+ MS: *m/z* 569 $[M + Na]^+$, 547 $[M + H]^+$, 511 $[M - Cl]^+$, 474/6 $[M - 2Cl]^{2+}$. IR (KBr disc): 1634, 1434, 1010, 317, 295 cm^{-1}.

$[PdCl_2\{Ph_2PN(C_3H_5)_2\}_2]$. (60): $(Ph_2P)_2N(C_3H_5)_2$ (124 mg, 0.4 mmol) and $[PdCl_2(cod)]$ (42 mg, 0.1 mmol) were dissolved in CH_2Cl_2 (5 cm^3) to yield an orange solution that was stirred for 30 minutes. The solvent was reduced to 1 cm^3 before precipitating a pale yellow solid upon addition of diethyl ether (20 cm^3) that was isolated by suction filtration. Yield 100 mg, 92 %. Microanalysis: Found (calculated for $C_{36}H_{40}P_2N_2PdCl_2$) C 57.56 (58.43), H 5.22 (5.45), N 3.40 (3.79) %. $^{31}P\{^1H\}$ NMR ($CDCl_3$): $\delta(P_A)$ 109.2 (d) ppm. $\delta(P_X)$ 44.7 (d) ppm. $^2J(^{31}P_A\text{-}^{31}P_X)$ 18 Hz. ^1H NMR ($CDCl_3$) δ 7.3-7.8 (m, 20 H, Ph), 5.6-5.7 (m, 3 H, $CH{=}CH_2$), 5.0-5.1 (m, 1 H, chelate $CH{=}CH_2$), 4.8-4.9 (m, 6 H, CH_2), 4.4-4.5 (m, 2 H, chelate CH_2), 3.4-3.5 (m, 8 H, CH_2) ppm. FAB^+ MS: *m/z* 704 $[M - Cl]^+$, 667/8 $[M - 2Cl]^{2+}$. IR(KBr disc): 1638, 1435, 995, 292, 277 cm^{-1}.

$[PdCl_2\{Ph_2PN(C_3H_5)_2\}]$. (61): $Ph_2PN(C_3H_5)_2$ (111 mg, 0.4 mmol) in CH_2Cl_2 (5 cm^3) was added dropwise to CH_2Cl_2 (5 cm^3) solution of $[PdCl_2(cod)]$ (112 mg, 0.4 mmol). After stirring for 30 minutes the solvent was reduced *in vacuo* to 0.5 cm^3 before

precipitating a yellow microcrystalline solid upon addition of hexane (10 cm^3) and isolation by suction filtration. Yield 164 mg, 91 %. Microanalysis: Found (calculated for $C_{18}H_{20}PNPdCl_2$) C 46.76 (47.14), H 4.18 (4.40), N 2.70 (3.05) %. $^{31}P\{^1H\}$ NMR ($CDCl_3$): 101.3 ppm. ^1H NMR ($CDCl_3$) δ 7.3-7.8 (m, 10 H, Ph), 5.6-5.7 (m, 1 H, $CH{=}CH_2$), 5.0-5.1 (m, 1 H, chelate $CH{=}CH_2$), 4.8-4.9 (m, 2 H, CH_2), 4.4-4.5 (m, 2 H, chelate CH_2), 3.4-3.5 (m, 4 H, CH_2)ppm. FAB^+ MS: *m/z* 422 $[M - Cl]^+$, 386 $[M - 2Cl]^{2+}$. IR (KBr disc): 1634, 1435, 999, 317, 290 cm^{-1}.

$[PtMe_2\{Ph_2PN(C_3H_5)_2\}]$. (62): $Ph_2PNH(C_3H_5)_2$ (96 mg, 0.3 mmol) in CH_2Cl_2 (5 cm^3) was added dropwise to a CH_2Cl_2 (5 cm^3) solution of $[PtMe_2(cod)]$ (114 mg, 0.3 mmol) over 2.5 hours. The solvent was reduced to 1 cm^3 before addition of hexane (10 cm^3) to yield an off white sticky solid on reduction of solvent. The sticky solid was subsequently dissolved in CH_2Cl_2 (0.5 cm^3) before addition of petroleum ether (40-60) (10 cm^3) to yield a colourless solid that was isolated by suction filtration. Yield 92 mg, 53 %. Microanalysis: Found (calculated for $C_{20}H_{26}NPPt$) C 46.90 (47.42), H 4.46 (5.18), N 2.35 (2.77) %. $^{31}P\{^1H\}$ NMR (CD_2Cl_2): 90.7 ppm $^1J(^{31}P\text{-}^{195}Pt)$ 1937 Hz. ^1H NMR (CD_2Cl_2) δ 7.8-7.4 (m, 10 H, aromatic), 5.3 (m, 2 H, CH), 5.1 (m, 2 H, CH_2), 4.7 (d, 1 H, $^3J(^{195}Pt\text{-}^1H)$ 54 Hz, $^2J(^{31}P\text{-}^1H)$ 8 Hz, CH_2), 4.1 (d, 1 H, $^3J(^{195}Pt\text{-}^1H)$ 59 Hz, $^2J(^{31}P\text{-}^1H)$ 13 Hz, CH_2) 3.5 (m, 4 H, NCH_2) ppm. FAB^+ MS: *m/z* 490 $[M - Me]^+$, 476 $[M - 2Me]^{2+}$. IR (KBr disc): 1636, 1432, 992 cm^{-1}.

$[Mo(CO)_4\{Ph_2PN(C_3H_5)_2\}]$. (63): To a CH_2Cl_2 (10 cm^3) solution of $[Mo(CO)_4(nbd)]$ (184 mg, 0.6 mmol) was added dropwise a CH_2Cl_2 (10 cm^3) solution of $(Ph_2P)N(C_3H_5)_2$ (172 mg, 0.6 mmol). After stirring for 30 minutes the solvent was reduced to 2 cm^3 before addition of petroleum ether (bp 40-60) (20 cm^3) and storing overnight at –18 °C. The yellow solid precipitated was isolated by filtration and dried

in vacuo. Yield 95 mg, 32 %. Microanalysis: Found (calculated for $C_{22}H_{20}PNO_4Mo$) C 54.04 (54.00), H 3.16 (4.12), N 2.76 (2.86) %. $^{31}P\{^1H\}$ NMR ($CDCl_3$): 116.2 ppm. ^1H NMR ($CDCl_3$) δ 7.4-7.2 (m, 10 H, aromatic), 5.3 (m, 1 H, CH), 5.0 (m, 2 H, CH_2), 4.7 (m, 1 H, CH), 4.0 (m, 2 H, chelate CH_2), 3.5 (m, 4 H, NCH_2) ppm. FAB^+ MS: *m/z* $[M]^+$, $[M - CO]^+$, $[M - 2CO]^+$, $[M - 3CO]^+$ 523 $[M - 4CO]^+$. IR (KBr disc): 1893, 1434, 987 cm^{-1}.

$[RuCl_2\{Ph_2PN(C_3H_5)_2\}(\eta^6\text{-}p\text{-}MeC_6H_4{}^iPr)]$. (64): $(Ph_2P)N(C_3H_5)_2$ (122 mg, 0.4 mmol) and $[RuCl(\mu\text{-}Cl)(\eta^6\text{-}p\text{-}MeC_6H_4{}^iPr)_2]$ (133 mg, 0.2 mmol) were dissolved in CH_2Cl_2 (5 cm^3) to yield a dark red solution. The solvent was reduced to 1 cm^3 before addition of diethyl ether (10 cm^3) to precipitate an orange solid that was isolated by suction filtration. Yield 118 mg, 92 %. Microanalysis: Found (calculated for $C_{28}H_{34}PNRuCl_2$) C 57.33 (57.24), H 5.65 (5.83), N 2.21 (2.38) %. $^{31}P\{^1H\}$ NMR ($CDCl_3$): 74.1 ppm. ^1H NMR ($CDCl_3$) δ 7.4-7.2 (m, 14 H, aromatic), 5.9 (m, 2 H, CH), 4.8 (m, 4 H, CH_2), 3.5 (m, 4 H, NCH_2), 2.7 (m, 1 H, CH), 1.9 (s, 3 H, $ArCH_3$), 1.2 (m, 6 H, CH_3) ppm. FAB^+ MS: *m/z* 552 $[M - Cl]^+$, 515/7 $[M - 2Cl]^{2+}$. IR (KBr disc): 1637, 1432, 994, 299, 278 cm^{-1}.

$[RhCl\{Ph_2PN(C_3H_5)_2\}_2]$. (65): $(Ph_2P)N(C_3H_5)_2$ (148 mg, 0.5 mmol) and $[\{Rh(\mu\text{-}Cl)(cod)\}_2]$ (65 mg, 0.1 mmol) were dissolved in CH_2Cl_2 (5 cm^3) to yield a dark red solution. The solvent was reduced to 1 cm^3 before addition of diethyl ether (10 cm^3) to precipitate an orange solid that was isolated by suction filtration. Yield 88 mg, 96 %. Microanalysis: Found (calculated for $C_{36}H_{40}P_2N_2RhCl$) C 61.00 (61.70), H 6.12 (5.75), N 3.83 (4.00) %. $^{31}P\{^1H\}$ NMR ($CDCl_3$): $\delta(P_A)$ 115.5 (d) ppm, $^1J(^{31}P_A\text{-}^{103}Rh)$ 154 Hz. $\delta(P_X)$ 84.7 (d) ppm, $^1J(^{31}P_X\text{-}^{103}Rh)$ 114 Hz. $^2J(^{31}P_A\text{-}^{31}P_X)$ 25 Hz. ^1H NMR ($CDCl_3$) δ 7.4-7.2 (m, 20 H, aromatic), 5.9 (m, 4 H, CH), 4.8 (m, 8 H, CH_2), 3.5 (m, 8

H, NCH_2) ppm. FAB^+ MS: *m/z* 665 $[M - Cl]^+$. IR (KBr disc): 1638, 1433, 990, 251 cm^{-1}.

$[PdCl(C_{14}H_{12}N)\{Ph_2PN(C_3H_5)_2\}]$. (66): To a CH_2Cl_2 (10 cm^3) suspension of $[\{Pd(\mu\text{-}Cl)(C_{14}H_{12}N)\}_2]$ (123 mg, 0.2 mmol) was added drop wise a CH_2Cl_2 solution of $Ph_2PN(C_3H_5)_2$ (111 mg, 0.4 mmol) over 10 minutes to yield a colourless solution. After stirring for a further 30 minutes the solution was filtered through a Celite plug to remove any insoluble material remaining before reducing the solvent volume to 1 cm^3 and addition of diethyl ether (20 cm^3) to precipitate a tan coloured microcrystalline solid that was isolated by filtration. Yield 108 mg, 92 %. Microanalysis: Found (calculated for $C_{30}H_{32}PN_2PdCl$) C 59.65 (60.72), H 5.52 (5.44), N 4.42 (4.72) %. $^{31}P\{^1H\}$ NMR ($CDCl_3$): 97.7 ppm. ^1H NMR ($CDCl_3$) δ 8.0-7.8 (m, 6 H, naphthalene aromatic), 7.4-7.2 (m, 10 H, aromatic), 5.8 (m, 2 H, CH), 5.2 (m, 4 H, CH_2), 4.0 (m, 4 H, CH_2), 3.4 (s, 6 H, $N(CH_3)_2$), ppm. FAB^+ MS: *m/z* 557 $[M - Cl]^+$. IR (KBr disc): 1638, 1435, 1003, 282 cm^{-1}.

References.

1. Andreu, M. G.; Zapf, A.; Beller, M.; *Chem. Commun. (Cambridge)*; (2000) 2475-2476
2. Wu, H-P.; Aumann, R.; Froehlich, R.; Wegelius, E.; *Organometallics*; **20**, (2001), 2183-2190
3. Hiraki, K.; Matsunaga, T.; Kawano, H.; *Organometallics*; **13**, (1994), 1878-1885
4. Moretó, J. M.; Ricart, S.; *J. Organomet. Chem.*, **617-618**, (2001), 334-338
5. Pares, J; Moretó, J. M.; Ricart, S.; Barluenga, J.; Fananas, F. J.; *J. Organomet. Chem.*; **586**, (1999), 247

6. Moretó, J. M.; Ricart, S.; Dotz, K-H.; Molins, E.; *Organometallics.*, **20**, (2001), 62-70

7. a) Aumann, R.; Jasper, B.; Lage, M.; Krebs, B.; *Chem. Ber.*, **127**, (1994), 2475. b) Aumann, R.; Jasper, B.; Frolich, R.; *Organometallics*, **14**, (1995), 231

8. Baya, M.; Crochet, P.; Esteruelas, M. A.; Onate, E.; *Organometallics*, **20**, (2001), 240

9. Eilmes, J.; Ptaszek, M.; Wozniak, K.; *Polyhedron*, **21**, (2002), 7-17

10. Legzdins, P.; Lumb, S. A.; Rettig, S. J.; *Organometallics*, **18**, (1999), 3128-3137 H. C. Clark; L. E. Manzer, *J. Organomet. Chem.*, 1973, **59**, 411.

11. Y. Tatsuno; T. Yoshida; Seiotsuka, *Inorg. Synth.*, 1979, **19**, 220.

12. H. C. Clark; L. E. Manzer, *J. Organomet. Chem.*, 1973, **59**, 411.

13. G. J. Kubas, *Inorg. Synth.*, 1979, **19**, 90.

14. R. Uson; A. Laguna; M. Laguna, *Inorg. Synth.*, 1989, **26**, 85.

15. D. Drew; J. R. Doyle, *Inorg. Synth.*, 1991, **28**, 346.

16. J. X. McDermott; J. F. White; G. M. Whiteside, *J. Am. Chem. Soc.*, 1976, **60**, 6521.

17. M. A. Bennett; T. N. Huang; T. W. Matheson; A. R. Smith, *Inorg. Synth.*, 1982, **21**, 74.

18. G. Giordano; R. H. Crabtree, *Inorg. Synth.*, 1979, **19**, 218.

19. M. A. Bennett; L. Pratt; G. Wilkinson, *J. Chem. Soc.*, 1961, 2037.

20. F. Maassarani; M. Pfeffer; G. Le Borgne, *Organometallics*, 1987, **6**, 2029.

CHAPTER 4: COORDINATION CHEMISTRY OF Z-1-DIPHENYLPHOSPHINO-3,3-DIMETHYL-2-PHENYLTHIOBUT-1-ENE AND Z-1-DIPHENYLPHOSPHINO-2-PHENYLTHIOPROPENE

4.1 Introduction

The work in this chapter involved looking at potentially new hemilabile P-S ligands. As with all hemilabile ligands it is necessary for the ligand to contain two binding units of which one is stronger than the other. In the case of P-S ligands the stronger binding unit is usually the phosphorus atom and the weaker more labile unit is the sulfur atom. This then provides the ligand with two possible binding motifs, one where both phosphorus and sulfur coordinate to the metal centre and the other where only phosphorus coordinates.

There are a few examples of metal complexes containing phosphorus and sulfur bonded atoms and most of these examples use iron as the coordinating metal. Samb *et al*[1] showed one example by using the readily available but unstable complex (**1**). (**1**) is easily converted to the more stable trimethylphosphine derivatives by treatment with a three-fold excess of PMe_3. Scheme 4.1 shows this conversion.

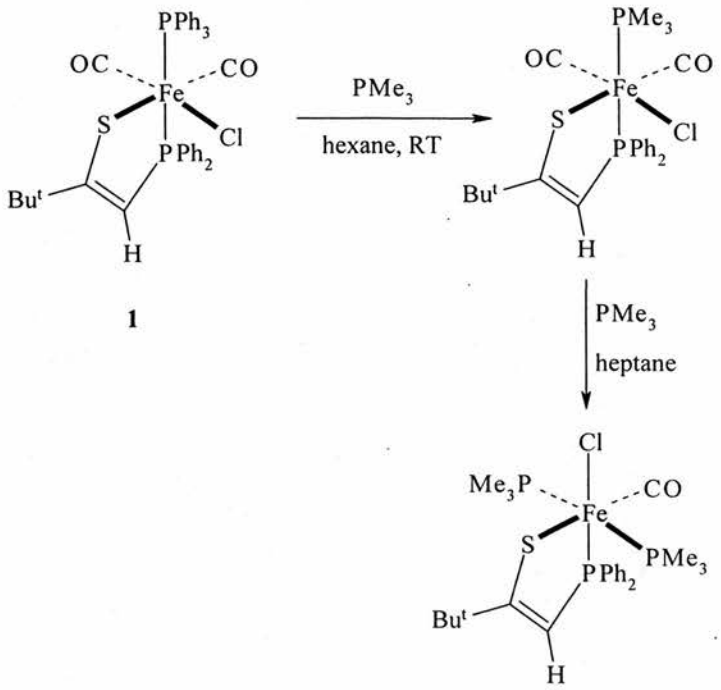

Scheme 4.1. Reaction of a β-phosphinothioketonate coordinated ligand with PMe_3.

Another example of a metal complex containing *Z*-1-diphenylphosphino-3,3-dimethyl-2-thiobut-1-ene was shown by Robert *et al*[2] who isolated red crystals of **4.1** from the reaction of $Fe(\eta^2\text{-}CS_2)(CO)_2(Ph_2PC{=}C\text{-}^tBu)_2$ in methanol. From this work it was noticed that S^- was bound to iron. Figure 4.1 shows the structure of the complex formed.

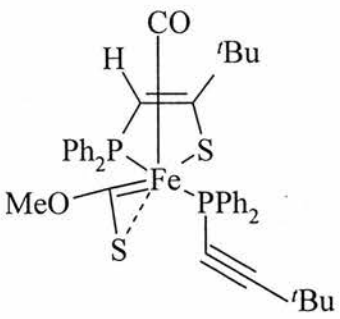

Figure 4.1. Product from the reaction of $Fe(\eta^2\text{-}CS_2)(CO)_2(Ph_2PC{=}C\text{-}^tBu)_2$ in methanol

In this work the preparation of metal complexes that demonstrate both coordination modes have been prepared.

Results and Discussion

4.2 *Synthesis of Z-1-Diphenylphosphino-3,3-dimethyl-2-phenylthiobut-1-ene and Z-1-Diphenylphosphino-2-phenylthiopropene.*

The ligands *Z*-1-Diphenylphosphino-3,3-dimethyl-2-phenylthiobut-1-ene (**67**) and *Z*-1-Diphenylphosphino-2-phenylthiopropene (**74**) were prepared and donated prior to this work[3]. Both ligands are prepared by flash vacuum pyrolysis at 650 °C and 10^{-2} Torr and upon furnace exit the crystalline deposit is recrystallised from ethyl acetate to give **67** as pale yellow plates in good yield and **74** as a colourless oil. The $^{31}P\{^{1}H\}$ NMR for **67** shows a single resonance at δ_P –19.8 ppm and for **74** a single resonance is observed at δ_P –22.7 ppm.

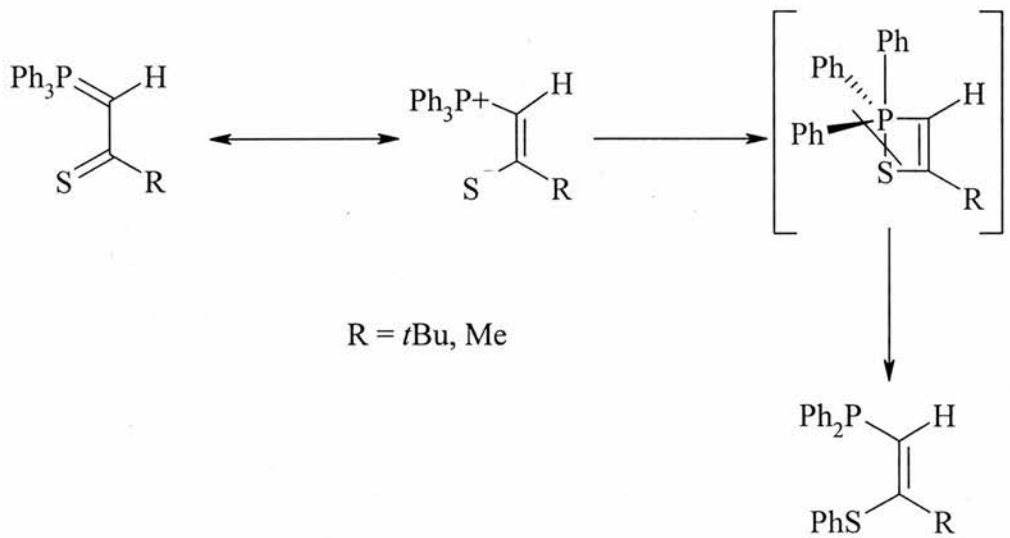

Scheme 4.2. Suggested formation of ligands **67** and **74**.

4.3 *Coordination chemistry of Z-1-Diphenylphosphino-3,3-dimethyl-2-phenylthiobut-1-ene, (dpptb), (**67**).*

Several new complexes of **67** have been prepared and characterised in the study of novel hemilabile ligands containing both phosphorus and sulfur binding units.

Reaction of $[PtCl_2(cod)]$ with one equivalent of **67** gives $[PtCl_2\{dpptb\}]$ (**68**) in good yield (79 %). The $^{31}P\{^1H\}$ NMR (CD_2Cl_2) exhibits a single resonance with platinum satellites (δ_P 29.4 ppm, $^1J(^{31}P\text{-}^{195}Pt)$ 3524 Hz and the ES^- mass spectrum shows the expected parent ion at $[M\text{-}H]^-$ 641 and fragmentation pattern. The microanalysis shows satisfactory results for the suggested structure and the IR spectrum shows bands at 1665, 1437 and 295 cm^{-1} that correspond to $\nu_{C=C}$ ν_{PPh2} ν_{PtCl} vibrations respectively.

Crystals of $[PtCl_2\{dpptb\}]$ (**68**) suitable for X-ray crystallography were grown overnight by layering a dichloromethane solution with diethyl ether. The crystal structure of the complex (Figure 4.2) and selected bond lengths and angles (Table 4.1) are shown below. The crystal structure shows that the molecule is square planar at platinum and forms *cis* geometry. The ligand {dpptb} is bound to the platinum centre through both the phosphorus and sulfur atoms and has a P(1)-Pt(1)-S(1) angle of 88.22(5) ^{o} with a P(1)-Pt(1) bond length of 2.2256(18) Å and a S(1)-Pt(1) bond length of 2.2617(14) Å.

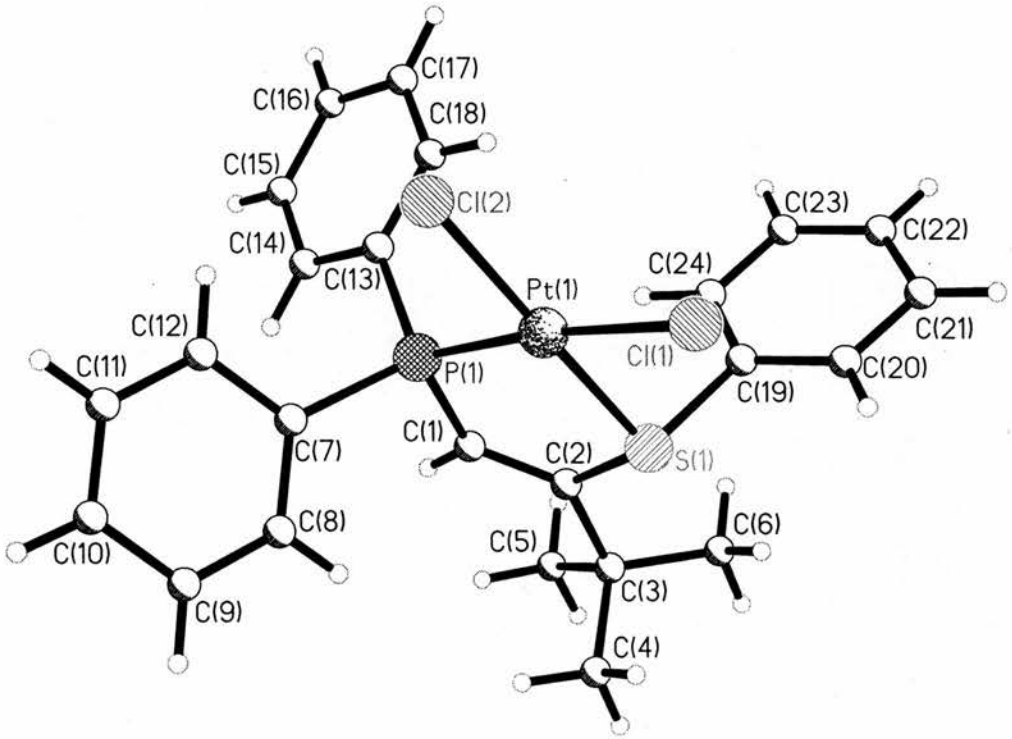

Figure 4.2. The X-ray structure of $[PtCl_2\{dpptb\}]$ **68**.

Table 4.1. Selected bond lengths (Å) and angles (°) for [$PtCl_2${dpptb}].

Selected bond lengths (Å) and angles (°)	*(68)*
M(1)-Cl(1)	2.3655(18)
M(1)-Cl(2)	2.3090(16)
M(1)-P(1)	2.2256(18)
M(1)-S(1)	2.2617(14)
P(1)-C(7)	1.835(6)
P(1)-C(13)	1.814(5)
S(1)-C(19)	1.792(6)
P(1)-C(1)	1.743(6)
S(1)-C(2)	1.846(7)
P(1)-M(1)-S(1)	88.22(5)
P(1)-M(1)-Cl(2)	91.67(6)
S(1)-M(1)-Cl(2)	178.50(7)
P(1)-M(1)-Cl(1)	174.08(5)
S(1)-M(1)-Cl(1)	87.11(5)
Cl(2)-M(1)-Cl(1)	93.09(6)
C(13)-P(1)-C(7)	106.2(2)
C(7)-P(1)-M(1)	112.8(2)
C(13)-P(1)-M(1)	119.0(2)
C(19)-S(1)-M(1)	102.74(17)

[$PdCl_2${dpptb}] (**69**) is prepared similarly to the platinum analogue by dropwise addition of [$PdCl_2$(cod)] to **67** in dichloromethane in good yield (73 %). The microanalysis shows satisfactory results for the suggested structure and is

isolated as a yellow solid. The $^{31}P\{^{1}H\}$ NMR (CD_2Cl_2) shows a single resonance at δ_P 50.4 ppm and ES^+ mass spectral analysis shows the expected fragmentation pattern and parent ion at $[M]^+$ 553. In the IR spectrum $\nu_{C=C}$, ν_{PPh2} and ν_{PdCl} vibrations are observed at 1575, 1436 and 289 cm^{-1} respectively.

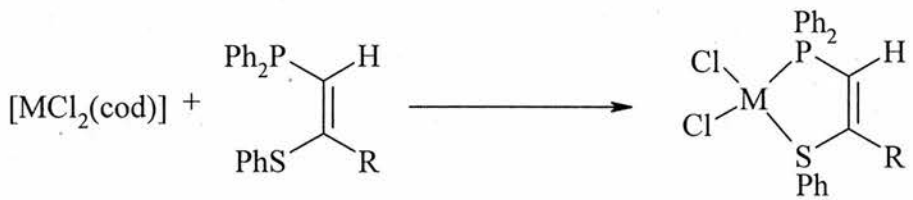

M = Pt, Pd
R = *t*Bu, Me

Scheme 4.3. Formation of *P,S*-chelated complexes.

Reaction of $[\{Pd(\mu\text{-}Cl)(\eta^3\text{-}C_3H_5)\}_2]$ with **67** proceeds to form $[PdCl(\eta^3\text{-}C_3H_5)\{$ dpptb$\}]$ (**70**) in a yield of 55 %. The $^{31}P\{^{1}H\}$ NMR (CD_2Cl_2) exhibits a single resonance at δ_P 40.9 ppm and microanalysis gave satisfactory results for the suggested structure. The ES^+ mass spectrum gave the expected parent ion and fragmentation pattern and the IR spectrum shows bands at 1599, 1435 and 296 cm^{-1} that correspond to $\nu_{C=C}$, ν_{PPh2} and ν_{PdCl} vibrations.

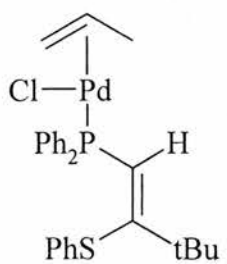

Figure 4.3. Suggested structure of $[PdCl(\eta^3\text{-}C_3H_5)\{$dpptb$\}]$ **70**

[AuCl{dpptb}] (**71**) is easily prepared by the addition of [AuCl(tht)] to **67** in one portion in dichloromethane in good yield (62 %). Microanalysis gives satisfactory results and ES^+ mass spectral analysis shows the expected parent ion and fragmentation pattern. The IR spectrum shows bands at 1577, 1436 and 253 cm^{-1} that correspond to $\nu_{C=C}$, ν_{PPh2} and ν_{AuCl} vibrations respectively and the $^{31}P\{^1H\}$ NMR ($CDCl_3$) shows a single peak at δ_P 18.2 ppm.

Crystals of [AuCl{dpptb}] (**71**) suitable for X-ray crystallography were grown overnight by layering a chloroform solution with diethyl ether. The crystal structure of the complex (Figure 4.4) and selected bond lengths and angles (Table 4.2) are shown below. The crystal structure shows that the molecule is linear at the gold centre and the ligand {dpptb} is bound to the gold centre through phosphorus and has a P(1)-Au(1)-Cl(1) angle of 175.08(12) °, which is just smaller than the ideal angle of 180 °. The P(1)-Au(1) bond length is 2.229(3) Å and a Au(1)-Cl(1) bond length is 2.284 (3) Å.

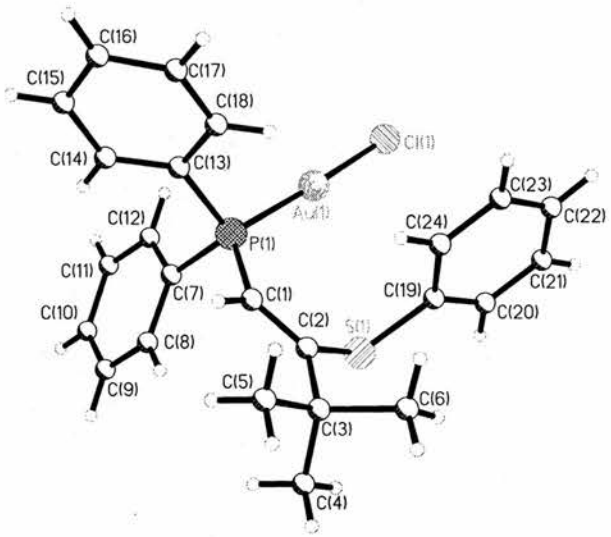

Figure 4.4. The X-ray structure of [AuCl{dpptb}] **71**.

Table 4.2. Selected bond lengths (Å) and angles (°) for [AuCl{dpptb}]

Selected bond lengths (Å) and angles (°)	*(71)*
M(1)-Cl(1)	2.284(3)
M(1)-P(1)	2.229(3)
P(1)-C(1)	1.790(12)
P(1)-C(7)	1.812(11)
P(1)-C(13)	1.836(11)
S(1)-C(19)	1.765(12)
C(2)-S(1)	1.780(12)
P(1)-M(1)-Cl(1)	175.08(12)
C(1)-P(1)-C(7)	106.6(5)
C(1)-P(1)-C(13)	98.9(5)
C(7)-P(1)-C(13)	106.4(5)
C(1)-P(1)-M(1)	121.6(4)
C(7)-P(1)-M(1)	109.4(4)
C(13)-P(1)-M(1)	112.6(3)

[IrCl(μ-Cl)(η^5-C_5Me_5){dpptb}] (**72**) was also prepared by slow addition of [{IrCl(μ-Cl)(η^5-C_5Me_5)}$_2$] to a dichloromethane solution of **67** in a yield of 57 %. The $^{31}P\{^1H\}$ NMR (CD_2Cl_2) shows a single resonance at δ_P –8.7 ppm. The ES^+ mass spectrum shows the expected fragmentation pattern and parent ion of $[M]^+$ at 739 and the microanalysis gave fairly satisfactory results. In the IR spectrum vibrations for $\nu_{C=C}$, ν_{PPh2} and ν_{IrCl} are observed at 1648, 1437 and 290 cm^{-1}.

Crystals of [IrCl(μ-Cl)(η^5-C_5Me_5){dpptb}] (**72**) suitable for X-ray crystallography were grown overnight by layering a dichlormethane solution with diethyl ether. The crystal structure of the complex (Figure 4.5) and selected bond lengths and angles (Table 4.3) are shown below. The crystal structure shows that the molecule is bound to the iridium centre through phosphorus and has a P(1)-Ir(1) bond length of 2.3080(10) Å with two Ir(1)-Cl bond lengths(Ir(1)-Cl(1) is 2.4097 (10) Å, and Ir(1)-Cl(2) is 2.4007(10) Å).

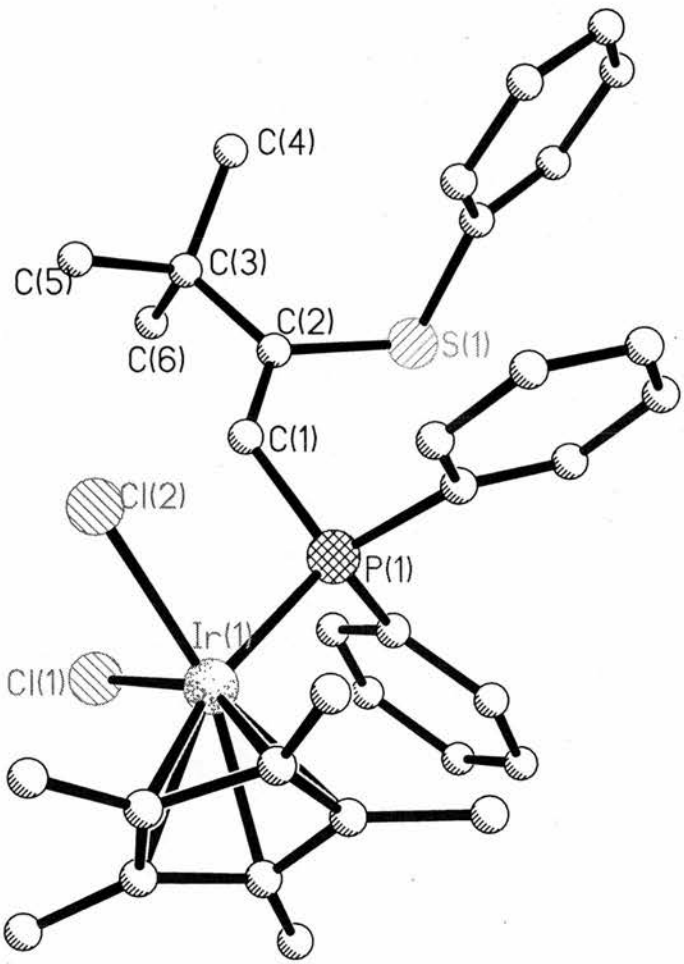

Figure 4.5. The X-ray structure of [IrCl(μ-Cl)(η^5-C_5Me_5){dpptb}] **72**.

Table 4.3. Selected bond lengths (Å) and angles (°) for [IrCl(μ-Cl)(η^5-C_5Me_5){dpptb}]

Selected bond lengths (Å) and angles (°)	*(72)*
M(1)-Cl(1)	2.4097(10)
M(1)-Cl(2)	2.4007(10)
M(1)-P(1)	2.3080(10)
P(1)-C(1)	1.823(4)
P(1)-C(7)	1.823(4)
P(1)-C(13)	1.823(4)
S(1)-C(19)	1.780(4)
C(2)-S(1)	1.785(4)
P(1)-M(1)-Cl(2)	98.94(11)
P(1)-M(1)-Cl(1)	83.23(4)
Cl(2)-M(1)-Cl(1)	89.19(4)
C(1)-P(1)-C(7)	105.97(18)
C(1)-P(1)-C(13)	106.16(19)
C(7)-P(1)-C(13)	107.85(19)
C(1)-P(1)-M(1)	109.31(14)
C(7)-P(1)-M(1)	114.83(14)
C(13)-P(1)-M(1)	112.20(13)

Reaction of [{RuCl(μ-Cl)(η^6-*p*-$MeC_6H_4{}^iPr$)}$_2$] and **67** proceeds easily to prepare [RuCl(μ-Cl)(η^6-*p*-$MeC_6H_4{}^iPr$){dpptb}] (**73**) in good yield (67 %) as an orange solid. Microanalysis shows fairly satisfactory results and the $^{31}P\{^1H\}$ NMR ($CDCl_3$) shows a single peak at δ_P 14.6 ppm. The IR spectrum shows bands at 1637,

1436 and 291 cm^{-1} that correspond to $\nu_{C=C}$ ν_{PPh2} ν_{RuCl} vibrations and the ES^+ mass spectrum shows the expected parent ion and fragmentation pattern for the suggested structure at *m/z* 647.

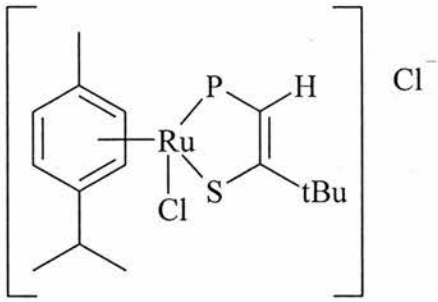

Figure 4.6. Suggested structure of [RuCl(μ-Cl)(η^6-*p*-$MeC_6H_4{}^iPr$){dpptb}] **73**.

4.4 *Coordination chemistry of Z-1-Diphenylphosphino-2-phenylthiopropene, (dpptp), (74).*

Due to purification problems with this ligand there has only been one successfully prepared and characterised metal complex of {dpptp}, (**74**). [$PdCl_2${dpptp}] (**75**) has been prepared by slow addition of [$PdCl_2$(cod)] to a solution of **74** in dichloromethane in good yield (73 %). The $^{31}P\{^1H\}$ NMR (CD_2Cl_2) exhibits a single resonance at δ_P 52.4 ppm and the IR spectrum shows bands at 1576, 1435 and 296 cm^{-1} that correspond to $\nu_{C=C}$ ν_{PPh2} ν_{PdCl} vibrations respectively. Microanalysis gives satisfactory results for the suggested structure and ES^+ mass spectral analysis shows the expected parent ion, $[M + Na]^+$ at 532, and fragmentation pattern.

Crystals of [$PdCl_2${dpptp}] (**75**) suitable for X-ray crystallography were grown overnight by layering a dichloromethane solution with diethyl ether. The crystal structure of the complex (Figure 4.7) and selected bond lengths and angles (Table 4.4)

are shown below. The crystal structure shows that the molecule is square planar at palladium and forms *cis* geometry. The ligand {dpptp} is bound to the platinum centre through both the phosphorus and sulfur atoms and has a P(1)-Pt(1)-S(1) angle of 87.07(7) ° with a P(1)-Pt(1) bond length of 2.229(2) Å and a S(1)-Pt(1) bond length of 2.2522(19) Å.

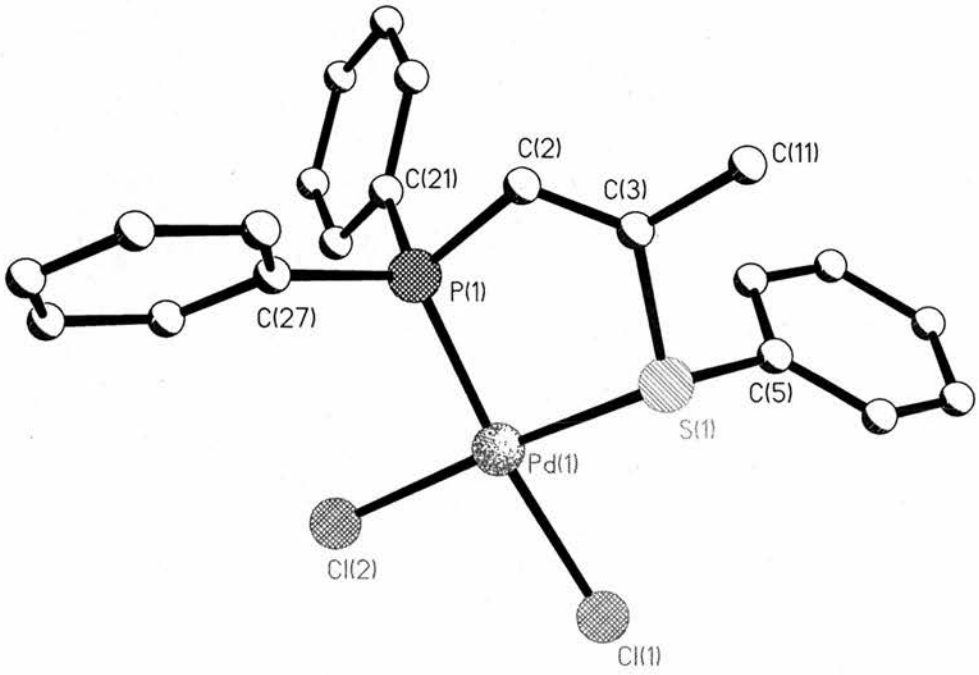

Figure 4.7. The X-ray structure of $[PdCl_2\{dpptp\}]$ **75**.

Table 4.4. Selected bond lengths (Å) and angles (°) for $[PdCl_2\{dpptp\}]$

Selected bond lengths (Å) and angles (°)	*(75)*
M(1)-Cl(1)	2.3608(19)
M(1)-Cl(2)	2.3221(18)
M(1)-P(1)	2.229(2)
M(1)-S(1)	2.2522(19)
P(1)-C(2)	1.799(7)
P(1)-C(27)	1.802(7)
P(1)-C(21)	1.825(7)
S(1)-C(5)	1.785(7)
C(3)-S(1)	1.796(7)
P(1)-M(1)-S(1)	87.07(7)
P(1)-M(1)-Cl(1)	174.30(7)
P(1)-M(1)-Cl(2)	94.63(7)
S(1)-M(1)-Cl(1)	87.67(7)
S(1)-M(1)-Cl(2)	174.72(6)
Cl(2)-M(1)-Cl(1)	90.80(7)
C(2)-P(1)-M(1)	107.1(2)
C(21)-P(1)-M(1)	114.5(2)
C(27)-P(1)-M(1)	117.5(2)
C(5)-S(1)-C(3)	101.2(3)
C(5)-S(1)-M(1)	110.6(2)
C(3)-S(1)-M(1)	106.9(2)

Table 4.5. Characterisation data for complexes of {dpptb} (**67**) and {dpptp} (**74**). ([a] $^1J\{^{31}P\text{-}^{195}Pt\}$ 3524 Hz.

Compound	*$^{31}P\{^1H\}$ NMR*	*IR/cm^{-1}*			*Microanalysis/ % Found (calc.)*	
	δ_p/ppm	$\nu_{C=C}$	ν_{PPh2}	ν_{MCl}	C	H
[$PtCl_2${dpptb}] (68)	29.4[a]	1637	1437	295	44.84 (44.87)	3.60 (3.92)
[$PdCl_2${dpptb}] (69)	50.4	1575	1436	289	49.69 (49.37)	4.44 (4.37)
[PdCl(η^3-C_3H_5){dpptb}] (70)	40.9	1599	1435	296	56.66 (56.36)	4.60 (5.29)
[AuCl{dpptb}] (71)	18.2	1577	1436	253	47.24 (47.34)	4.11 (4.14)
[IrCl(μ-Cl)(η^5-C_5Me_5){dpptb}] (72)	-8.7	1643	1437	290	48.07 (48.06)	4.65 (4.86)
[RuCl(μ-Cl)(η^6-*p*-$MeC_6H_4{}^iPr$){dpptb}] (73)	14.6	1637	1436	291	56.86 (57.14)	4.04 (5.56)
[$PdCl_2${dpptp}] (75)	52.4	1576	1435	296	49.50 (49.29)	3.21 (3.74)

Experimental

General experimental conditions and instruments were as set out on page xvii. The complexes [AuCl(tht)] (tht = tetrahydrothiophene)[4], $[MCl_2(cod)]$ (M = Pt or Pd; cod = cycloocta-1,5-diene)[5, 6], $[\{RuCl(\mu\text{-}Cl)(\eta^6\text{-}p\text{-}MeC_6H_4{}^iPr)_2\}]$[7], $[\{MCl(\mu\text{-}Cl)(\eta^5\text{-}C_5Me_5)\}_2]$ (M = Rh or Ir)[8] and $[\{Pd(\mu\text{-}Cl)(\eta^3\text{-}C_3H_5)\}_2]$[9] were prepared using literature procedures. Reagent grade KBr was used without further purification. Infra-red spectra were recorded as KBr discs in the range 4000-200 cm^{-1} on a Perkin-Elmer 2000 FTIR/RAMAN spectrometer. NMR spectra were recorded on a Gemini 2000 spectrometer (operating at 121.4 MHz for ^{31}P and 300 MHz for ^1H). Microanalyses were performed by the St. Andrews University service and mass spectra by the Swansea Mass Spectrometer Service.

_Z_-1-Diphenylphosphino-3,3-dimethyl-2-phenylthiobut-1-ene[3]. (dpptb). (67)

$[PtCl_2\{dpptb\}]$. (68): To a dichloromethane (5 cm^3) solution of $[PtCl_2(cod)]$ (66 mg, 0.2 mmol) was added a dichloromethane (5 cm^3) solution of **67** (66 mg, 0.2 mmol) dropwise over 30 minutes. The resultant reaction mixture was stirred for a further 1 hour before the solvent was reduced to 1 cm^3 and addition of diethyl ether (15 cm^3) to precipitate an off- white solid that was isolated by suction filtration. Yield 89 mg, 79 %. Microanalysis: Found (calculated for $C_{24}H_{25}PSPtCl_2$) C 44.84 (44.87), H 3.60 (3.92), S 4.81 (4.99) %. $^{31}P\{^1H\}$ NMR (CD_2Cl_2): 29.4 ppm $^1J(^{31}P\text{-}^{195}Pt)$ 3524 Hz. ^1H NMR (CD_2Cl_2) δ 8.0-7.5 (m, 15 H, aromatic), 6.7 (d, 1 H, $^3J(^{195}Pt\text{-}^1H)$ 67 Hz, $^2J(^{31}P\text{-}^1H)$ 10 Hz, CH) and 1.2 (s, 9 H, ^tBu). ES^- MS: *m/z* 641 $[M - H]^-$. IR (KBr disc): 1665, 1437, 295 cm^{-1}.

[$PdCl_2${dpptb}]. (69): To a dichloromethane (5 cm^3) solution of [$PdCl_2$(cod)] (38 mg, 0.1 mmol) was added a dichloromethane (5 cm^3) solution of **67** (50 mg, 0.1 mmol) dropwise over 30 minutes. The resultant reaction mixture was stirred for a further 2 hours before the solvent was reduced to 1 cm^3 and addition of diethyl ether (15 cm^3) to precipitate a yellow solid that was isolated by suction filtration and dried *in vacuo*. Yield 63 mg, 73 %. Microanalysis: Found (calculated for $C_{24}H_{25}PSPdCl_2.0.5CH_2Cl_2$) C 49.69 (49.37), H 4.44 (4.37) %. $^{31}P\{^1H\}$ NMR (CD_2Cl_2): 50.4 ppm. ^1H NMR (CD_2Cl_2) δ 8.0-7.5 (m, 15 H, aromatic), 6.7 (d, 1 H, $^2J(^{31}P\text{-}^1H)$ 8 Hz, CH) and 1.2 (s, 9 H, ^{t}Bu). ES^+ MS: *m/z* 553 $[M]^+$. IR (KBr disc): 1575, 1436, 289 cm^{-1}.

[$PdCl(\eta^3\text{-}C_3H_5)${dpptb}]. (70): To a dichloromethane (5 cm^3) solution of [$PdCl(\eta^3\text{-}C_3H_5)$] (32 mg, 0.1 mmol) was added a dichloromethane (5 cm^3) solution of **67** (66 mg, 0.2 mmol) dropwise over 30 minutes. The resultant reaction mixture was stirred for a further 2 hours before the solvent was reduced to 0.5 cm^3 and addition of diethyl ether (10 cm^3) to precipitate a yellow solid that was isolated by suction filtration and dried *in vacuo*. Yield 54 mg, 55 %. Microanalysis: Found (calculated for $C_{27}H_{30}PSPdCl.0.25CH_2Cl_2$) C 56.66 (56.36), H 4.60 (5.29) %. $^{31}P\{^1H\}$ NMR (CD_2Cl_2): 40.9 ppm. ^1H NMR (CD_2Cl_2) δ 8.0-7.5 (m, 15 H, aromatic), 6.7 (d, 1 H, $^2J(^{31}P\text{-}^1H)$ 8 Hz, CH) and 1.2 (s, 9 H, ^{t}Bu). ES^+ MS: *m/z* 523 $[M - Cl]^+$. IR (KBr disc): 1599, 1435, 296 cm^{-1}.

[AuCl{dpptb}]. (71): [AuCl(tht)] (18 mg, 0.06 mmol) and **67** (21 mg, 0.06 mmol) was added to dichloromethane (2 cm^3) in one portion before stirring overnight. The solvent was reduced to 0.5 cm^3 and addition of diethyl ether (10 cm^3) to precipitate a white solid that was isolated by suction filtration and dried *in vacuo*. Yield 21 mg, 62 %. Microanalysis: Found (calculated for $C_{24}H_{25}PSAuCl$) C 47.24 (47.34), H 4.11

(4.14) %. $^{31}P\{^{1}H\}$ NMR ($CDCl_3$): 18.2 ppm. ^{1}H NMR (CD_2Cl_2) δ 7.5-7.0 (m, 15 H, aromatic), 6.7 (d, 1 H, $^{2}J(^{31}P\text{-}^{1}H)$ 12 Hz, CH) and 1.2 (s, 9 H, ^{t}Bu). ES^{+} MS: *m/z* 523 $[M + Na]^{+}$. IR (KBr disc): 1577, 1436, 253 cm^{-1}.

[IrCl(μ-Cl)(η^5-C_5Me_5){dpptb}]. (72): To a dichloromethane (5 cm^3) solution of [{IrCl(μ-Cl)(η^5-C_5Me_5)}$_2$] (75 mg, 0.1 mmol) was added a dichloromethane (5 cm^3) solution of **67** (71 mg, 0.2 mmol) dropwise over 30 minutes. The resultant reaction mixture was stirred for a further 2 hours before the solvent was reduced to 0.5 cm^3 and addition of diethyl ether (20 cm^3) to precipitate a yellow solid that was isolated by suction filtration and dried *in vacuo*. Yield 84 mg, 57 %. Microanalysis: Found (calculated for $C_{34}H_{40}PSIrCl_2.1.25CH_2Cl_2$) C 48.07 (48.06), H 4.65 (4.86) %. $^{31}P\{^{1}H\}$ NMR (CD_2Cl_2): -8.7 ppm. ^{1}H NMR (CD_2Cl_2) δ 8.0-7.5 (m, 15 H, aromatic), 6.7 (d, 1 H, $^{2}J(^{31}P\text{-}^{1}H)$ 8 Hz, CH), 1.2 (s, 9 H, ^{t}Bu), 1.0 (s, 15 H, Cp*). ES^{+} MS: *m/z* 739 $[M]^{+}$. IR (KBr disc): 1648, 1437, 290 cm^{-1}.

[RuCl(μ-Cl)(η^6-*p*-$MeC_6H_4{}^{i}Pr$){dpptb}]. (73): To a dichloromethane (5 cm^3) solution of [{RuCl(μ-Cl)(η^6-*p*-$MeC_6H_4{}^{i}Pr$)}$_2$] (26 mg, 0.04 mmol) was added a dichloromethane (5 cm^3) solution of **67** (32 mg, 0.08 mmol) dropwise over 30 minutes. The red solution was stirred for overnight before the solvent was reduced to 0.5 cm^3 and addition of diethyl ether (10 cm^3) to precipitate an orange solid that was isolated by suction filtration and dried *in vacuo*. Yield 39 mg, 67 %. Microanalysis: Found (calculated for $C_{34}H_{39}PSRuCl_2.0.\ 5CH_2Cl_2$) C 56.86 (57.14), H 4.04 (5.56) %. $^{31}P\{^{1}H\}$ NMR ($CDCl_3$): 14.6 ppm. ^{1}H NMR ($CDCl_3$) δ 8.0-7.5 (m, 19 H, aromatic), 6.7 (d, 1 H, $^{2}J(^{31}P\text{-}^{1}H)$ 8 Hz, CH), 2.5 (m, 1 H, CH), 1.8 (s, 3 H, CH_3) 1.2 (s, 9 H, ^{t}Bu), 0.7 (m, 6 H, ^{i}Pr). ES^{+} MS: *m/z* 647 $[M - Cl]^{+}$. IR (KBr disc):1637, 1436, 291 cm^{-1}.

***Z*-1-Diphenylphosphino-2-phenylthiopropene[3]. (dpptp) (74)**

[$PdCl_2${dpptp}]. (75): To a dichloromethane (5 cm^3) solution of [$PdCl_2$(cod)] (33 mg, 0.1 mmol) was added a dichloromethane (5 cm^3) solution of **74** (64 mg, 0.2 mmol) dropwise over 30 minutes. The resultant reaction mixture was stirred for a further 2 hours before the solvent was reduced to 0.5 cm^3 and addition of diethyl ether (10 cm^3) to precipitate a yellow solid that was isolated by suction filtration and dried *in vacuo*. Yield 43 mg, 73 %. Microanalysis: Found (calculated for $C_{21}H_{19}PSPdCl$) C 49.50 (49.29), H 3.21 (3.74) %. $^{31}P\{^1H\}$ NMR (CD_2Cl_2): 52.4 ppm. ^1H NMR (CD_2Cl_2) δ 8.0-7.5 (m, 15 H, aromatic), 6.7 (d, 1 H, $^2J(^{31}P\text{-}^1H)$ 8 Hz, CH) and 1.2 (s, 9 H, ^{t}Bu). ES^+ MS: *m/z* 532 $[M + Na]^+$. IR (KBr disc): 1576, 1435, 296 cm^{-1}.

References.

1. A. Samb; B. Demerseman; P. H. Dixneuf; C. Mealli, *J. Chem. Soc., Chem. Commun.*, 1988, 1408.
2. P. Robert; H. Le Bozec; P. H. Dixneuf; F. Hartstock; N. J. Taylor; A. J. Carty, *Organometallics*, 1982, **1**, 1148.
3. R. A. Aitkin, unpublished results.
4. R. Uson; A. Laguna; M. Laguna, *Inorg. Synth.*, 1989, **26**, 85.
5. D. Drew; J. R. Doyle, *Inorg. Synth.*, 1991, **28**, 346.
6. J. X. McDermott; J. F. White; G. M. Whiteside, *J. Am. Chem. Soc.*, 1976, **60**, 6521.
7. M. A. Bennett; T. N. Huang; T. W. Matheson; A. R. Smith, *Inorg. Synth.*, 1982, **21**, 74.
8. C. White; A. Yates; P. M. Maitlis, *Inorg. Synth.*, 1992, **29**, 228.
9. Y. Tatsuno; T. Yoshida; Seiotsuka, *Inorg. Synth.*, 1979, **19**, 220.

CHAPTER 5: MOLECULAR MODELLING OF IMIDAZOLIDINETHIONE AND BENZIMIDAZOLETHIOL LIGANDS.

5.1 *Introduction*

Molecular modelling has in recent years been used in many applications such as in pharmaceutical drug design and ligand design for catalysts. By performing these calculations it can be determined whether the ligand of choice has the potential to firstly be prepared and secondly the likelihood that the ligand will behave in a hemilable manner.

For details on molecular calculation theory see references 1-6.

5.2 *Results and Discussion*

The phosphorus-nitrogen bond lengths calculated for this work are longer than those obtained by crystallographic means and suggest that the calculations are not perfect. However, this does not make the calculations invalid as the data obtained can still be used to look for trends within ligand types and the bond lengths and angles should only be used as a guide to the quality of the calculations performed.

We carried out similar calculations for series of target ligands to investigate the ideal ligand for synthesis. During the calculations monodentate, bidentate and chelated complexes were modelled to compare the ligands under investigation.

The first ligand to consider is *N*-diphenylphosphino-2-thioimidazolidine (**76**). Considering the platinum complexes of **76** the data shows the *trans* 2:1

chelate complex forms the most stable complex with a heat of formation of –381 kcal/mol. The *trans* 2:1 complex is also formed favourably with a heat of formation of –368 kcal/mol. The 2:1 *cis* analogues show that chelation of one ligand is comparable to the monodentate chelated complex. However, when palladium is considered, the formation of the *cis* 2:1 complex is less favourable due to a more endothermic reaction being required and chelation of this complex is not favoured. The *trans* 2:1 unchelated complex forms a more favourable conformation but the most stable palladium complex formed by these calculations is the chelated monodentate complex with a heat of formation of –39 kcal/mol. This complex is possibly the most stable conformation for palladium due to little steric hindrance occurring within the molecule. The [Pd(allyl)Cl] and [RhCp*Cl_2] complexes of **76** appear to form the most stable complexes when there is no chelation involved with the ligand.

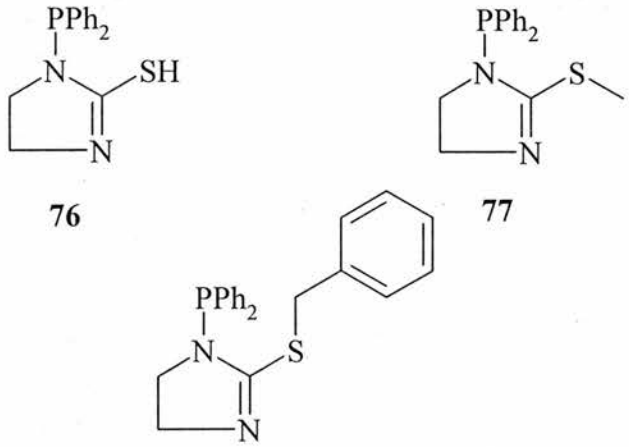

Figure 5.1. Derivatives of *N*-diphenylphosphino-2-thioimidazolidine.

A similar study for the complexes of *N*-diphenylphosphino-2-(methylthio)imidazolidine (**77**) was performed using the same calculations.

Again it was observed that the phosphorus-nitrogen bond lengths measured were longer than expected which showed some consistency with the previous ligand data. As the results for the bond lengths are similar, the data obtained can be used to compare this ligand with **76**. The most stable complexes formed with this ligand were with platinum. The palladium complexes of **77** again showed that these were the least stable and the complexes of [RhCp*Cl_2] and [Pd(allyl)Cl] were the most stable when there was no chelation. *N*-diphenylphosphino-2-(benzylthio)imidazolidine (**78**) was the next ligand studied in our design process. Again the phosphorus-nitrogen bond lengths are longer than the crystallographic bond lengths observed for phosphorus-nitrogen bonds. The platinum complexes of **78** proved to form the most stable complexes and the palladium formed the least stable complexes including the complexes of [Pd(allyl)Cl] which do not seem to form stable complexes unlike when prepared with ligands **76** and **77**. When comparing the three ligands mentioned above the first ligand to be prepared should be *N*-diphenylphosphino-2-(methylthio)imidazolidine (**77**) though some heat is required to force the reaction to proceed. Table 5.1 shows the heats of formation for ligands **76**, **77** and **78**.

Table 5.1. Heats of formation for derivatives of *N*-diphenylphosphino-2-thioimidazolidine.

	Heat of formation (kcal/mol)	*Heat of formation (kcal/mol)*	*Heat of formation (kcal/mol)*
Compound	**76**	**77**	**78**
Ligand	77.040	70.636	102.914
***cis* $PtCl_2L_2$**	-351.243	-367.904	-294.698
***trans* $PtCl_2L_2$**	-368.389	-375.978	-333.526
***cis* $PtClL_2$ chelate**	-333.483	-356.061	-357.06
***trans* $PtClL_2$ chelate**	-381.239	-394.093	-329.632
$PtCl_2L$ chelate	-331.010	-347.746	-363.599
***cis* $PdCl_2L_2$**	1.346	1.031	50.486
***trans* $PdCl_2L_2$**	-18.292	-11.026	39.746
***cis* $PdClL_2$ chelate**	31.881	7.468	52.858
***trans* $PdClL_2$ chelate**	8.165	13.417	52.801
$PdCl_2L$ chelate	-39.694	-50.247	-21.383
Pd(allyl)ClL	-13.354	-28.001	5.794
Pd(allyl)L chelate	1.907	-3.625	10.034
***trans* $RhCp^*Cl_2L$**	-344.025	-348.39	-318.606
***trans* $RhCp^*ClL$ chelate**	-324.198	-328.635	-304.493

The next ligands considered in these calculations were the benzimidazolethiol ligands. The first of these ligands is *N*-diphenylphosphino-2-thiobenzimidazole (**79**). The most stable complex predicted by the calculations is the *trans* 2:1 chelate platinum complex closely followed by the *trans* RhCp*Cl chelate complex. The palladium complexes of **79** again prove to be difficult to prepare. The second ligand from this ligand set is *N*-diphenylphosphino-2-(methylthio)benzimidazole (**80**). Again the most stable complexes predicted by the calculations were the platinum complexes but unlike shown with the **79** the chelated RhCp*is slightly more difficult to prepare than the non-chelated

complex. Again the palladium complexes appear to be difficult to prepare, as the heats of formation are slightly endothermic.

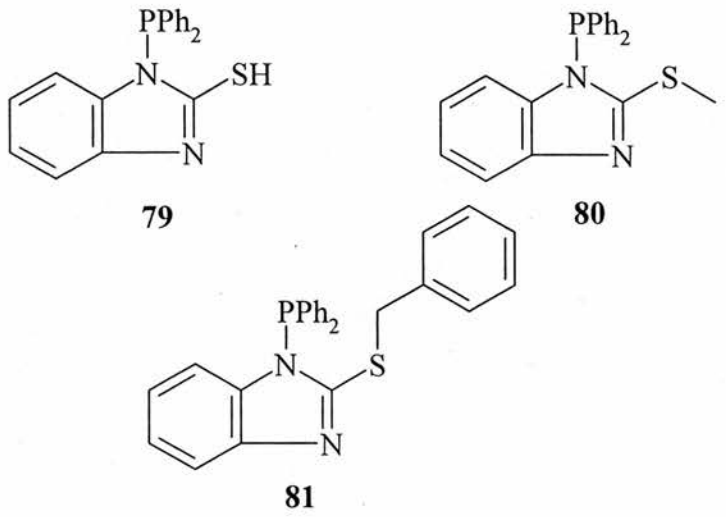

Figure 5.2. Derivatives of *N*-diphenylphosphino-2-thiobenzimidazole.

N-diphenylphosphino-2-(benzylthio)benzimidazole **81** was then used in the ligand design study. The most stable complex formed by the calculation was the 1:1 monodentate $PtCl_2$ complex with a heat of formation of –330 kcal/mol. The RhCp*Cl complexes of **81** were shown to form stable complexes in this calculation and the palladium complexes again seemed to form the least stable complexes. When comparing the three ligands mentioned above the most likely ligand to be prepared is *N*-diphenylphosphino-2-(methylthio)benzimidazole (**80**) though some heat is required to force the reaction to proceed which is consistent with the imidazolidinethione ligands. The heats of formation for several metal complexes of **79**, **80** and **81** are shown below (Table 5.2).

Table 5.2. Heats of formation for derivatives of *N*-diphenylphosphino-2-thiobenzimidazole.

	Heat of formation (kcal/mol)	*Heat of formation (kcal/mol)*	*Heat of formation (kcal/mol)*
Compound	**79**	**80**	**81**
Ligand	110.567	102.999	132.71
***cis* $PtCl_2L_2$**	-282.262	-293.866	-245.63
***trans* $PtCl_2L_2$**	-305.449	-313.89	-269.993
***cis* $PtClL_2$ chelate**	-273.249	-307.464	-267.446
***trans* $PtClL_2$ chelate**	-333.626	-315.878	-272.457
$PtCl_2L$ chelate	-307.082	-323.747	-330.59
***cis* $PdCl_2L_2$**	67.864	56.101	111.989
***trans* $PdCl_2L_2$**	51.515	43.497	104.828
***cis* $PdClL_2$ chelate**	94.754	82.865	127.644
***trans* $PdClL_2$ chelate**	46.304	56.981	129.66
$PdCl_2L$ chelate	-7.774	-18.027	0.132
Pd(allyl)ClL	12.122	7.975	39.593
Pd(allyl)L chelate	46.565	24.788	40.697
***trans* $RhCp^*Cl_2L$**	-313.713	-312.693	-281.358
***trans* $RhCp^*ClL$ chelate**	-331.491	-303.737	-280.608

The next four ligands considered for these calculations were the non-thiolated imidazolidine and benzimidazole analogues containing allyl and pyridyl R groups shown below (Figure 5.3). Considering the allyl analogues first the easiest ligand to prepare is shown to be 2-allylimidazolidine **82** that has a heat of formation of 85 kcal/mol. The most stable metal complex formed was shown to be the *trans* 2:1 platinum chelate complex. It was observed that the palladium complexes again proved to be the least stable with heat being required to make the reaction proceed apart from the monodentate $PdCl_2$ chelate complex and Pd(allyl)Cl complex that were exothermic. The *trans* $RhCp^*Cl_2$ complex

and the chelate analogue were also observed to form fairly easily to give stable complexes from the calculations. For 2-allylbenzimidazole **83** the most stable complex formed is the 1:1 $PtCl_2$ chelate complex. The other platinum complexes are formed easily according to the calculations thought he palladium complexes appear to form in more difficulty. Again the rhodium complexes studied for these calculations are stable.

Considering the pyridyl analogues the easiest ligand to prepare appears to be 2-pyridylimidazolidine **84** with a heat of formation of 105 kcal/mol. The most stable complexes that seem to be prepared by the calculations are the chelates of the monodentate 1:1 platinum complex and the *trans* 2:1 platinum complex. The rhodium complexes also appear to be prepared fairly easily though most of the palladium analogues appear to require heat to force the reaction to proceed. The most stable complex calculated for 2-pyridylbenzimidazole **85** is the 1:1 platinum monodentate chelate. For this ligand all the palladium complexes appear to form via an endothermic reaction making them less stable. The heat of formation for complexes of **82**, **83**, **84** and **85** are shown below (Table 5.3).

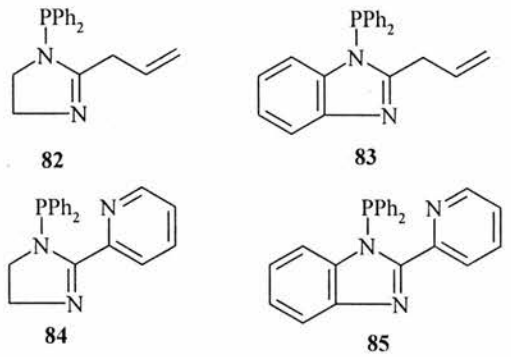

Figure 5.3. Derivatives of *N*-diphenylphosphino-2-imidazolidine and Derivatives of *N*-diphenylphosphino-2-benzimidazole.

Table 5.3. Heats of formation for derivatives of *N*-diphenylphosphino-2-imidazolidine and Derivatives of *N*-diphenylphosphino-2-benzimidazole.

	Heat of formation (kcal/mol)	*Heat of formation (kcal/mol)*	*Heat of formation (kcal/mol)*	*Heat of formation (kcal/mol)*
Compound	**82**	**83**	**84**	**85**
Ligand	85.063	115.538	105.996	141.071
***cis* $PtCl_2L_2$**	-359.771	-277.974	-305.775	-234.644
***trans* $PtCl_2L_2$**	-376.415	-312.533	-323.973	-251.949
***cis* $PtClL_2$ chelate**	-385.263	-332.281	-296.286	-248.559
***trans* $PtClL_2$ chelate**	-410.921	-385.032	-326.030	-261.889
$PtCl_2L$ chelate	-378.508	-410.412	-328.973	-294.369
***cis* $PdCl_2L_2$**	13.330	76.867	111.007	120.120
***trans* $PdCl_2L_2$**	8.955	58.657	42.530	102.000
***cis* $PdClL_2$ chelate**	36.735	86.579	85.044	130.462
***trans* $PdClL_2$ chelate**	31.100	74.519	59.516	164.257
$PdCl_2L$ chelate	-68.417	-35.897	-23.652	9.655
Pd(allyl)ClL	-16.262	16.176	-1.846	42.911
Pd(allyl)L chelate	1.454	14.929	32.324	47.295
***trans* $RhCp^*Cl_2L$**	-335.921	-306.540	-316.689	-279.486
***trans* $RhCp^*ClL$ chelate**	-288.802	-298.486	-301.086	-270.773

The final ligand set considered for the calculations contained three possible binding sites within the molecule. This was split into two sections: one containing an allyl group and the second containing a picolyl group shown below (Figure 5.4). Considering the complexes of *N*-diphenylphosphino-2-(allylthio)imidazolidine **86** first the calculations show that the most stable complex to form is the 1:1 monodentate platinum complex that is chelated through the allyl R group with the *trans* 2:1 allyl platinum chelate also forming a fairly stable complex. Again it is observed that the palladium complexes form

less stable complexes as has been shown previously and the rhodium complexes of **86** are also formed fairly easily. For *N*-diphenylphosphino-2-(allylthio)benzimidazole **87** the most stable complexes prepared are the platinum complexes when chelated through the allyl group and the least stable complexes are the palladium complexes possibly due to steric hindrance of the bulky benzimidazole group of the ligand.

The most stable complex of *N*-diphenylphosphino-2-(picolylthio)imidazolidine **88** is the 1:1 monodentate palladium *N*-chelated complex with a heat of formation of –349 kcal/mol. This is the first instance that the palladium complex has formed a very stable complex using these calculations. However, the palladium complexes of *N*-diphenylphosphino-2-(picolylthio)benzimidazole **89** do not appear to be very stable as they form endothermic reactions from the calculations. The most stable complexes formed for ligand **89** is the monodentate 1:1 platinum *N*-chelated complex with a heat of formation of –363 kcal/mol. For both ligands **88** and **89** the rhodium complexes are formed in exothermic reactions making them fairly stable. The heats of formation for complexes of **86**, **87**, **88** and **89** are shown below (Tables 5.4, 5.5).

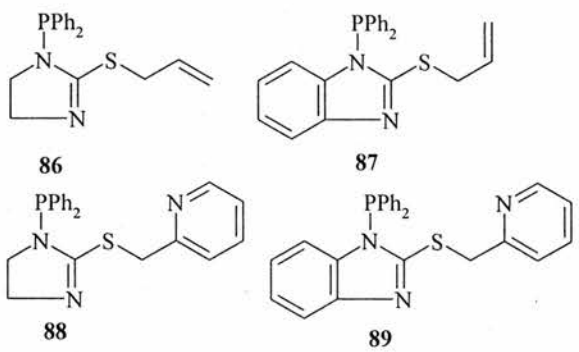

Figure 5.4. Derivatives of *N*-diphenylphosphino-2-thioimidazolidine and Derivatives of *N*-diphenylphosphino-2-thiobenzimidazole.

Table 5.4. Heats of formation for derivatives of *N*-diphenylphosphino-2-thioimidazolidine.

	Heat of Formation (kcal/mol)	*Heat of Formation (kcal/mol)*
Compound	**86**	**87**
Ligand	92.316	124.02
***cis* $PtCl_2L_2$**	-293.264	-276.227
***trans* $PtCl_2L_2$**	-343.904	-263.785
***cis* $PtClL_2$ chelate (S)**	-330.391	-309.463
***trans* $PtClL_2$ chelate (S)**	-352.714	-330.294
***cis* $PtClL_2$ chelate (allyl)**	-334.943	-249.276
***trans* $PtClL_2$ chelate (allyl)**	-422.945	-283.514
$PtCl_2L$ chelate (S)	-341.89	-409.897
$PtCl_2L$ chelate (allyl)	-446.233	-329.878
***cis* $PdCl_2L_2$**	44.258	102.202
***trans* $PdCl_2L_2$**	21.371	85.986
***cis* $PdClL_2$ chelate (S)**	61.879	107.453
***trans* $PdClL_2$ chelate (S)**	55.701	93.017
***cis* $PdClL_2$ chelate (allyl)**	34.104	134.175
***trans* $PdClL_2$ chelate (allyl)**	12.477	108.628
$PdCl_2L$ chelate (S)	-28.786	-23.898
$PdCl_2L$ chelate (allyl)	-57.08	-5.631
Pd(allyl)ClL	-3.818	28.999
Pd(allyl)L chelate (S)	26.954	30.602
Pd(allyl)L chelate (allyl)	-56.086	39.442
***trans* $RhCp^*Cl_2L$**	-327.286	-298.064
***trans* $RhCp^*ClL$ chelate (S)**	-309.389	-288.209
***trans* $RhCp^*ClL$ chelate (allyl)**	-277.793	-252.436

Table 5.5. Heats of formation for derivatives of *N*-diphenylphosphino-2-thiobenzimidazole.

	Heat of Formation (kcal/mol)	*Heat of Formation (kcal/mol)*
Compound	**88**	**89**
Ligand	110.217	139.7
***cis* $PtCl_2L_2$**	-307.918	-215.322
***trans* $PtCl_2L_2$**	-311.847	-262.418
***cis* $PtClL_2$ chelate (N)**	-340.2187	-249.475
***trans* $PtClL_2$ chelate (N)**	-345.605	-253.467
***cis* $PtClL_2$ chelate (S)**	-296.122	-235.351
***trans* $PtClL_2$ chelate (S)**	-296.854	-261.501
$PtCl_2L$ chelate (N)	-343.869	-363.132
$PtCl_2L$ chelate (S)	-25.873	-317.38
***cis* $PdCl_2L_2$**	73.24	123.842
***trans* $PdCl_2L_2$**	54.071	116.315
***cis* $PdClL_2$ chelate (N)**	56.519	130.518
***trans* $PdClL_2$ chelate (N)**	61.016	117.92
***cis* $PdClL_2$ chelate (S)**	84.04	150.305
***trans* $PdClL_2$ chelate (S)**	82.611	164.827
$PdCl_2L$ chelate (N)	-349.116	6.018
$PdCl_2L$ chelate (S)	-22.518	5.612
Pd(allyl)ClL	20.579	46.18
Pd(allyl)L chelate (N)	20.133	54.255
Pd(allyl)L chelate (S)	31.493	45.589
***trans* $RhCp^*Cl_2L$**	-308.69	-279.296
***trans* $RhCp^*ClL$ chelate (N)**	-285.766	-247.693
***trans* $RhCp^*ClL$ chelate (S)**	-298.22	-272.078

From the calculations performed for this work the ligands that should be investigated further by practical preparation appear to be *N*-diphenylphosphino-2-(methylthio)imidazolidine (**77**), *N*-diphenylphosphino-2-(methylthio)benzimidazole (**80**), 2-allylimidazolidine (**82**), 2-

pyridylimidazolidine (**84**), *N*-diphenylphosphino-2-(allylthio)imidazolidine (**86**) and *N*-diphenylphosphino-2-(picolylthio)imidazolidine (**88**).

References.

1. http://cmm.info.nih.gov/modelling/guide_documents/quantum_mechanics_documents.html
2. http://cmm.info.nih.gov/modelling/guide_documents/tocs/computation_software.html
3. PC Spartan *Pro* User's Guide, Wavefunction, Inc., Irvine, California, 1990.
4. W. J. Hehre, J. Yu, P. E. Klunzinger and L. Lou, A Brief Guide to Molecular Mechanics and Quantum Chemical Calculations, Wavefunction, Inc., Irvine, California, 1998 and references therein.
5. W. J, Hehre, B. J. Deppmeier and P. E. Klinzinger, A PC Spartan *Pro* Tutorial, Wavefunction, Inc., Irvine, California, 1999.
6. M. Rodriguez i Zubiri, PhD thesis, University of St. Andrews, 2002 and references therein.

CHAPTER 6: CONCLUSIONS

This work has investigated a variety of ligands with varying backbones to develop our understanding of the criteria for hemilability.

The initial work focused on the preparation of 2-(diphenylphosphinohydrazino)pyridine and its potential to act as a hemilable ligand. Within the investigation illustrative examples of coordination complexes were prepared which demonstrated the ability to form chelated complexes. Specific examples included the preparation of $[Cu(Ph_2PNHNHpy)_2][PF_6]$ in which the pyridyl nitrogen coordinates to the copper centre to form a six-member ring. Clarke *et al*[1] also reported chelation of 2-(diphenylphosphinohydrazino)pyridine in [RhCp*] complexes and this work showed the ability of the ligand to act as a hemilable ligand. However, further more detailed work would have to be carried out to prove that 2-(diphenylphosphinohydrazino)pyridine can behave as a hemilable ligand though the work performed suggests that this ligand has some hemilabile properties[2].

The next ligand investigated in this work was *p*-(xylylenediaminodiphenyl)phosphine which behaved as a bridging ligand. Bimetallic metal complexes such as $[RhCl(\mu\text{-}Cl)(\eta\text{-}C_5Me_5)]_2$, were used as the precursors to the bridged complexes. Figure 6.1 gives a schematic representation of how the bridging ligand coordinated to the metal centres.

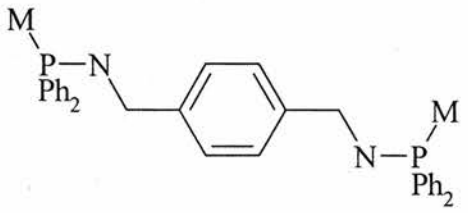

Figure 6.1. Schematic representation of a bridging ligand.

The work performed in this investigation only used metal complexes containing two identical metal centres. Further work that could be carried out on this ligand includes the use of mixed bimetallic to provide a new type of bridging complex. Figure 6.2 illustrates the potential mixed metallic bridging ligand that could be investigated.

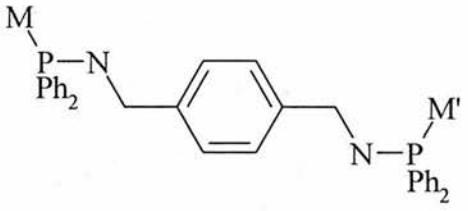

Figure 6.2. Schematic representation of a mixed bimetallic bridging ligand.

Chapter 3 describes the main focus of this work; centred on the ligands *N*-allylaminophosphine, *N*-allylaminobisphosphine and *N*-diallylaminophosphine. Considering *N*-allylaminophosphine first a variety of metal complexes were prepared using standard techniques in good yield and purity. The chelated complex $[Pt\{Ph_2PNH(C_3H_8O)\}_2]$ was prepared by reaction of K^{t}BuO in methanol with $[Pt\{Ph_2PNH(C_3H_5)\}]$. However, the reverse reaction was not attempted to prove whether or not the *N*-allylaminophosphine ligand behaves as a hemilabile ligand. Further work on this ligand would be to

investigate the possibility of hemilabilty. *N*-allylaminobisphosphine was easily prepared and behaved as a pincer ligand. In square planar platinum complexes this ligand coordinated with *cis* geometry. A novel complex was formed during the reaction of $[\{RuCl(\mu\text{-}Cl)(\eta^6\text{-}p\text{-}MeC_6H_4{}^iPr)\}_2]$ with *N*-allylaminobisphosphine where (η^6-*p*-$MeC_6H_4{}^iPr$) was replaced by the ligand. The final allyl ligand prepared for this work was *N*-diallylaminophosphine. There were unusual results observed with $[PtCl_2(cod)]$. When three equivalents of $[PtCl_2(cod)]$ were reacted with *N*-diallylaminophosphine a complex containing three different phosphorus groups was produced and the structure was assigned by ^{31}P NMR. However, crystallographic evidence was not available to prove the suggested structure of this novel complex.

Work carried out on *Z*-1-diphenylphosphino-3,3-dimethyl-2-phenylthiobut-1-ene and *Z*-1-diphenylphosphino-2-phenylthiopropene showed a potentially new hemilabile ligand containing both phosphorus and sulfur.

The final chapter investigates some potential hemilabile ligands using a computational approach. This work gives suggestions as to where to begin the synthetic work on the basis of the molecular modelling calculations. The ligands that would seem to be the best starting place for any future work would be *N*-dimethylphosphino-2-(methylthio)imidazolidine, *N*-diphenylphosphino-2-(methylthio)benzimidazole, 2-allylimidaoline, 2-pyridylimidazolidine, *N*-diphenylphosphino-2-(allylthio)imdazolidine and *N*-diphenylphosphino-2-(picolylthio)imidazolidine.

References.

1. M. L. Clarke, A. M. Z.Slawin, M. V. Wheatley, J. D. Woollins, *J. Chem. Soc. Dalton Trans.*, 2001, 3421.
2. A. M. Z. Slawin, J. Wheatley, M. V. Wheatley, J. D. Woolins, *Polyhedron*, 2003, **22**, 1397.

Appendix 1.

Table A1.1: Selected modelling data for N-diphenylphosphino-2-imidazolidinethiol complexes.

Compound	*Heat of formation (kcal/mol)*	P_1-N_1 (Å)	P_{11}-N_{11} (Å)	P_1-M (Å)	P_{11}-M (Å)	Cl_1-M (Å)	Cl_2-M (Å)	S-M (Å)
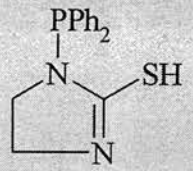 **76**	77.040	1.806	-	-	-	-	-	-
cis **$PtCl_2L_2$**	-351.243	1.834	1.832	2.292	2.294	2.399	2.396	-
trans **$PtCl_2L_2$**	-368.389	1.807	1.828	2.287	2.294	2.390	2.389	-
cis **$PtClL_2$ chelate**	-333.483	1.825	1.804	2.308	2.267	2.410	-	2.405
trans **$PtClL_2$ chelate**	-381.239	1.810	1.830	2.259	2.284	2.390	-	2.422
$PtCl_2L$ chelate	-331.010	1.844	-	2.240	-	2.360	2.375	2.368
cis **$PdCl_2L_2$**	1.346	1.835	1.841	2.299	2.279	2.322	2.315	-
trans **$PdCl_2L_2$**	-18.292	1.837	1.838	2.264	2.263	2.337	2.338	-
cis **$PdClL_2$ chelate**	31.881	1.871	1.821	2.290	2.297	2.323	-	2.421
trans **$PdClL_2$ chelate**	8.165	1.855	1.829	2.283	2.302	2.324	-	2.432
$PdCl_2L$ chelate	-39.694	1.872	-	2.258	-	2.310	2.304	2.393
Pd(allyl)ClL	-13.354	1.828	-	2.269	-	2.334	-	-
Pd(allyl)L chelate	1.907	1.866	-	2.279	-	-	-	2.419
trans **$RhCp^*Cl_2L$**	-344.025	1.841	-	2.319	-	2.303	2.302	-
trans **$RhCp^*ClL$ chelate**	-324.198	1.843	-	2.342	-	2.302	-	2.387

Table A1.2: Selected modelling data for N-diphenylphosphino-2-methylthioimidazolidine complexes.

Compound	*Heat of formation (kcal/mol)*	P_1-N_1 (Å)	P_{11}-N_{11} (Å)	P_1-M (Å)	P_{11}-M (Å)	Cl_1-M (Å)	Cl_2-M (Å)	S-M (Å)
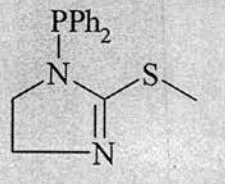 77	70.636	1.802	–	–	–	–	–	–
cis **$PtCl_2L_2$**	-367.904	1.822	1.821	2.293	2.285	2.394	2.397	–
trans **$PtCl_2L_2$**	-375.978	1.826	1.823	2.326	2.305	2.391	2.387	–
cis **$PtClL_2$ chelate**	-356.061	1.823	1.803	2.304	2.296	2.414	–	2.404
trans **$PtClL_2$ chelate**	-394.093	1.822	1.821	2.291	2.323	2.379	–	2.417
$PtCl_2L$ chelate	-347.746	1.842	–	2.239	–	2.359	2.376	2.368
cis **$PdCl_2L_2$**	1.031	1.839	1.847	2.293	2.275	2.323	2.32	–
trans **$PdCl_2L_2$**	-11.026	1.833	1.833	2.276	2.276	2.335	2.336	–
cis **$PdClL_2$ chelate**	7.468	1.856	1.847	2.303	2.304	2.33	–	2.408
trans **$PdClL_2$ chelate**	13.417	1.842	1.852	2.349	2.308	2.326	–	2.42
$PdCl_2L$ chelate	-50.247	1.869	–	2.256	–	2.31	2.306	2.387
Pd(allyl)ClL	-28.001	1.836	–	2.262	–	2.339	–	–
Pd(allyl)L chelate	-3.625	1.884	–	2.287	–	–	–	2.401
trans **$RhCp^*Cl_2L$**	-348.39	1.84	–	2.319	–	2.304	2.303	–
trans **$RhCp^*ClL$ chelate**	-328.635	1.812	–	2.355	–	2.296	–	2.399

Table A1.3: Selected modelling data for N-diphenylphosphino-2-benzylthioimidazolidine complexes.

Compound	*Heat of Formation (kcal/mol)*	P_1-N_1(Å)	P_{11}-N_{11}(Å)	P_1-M(Å)	P_{11}-M(Å)	Cl_1-M(Å)	Cl_2-M(Å)	S_2-M(Å)
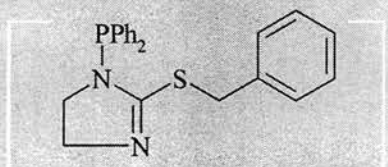	102.914	1.802	–	–	–	–	–	–
78								
cis **$PtCl_2L_2$**	-294.698	1.832	1.837	2.284	2.301	2.396	2.402	–
trans **$PtCl_2L_2$**	-333.526	1.821	1.823	2.302	2.279	2.387	2.386	–
trans **$PtClL_2$ chelate (S)**	-357.06	1.809	1.827	2.297	2.332	2.382	–	2.422
cis **$PtClL_2$ chelate (S)**	-329.632	1.835	1.821	2.28	2.304	2.385	–	2.415
$PtCl_2L$ chelate (S)	-363.599	1.839	–	2.276	–	2.371	2.391	2.408
cis **$PdCl_2L_2$**	50.486	1.833	1.855	2.273	2.279	2.33	2.321	–
trans **$PdCl_2L_2$**	39.746	1.836	1.837	2.297	2.263	2.338	2.333	–
trans **$PdClL_2$ chelate (S)**	52.858	1.841	1.829	2.29	2.294	2.325	–	2.438
cis **$PdClL_2$ chelate (S)**	52.801	1.862	1.835	2.283	2.289	2.321	–	2.417
$PdCl_2L$ chelate (S)	-21.383	1.864	–	2.256	–	2.306	2.308	2.39
Pd(allyl)ClL	5.794	1.852	–	2.258	–	2.336	–	–
Pd(allyl)L chelate (S)	10.034	1.871	–	2.263	–	–	–	
trans **$RhCp^*Cl_2L$**	-318.606	1.84	–	2.32	–	2.303	2.302	–
trans **$RhCp^*ClL$ chelate (S)**	-304.493	1.855	–	2.34	–	2.301	–	2.393

Table A1.4: Selected modelling data for N-diphenylphosphino-2-benzimidazolethiol complexes.

Compound	*Heat of Formation (kcal/mol)*	P_1-N_1(Å)	P_{11}-N_{11}(Å)	P_1-M(Å)	P_{11}-M(Å)	Cl_1-M(Å)	Cl_2-M(Å)	S_2-M(Å)
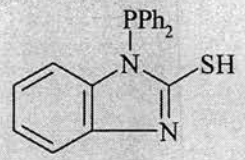 **79**	110.567	1.814	–	–	–	–	–	–
cis **$PtCl_2L_2$**	-282.262	1.85	1.836	2.275	2.269	2.395	2.391	–
trans **$PtCl_2L_2$**	-305.449	1.824	1.823	2.302	2.282	2.403	2.389	–
cis **$PtClL_2$ chelate**	-273.249	1.862	1.818	2.315	2.289	2.42	–	2.41
trans **$PtClL_2$ chelate**	-333.626	1.829	1.832	2.305	2.288	2.39	–	2.43
$PtCl_2L$ chelate	-307.082	1.866	–	2.255	–	2.36	2.373	2.365
cis **$PdCl_2L_2$**	67.864	1.872	1.871	2.291	2.284	2.319	2.326	–
trans **$PdCl_2L_2$**	51.515	1.861	1.861	2.266	2.276	2.337	2.336	–
cis **$PdClL_2$ chelate**	94.754	1.876	1.856	2.358	2.292	2.326	–	2.413
trans **$PdClL_2$ chelate**	46.304	1.848	1.864	2.294	2.287	2.332	–	2.436
$PdCl_2L$ chelate	-7.774	1.891	–	2.255	–	2.307	2.303	2.399
Pd(allyl)ClL	12.122	1.885	–	2.26	–	2.338	–	–
Pd(allyl)L chelate	46.565	1.878	–	2.344	–	–	–	2.397
trans **$RhCp^*Cl_2L$**	-313.713	1.843	–	2.312	–	2.297	2.298	–
trans **$RhCp^*ClL$ chelate**	-331.491	1.832	–	2.324	–	2.299	–	2.389

Table A1.5: Selected modelling data for N-diphenylphosphino-2-methylthiobenzimidazole complexes.

Compound	*Heat of Formation (kcal/mol)*	P_1-N_1(Å)	P_{11}-N_{11}(Å)	P_1-M(Å)	P_{11}-M(Å)	Cl_1-M(Å)	Cl_2-M(Å)	S_2-M(Å)
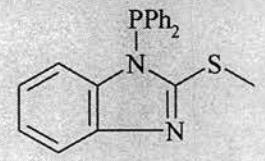	102.999	1.815	–	–	–	–	–	–
80								
cis **$PtCl_2L_2$**	-293.866	1.838	1.838	2.281	2.278	2.385	2.398	–
trans **$PtCl_2L_2$**	-313.89	1.834	1.822	2.283	2.309	2.395	2.395	–
cis **$PtClL_2$ chelate**	-307.464	1.851	1.81	2.306	2.273	2.44	–	2.432
trans **$PtClL_2$ chelate**	-315.878	2.012	1.828	2.318	2.287	2.381	–	2.402
$PtCl_2L$ chelate	-323.747	1.865	–	2.254	–	2.375	2.36	2.369
cis **$PdCl_2L_2$**	56.101	1.869	1.87	2.288	2.288	2.315	2.315	–
trans **$PdCl_2L_2$**	43.497	1.863	1.859	2.277	2.266	2.337	2.336	–
cis **$PdClL_2$ chelate**	82.865	1.889	1.836	2.305	2.285	2.325	–	2.426
trans **$PdClL_2$ chelate**	56.981	1.862	1.85	2.294	2.276	2.331	–	2.433
$PdCl_2L$ chelate	-18.027	1.89	–	2.255	–	2.306	2.304	2.391
Pd(allyl)ClL	7.975	1.865	–	2.257	–	2.334	–	–
Pd(allyl)L chelate	24.788	1.888	–	2.282	–	–	–	2.409
trans **$RhCp^*Cl_2L$**	-312.693	1.866	–	2.326	–	2.348	2.314	–
trans **$RhCp^*ClL$ chelate**	-303.737	1.876	–	2.333	–	2.303	–	2.392

Table A1.6: Selected modelling data for N-diphenylphosphino-2-benzylthiobenzimidaole complexes.

Compound	*Heat of Formation (kcal/mol)*	P_1-N_1(Å)	P_{11}-N_{11}(Å)	P_1-M(Å)	P_{11}-M(Å)	Cl_1-M(Å)	Cl_2-M(Å)	S_2-M(Å)
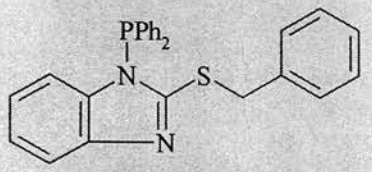 **81**	132.71	1.817	–	–	–	–	–	–
cis **$PtCl_2L_2$**	-245.63	1.846	1.844	2.286	2.28	2.38	2.399	–
trans **$PtCl_2L_2$**	-269.993	1.832	1.84	2.305	2.294	2.383	2.407	–
trans **$PtClL_2$ chelate (S)**	-267.446	1.849	1.827	2.323	2.303	2.376	–	2.45
cis **$PtClL_2$ chelate (S)**	-272.457	1.85	1.826	2.346	2.307	2.418	–	2.417
$PtCl_2L$ chelate (S)	-330.59	1.871	–	2.278	–	2.37	2.388	2.402
cis **$PdCl_2L_2$**	111.989	1.861	1.854	2.272	2.273	2.325	2.327	–
trans **$PdCl_2L_2$**	104.828	1.86	1.86	2.279	2.279	2.336	2.336	–
trans **$PdClL_2$ chelate (S)**	127.644	1.857	1.959	2.296	2.25	2.388	–	2.417
cis **$PdClL_2$ chelate (S)**	129.66	1.888	1.845	2.292	2.28	2.321	–	2.425
$PdCl_2L_2$ chelate (S)	0.132	1.89	–	2.254	–	2.309	2.308	2.416
Pd(allyl)ClL	39.593	1.881	–	2.247	–	2.345	–	–
Pd(allyl)L chelate (S)	40.697	1.899	–	2.264	–	–	–	2.423
trans **$RhCp^*Cl_2L$**	-281.358	1.848	–	2.324	–	2.293	2.299	–
trans **$RhCp^*ClL$ chelate (S)**	-280.608	1.846	–	2.32	–	2.287	–	2.4

Table A1.8: Selected modelling data for N-diphenylphosphino-2-allylbenzimidaole complexes.

Compound	*Heat of formation (kcal/mol)*	P_1-N_1 (Å)	P_{11}-N_{11} (Å)	P_1-M (Å)	P_{11}-M (Å)	Cl_1-M (Å)	Cl_2-M (Å)	allyl-M (Å)
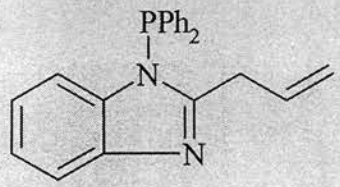 **83**	115.538	1.812	-	-	-	-	-	-
cis **$PtCl_2L_2$**	-277.974	1.832	1.832	2.252	2.277	2.391	2.395	-
trans **$PtCl_2L_2$**	-312.533	1.820	1.820	2.269	2.270	2.391	2.390	-
cis **$PtClL_2$ chelate**	-332.281	1.830	1.817	2.300	2.406	2.434	-	2.102
trans **$PtClL_2$ chelate**	-385.032	1.850	1.801	2.336	2.343	2.501	-	2.127
$PtCl_2L$ chelate	-410.412	1.831	-	2.255	-	2.448	2.398	2.090
cis **$PdCl_2L_2$**	76.867	1.856	1.859	2.282	2.283	2.315	2.315	-
trans **$PdCl_2L_2$**	58.657	1.850	1.850	2.278	2.279	2.335	2.337	-
cis **$PdClL_2$ chelate**	86.579	1.861	1.841	2.331	2.328	2.328	-	2.079
trans **$PdClL_2$ chelate**	74.519	1.825	1.858	2.290	2.304	2.319	-	2.079
$PdCl_2L$ chelate	-35.897	1.858	-	2.265	-	2.297	2.307	2.025
Pd(allyl)ClL	16.176	1.874	-	2.265	-	2.346	-	-
Pd(allyl)L chelate	14.929	1.832	-	2.282	-	-	-	2.038
trans **$RhCp^*Cl_2L$**	-306.540	1.826	-	2.323	-	2.294	2.302	-
trans **$RhCp^*ClL$ chelate**	-298.486	1.826	-	2.330	-	2.310	-	2.068

Table A1.9: Selected modelling data for N-diphenylphosphino-2-picolylimidazolidine complexes.

Compound	*Heat of formation (kcal/mol)*	P_1-N_1 (Å)	P_{11}-N_{11} (Å)	P_1-M (Å)	P_{11}-M (Å)	Cl_1-M (Å)	Cl_2-M (Å)	*pyridyl-M (Å)*
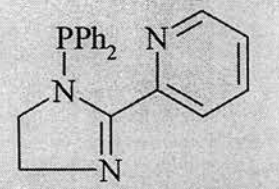 **84**	105.996	1.801	-	-	-	-	-	-
cis **$PtCl_2L_2$**	-305.775	1.841	1.824	2.275	2.269	2.405	2.390	-
trans **$PtCl_2L_2$**	-323.973	1.827	1.827	2.294	2.294	2.389	2.387	-
cis **$PtClL_2$ chelate**	-296.286	1.805	1.816	2.290	2.298	2.430	-	2.038
trans **$PtClL_2$ chelate**	-326.030	1.824	1.795	2.315	2.322	2.365	-	2.030
$PtCl_2L$ chelate	-328.973	1.830	-	2.243	-	2.362	2.417	2.016
cis **$PdCl_2L_2$**	111.007	1.836	1.842	2.298	2.280	2.317	2.315	-
trans **$PdCl_2L_2$**	42.530	1.827	1.836	2.291	2.295	2.328	2.344	-
cis **$PdClL_2$ chelate**	85.044	1.838	1.820	2.320	2.298	2.350	-	2.024
trans **$PdClL_2$ chelate**	59.516	1.850	1.815	2.286	2.286	2.317	-	2.030
$PdCl_2L$ chelate	-23.652	1.854	-	2.242	-	2.311	2.344	2.010
Pd(allyl)ClL	-1.846	1.829	-	2.265	-	2.339	-	-
Pd(allyl)L chelate	32.324	1.841	-	2.322	-	-	-	2.026
trans **$RhCp^*Cl_2L$**	-316.689	1.829	-	2.321	-	2.302	2.294	-
trans **$RhCp^*ClL$ chelate**	-301.086	1.821	-	2.318	-	2.308	-	2.007

Table A1.10: Selected modelling data for N-diphenylphosphino-2-picolylbenzimidaole complexes.

Compound	*Heat of formation (kcal/mol)*	P_1-N_1 (Å)	P_{11}-N_{11} (Å)	P_1-M (Å)	P_{11}-M (Å)	Cl_1-M (Å)	Cl_2-M (Å)	*pyridyl-M (Å)*
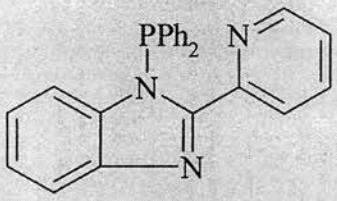 **85**	141.071	1.829	-	-	-	-	-	-
cis **$PtCl_2L_2$**	-234.644	1.849	1.843	2.254	2.259	2.382	2.399	-
trans **$PtCl_2L_2$**	-251.949	1.839	1.825	2.260	2.271	2.384	2.387	-
cis **$PtClL_2$ chelate**	-248.559	1.945	1.848	2.304	2.278	2.450	-	2.045
trans **$PtClL_2$ chelate**	-261.889	2.067	1.831	2.288	2.315	2.374	-	2.014
$PtCl_2L$ chelate	-294.369	1.865	-	2.245	-	2.361	2.391	2.011
cis **$PdCl_2L_2$**	120.120	1.860	1.857	2.291	2.283	2.318	2.319	-
trans **$PdCl_2L_2$**	102.000	1.855	1.852	2.286	2.285	2.332	2.337	-
cis **$PdClL_2$ chelate**	130.462	1.899	1.856	2.270	2.279	2.337	-	2.021
trans **$PdClL_2$ chelate**	164.257	1.866	1.834	2.289	2.330	2.316	-	2.045
$PdCl_2L$ chelate	9.655	1.885	-	2.240	-	2.305	2.324	2.008
Pd(allyl)ClL	42.911	1.858	-	2.257	-	2.334	-	-
Pd(allyl)L chelate	47.295	1.885	-	2.257	-	-	-	2.033
trans **$RhCp^*Cl_2L$**	-279.486	1.839	-	2.313	-	2.302	2.296	-
trans **$RhCp^*ClL$ chelate**	-270.773	2.009	-	2.356	-	2.309	-	2.004

Table A1.11: Selected modelling data for N-diphenylphosphino-2-allylthioimidazolidine complexes.

Compound	*Heat of Formation (kcal/mol)*	P_1-N_1(Å)	P_{11}-N_{11}(Å)	P_1-M(Å)	P_{11}-M(Å)	Cl_1-M(Å)	Cl_2-M(Å)	allyl-M(Å)	S_2-M(Å)
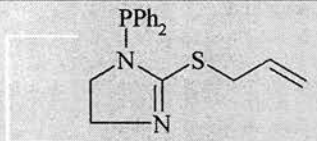	92.316	1.802	–	–	–	–	–	–	–
86									
cis **$PtCl_2L_2$**	-293.264	1.816	1.827	2.276	2.298	2.396	2.382	–	–
trans **$PtCl_2L_2$**	-343.904	1.822	1.827	2.306	2.32	2.394	2.385	–	–
cis **$PtClL_2$ chelate (S)**	-330.391	1.821	1.802	2.313	2.28	2.41	–	–	–
trans **$PtClL_2$ chelate (S)**	-352.714	1.823	1.84	2.322	2.325	2.381	–	–	–
cis **$PtClL_2$ chelate (allyl)**	-334.943	1.811	1.801	2.335	2.301	2.429	–	2.093	–
trans **$PtClL_2$ chelate (allyl)**	-422.945	1.814	1.967	2.307	2.33	2.504	–	2.474	2.415
$PtCl_2L$ chelate (S)	-341.89	1.836	–	2.259	–	2.36	2.379	–	–
$PtCl_2L$ chelate (allyl)	-446.233	1.825	–	2.289	–	2.491	2.397	2.08	2.426
cis **$PdCl_2L_2$**	44.258	1.838	1.832	2.291	2.294	2.321	2.315	–	–
trans **$PdCl_2L_2$**	21.371	1.834	1.835	2.268	2.295	2.34	2.34	–	2.427
cis **$PdClL_2$ chelate (S)**	61.879	1.833	1.825	2.347	2.29	2.33	–	–	–
trans **$PdClL_2$ chelate (S)**	55.701	1.832	1.818	2.344	2.311	2.324	–	–	2.41
cis **$PdClL_2$ chelate (allyl)**	34.104	1.846	1.836	2.301	2.349	2.332	–	2.075	2.392
trans **$PdClL_2$ chelate (allyl)**	12.477	1.836	1.842	2.301	2.3	2.344	–	2.088	–
$PdCl_2L$ chelate (S)	-28.786	1.866	–	2.254	–	2.306	2.307	–	2.378
$PdCl_2L$ chelate (allyl)	-57.08	1.836	–	2.27	–	2.3	2.311	2.026	–
Pd(allyl)ClL	-3.818	1.859	–	2.262	–	2.337	–	–	–
Pd(allyl)L chelate (S)	26.954	1.859	–	2.314	–	–	–	–	2.399
Pd(allyl)L chelate (allyl)	-56.086	1.852	–	2.249	–	–	–	2.031	–
trans **$RhCp^*Cl_2L$**	-327.286	1.841	–	2.32	–	2.302	2.304	–	–
trans **$RhCp^*ClL$ chelate (S)**	-309.389	1.815	–	2.355	–	2.299	–	–	2.387
trans **$RhCp^*ClL$ chelate (allyl)**	-277.793	1.802	–	2.331	–	2.32	–	2.627	–

Table A1.12: Selected modelling data for N-diphenylphosphino-2-allylthiobenzimidaole complexes.

Compound	*Heat of Formation (kcal/mol)*	P_1-N_1(Å)	P_{11}-N_{11}(Å)	P_1-M(Å)	P_{11}-M(Å)	Cl_1-M(Å)	Cl_2-M(Å)	*allyl*-M(Å)	S_2-M(Å)
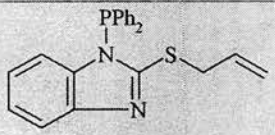	124.02	1.816	–	–	–	–	–	–	–
87									
cis **$PtCl_2L_2$**	-276.227	1.833	1.849	2.297	2.279	2.389	2.398	–	–
trans **$PtCl_2L_2$**	-263.785	1.825	1.832	2.267	2.266	2.383	2.392	–	–
cis **$PtClL_2$ chelate (allyl)**	-309.463	1.818	1.828	2.348	2.396	2.438	–	2.098	–
trans **$PtClL_2$ chelate (allyl)**	-330.294	1.831	1.837	2.329	2.311	2.429	–	2.559	–
cis **$PtClL_2$ chelate (S)**	-249.276	1.865	1.849	2.262	2.279	2.398	–	–	2.419
trans **$PtClL_2$ chelate (S)**	-283.514	1.846	1.821	2.308	2.284	2.383	–	–	2.411
$PtCl_2L$ chelate (allyl)	-409.897	1.836	–	2.269	–	2.448	2.403	2.092	–
$PtCl_2L$ chelate (S)	-329.878	1.865	–	2.267	–	2.364	2.383	–	2.381
cis **$PdCl_2L_2$**	102.202	1.865	1.861	2.284	2.278	2.323	2.315	–	–
trans **$PdCl_2L_2$**	85.986	1.862	1.858	2.279	2.282	2.333	2.334	–	–
cis **$PdClL_2$ chelate (allyl)**	107.453	1.828	1.878	2.318	2.321	2.318	–	2.071	–
trans **$PdClL_2$ chelate (allyl)**	93.017	1.883	1.882	2.299	2.313	2.318	–	2.062	–
cis **$PdClL_2$ chelate (S)**	134.175	1.889	1.848	2.299	2.317	2.319	–	–	2.423
trans **$PdClL_2$ chelate (S)**	108.628	2.087	1.847	2.317	2.287	2.319	–	–	2.423
$PdCl_2L$ chelate (allyl)	-23.898	1.858	–	2.271	–	2.3	2.31	2.03	–
$PdCl_2L$ chelate (S)	-5.631	1.899	–	2.254	–	2.307	2.311	–	2.386
Pd(allyl)ClL	28.999	1.866	–	2.275	–	2.334	–	–	–
Pd(allyl)L chelate (allyl)	30.602	1.846	–	2.282	–	–	–	2.089	–
Pd(allyl)L chelate (S)	39.442	2.092	–	2.318	–	–	–	–	2.399
trans **$RhCp^*Cl_2L$**	-298.064	1.84	–	2.312	–	2.297	2.301	–	–
trans **$RhCp^*ClL$ chelate (allyl)**	-288.209	1.837	–	2.336	–	2.322	–	2.058	–
trans **$RhCp^*ClL$ chelate (S)**	-252.436	1.816	–	2.341	–	2.293	–	–	2.404

Table A1.13: Selected modelling data for N-diphenylphosphino-2-picolylthioimidazolidine complexes.

Compound	*Heat of Formation (kcal/mol)*	P_1-N_1(Å)	P_{11}-N_{11}(Å)	P_1-M(Å)	P_{11}-M(Å)	Cl_1-M(Å)	Cl_2-M(Å)	N_{10}-M(Å)	S_2-M(Å)
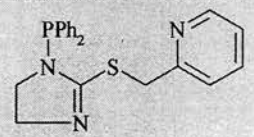 **88**	110.217	1.805	–	–	–	–	–	–	–
cis **$PtCl_2L_2$**	-307.918	1.836	1.819	2.292	2.283	2.389	2.401	–	–
trans **$PtCl_2L_2$**	-311.847	1.818	1.822	2.327	2.317	2.389	2.387	–	–
cis **$PtClL_2$ chelate (N)**	-340.2187	1.805	1.799	2.291	2.308	2.402	–	2.034	–
trans **$PtClL_2$ chelate (N)**	-345.605	1.8	1.8	2.296	2.318	2.409	–	2.022	–
cis **$PtClL_2$ chelate (S)**	-296.122	1.839	1.824	2.26	2.32	2.405	–	–	2.415
trans **$PtClL_2$ chelate (S)**	-296.854	1.829	1.833	2.335	2.332	2.378	–	–	2.4
$PtCl_2L$ chelate (N)	-343.869	1.83	–	2.259	–	2.361	2.375	3.763	–
$PtCl_2L$ chelate (S)	-25.873	1.832	–	2.257	–	2.362	2.384	–	2.386
cis **$PdCl_2L_2$**	73.24	1.847	1.839	2.277	2.295	2.32	2.32	–	–
trans **$PdCl_2L_2$**	54.071	1.839	1.835	2.297	2.263	2.335	2.336	–	–
cis **$PdClL_2$ chelate (N)**	56.519	1.852	1.835	2.29	2.308	2.329	–	2.031	–
trans **$PdClL_2$ chelate (N)**	61.016	1.833	1.828	2.3	2.288	2.327	–	2.065	–
cis **$PdClL_2$ chelate (S)**	84.04	1.835	1.82	2.35	2.31	2.333	–	–	2.416
trans **$PdClL_2$ chelate (S)**	82.611	1.845	1.823	2.346	2.284	2.327	–	–	2.427
$PdCl_2L$ chelate (N)	-349.116	1.858	–	2.26	–	2.313	2.314	2.019	–
$PdCl_2L$ chelate (S)	-22.518	1.866	–	2.255	–	2.306	2.312	–	2.414
Pd(allyl)ClL	20.579	1.839	–	2.255	–	2.34	–	–	–
Pd(allyl)L chelate (N)	20.133	1.841	–	2.292	–	–	–	2.05	–
Pd(allyl)L chelate (S)	31.493	1.833	–	2.333	–	–	–	–	–
trans **$RhCp^*Cl_2L$**	-308.69	1.806	–	2.324	–	2.293	2.298	–	–
trans **$RhCp^*ClL$ chelate (N)**	-285.766	1.832	–	2.345	–	2.325	–	2.034	–
trans **$RhCp^*ClL$ chelate (S)**	-298.22	1.849	–	2.334	–	2.304	–	–	2.398

Table A1.14: Selected modelling data for N-diphenylphosphino-2-picolylthiobenzimidaole complexes.

Compound	*Heat of Formation (kcal/mol)*	P_1-N_1(Å)	P_{11}-N_{11}(Å)	P_1-M(Å)	P_{11}-M(Å)	Cl_1-M(Å)	Cl_2-M(Å)	N_{10}-M(Å)	S_2-M(Å)
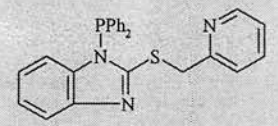	139.7	1.831	–	–	–	–	–	–	–
89									
cis **$PtCl_2L_2$**	-215.322	1.844	1.842	2.281	2.26	2.391	2.392	–	–
trans **$PtCl_2L_2$**	-262.418	1.832	1.827	2.287	2.299	2.393	2.404	–	–
cis **$PtClL_2$ chelate (N)**	-249.475	1.838	1.824	2.299	2.311	2.385	–	2.034	–
trans **$PtClL_2$ chelate (N)**	-253.467	1.829	1.831	2.338	2.31	2.394	–	2.038	–
cis **$PtClL_2$ chelate (S)**	-235.351	1.863	1.839	2.308	2.269	2.412	–	–	2.409
trans **$PtClL_2$ chelate (S)**	-261.501	1.859	1.815	2.344	2.323	2.403	–	4	–
$PtCl_2L$ chelate (N)	-363.132	1.814	–	2.263	–	2.434	2.4	2.781	–
$PtCl_2L$ chelate (S)	-317.38	1.863	–	2.258	–	2.381	2.362	–	2.383
cis **$PdCl_2L_2$**	123.842	1.853	1.878	2.279	2.284	2.318	2.328	–	–
trans **$PdCl_2L_2$**	116.315	1.863	1.859	2.276	2.265	2.338	2.34	–	–
cis **$PdClL_2$ chelate (N)**	130.518	1.871	1.856	2.279	2.288	2.324	–	2.037	–
trans **$PdClL_2$ chelate (N)**	117.92	1.872	1.857	2.293	2.288	2.331	–	2.032	–
cis **$PdClL_2$ chelate (S)**	150.305	1.885	1.862	2.292	2.279	2.318	–	–	2.414
trans **$PdClL_2$ chelate (S)**	164.827	1.879	1.834	2.304	2.289	2.319	–	–	2.429
$PdCl_2L$ chelate (N)	6.018	1.882	–	2.273	–	2.312	2.314	2.02	–
$PdCl_2L$ chelate (S)	5.612	1.888	–	2.274	–	2.308	2.311	–	2.41
Pd(allyl)ClL	46.18	1.866	–	2.24	–	2.335	–	–	–
Pd(allyl)L chelate (N)	54.255	1.905	–	2.263	–	–	–	3.617	–
Pd(allyl)L chelate (S)	45.589	1.882	–	2.279	–	–	–	–	2.436
trans **$RhCp^*Cl_2L$**	-279.296	1.844	–	2.325	–	2.294	2.303	–	–
trans **$RhCp^*ClL$ chelate (N)**	-247.693	1.827	–	2.337	–	2.307	–	2.015	–
trans **$RhCp^*ClL$ chelate (S)**	-272.078	1.877	–	2.332	–	2.303	–	–	2.39

APPENDIX 2: CRYSTAL STRUCTURE DATA

Details of collection and refinements for	*Compound (Local ID Number)*
$Ph_2PNHNHpy$	**1** (mwas1)
$Ph_2P(Se)NHNHpy$	**4** (mwas2)
$[RuCl_2(\eta^3:\eta^3\text{-}C_{10}H_{16})\{Ph_2PNHNHpy\text{-}P\}]$	**10** (jo1)
$[IrCl(\mu\text{-}Cl)(\eta^5\text{-}C_5Me_5)\{Ph_2PNHNHpy\text{-}P\}]$	**12** (wheat3)
$p\text{-}Ph_2P(S)NHCH_2(C_6H_4)CH_2NHP(S)Ph_2$	**19** (HMASJ24)
$p\text{-}Ph_2P(Se)NHCH_2(C_6H_4)CH_2NHP(Se)Ph_2$	**20** (HMASJ34)
$Ph_2P(Se)NH(C_3H_5)$	**32** (HMASJ15)
$[PtCl_2\{Ph_2PNH(C_3H_5)\}_2]$	**33** (jo6)
$[RuCl(\mu\text{-}Cl)(\eta^6\text{-}p\text{-}MeC_6H_4{}^iPr)\{Ph_2PNH(C_3H_5)\}]$	**38** (HMASJ17)
$[Pt\{Ph_2PNH(C_3H_8O)\}_2]$	**39** (alex5)
$[Pt(PEt)_3Cl_2\{Ph_2PNH(C_3H_5)\}]$	**42** (HMASJ13)
$[Pt(PPhMe_2)Cl_2\{Ph_2PNH(C_3H_5)\}]$	**43** (HMASJ14)
$[PtCl_2\{(Ph_2P)_2N(C_3H_5)\}]$	**46** (HMASJ2)
$[RuCl_2\{(Ph_2P)_2N(C_3H_5)\}_2]$	**51** (HMASJ8)
$[PdCl_2\{Ph_2PN(C_3H_5)_2\}]$	**61** (jo3)
$[PtCl_2\{X\}]$	**68** (jo7)
$[AuCl\{X\}]$	**71** (jo8)
$[IrCl(\mu\text{-}Cl)(\eta^5\text{-}C_5Me_5)\{X\}$	**72** (HMASJ25)
$[PdCl_2\{Y\}]$	**75** (HMASJ23)

Table A2.1 Selected Crystal Data for $Ph_2PNHNHpy$ and Derivatives.

Compound (Local ID number)	*1 (mwas1)*	*4 (mwas2)*	*10 (jo1)*	*12 (wheat3)*
Empirical Formula	$C_{17}H_{16}N_3P$	$C_{17}H_{16}N_3PSe$	$C_{28}H_{33}Cl_5N_3PRu$	$C_{27}H_{31}Cl_2IrN_3P$
M	293.31	372.26	720.86	691.62
Crystal system	Monoclinic	Monoclinic	Triclinic	Triclinic
Space group	$P2_{1/c}$	$P2_{1/c}$	P-1	P-1
a (Å)	5.592(4)	15.7931(19)	8.9712(2)	13.2992(3)
b (Å)	17.947(6)	11.8898(14)	13.5564(7)	14.4656(3)
c (Å)	15.139(3)	9.3268(11)	13.6359(7)	16.7774(4)
α (°)	90	90	106.947(2)	71.7020(10)
β (°)	97.81(3)	98.024(3)	103.608(2)	83.7060(10)
γ (°)	90	90	93.094(3)	64.4440(10)
U ($Å^3$)	1505.3(9)	1734.2(4)	1528.36(12)	2763.38(11)
Z	4	4	2	4
μ (mm^{-1})	1.579	2.257	1.026	5.103
Reflections measured	2605	7237	7628	13884
Independent reflections	2339	2439	4303	7819
Final R_1, $\omega R_2[I > 2\sigma(I)]$	0.070, 0.057	0.0553, 0.1283	0.0676, 0.1129	0.0269, 0.0460

Table A2.2 Selected Crystal Data for p-$Ph_2PNHCH_2(C_6H_4)CH_2NHPPh_2$ chalcogens.

Compound (Local ID number)	*19 (HMASJ24)*	*20 (HMASJ34)*
Empirical Formula	$C_{32}H_{30}N_2P_2S_2$	$C_{32}H_{32}N_2P_2Se_2$
M	568.64	664.46
Crystal system	Triclinic	Monoclinic
Space group	P-1	$P2_{1/n}$
a (Å)	9.2393(15)	10.950(5)
b (Å)	10.6234(17)	10.964(5)
c (Å)	16.444(3)	12.459(6)
α (°)	92.828(3)	90
β (°)	100.309(3)	96.528(10)
γ (°)	112.799(3)	90
U ($Å^3$)	1451.3(4)	1486.1(12)
Z	2	2
μ (mm^{-1})	0.318	2.620
Reflections measured	7413	6267
Independent reflections	4150	2100
Final R_1, $\omega R_2[I > 2\sigma(I)]$	0.0402, 0.1035	0.0401, 0.0651

Table A2.3 Selected Crystal Data for $Ph_2PNH(C_3H_5)$ and Derivatives.

Compound (Local ID number)	*32 (HMASJ15)*	*33 (jo6)*	*38 (HMASJ17)*	*39 (alex5)*	*42 (HMASJ13)*	*43 (HMASJ14)*
Empirical Formula	$C_{17}H_{16}N_3PSe$	$C_{30}H_{32}Cl_2N_2P_2Pt$	$C_{25}H_{30}Cl_2NPRu$	$C_{32}H_{38}N_2P_2O_2Pt$	$C_{21}H_{31}NP_2Cl_2Pt$	$C_{28}H_{33}Cl_5N_3PRu$
M	320.22	748.51	547.44	739.67	625.40	720.86
Crystal system	Monoclinic	Monoclinic	Monoclinic	Monoclinic	Triclinic	Triclinic
Space group	$P2_{1/n}$	$P2_{1/n}$	$P2_{1/c}$	$C2/_c$	P-1	P-1
a (Å)	12.246(3)	10.012(3)	9.918(3)	20229(3)	8.835(2)	8.9712(2)
b (Å)	9.317(2)	15.065(4)	13.782(4)	10.8193(17)	9.741(2)	13.5564(7)
c (Å)	12.711(3)	19.717(6)	17.566(5)	16.926(3)	14.634(3)	13.6359(7)
α (°)	90	90	90	90	87.302(4)	106.947(2)
β (°)	92.261(5)	91.56(10)	94.880(5)	123.002(2)	87.343(4)	103.608(2)
γ (°)	90	90	90	90	71.362(3)	93.094(3)
U ($Å^3$)	1449.1(6)	2972.9(15)	2392.5(11)	3106.8(8)	1191.4(5)	1528.36(12)
Z	4	4	4	4	2	2
μ (mm^{-1})	2.684	5.029	0.958	4.650	6.254	1.026
Reflections measured	5982	12495	10269	8848	5879	7628
Independent reflections	2066	4181	3421	2765	3327	4303
Final R_1, $\omega R_2[I > 2\sigma(I)]$	0.0381, 0.0917	0.0214, 0.0515	0.0343, 0.0783	0.0229, 0.0473	0.0361, 0.0967	0.0676, 0.1129

Table A2.4 Selected Crystal Data for $(Ph_2)_2PN(C_3H_5)$ and Derivatives.

Compound (Local ID number)	*46 (HMASJ2)*	*51 (HMASJ8)*
Empirical Formula	$C_{27}H_{25}NP_2Cl_2Pt$	$C_{54}H_{50}N_2P_4Cl_2Ru$
M	691.41	1022.81
Crystal system	Monoclinic	Triclinic
Space group	$P2_{1/n}$	P-1
a (Å)	10.8188(16)	10.1826(17)
b (Å)	14.661(2)	11.1207(19)
c (Å)	16.563(2)	12.597(2)
α (°)	90	111.490(3)
β (°)	85.488(3)	95.557(3)
γ (°)	90	113.376(3)
U ($Å^3$)	2618.9(7)	1168.3(3)
Z	4	1
μ (mm^{-1})	5.700	0.627
Reflections measured	12793	5901
Independent reflections	3741	3306
Final R_1, $\omega R_2[I > 2\sigma(I)]$	0.0419, 0.0965	0.0288, 0.0701

Table A2.5 Selected Crystal Data for $Ph_2PNH(C_3H_5)_2$ and Derivatives.

Compound (Local ID number)	*61 (jo3)*
Empirical Formula	$C_{18}H_{20}Cl_2NPPd$
M	458.62
Crystal system	Monoclinic
Space group	$P2_{1/c}$
a (Å)	8.514(2)
b (Å)	10.628(2)
c (Å)	20.307(10)
α (°)	90
β (°)	90.21(10)
γ (°)	90
U (Å^3)	1837.4(6)
Z	4
μ (mm^{-1})	1.386
Reflections measured	7708
Independent reflections	2624
Final R_1, $\omega R_2[I > 2\sigma(I)]$	0.019, 0.046

Table A2.6 Selected Crystal Data for Metal Complexes of dpptb and dpptp..

Compound (Local ID number)	*68 (jo7)*	*72 (jo8)*	*71 (HMASJ25)*	*75 (HMASJ23)*
Empirical Formula	$C_{24}H_{25}Cl_2SPPt$	$C_{24}H_{25}PAuClS$	$C_{34}H_{40}Cl_2IrSP$	$C_{21}H_{19}Cl_2PdSP$
M	642.46	608.89	774.79	511.69
Crystal system	Triclinic	Monoclinic	Triclinic	Triclinic
Space group	P1	$P2_{1/c}$	P-1	P-1
a (Å)	8.371(3)	18.290(6)	10.2041(15)	8.677(3)
b (Å)	9.178(3)	7.007(2)	10.2862(15)	11.063(4)
c (Å)	9.282(3)	17.660(6)	16.724(3)	11.665(4)
α (°)	103.72(5)	90	80.903(2)	76.460(6)
β (°)	116.14(4)	96.966(6)	82.655(2)	87.468(6)
γ (°)	103.02(4)	90	65.666(2)	71.174(5)
U ($Å^3$)	575.8(3)	2246.7(13)	1575.5(4)	1029.8(6)
Z	1	4	2	2
μ (mm^{-1})	6.494	6.839	4.546	1.342
Reflections measured	2742	11570	7887	5164
Independent reflections	2212	4032	4491	2910
Final R_1, $\omega R_2[I > 2\sigma(I)]$	0.0400, 0.1003	0.0571, 0.1252	0.0245, 0.0655	0.0483, 0.1280